Comparison of the chloroplast peroxidase system and characterization of the *Physcomitrella patens* thylakoid-bound APx

Inaugural-Dissertation
to obtain the academic degree
Doctor rerum naturalium (Dr. rer. nat.)

Submitted to the Department of Biology, Chemistry and Pharmacy
of the Freie Universität Berlin

by

Nicola Tatjana Pitsch

from Stuttgart (Germany)

Berlin, July 2013

The investigations described in the following thesis were started under supervision of Prof. Dr. Margarete Baier at the Institute of Plant Sciences of the Heinrich-Heine University Düsseldorf (12/2007 - 9/2010) and continued after moving of the group at the Institute of Biology, Section Plant Physiology of the Freie Universität Berlin (10/2010 – 7/2013).

1st Reviewer: Prof. Dr. Margarete Baier (FU Berlin)

2nd Reviewer: Prof. Dr. Tina Romeis (FU Berlin)

Date of defense: 17. September 2013

This thesis is dedicated to my mother…

R. I. P.

Acknowledgements

I would like to thank Prof. Dr. Margarete Baier for the opportunity to prepare my PhD thesis in her labs and research group. Thank you for your supervision and long discussions about science.

Many thanks to Prof. Dr. Tina Romeis for being the second reviewer of my thesis.

I thank the research groups in Düsseldorf and Berlin for their support and nice discussions about diverse topics - especially, Dr. Hans-Peter Haschke and Dr. Christiane Hedtmann, who spend time for reading and discussing my PhD thesis.

I am thanking my mom who was always there for me. She supported me in good and bad times. You will always stay in my heart. R. I. P.

A big thank you to Joachim Meeßen and Marc Wenczek! You are the best friends in the world, helping me through all times! Thank you so much!

I would like to thank Ilona Juszczak for being my friend, for nearly endless shopping tours, and deep discussions about science and other things.

Many thanks to Manfred Loell who became a friend for many grocery shopping tours and long discussions in nice evenings.

A big thank you to my remaining family in Stuttgart. Thank you for your help and support! For many relaxed evenings with nice food and discussions on sunny and rainy days.

Furthermore I would like to thank Benjamin Witsch, who helped in the lab work and who brought so many gummibears to survive long computer and lab days.

Finally, I would like to thank all my friends and the people I got to know in Düsseldorf and Berlin for their support and having an open ear for PhD problems.

List of abbreviations

$^1O_2$	singlet oxygen
2CP	2-Cys peroxiredoxin
3D	three dimensional
A	Absorbtion
Aa	amino acid
ABA	abscisic acid
ABI3	absisic-acid-insensitive3
AOS	active oxygen species
APx	ascorbate peroxidase
AsA	Ascorbate
At	*Arabidopsis thaliana*
ATP	adenosine triphosphate
BLAST	basic local alignment search tool
Bp	base pairs
BSA	bovine serum albumine
CaMV	cauliflower mosaic virus
CCD	charge-coupled device
cDNA	complementary deoxyribonucleic acid
CO_2	carbon dioxide
Col-0	Columbia-0
Cr	*Chlamydomonas reinhardtii*
C_t	threshold cycle
Cyp	Cyclophilin
$Cytb_6/f$	cytochrome b_6/f complex
DHA	Dehydroascorbate
DHAR	dehydroascorbate reductase
DNA	deoxyribonucleic acid
EDTA	Ethylenediaminetetraacetic acid
EST	expressed sequence tag
EVaLo	evolutionary variable loop
Fd	Ferredoxin
Fe	Iron

Fig.	Figure
Fts	filamentous temperature-sensitive
gDNA	genomic deoxyribonucleic acid
GFP	green fluorescent protein
glucose-6-P	glucose-6-phosphate
glutathione^{ox}	oxidized glutathione
glutathione^{red}	reduced glutathione
GPx	glutathione peroxidase
GR	glutathione reductase
Grx	Glutaredoxin
GSH1	γ-glutamylcysteine synthetase
GSH2	glutathione synthetase
H_2O	Water
H_2O_2	hydrogen peroxide
Hedw.	Hedwig
Heynh.	Gustav Heynhold
hnRNA	heterogenous nuclear ribonucleic acid
Hs	*Homo sapiens*
ID	Identity
L.	Carl von Linné
LHC	light harvesting complex
LTR	long terminal repeat
LUC	Luciferase
MDA	monodehydroascorbate
MDAR	monodehydroascorbate reductase
MES	2-(N-morpholino)ethanesulfonic acid
MOPS	3-(N-Morpholino)propanesulfonic acid
mRNA	messenger ribonucleic acid
MS	Murashige and Skoog
$NAD(P)^+$	oxidized nicotinamide adenine dinucleotide (phosphate)
NAD(P)H	reduced nicotinamide adenine dinucleotide (phosphate)
O_2^-	Superoxide
OD_{600}	optical density at 600 nm

$ONOO^-$	Peroxinitrites
ORF	open reading frame
PC	Plastocyanine
PCR	polymerase chain reaction
PEG	polyethylene glycol
PHGPx	phospholipid hydroperoxid glutathione peroxidase
Pp	*Physcomitrella patens*
PQ	Plastoquinone
Prx	Peroxiredoxin
PrxII	peroxiredoxin type II
PrxQ	peroxiredoxin Q
PSI	photosystem I
PSII	photosystem II
qRT-PCR	quantitative real time polymerase chain reaction
*rax*1-1	regulator of APx2 1-1 *Arabidopsis* mutant
RNA	ribonucleic acid
ROS	reactive oxygen species
RT-PCR	reverse transcriptase polymerase chain reaction
RbcS	small subunit of ribulose-1,5-bisphosphate carboxylase oxygenase
sAPx	stromal ascorbate peroxidase
Sm	*Selaginella moellendorffii*
SNP	single nucleotide polymorphism
SOD	superoxide dismutase
spec.	Species
TAE	Tris-acetate, ethylenediaminetetraacetic acid
TAE	Tris-acetate, ethylenediaminetetraacetic acid
TAP	Tris-acetate phosphate
tAPx	thylakoid-bound ascorbate peroxidase
Taq polymerase	*Thermus aquaticus* polymerase
T_m	melting temperature
TP	transit peptide
Trx	Thioredoxin
UTR	untranslated region

UTRE	upstream transcription regulating element
UV	Ultraviolet
var.	Variation
vtc-1	vitamin c 1 *Arabidopsis* mutant
WWC	water-water-cycle
YEB	yeast extract broth
YFP	yellow fluorescent protein

1 Introduction

1.1 Plant evolution

The conquest of land was accompanied by various hostile conditions which challenged plants to adapt. Green algae, also called chlorophyta, comprise approximately 11,000 species, appear green since their chlorophyll is not covered by accessory pigments (Fig. I1, Frey *et al.* 1988, Sitte *et al.* 2002). They separated from streptophytes more than a billion years ago (Merchant *et al.* 2007). On the one hand, chlorophytes show similarity to the animal kingdom, due to some stages showing flagella. On the other hand, green algae are photosynthetic organisms having one single cup-shaped chloroplast with one or more pyrenoids, where the Calvin cycle resides (Harris *et al.* 2001).

Bryophytina were among the first plants conquering land. Their adaptation to this environment is less sophisticated than that of higher plants, placing them at an evolutionary stage in between algae and lycophytes (Fig. I1, Frahm 2001). Reski (2005) suggested that mosses and seed plants diverged approximately 450 million years ago. In contrast to the cormophyta, they do not have an epidermis in their leaf-like organs and no fully functional cuticula (Frahm 2001). Only further evolved mosses have simple tissues to transport water or assimilates and to stabilize their body (Frey *et al.* 1988). Being haploid, the general habitus of musci, also called mosses, appears similar to true cormophytes since it is differentiated into phylloids, cauloids, and rhizoids. To regulate the rate of transpiration cormophytes evolved stomata. Mosses also can have stomata but only at the apophysis of their sporophytes (Frey *et al.* 1988, Sitte *et al.* 2002). Whereas the haploid gametophyte is the dominating generation in the moss life cycle, the diploid sporophyte stage dominates the in higher plants life cycle (Reski 1998a, Frahm 2001).

The life on land forced plants to evolve tissues stabilizing the cormus and ensuring the uptake of water and nutrients from soil, their transport within the plant body, and protection from excess transpiration (Frey *et al.* 1988). While pteridophyta already evolved tissues fulfilling these functions, higher plants show a more sophisticated differentiation of cells. Additionally, the latter protect their gametophyte with sporophyte tissue and gamets do not have any flagella (Banks 2009). All this increases the capability to survive the water deficit on land.

Higher plants are true cormophytes and organized in root, stem, and leaves (Frey *et al.* 1988). Xylem and phloem transport water and assimilates. Turgor pressure as well as collenchyma and sclerenchyma stabilize the cormus (Frey *et al.* 1988). During evolution, plants adapted to

the environment on land and became more tolerant to abiotic stresses, like water deficit, varying light intensities, and temperature changes, to survive trough times (Rensing *et al.* 2008). Besides this, they evolved more sophisticated signaling cascades in response to stress.

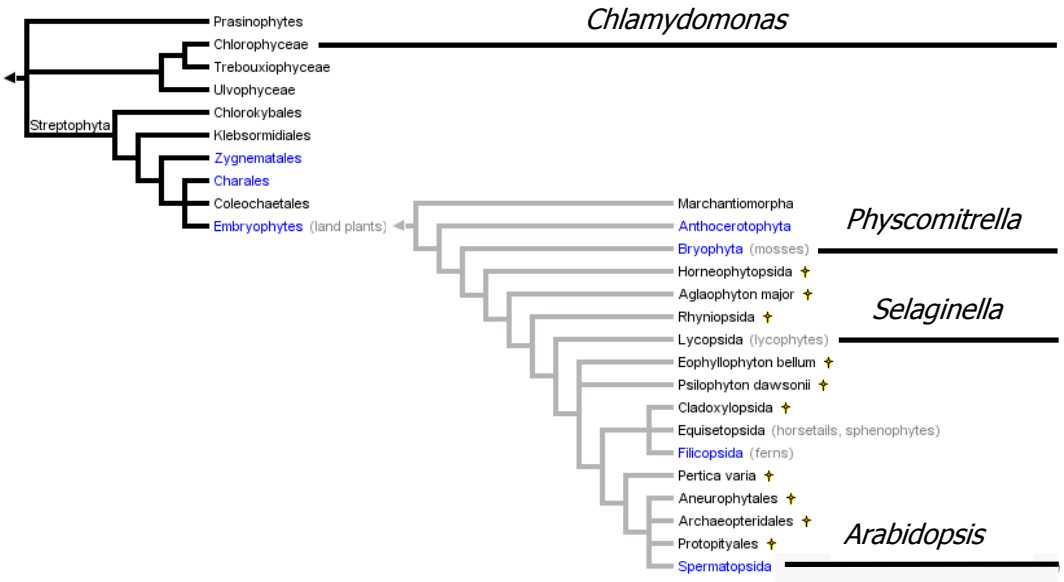

Fig. I1: According to „The Tree of Life"-project: http://www.tolweb.org/tree/. *Chlamydomonas* is a single celled green alga belonging to the chlorophytes. The moss *Physcomitrella*, the spikemoss *Selaginella*, and the seed plant *Arabidopsis* are streptophytes.

In the present study, plants representing different stages during plant evolution were investigated. The higher plant *Arabidopsis thaliana*, the lycophyte *Selaginella moellendorffii*, the moss *Physcomitrella patens*, and the green alga *Chlamydomonas reinhardtii* were included. Their genomes had been sequenced and were accessible online for bioinformatic analyses.

1.2 *Chlamydomonas reinhardtii*

Chlamydomonas reinhardtii is a single celled chlorophytic alga species (Fig. I2, Harris *et al.* 2001). The natural habitat of these algae can be stagnant or fresh water, where they are less exposed to high light conditions (Stauber *et al.* 2009, van den Hoek 1978, Sze 1986). Besides this, they are also capable of living on damp soil (Merchant *et al.* 2007, van den Hoek 1978, Sze 1986). *Chlamydomonas* moves and mates within its aqueous environment with two anterior flagella (Fig. I2). Like other green algae, it has many mitochondria but only one single cup-shaped chloroplast comprising most of the cell and partially surrounding the nucleus (Fig. I2, Harris *et al.* 2001). During times, it became a well known model for scientific studies (Harris *et al.* 2001). The 121 Mbp *Chlamydomonas reinhardtii* genome sequence was published in 2007 by Merchant *et al.*. Comparative genome analyses revealed that the green alga encodes proteins with plant origin but also genes which are more similar to animal homologs.

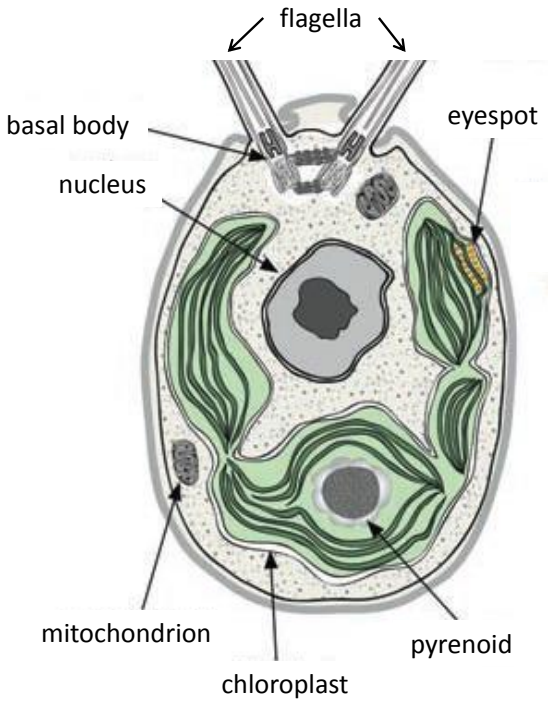

Fig. I2: Schematic *Chlamydomonas reinhardtii* cell. Figure was adapted from Merchant *et al.* 2007.

1.3 *Physcomitrella patens*

Bryophytes comprise mosses, hornworts, and liverworts (Frahm 2001, Rensing *et al* 2008) and belong to the first plants colonizing land approximately 450 million years ago (Rensing *et al.* 2008). *Physcomitrella patens*, a moss, lives in open and disturbed habitats (Fig. I3, Schaefer and Zrÿd, 2001). It usually colonizes damp soils or areas fallen dry at low water, *e. g.* shores of lakes and riversides (Frahm and Frey 2004). In these environments, *Physcomitrella* can be exposed to varying light conditions (Wolf *et al.* 2010).

Mosses in general, are still dependent on water for reproduction and due to their morphology being less adapted to water loss than higher plants. Nevertheless, *Physcomitrella* shows a high capability to survive times of drought (Frank *et al.* 2005). Taking three months, its life cycle is dominated by a haploid gametophyte comprising two developmental stages: (i) a filamentous cell network, the protonema, and (ii) a cauloid with various phylloids, the gametophore (Cove and Knight 1993, Frahm 2001, Schaefer and Zrÿd 2001). Filamentous rhizoids and reproductive organs are situated on the gametophore (Reski 1998b, Schaefer and Zrÿd 2001). The monoecious moss carries both sex organs on one single gametophore and is capable of self-fertilization (Cove and Knight 1993, Schaefer and Zrÿd 2001). The genome sequence of the model plant *Physcomitrella patens* was published in 2008 (Rensing *et al.* 2008) and revealed to include 480 Mbp.

Fig. I3: *Physcomitrella patens*. Picture from http://genome.jgi-psf.org/Phypa1_1/ Phypa1_1.home.html.

1.4 *Selaginella moellendorffii*

Belonging to lycophytes, Selaginellales emerged approximately 300 - 400 million years ago (Wang *et al.* 2005, Banks 2009). The natural habitat of the *Selaginella* species ranges from wet and tropical forests to deserts as well as alpine areas (Little *et al.* 2006). Its members are distributed nearly worldwide (Tryon and Lugardon 1990)

Selaginella moellendorffii became a model plant for scientific purposes (Fig. I4). Wang *et al.* (2005) constructed a bacterial artificial chromosome library from *Selaginella moellendorffii*. In 2007, the genome was sequenced by the Department of Energy Joint Genome Institute (JGI) and its sequence released to be available online. This assembly of the *Selaginella* genome was published by Banks *et al.* (2011). This spikemoss has the smallest genome among all sequenced species comprising only approximately 106 Mbp (Wang *et al.* 2005).

Fig. I4: *Selaginella moellendorffii*, Picture from http://www.chromdb.org/org_specific.html?o=SELMO.

1.5 *Arabidopsis thaliana*

The higher plant *Arabidopsis thaliana* is an angiosperm and belongs to the family of Brassicaceae (Fig. I5, Meinke *et al.* 1998, Reski 1998a). The species is widely distributed over North America, Asia, and Europe (Hoffmann 2002). Being found in waste lands, rotation crop fields, and grass lands, its natural habitats are open and disturbed (Häflinger and Wolf 1988, Polunin 1971).

Arabidopsis is capable of self-fertilization and its seeds develop in siliques (Meinke *et al.* 1998). The genome of this well known model plant was published in 2000 by the *Arabidopsis* Genome Initiative. Bennet *et al.* (2003) estimated the *Arabidopsis* genome size to be approximately 157 Mbp.

Fig. I5: *Arabidopsis thaliana* var. Col-0.

1.6 Reactive oxygen species

Since the evolution of oxygenic photosynthesis all living organisms have to deal with the formation of reactive oxygen species (ROS). Stressful environmental conditions, no matter whether they are biotic or abiotic, cause an increase in these toxic compounds (Jahnke *et al.* 1991, Okuda *et al.* 1991, Karpinski *et al.* 1997). They are capable to damage diverse cellular components by oxidizing lipids, proteins, carbohydrates, and nucleic acids (Elstner 1990, Baier and Dietz 1999). Beside this deleterious role, ROS are also known as important signaling molecules. Upon accumulation they induce cascades involved in developmental processes, cell death, and the production of low molecular weight antioxidants as well as antioxidative defense enzymes (Leung and Giraudat 1998, Desikan *et al.* 2001, Pfannschmidt *et al.* 2003).

Between 1951 and 1952, Mehler discovered and studied the photoreduction of oxygen to hydrogen peroxide in illuminated chloroplasts (Mehler 1951, Mehler *et al.* 1952). Even under comfortable conditions, ROS are produced as by-products during photosynthesis (Asada 1999, Baier and Dietz 1999). Excess electrons are transferred from photosystem I to oxygen and, as a result, superoxide anions are generated (Mehler 1951, Mehler *et al.* 1952, Asada 1974). These compounds are highly reactive and toxic to various molecules, *e. g.* by oxidation of metal components within enzymes, thereby influencing their functions or causing their inactivation (Flint *et al.* 1993). Additonally, they can lead to the formation of other ROS, such as hydroxyl radicals during the Haber-Weiss and Fenton reactions (Fenton 1894, Haber and Weiss 1932). At the thylakoid membrane, superoxide dismutases (SODs) are localized to rapidly scavenge superoxide anions and convert them into hydrogen peroxide (Ogawa *et al.* 1995). The latter is less toxic than its precursor anions but still capable of reacting with diverse biomolecules. Hydrogen peroxide can react with transitional metals, such as copper or iron, to create hydroxyl radicals (Fenton 1894, Haber and Weiss 1932). These are very reactive oxygen species and no specific enzyme is known, which is capable to detoxify them. Polyols represent effective scavenges of hydroxyl radicals (Shen *et al.* 1997). In addition, another highly toxic ROS, singlet oxygen, can be produced by the reaction of chlorophyll molecules in the triplet state with oxygen in the ground state (Gorman and Rodgers 1992, Krieger-Lizskay 2005). Like for hydroxyl radicals, no enzymatic scavenger is known. Tocopherol and β-carotene serve as main quenchers directly in membranes (Telfer *et al.* 1994, Neely *et al.* 1988, Trebst 2003).

Taken together, the most prominent ROS within a plant cell are superoxide anions, hydrogen peroxide, hydroxyl radicals, and singlet oxygen (Elstner 1990). The main sources of these toxic compounds within a plant cell are chloroplasts (Asada 1974), mitochondria (Turrens 1997), and peroxisomes (Sandalio *et al.* 1987, López-Huertas *et al.* 1999). Additionally, ROS are produced within the cytosol, apoplast, and plasma membrane (Kanematsu and Asada 1990, Blokhina *et al.* 2001).

1.7 Antioxidative defense systems

To protect themselves from oxidative damage, plants evolved a highly sophisticated antioxidant defense (Asada 1999). Beside their toxic impact, ROS also have important roles as signaling molecules (Desikan *et al.* 2001, Halliwell 2006). Thus, low molecular weight antioxidants and antioxidant enzymes facilitate the maintenance of a balance between ROS accumulation and scavenging. In general, Noctor and Foyer (1998) considered an antioxidant to be "any compound capable of quenching AOS without itself undergoing conversion to a destructive radical" and antioxidant enzymes "as those that either catalyze such reactions or are involved in the direct processing of AOS" (AOS – Active Oxygen Species, synonym for ROS).

1.7.1 Non-enzymatic antioxidative defense systems: Low molecular weight antioxidants

1.7.1.1 Ascorbate

Ascorbate is ubiquitously present within the plant and animal kingdoms. To date, the only known exceptions are guinea pigs and primates, including their descendants, which are not able to synthesize this low molecular weight antioxidant (Burns 1957, Noctor and Foyer 1998, Wheeler *et al.* 1998). In plant cells, ascorbate represents one of the most prominent and important scavengers of ROS (Fig. I6, Koch 1968, Nishikimi 1975, Larson 1988, Foyer and Lelandais 1996). It can be used as a substrate by diverse peroxidases, such as ascorbate peroxidases (Fig. I8, Groden and Beck 1979, Asada 1992). Additionally, the low molecular weight antioxidant is involved in the regeneration of tocopherol, another antioxidant molecule (Mukai *et al.* 1991).

In addition, ascorbate plays an important role in the violaxanthin cycle (Hager 1969). In excess light conditions, violaxanthin is rapidly converted to zeaxanthin under the expense of

ascorbate (Hager 1969, Demming *et al.* 1987, Eskling *et al.* 1997). Zeaxanthin can quench triplet state chlorophylls. The excess excitation energy is thereby dissipated as heat (Demming *et al.* 1987, Eskling *et al.* 1997).

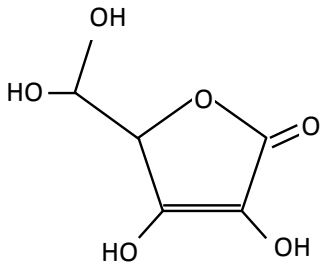

Fig. I6: Chemical structure of ascorbate

The oxidized form of ascorbate, monodehydroascorbate, can be reduced enzymatically under the expense of reduction equivalents by monodehydroascorbate reductases (Fig. I8, Hossain *et al.* 1984):

2 monodehydroascorbate + NAD(P)H → 2 ascorbate + $NAD(P)^+$

Monodehydroascorbate, can also spontaneously disproportionate to ascorbate and dehydroascorbate (Fig. I8, Bielski *et al.* 1981):

monodehydroascorbate + monodehydroascorbate → ascorbate + dehydroascorbate

Dehydroascorbate, in turn, is reduced to ascorbate by dehydroascorbate reductases, which use reduced glutathione ($glutathione^{red}$) as electron donor (Fig. I8, Crook and Hopkins 1938, Crook and Morgan 1943, Foyer and Halliwell 1977). As a result, two glutathione molecules are oxidized and form a dimer ($glutathione^{ox}$):

dehydroascorbate + 2 $glutathione^{red}$ → ascorbate + $glutathione^{ox}$

Under physiological conditions, ascorbate is highly abundant and accumulates to millimolar concentrations (Foyer and Lelandais 1996). The low molecular weight antioxidant is synthesized from glucose-6-P with the last biosynthetic step being localized in mitochondria (Wheeler *et al.* 1998). Ascorbate represents not only one of the most essential antioxidants within plant cells but has also a great influence on cell division and a signaling role in the

expressional control of defense genes (Liso *et al.* 1988, Kiddle *et al.* 2003, Pastori *et al.* 2003). The fact that its regulatory impact also includes the phytohormone abscisic acid (ABA) even stresses its importance in the plant metabolism (Pastori *et al.* 2003).

1.7.1.2 Glutathione

Another highly abundant and essential low molecular weight antioxidant is glutathione (Foyer and Halliwell 1976, Noctor and Foyer 1998). Like ascorbate, γ-glutamylcysteinylglycine can accumulate to millimolar concentrations (Fig. I7, Foyer and Halliwell 1976). The thiol is synthesized in two steps catalyzed by γ-glutamylcysteine synthetase (GSH1) and glutathione synthetase (GSH2) (Rennenberg 1982, Law and Halliwell 1986). The previous resides in chloroplasts while the latter is localized either to the plastids or the cytosol (Wachter *et al.* 2005). Glutathione is one of the most important scavengers of ROS, being capable to detoxify singlet oxygen, superoxide anions, hydroxyl radicals, and hydrogen peroxide (Foyer and Halliwell 1976, Larson 1988). Apart from this, the antioxidant is part of the ascorbate regeneration machinery (Mapson 1958, Foyer and Halliwell 1976, Asada 1999).

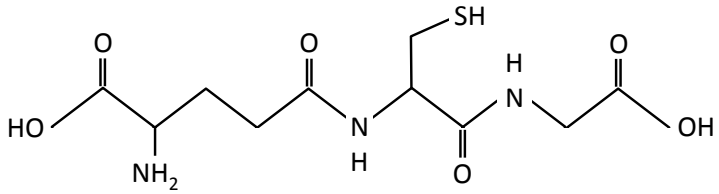

Fig. I7: Chemical structure of glutathione.

Upon oxidation, two glutathione molecules (glutathione^{red}) form disulphide bridges and, thereby, generate dimers (glutathione^{ox}). The compound can be reduced by glutathione reductases under the consumption of reduction equivalents (Fig. I8, Foyer and Halliwell 1976, Asada 1999):

glutathione^{ox} + 2 NADPH → 2 NADP+ + 2 glutathione^{red}

In addition, this low molecular weight antioxidant is known to have an essential signaling role influencing the expression of various genes involved in abiotic and biotic stress responses (Wingate *et al.* 1988, Wingsle and Karpinsky 1996, Ball *et al.* 2004).

1.7.1.3 Other low molecular weight antioxidants

The most abundant low molecular weight antioxidants in plant cells are ascorbate and glutathione (Foyer and Halliwell 1976, Foyer and Lelandais 1996). Together with their oxidized forms, they are important for balancing the redox status of plant cells. In addition to these molecules, other antioxidants serve to scavenge ROS. Being capable of directly scavenging singlet oxygen, carotenoids can also quench triplet state chlorophylls, thereby preventing the formation of singlet oxygen (Cogdell 1985, Siefermann-Harms 1987). A common example of carotenoids is zeaxanthin, mentioned before as a part of the violaxanthin cycle (Hager 1969, Eskling *et al.* 1997).

In addition, tocopherols, such as flavonoids, tannins and precursors of lignin, are hydrophobic antioxidants, efficiently detoxifying ROS at and within membranes (Fryer 1992, Wang and Quinn 2000, Trebst *et al.* 2003).

1.7.2 Enzymatic antioxidative defense systems

In 1772, Priestley published the generation of "air" by plants. Since his discovery, chloroplasts have been identified as the site of oxygen evolution within plant cells (Asada *et al.* 1974, Navari-Izzo *et al.* 1999). At photosystem II, which is located in thylakoids, water is split (Fig. I8, Hill 1939). Mehler (1951) found that the resulting oxygen is photoreduced to hydrogen peroxide and dedicated oxygen to be a Hill oxidant. Afterwards, during several years of research, photosystem I was suggested to be the site of oxygen photoreduction (Fig. I8, Asada *et al.* 1974). Excess electrons within the photosynthetic electron transport chain (PET) are transferred to oxygen, generating superoxide anions (O_2^-, Fig. I8, Asada *et al.* 1974). These highly reactive compounds are rapidly converted to hydrogen peroxide (H_2O_2). The reaction is catalyzed by superoxide dismutases (SODs) (Fig. I8, McCord and Fridovich 1969, Sawada *et al.* 1971):

$$O_2^- + O_2^- + 2\ H^+ \rightarrow H_2O_2 + O_2$$

Being ubiquitously present in all aerobic organisms, the enzymes are 10,000 times more effective than the spontaneous dismutation of superoxide anions by interaction with low molecular weight antioxidants (Asada 1999).

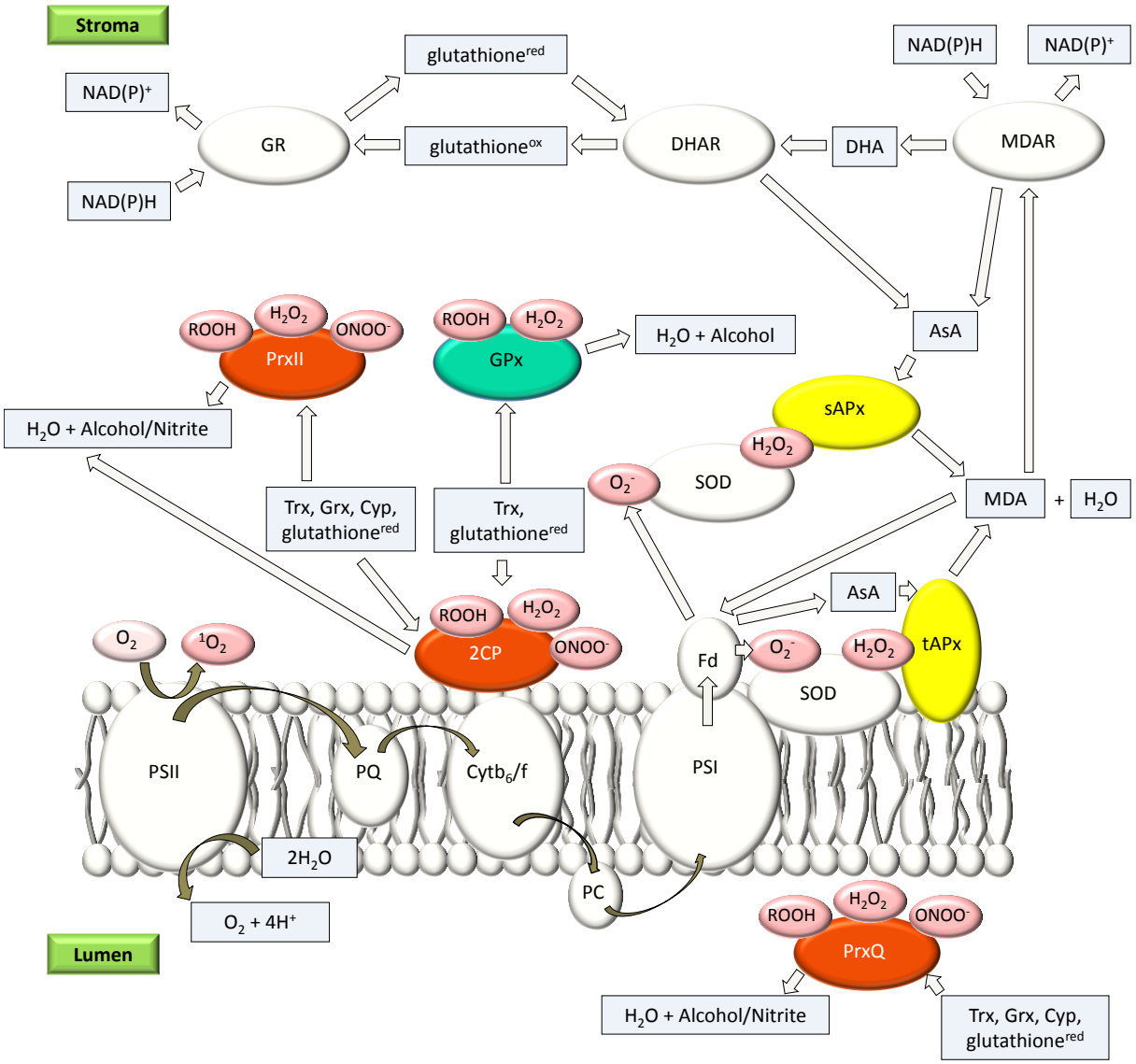

Fig. I8: Schematic light reaction of photosynthesis and the *Arabidopsis thaliana* chloroplast enzymatic defense against ROS in stroma and lumen (figure was adapted from Asada 1999 and modified according to Dietz *et al.* 2006 and Rodriguez Milla *et al.* 2003). ROS: $^1O_2$ – singlet oxygen, ROOH – organic hydroperoxides, $ONOO^-$ - peroxinitrites, O_2^- - superoxide anions, H_2O_2 – hydrogen peroxide. Enzymes and protein complexes: PSII – photosystem I, PQ – plastoquinone, $Cytb_6/f$ – cytochrome b_6/f complex, PC – plastocyanine, PSI – photosystem I, Fd – ferredoxin, SOD – superoxide dismutase, tAPx – thylakoid-bound ascorbate peroxidase, sAPx – stromal ascorbate peroxidase, MDAR – monodehydroascorbate reductase, DHAR – dehydroascorbate reductase, GR – glutathione reductase, 2CP – 2-Cys peroxiredoxin, PrxQ – peroxiredoxin Q, PrxII – peroxiredoxin type II, GPx – glutathione peroxidase, Trx – thioredoxin, Grx – glutaredoxin, Cyp - cyclophilin. Antioxidants and other molecules: AsA – ascorbate, MDA – monodehydroascorbate, H_2O – water, DHA – dehydroascorbate, NAD(P)H – reduced nicotinamide adenine dinucleotide (phosphate), $NAD(P)^+$ – oxidized nicotinamide adenine dinucleotide (phosphate), $glutathione^{red}$ – reduced glutathione, $glutathione^{ox}$ – oxidized glutathione.

Within chloroplasts, SODs are capable of scavenging superoxide anions at the site of production since they are attached to thylakoids (Fig. I8, Ogawa *et al.* 1995). Other, soluble isoforms, convert radicals which escaped thylakoids and diffused into the stroma (Fig. I8, Asada *et al.* 1973).

Being less reactive than superoxide anions, hydrogen peroxide is still capable of oxidizing lipids, proteins, and DNA (Elstner 1990, Baier and Dietz 1999). Several peroxidases are at service to scavenge and detoxify these ROS. Hydrogen peroxide is generated via superoxide anions from the split of water. Since peroxidases catalyze the conversion of hydrogen peroxide back to water, these proteins represent key enzymes of the chloroplast antioxidant defense (Asada 1999, Dietz *et al.* 2006). Ascorbate peroxidases (APxs) detoxify ROS under the expense of ascorbate (Fig. I8). To regenerate their substrate glutathione is consumed (Fig. I8). Together with the regeneration of ascorbate as well as glutathione, APxs comprise the ascorbate-dependent water-water-cycle (WWC) (Asada 1999). These enzymes are specific for hydrogen peroxide while peroxiredoxins (Prxs) and glutathione peroxidases (GPxs) are capable of detoxifying also other hydroperoxides (Fig. I8, Eshdat *et al.* 1997, Raven 2003, Baier and Dietz 1996, Rouhier and Jacquot 2005).

1.7.2.1 Ascorbate peroxidases

Ascorbate peroxidases (APxs) are members of the heme peroxidase family (Asada 1999). This group is divided into three classes of enzymes: Class I comprises peroxidases in bacteria, fungi, green algae, and higher plants. It includes ascorbate peroxidases from green algae, higher plants, and mammals as well as cytochrome c peroxidases, and catalase-peroxidases (Welinder 1992, Zámocky *et al.* 2000). The different isoforms are thought to have emerged due to gene duplication of an ancestral hydroperoxidase (Asada 1999, Zamocky *et al.* 2000). Sharing a prokaryotic origin, they are found in all three domains of life: archaea, bacteria, and eukarya (Zamocky *et al.* 2000). Class II covers extracellular fungal peroxidases and class III includes secretory plant peroxidases (Welinder 1992).

Commonly, higher plants have two chloroplast ascorbate peroxidase isoforms: soluble stromal and thylakoid-bound APxs (Fig. I8, Ishikawa *et al.* 1996, Jespersen *et al.* 1997, Mano *et al.* 1997, Yoshimura *et al.* 1999, Teixeira *et al.* 2004). They can be encoded by different genes or one single gene codes for both isoforms. The latter is alternatively spliced upon induction of expression (Ishikawa *et al.* 1996, Jespersen *et al.* 1997). The enzymes are also present in other subcellular compartments, such as cytosol, peroxisomes and mitochondria

(Chew *et al.* 2003, Davletova *et al* 2005, Teixeira *et al.* 2006). APxs catalyze the conversion of hydrogen peroxide to water under the expense of two ascorbate molecules (Fig. I8, Yamazaki and Piette 1961, Nakano and Asada 1981):

H_2O_2 + 2 ascorbate → 2 H_2O + 2 monodehydroascorbate

ROS, which were failed to be scavenged at the thylakoid by the thylakoid-bound APx isoform, enter the stroma, where they are detoxified by a soluble ascorbate peroxidase. Subsequent to hydrogen peroxide reduction, APxs are regenerated. Two ascorbate molecules are oxidized to convert the two-electron oxidized APx back to its ferric resting state (Asada 1999). The two intermediates during catalysis and regeneration are called compounds I and II (Yamazaki and Piette 1961, Asada 1999):

APx-Fe(III)-R + H_2O_2 → APx-Fe(IV)=O-R^+ + H_2O

Formation of compound I

APx-Fe(IV)=O-R^+ + ascorbate → APx-Fe(IV)=O-R + monodehydroascorbate

Formation of compound II

APx-Fe(IV)=O-R + ascorbate → APx-Fe(III)-R + monodehydroascorbate + H_2O

Regeneration of APx to its functional form

The rest R represents either porphyrin or a conserved tryptophan residue (Asada 1999).

In comparison to cytosolic isoforms, chloroplast APxs are more specific for ascorbate and susceptible to hydrogen peroxide (Jespersen *et al.* 1997, Wada *et al.* 2003). In an ascorbate depleted environment, the plastid enzymes are rapidly inactivated by this ROS (Miyake and Asada 1996, Kitajima 2008). Kitajima (2008) suggested that this sensitivity evolved as a sensor for hydrogen peroxide accumulation. Another possibility may be that it represents a defect, being inserted during plant evolution (Kitajima 2008). Maybe due to the susceptibility to ROS mediated inactivation, chloroplast APxs represent the primary targets of photooxidative stress (Mano *et al.* 2001, Ishikawa and Shigeoka 2008).

1.7.2.2 Peroxiredoxins

Peroxiredoxins (Prxs) are non-heme peroxidases which are ubiquitously present among the kingdoms of life (Baier and Dietz 1996, Verdoucq *et al.* 1999, Horling *et al.* 2001). Within plants, they are highly abundant in green tissues and can be found in all cellular compartments (Baier and Dietz 1996, Horling *et al.* 2003). These enzymes scavenge hydrogen peroxide as well as other hydroperoxides and convert them into water and their corresponding alcohol (Fig. I9, Baier and Dietz 1997, Horling *et al* 2003, König *et al.* 2003).

The peroxiredoxin family comprises three classes of enzymes: (i) typical peroxiredoxins (2-Cys peroxiredoxins, 2CPs), (ii) atypical peroxiredoxins (peroxiredoxins Q, PrxQs, as well as peroxiredoxins type II, PrxIIs), and 1-Cys peroxiredoxins (1CPs) (Verdoucq *et al.* 1999, Horling *et al.* 2002). The latter contain only one conserved active site cysteine, while the other peroxiredoxin classes comprise two residues, the peroxidatic and resolving cysteines (Fig. I9, Baier and Dietz 1996, Verdoucq *et al.* 1999, Horling *et al.* 2002). During the first catalysis step, the peroxidatic residue is oxidized to a cysteine sulfenic acid while in the second step stable disulfide bridges are created (Fig. I9, Chae *et al.* 1994, Baier and Dietz 1999). 2CPs are functional as homodimers forming intermolecular disulfide bonds (Fig. I9). They can be also found in a decameric form, which is attached to thylakoid membranes (König *et al.* 2002). Atypical peroxiredoxins, in contrast, detoxify hydroperoxides as monomers generating intramolecular disulfide bridges (Fig. I9, Kong *et al.* 2000, Seo *et al.* 2000). The oxidized enzymes can be regenerated under expense of thioredoxins, glutaredoxins, cyclophilins, or glutathione (Fig.s I8 and I9, Kong *et al.* 2000, Seo *et al.* 2000, König *et al.* 2002, Rouhier *et al.* 2001, Laxa *et al.* 2007). Both, thioredoxins and glutaredoxins, represent protein disulfide oxidoreductases (Meyer *et al.* 1999).

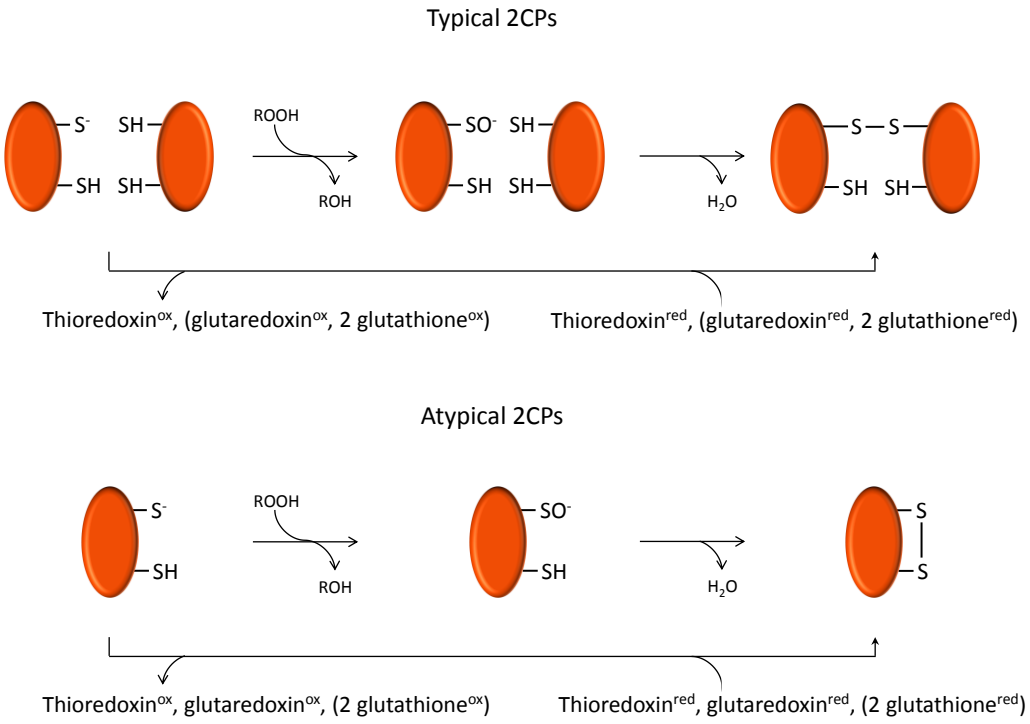

Fig. I9: Catalytic cycle of peroxiredoxins according to Dietz (2011). Upper part: Catalytic cycle of typical peroxiredoxins (2CPs). Lower part: Catalytic cycle of atypical peroxiredoxins (PrxQs, PrxIIs). ROOH - organic hydroperoxide, H_2O - water. Peroxidatic and resolve cysteine residues are indicated by their sulfate residues. During the catalytic cycle, first the peroxidatic cysteine is oxidized to sulfenic acid. A second oxidation step leads to formation of an intermolecular (typical 2CPs) or intramolecular (atypical 2CPs) disulfide bridge. Oxidized typical 2CPs are preferentially reduced by the thioredoxin system while glutaredoxins are additional effective regenerators of atypical peroxiredoxins.

1.7.2.3 Glutathione peroxidases

Glutathione peroxidases (GPxs) represent another class of peroxiredoxins (Rouhier and Jacquot 2005). Being present in animals as well as plants, they can be divided into selenocysteine and non-selenocysteine isoforms. All GPxs contain at least two conserved cysteine residues within their active site. In most animal isoforms, one of them is a selenocysteine while all known GPxs higher plants contain non-selenocysteines (Eshdat *et al.* 1997, Navrot *et al.* 2006). In contrast, being also a member of the plant kingdom, the green alga *Chlamydomonas reinhardtii* was found to encode both forms of GPxs (Fu *et al.* 2002, Novoselov *et al.* 2002, Dayer *et al.* 2008).

In general, glutathione peroxidases are capable of scavenging hydrogen peroxide and other hydroperoxides by using redox molecules or proteins, *e. g.* thioredoxins, as electron donors (Fig. I8, Eshdat *et al.* 1997, Tanaka *et al.* 2005, Navrot *et al.* 2006). In 1957, Mills published

these enzymes to protect haemoglobin from oxidative damage under the expense of glutathione:

$H_2O_2 + 2\ \text{glutathione}^{red} \rightarrow H_2O + \text{glutathione}^{ox}$

Although their active sites are different, GPxs and atypical Prxs have a similar catalytic cycle (Fig. I9, Tanaka *et al.* 2005, Navrot *et al.* 2006). First, the peroxidatic cysteine is oxidized to a sulfenic acid. The reaction cycle can stop at this step, but in general it continues with the second, resolving, cysteine attacking the sulfenic acid to form an intramolecular disulfide bridge (Fig. I9, Tanaka *et al.* 2005, Navrot *et al.* 2006).

1.8 Aim of the study

All key peroxidases of the chloroplast antioxidant defense are found in every kingdom of life. Being already present in cyanobacteria (Miyake *et al.* 1991, Stork *et al.* 2005, Margis *et al.* 2008), they most likely emerged in eukaryotic photosynthesizing organisms as a result of the cyanobacterial endosymbiont incorporation into the plant cell ancestor (Mereschkowsky 1905). During plant evolution, DNA was exchanged between the endosymbiont and nucleus. Nowadays, all chloroplast peroxidases are not encoded within the plastome anymore but the genes appeared in the nuclear genome (Jespersen *et al.* 1997, Horling *et al.* 2003, Mullineaux *et al.* 1998, Rodriguez Milla *et al.* 2003). However, chloroplasts are still the sites of oxygenic photosynthesis. As a consequence, ROS are produced and need to be rapidly detoxified. Therefore, the presence and detoxification function of these enzymes within chloroplasts is essential. Thus, after integration of the peroxidase genes, plants had to evolve a new transport machinery targeting the proteins into organelles. Additionally, they developed a fine-tuned expressional regulation to successfully adapt to environmental changes and hostile conditions.

The present study focuses on different types of chloroplast peroxidases: ascorbate peroxidases (APxs), peroxiredoxins (Prxs), and glutathione peroxidases (GPxs). All of these enzymes were conserved during evolution, stressing their importance for plants to survive stressful times (Baier and Dietz 1996, Zamocky *et al.* 2000, Margis *et al.* 2008). The higher plant *Arabidopsis thaliana* has two APxs, four Prx isoforms, and two GPxs, which are targeted to chloroplasts. It was hypothesized, that the composition of the organellar antioxidant defense might have changed during plant evolution. In addition, amino acid sequences may have accumulated substitutions with possible impacts on function and effectivity of the enzymes.

The model *Arabidopsis thaliana* was chosen as a reference plant to be compared to organisms representing more ancient times during evolution. The genomes of the spikemoss *Selaginella moellendorffii*, the moss *Physcomitrella patens*, and the green alga *Chlamydomonas reinhardtii* were screened for genes encoding chloroplast APxs, Prxs, and GPxs. Comparisons of the identified open reading frames (ORFs), cDNAs, and amino acid sequences led to conclusions on relation, origin, and possible changes in function and effectiveness. In addition, EST data were analyzed to hint at expression of the encoded peroxidases and their degrees of importance for the chloroplast antioxidant defense.

These bioinformatic analyses indicated the *Physcomitrella* thylakoid-bound ascorbate peroxidase (PptAPx) to have an atypical gene structure but to be very similar to its *Arabidopsis* homolog on amino acid as well as on protein secondary structure level. Further investigatory focus was set on this peroxidase. The studies included its regulation of transcription as well as transcript level besides the organellar targeting and function of PptAPx. Additionally, light was shed on parallels between higher plants and the moss *Physcomitrella patens*.

2 Material and Methods

2.1 Plant material and growth conditions

2.1.1 Cultivation of *Arabidopsis thaliana*

Arabidopsis thaliana (L.) Heynh. var. Col-0 seedlings were cultivated on plates containing sterile Murashige and Skoog medium (MS, Duchefa, Haarlam, The Netherlands), pH 5.7 and supplemented with 1 % (w/v) sucrose and 0.5 % (w/v) Phytagel. Prior to transfer onto plates, the seeds were surface sterilized by incubating them in 80 % (v/v) ethanol followed by a washing step with sterile water and a further sterilization by applying 30 % (v/v) Glorix for 10 min. After three washing steps with sterile water, seeds were transferred onto solid MS medium and cultivated in climate-controlled chambers (CU-41L4X, Percival Scientific Inc. Perry, USA) at a day/night temperature of 20 °C / 18 °C and 120 µmol quanta m^{-2} s^{-1} light with a 10 h light / 14 h dark photoperiod. Stress treatments and transfections were performed with ten day old seedlings.

For reverse transcriptase PCRs, six week old *Arabidopsis* plants were used. They had been cultivated on soil [Terreau Professionell Gepac Einheitserde Typ T (Einheitserde, Germany), Perligran G (Knauf Perlite, Germany) (1:1:1)] in a growth chamber at 20 °C and illuminated with 80-100 µmol quanta m^{-2} s^{-1} for 10 h per day.

2.1.1 Cultivation of *Selaginella moellendorffii*

Selaginella moellendorffii plants were kindly provided by the Botanical Garden Berlin and used for transfection experiments immediately after delivery. For reverse transcriptase PCRs, *Selaginella moellendorffii* sporophytes were grown in a green house on soil and 14 h per day illumination with 50 µmol quanta m^{-2} s^{-1}.

2.1.2 Cultivation of *Physcomitrella patens*

Physcomitrella patens patens (Hedw.) Bruch and Schimp var. Gransden gametophytes were ordered via http://www.cosmoss.org (Freiburg, Germany). They were cultivated on plates containing sterile modified Knop medium according to Bopp and Brandes (1964) (25 g/L KH_2PO_4, 25 g/L KCl, 25 g/L $MgSO_4$*7 H_2O, 100 g/L $Ca(NO_3)_2$, 12.5 mg $FeSO_4$*7 H_2O, pH 5.8 was adjusted with KOH and HCl) supplemented with 0.5 % (w/v) Phytagel. After

propagation by dividing gametophytes under sterile conditions, they were transferred onto solid medium and further cultivated in climate-controlled chambers (CU-41L4X, Percival Scientific Inc. Perry, USA) at a day/night temperature of 20 °C / 18 °C and 55 µmol quanta m^{-2} s^{-1} light a with a 10 h light / 14 h dark photoperiod.

Prior to stress treatments, *Physcomitrella* gametophytes were transferred to fresh medium and cultivated for ten days. Gametophytes which were grown on sterile plates containing modified Knop medium at 70-80 µE m^{-2} s^{-1} and 14 h light/10 h dark were used for reverse transcriptase PCRs.

2.1.3 Cultivation of *Chlamydomonas reinhardtii*

Chlamydomonas reinhardtii Dangeard strain CC125 *Chlamydomonas* algae were kindly provided by Prof. Dr. Olaf Kruse (University of Bielefeld, Germany). The algae were grown either at 12-20 µmol quanta m^{-2} s^{-1} and a 12 h light / 12 h dark photoperiod under sterile conditions in liquid TAP medium (Gorman and Levine, 1965) (25 ml/L 2 x Filner's Beijernicks solution, 1 mM K_3PO_4, 5 ml/L trace mineral solution, 2.42 g/L Tris-base, 0.1 % (v/v) glacial acetic acid, pH 7.2) or at 80-100 µmol quanta m^{-2} s^{-1} and 12 h light / 12 h dark photoperiod on plates containing sterile TAP medium supplemented with 1 % (w/v) agar-agar (Gorman and Levine, 1965).

2.1.4 Cultivation of *Nicotiana benthamiana*

Nicotiana benthamiana were available at the Freie Universität Berlin. Seeds were sown on Floraton1 soil (Floragard, Osternburg/Tweelbäke, Germany) by the gardeners at the FU Berlin. After approximately one week of growth at 250-350 µmol quanta m^{-2} s^{-1} in a 14 h light/10 h dark photoperiod, the seedlings were transferred into pots containing Floraton1 soil (one seedling per pot). Further cultivation took place under the standard conditions described above. During the light phase the temperature was 22-24 °C and 18 °C during night.

2.2 Stress treatments

2.2.1 Exposure to varying light intensities and chilling temperatures

Physcomitrella gametophytes, which had been cultivated on fresh Knop medium for ten days, were exposed to diverse light intensities. These intensities included darkness, 55 µmol quanta m^{-2} s^{-1}, and 1000-1100 µmol quanta m^{-2} s^{-1}. Since the light source for 1000-1100 µmol quanta m^{-2} s^{-1} produced heat, the experiment was performed at 4 °C reducing the temperature at the plant surface to approximately 20 °C. Nevertheless, temperature controls were performed by transferring gametophytes to 4 °C and 55 µmol quanta m^{-2} s^{-1}. These plants represented not only the controls but also *Physcomitrella* treated with chilling stress. Light controls were cultivated in standard growth conditions. Samples were collected between 0 h and 6 h after transfer into the different environmental conditions. The experiments started with the standard onset of light in the Percivals (CU-41L4X, Percival Scientific Inc. Perry, USA). One plate with three gametophytes was harvested per light intensity and time point. Subsequently, the plants were frozen in liquid nitrogen and transferred to -80 °C until RNA extraction.

2.2.2 Application of ascorbate, dehydroascorbate, reduced and oxidized glutathione

For redox experiments, *Physcomitrella* gametophytes were cultivated on fresh Knop medium for ten days before treatment. Ascorbate, dehydroascorbate, reduced and oxidized glutathione were applied to the plants in different concentrations (20 mM ascorbate, 20 mM and 50 mM dehydroascorbate, 20 mM and 50 mM reduced glutathione, 10 mM oxidized glutathione). All compounds were dissolved in autoclaved tap water. *Physcomitrella* gametophytes were soaked with freshly prepared solutions and subsequently incubated at standard growth conditions for 4 h. Plants treated with pure autoclaved tap water served as control. Three gametophytes per compound and concentration were harvested. The samples were immediately frozen in liquid nitrogen and transferred to -80 °C until RNA extraction.

2.2.3 Application of abscisic acid

A 1 mM stock of abscisic acid (ABA) was prepared in pure ethanol. To treat *Physcomitrella* gametophytes, a 10 µM dilution with autoclaved tap water was used. After ten days of cultivation on fresh Knop medium, *Physcomitrella* gametophytes were soaked in the 10 µM ABA solution. Control plants, treated with pure autoclaved tap water were included in the

experiment. After 1 h of incubation at standard growth conditions, three treated and three control gametophytes were harvested. The samples were frozen in liquid nitrogen and stored at -80 °C until RNA isolation.

2.2.4 Treatment with methylviologen

Physcomitrella gametophytes or *Arabidopsis* seedlings were soaked with 300 µl or 100 µl of 0 µM, 25 µM, or 2 mM methylviologen in autoclaved tap water supplemented with 0.1 % (v/v) Tween-20, respectively. For each concentration, a separate plate with either ten *Arabidopsis* seedlings or three *Physcomitrella* gametophytes was used. Following application of the solutions either by pipetting or by spraying, the plants were transferred to standard growth conditions and measurements of the photosynthetic yield took place between 0 h and 6 h of treatment starting one hour after the onset of light.

2.3 Isolation of DNA from plant material

2.3.1 Isolation of DNA from *Arabidopsis thaliana*

One *Arabidopsis* seedling or 1-10 mg of leaf material were homogenized in 200 µl REB buffer (50 mM Tris-HCl pH 8.0, 25 mM EDTA, 250 mM NaCl, 0.5 % (w/v) SDS) with a plastic micropistill. The homogenate was extracted with 200 µl phenol / chloroform / isoamylalcohol (25:24:1). After centrifugation at 16,000 rpm and room temperature (Centrifuge 5424, Eppendorf, Hamburg, Germany) for 3 min, the "upper" water phase was transferred to 200 µl isopropanol and DNA precipitation was performed for minimum 10 min at -20 °C. Following centrifugation at 16,000 rpm and room temperature for 15 min, supernatants were discarded and the DNA pellet was suspended in 50-100 µl deionized autoclaved water. All DNA samples were either used immediately or transferred to -20 °C for further storage.

2.3.2 Isolation of DNA from *Selaginella moellendorffii* and *Physcomitrella patens*

10-100 mg *Physcomitrella* gametophyte material were homogenized in 200 µl cetyl trimethyl ammonium bromide (CTAB) buffer (100 mM Tris-HCl pH 8, 1.4 M NaCl, 20 mM EDTA, 2 % (w/v) CTAB) with a plastic micropistill. After homogenization, additional 800 µl CTAB buffer were added. The same amount of *Selaginella* phylloids was homogenized in liquid nitrogen and 1 ml CTAB buffer was added prior to thawing. The suspension was incubated at 60 °C for 30 min under continuous shaking. Subsequently, 1 ml chloroform was added. For phase separation, the mixture was centrifuged at 13,000 rpm and room temperature for 10 min. Supernatants were mixed with 1/10 volume 3 M sodium acetate pH 5.2 and 0.8 x volume isopropanol and incubated for minimum 10 min at room temperature to precipitate DNA. Following sedimentation of the DNA at 13,000 rpm and room temperature for 5 min, the supernatants were discarded. The pellets were first dried at room temperature, and then re-dissolved over night in 50 µl deionized autoclaved water. All DNA samples were either used immediately or transferred to -20 °C for further storage.

2.3.3 Isolation of DNA from *Chlamydomonas reinhardtii*

Chlamydomonas algae were grown for 3-5 days in 100 ml liquid TAP medium (see chapter 2.1.3) and harvested by centrifugation at 10,000 x g and room temperature for 10 min. After discarding the supernatants, the pellets were frozen in liquid nitrogen and subsequently transferred to 50-60 °C. After repeating this disruption step for three times, the DNA was isolated with the DNeasy Plant Mini kit (Qiagen, Hilden, Germany) according to manufacturer's instructions.

2.4 Polymerase chain reactions (PCRs)

2.4.1 Primer design

Primers spanning 19-22 bp were manually designed to have a melting temperature (T_m) of approximately 60 °C and minimal probabilities for primer-dimer formation and self-ligation. Oligonucleotides used for sequencing constructs annealed 100-200 bp up- or downstream of the inserted DNA to ensure a precise result. To amplify specific promoters, primers were designed to span the genomic DNA region directly upstream of the start-ATGs (approximately 1500-2000 bp). Upstream primers were designed as described above while the

downstream primer spanned the first 19-21 bp upstream of the respective start-ATG, irrespective of possible self-ligation. For amplification of the ORF cDNAs, the primers were located at the start-ATGs and the stop-codons. The only exception was SmtAPx, for which its 3'- region encoding the transmembrane helix was excluded.

Primers used for qRT-PCRs were designed as described above. They were located close to the 3'terminus of the respective cDNA. The PptAPx qRT-PCR primers amplified a 134 bp region of the second exon. The whole PptAPx ORF comprises 1454 bp and is interrupted by a 131 bp intron. The first exon is 754 bp long. The PptAPx_Q_S2 primer was located at nucleotide 1148 within the complete ORF while PptAPx_Q_A2 positioned at nucleotide 1281. Primers to amplify a region of the actin1 gene in *Physcomitrella* (PpAct1), had been published by Wang *et al.* 2008 and were also used in the presented study.

All primers were obtained from Sigma-Aldrich Chemie GmbH (Steinheim, Germany) and are listed in Table M1. Specificity of the primers used for qRT-PCRs was evaluated in two ways: (i) by performing saturating RT-PCRs (40 cycles). If one single product of desired length had been amplified within 40 reaction cycles, the primers were applied in qRT-PCRs. (ii) Each primer pair was analyzed during quantitative reactions by generating melting curves with the CFX96 thermocycler (BioRAD, Munich, Germany). One single sharp peak indicated high specificity of the investigated oligonucleotides. Since the efficiency of qRT-PCRs can vary depending on the applied primer pair, amplification rates were evaluated by performance of a qRT-PCR with a 10-fold dilution series of cDNA as template. All primer pairs used for qRT-PCRs revealed reaction efficiencies between 95 % and 100 %.

Table M1: Primers used for sequencing, construct design, RT-PCRs, and qRT-PCRs.

Primers for sequencing	**Orientation**	**Sequence**	**T_m [°C]**	**Genomic target**
M13-F(-20)	sense	GTAAAACGACGGCCAG	57.6	pCR®8/GW/TOPO®
M13-R	antisense	CAGGAAACAGCTATGAC	50.6	pCR®8/GW/TOPO®
LUC-72bp-A	antisense	CAACTGCATAAGGCTATGAA	58.0	pHGWL7.0
pHGWFS7-4089-A	antisense	GTGGTGCAGATGAACTTCAGG	64.7	pHGWFS7.0
pXCLSG-YFP-F	sense	AGCGAAACCCTATAAGAA	53.9	pXCSG-YFP
pMDC83_mgfp6_A	antisense	GTATGTTGCATCACCTTCAC	58.0	pMDC83

Primers for constructs	**Orientation**	**Sequence**	**T_m [°C]**	**Genomic target**
Phy4ApxProm-S	sense	GTTGCCTTAAGAGTAAGTTTAG	53,5	PptAPx promoter
Phy4ApxProm-A	antisense	GACGCGTCAAACCAACTAC	60,8	PptAPx promoter

Phypa_227509-5-UTR-A	antisense	GAGAGATTGGATCCACAAGC	61,2	PptAPx promoter
PptAPx_5'-UTR_S	sense	GCTTGTGGATCCAATCTCTC	61,2	PptAPx promoter
PpftsZ1-1_TP_S	sense	ATGATGAGCTCCATGGTGAG	62,8	PpftsZ1-1 transit peptide
PpftsZ1-1_TP_A	antisense	GCCTACACCAATGACCTTG	60,6	PpftsZ1-1 transit peptide
PptAPx_TP_S	sense	ATGGCGACTTCGGCTTC	64,1	PptAPx transit peptide
PptAPx_TP_A	antisense	GGCAGATCTCAGCTGGG	62,3	PptAPx transit peptide

Primers for RT-PCRs	**Orientation**	**Sequence**	**T_m [°C]**	**Genomic target**
CrsAPxA-cDNA-S	sense	GTTGAGCAGCTGAAGGCG	65	CrsAPxA
CrsAPxA-cDNA-A	antisense	CTCAGTCCAGAGTAACGGGC	63,7	CrsAPxA
CrsAPxB-cDNA-S	sense	CCCGGCGACTACGCG	68,1	CrsAPxB
CrsAPxB-cDNA-A	antisense	CAACTACCGTACTGCTGCAACG	66,6	CrsAPxB
PptAPxforwneu	sense	GCCATAGCCTCTGATCC	58,2	PptAPx
PptAPxrev	antisense	GACATTGTTAAATAAACTAGCCAAG	58,8	PptAPx
PptAPx_Q_S3	sense	CAGTGTGTGAAGGAGGGCAATC	68	PptAPx (used for cDNA quality check)
PptAPx_Q_A4	antisense	AACCCTTCCTAGAGTATGTGCAC	62,2	PptAPx (used for cDNA quality check)
SmtAPxforw	sense	GCGAATGATCTCGAAGAAG	60,1	SmtAPx
SmtAPxrevohne TMH	antisense	CTAAAACCCACCGAATAGCC	62,1	SmtAPx
SmsAPx1forw	sense	CTCGATCAGCTAGTGGGA	59	SmsAPx
SmsAPxrev	antisense	CTAACTTGTGCTCTCGTCGAT	61,1	SmsAPx
CrGPxA_s	sense	CTGGACATTGACAAGAAGAAC	58,8	CrGPxA
CrGPxA_a	antisense	CGACAATGTACTTCTCGAGC	60,1	CrGPxA
CrGPxB_s	sense	GACTCCATCTACCAGTTCAG	56,2	CrGPxB
CrGPxB_a	antisense	CGTAGTTCCACTCGATGTC	58,2	CrGPxB
CrGPxC_s	sense	CCTAACACCTGTGCTAGCTTC	60,5	CrGPxC
CrGPxC_a	antisense	GCTCTTCAGGTACTTGAACAC	58	CrGPxC
PpGPxA_s	sense	CTTCAGCATGTGGATTGA	59,2	PpGPxA
PpGPxA.1_a	antisense	CTGGATGTCGTTCTCTATCTTTG	61,6	PpGPxA
PpGPxA.2_a	antisense	CTGGGAGAGGAAGACTACCT	58,9	PpGPxA
PpGPxB_s	sense	GTGGACATTGACGGAGTG	60,2	PpGPxB
PpGPxB_a	antisense	CACTTCAATCTTGGCAAAGAG	61,4	PpGPxB
SmGPxA.1_s	sense	GCATAGCTTTAGCCTTGTGAC	60,5	SmGpxA.1
SmGPxA.2_s	sense	CTTTAGGGCATTTGTTGATT	58,2	SmGPxA.2
SmGPxA.1/2_a	antisense	GTCAATCCACATTGAGAAGC	59,7	SmGPxA.1 and 2
SmGPxB.1_s	sense	CAGACACAAGAATCCACAGC	61	SmGPxB.1
SmGPxB.2_s	sense	GCTTGTTCTTCCAGACAC	55,5	SmGPxB.2
SmGPxB.1/2_a	antisense	GTGAAGCCACATTGCGATG	65,5	SmGPxB.1 and 2

Primers for qRT-PCRs	Orientation	Sequence	T_m [°C]	Genomic target
PpACT1_S	sense	TTTCAGCACACTCCCTTCCC	66,4	PpAct1
PpACT1_A	antisense	AACCATAGTCATCTGCGAAATAAAC	62,9	PpAct1
PptAPx_Q_S2	sense	CAACGACTACGCCATCTCTC	62,5	PptAPx
PptAPx_Q_A2	antisense	GCGTGGAGTATTTGGATGC	63,1	PptAPx

2.4.2 Standard PCRs

To amplify specific DNA fragments, PCRs were performed in a total volume of 20 µl containing 2 µl *Thermus aquaticus* (*Taq*) buffer (20 mM Tris-HCl pH 8.4, 50 mM KCl, 1.5 mM $MgSO_4$ and 0.5 mM $MgCl_2$), 2 mM dNTPs (deoxynucleotide triphosphates), 0.5 mM of each primer, and 1 µl of DNA. Prior to reactions, template DNAs were diluted 1:10 with autoclaved deionized water. If the PCR was performed to amplify a specific region of the *Physcomitrella* genome, 0.24 mM spermidine was included in the reaction mixture. PCRs were catalyzed either by a heat-stable *Taq* polymerase, which had been produced and isolated according to Pluthero (1993), or by a mixture of a DNA polymerase having proofreading activity and *Taq* polymerase (High Fidelity PCR Enzyme Mix, Fermentas, St. Leon-Rot, Germany). Being initialized with a single DNA denaturation step at 94 °C for 7 min, forty reaction cycles were performed. Each cycle included a denaturation step of 1 min, a primer annealing step for 0.5-1 min, and elongation. The annealing temperature of oligonucleotides was adjusted to the melting temperatures of the used primers (T_m - 5 °C) (see table M1). The duration of the elongation depended on the length of the desired product set to approximately 1 min per 1 kbp. The temperatures during this step were set to 72 °C for the *Taq* polymerase or to 62 °C, if the High Fidelity PCR Enzyme Mix was used.

For each PCR, a control sample, containing no template, was included to ensure purity of the reagents used. Amplified PCR products were analyzed by gel electrophoresis as described in chapter 2.4.3.

2.4.3 Electrophoretic separation of DNA

Following termination of the reactions, restriction digests and PCR mixtures were analyzed by separating the DNA fragments by gel electrophoresis. Agarose gels were prepared by melting 1.2 % (w/v) agarose in 1 x TAE buffer containing 0.8 mM Tris-acetate pH 7.5, 0.02 mM EDTA (Ethylenediamine-N,N,N',N'-tetraacetic Acid). After cooling the mixture to

approximately 60 °C and addition of 0.5 µg/ml ethidium bromide the mixture was casted in horizontal gel trays. Prior to loading them onto solidified gels, samples were mixed with 25 % (v/v) DNA loading buffer (0.05 % (w/v) bromophenol blue, 0.05 % (w/v) xylenecyanol, 6 % (v/v) glycerol). Electrophoretic separation took place in 1 x TAE buffer by applying a constant voltage of 120 V. The duration was adjusted to the expected size of the fragments. Ethidium bromide stained DNA bands were visualized with UV light (312 nm) and the patterns documented by using a gel imager with a CCD camera (Intas, Göttingen, Germany).

2.4.4 Gel extraction of PCR products

PCR products, which should be used for cloning procedures, were purified from 1.2 % (w/v) agarose gels (see chapter 2.4.3). Stained with ethidium bromide and visualized with UV light (312 nm), the desired band was excised from the gel and the contained DNA fragment was extracted. Various kits were used according to manufacturer's recommendations [GeneJET Gel Extraction Kit (Fermentas, St. Leon-Rot, Germany), innuPREP Gel Extraction Kit (Analytik Jena AG, Jena, Germany)]. The purification principle is equal for all used kits. After melting the gel in high salt conditions, the sample purification takes place by binding of the DNA fragment to silica membranes and removal of contaminations by several washing steps. Fragments were eluted with deionized autoclaved water and directly used for plasmid modifications (see chapter 2.6) or stored at -20 °C for further use.

2.5 *Escherichia coli* modifications

2.5.1 Generation of competent *Escherichia coli*

For most *E. coli* transformations the strain TOP10 (One shot TOP10, Invitrogen, Carlsbad, USA) was used. If the cloning failed twice, the procedure was repeated with the *E. coli* strain DH5α. The genomes of theses strains show different mutations (for genotypes see Table M2) which influence the transformations efficiency. To generate chemically competent bacteria, 5 ml Lysogeny Broth (LB) medium were inoculated under sterile conditions and cultivated over night at 37 °C with continuous shaking (200 rpm). The culture volume was increased to 100 ml. The cells were grown to an OD_{600} of 0.4-0.6 and, subsequently, cooled down on ice for 10 min. Harvesting of the cells was performed by centrifugation at 16,000 x g and room temperature for 7 min. Supernatants were discarded and the pellet was resuspended in 5 ml

ice-cold 60 mM $CaCl_2$ supplemented with 15 % (v/v) glycerol and 10 mM PIPES pH 7.0 (adjusted with KOH). Afterwards, sedimentation was repeated by centrifuging at 16,000 x g and room temperature for 7 min. Supernatants were again discarded and the pellets resuspended in 2 ml ice-cold $CaCl_2$ supplemented with 15 % (v/v) glycerol and 10 mM PIPES pH 7.0 (adjusted with KOH). 100 µl aliquots were prepared, frozen in liquid nitrogen and transferred to -80 °C for further storage. To perform one transformation procedure, an aliquot was thawed on ice and 16 µl were used. Subsequently the remaining suspension was transferred back to -80 °C.

Table M2: *E. coli* strains and their genotypes (Sambrook and Russel, 2001).

***E. coli* strain**	**Genotype**
DH5α	F-, *Δ(argF-lac)169*, φ80d*lacZ58*(M15), *ΔphoA8*, *glnV44*(AS), *λ*⁻, *deoR481*, *rfbC1*?, *gyrA96* (NalR), *recA1*, *endA1*, *thiE1*, *hsdR17*
TOP10	F⁻ *mcr*A Δ(*mrr-hsd*RMS-*mcr*BC) φ80*lacZ*ΔM15 Δ*lac*X74 *rec*A1 *ara*D139 Δ(*ara-leu*) 7697 *gal*U *gal*K *rps*L (Str^R) *end*A1 *nup*G λ-

2.5.2 Transformation of *Escherichia coli*

Chemically competent *E. coli* were transformed with different constructs for the analyses of promoter activities and to study protein targeting. For each transformation an aliquot of competent *E. coli* was thawed on ice. 16 µl bacterial suspension were mixed with a plasmid preparation. After incubation on ice for 5-30 min, the cells were heat-shocked for 60 s at 42 °C and immediately transferred back to ice. 250 µl LB were added. The bacteria were incubated at 37 °C for 1 h to enable recovery. 75 µl bacteria suspension were spread on plates containing LB medium supplemented with antibiotics and 1 % (w/v) agar-agar. The kind of antibiotic depended on the resistance encoded on the plasmid used for the transformation procedure.

2.5.3 *Escherichia coli* colony PCRs

Cells from one single *E. coli* colony were transferred to 20 µl PCR mixture (see chapter 2.4.2). The colonies were picked from a plate containing selecting antibiotics, which was incubated over night at 37 °C. Following an initial denaturation for 13 min for cell lysis, the reactions were performed according to the protocol described for standard PCRs (see chapter 2.4.2) using a FlexCycler (Analytik Jena AG, Jena, Germany). For each colony PCR, a control sample, containing no template, was included to ensure purity of the used reagents. Products were analyzed by performing gel electrophoresis (see chapter 2.4.3).

2.5.4 Plasmid isolation from *Escherichia coli*

Plasmids were isolated from 5 ml LB medium cultures [1 % (w/v) tryptone, 0.5 % (w/v) yeast extract, 1 % (v/v) NaCl] cultures supplemented with antibiotics. They had been incubated over night at 37 °C under continuous shaking at 200 rpm. The type of antibiotic depended on the resistance conferred by the plasmid contained in the *E. coli* strain. The extraction was performed by using different commercially available kits [Wizard® *Plus* SV Minipreps (Promega, Madison, USA), innuPREP Plasmid Mini Kit (Analytik Jena AG, Jena, Germany), GeneMATRIX Plasmid Miniprep DNA Purification Kit (EURx Ltd. Gdansk, Poland)] according to the manufacturer's instructions. The extractions base on the ability of silica membranes to bind plasmid DNA under high salt conditions. Cell debris and precipitated proteins are removed by centrifugation prior to loading the column. RNase H (supplied in the kits) digested RNA and remaining contaminations were discarded in several washing steps. Elution of the plasmids from membranes was performed with autoclaved deionized water. Usually, these kits yield 250-400 µg/ml. If a higher concentration and more DNA were necessary, *e. g.* for protoplast transfection, the desired plasmids were isolated with the Plasmid Maxi Kit (Qiagen, Hilden, Germany) according to recommendations of the manufacturer. Subsequent to extraction, the DNA content was quantified and checked for quality and purity using the NanoPhotometer P300 (Implen, Munich, Germany) (see chapter 2.14.5). All samples were either stored at -20 °C or directly used for restriction digests, sequencing or cloning procedures.

2.5.5 Preparation of *Escherichia coli* glycerol stocks

For the long term storage of *E. coli* glycerol stocks were prepared. 5 ml of LB medium containing antibiotics were inoculated and cultured over night at 37 °C under continuous shaking (200 rpm). Afterwards, 800 µl *E. coli* culture were mixed with 200 µl glycerol and frozen at -80 °C for further storage.

2.6 Plasmid modifications

Several different vectors were used to generate constructs for promoter-reporter gene analyses and to verify the chloroplast targeting prediction of PptAPx. All constructs used for this study are listed below.

Table M3: Constructs for promoter-reporter gene analyses or protein targeting studies (see "Construct use"). Primers used to create the constructs are listed in the "Primer combination" section.

Construct	Primer combination	Destination clone	Construct use
PptAPx+5'-UTR x pHGWL (UTRE1/2)	Phy4ApxProm-S x Phy4ApxProm-A	pHGWL7.0	Promoter analyses
PptAPxw/o5'-UTR x pHGWL (UTRE1)	Phy4ApxProm-S x Phypa_227509-5-UTR-A	pHGWL7.1	Promoter analyses
PptAPx5'-UTR x pHGWL (UTRE2)	PptAPx_5'-UTR_S x Phypa_227509-5-UTR-A	pHGWL7.2	Promoter analyses
PptAPx+5'-UTR x pHGWFS	Phy4ApxProm-S x Phy4ApxProm-A	pHGWFS7.0	Promoter analyses
AtsAPx x pHGWL	designed by U. Ellersiek	pHGWL7.1	Promoter analyses
AttAPx x pHGWL	designed by U. Ellersiek	pHGWL7.1	Promoter analyses
PpftsZ1-1_TP in pMDC83	PpftsZ1-1_TP_S x PpftsZ1-1_TP_A	pMDC83	Targeting analyses
PpftsZ1-1_TP in pXCSG-YFP	PpftsZ1-1_TP_S x PpftsZ1-1_TP_A	pXCSG-YFP	Targeting analyses
PptAPx_TP in pMDC83	PptAPx_TP_S x PptAPx_TP_A	pMDC83	Targeting analyses
PptAPx_TP in pXCSG-YFP	PptAPx_TP_S x PptAPx_TP_A	pXCSG-YFP	Targeting analyses

2.6.1 Ligation of PCR products into pCR8/GW/TOPO

The pCR8/GW/TOPO vector was used as entry clone for Gateway cloning. Ligation into this plasmid is based on overhanging thymidine residues at the cloning site. PCR products were produced either with a polymerase derived from *Thermus aquaticus* (*Taq*) or using a mixture of a DNA polymerase having proofreading activity and *Taq* polymerase (High Fidelity PCR Enzyme Mix, Fermentas, St. Leon-Rot, Germany). The *Taq* polymerase transfers overhanging sticky adenine residues to 3'- and 5'-ends which make the ligation into pCR8/GW/TOPO

feasible. Ligations were performed according to the manufacturer's instructions (Invitrogen, Carlsbad, USA).

After transformation of *E. coli* with modified pCR8/GW/TOPO (see chapter 2.5.2), selection was carried out on LB medium supplemented with 50 µg/ml spectinomycin and 1 % (w/v) agar-agar. Positive clones survive addition of this antibiotic since the vector confers resistance.

2.6.2 Ligation of PCR products into pJET1.2/blunt

The pJET1.2/blunt plasmid was used as an intermediate vector. After performance of *E. coli* transformation and plasmid isolation (see chapters 2.7.2, 2.7.5), this intermediate construct was used for re-amplification by PCR. Usually, ligation of this PCR product into pCR8/GW/TOPO was feasible without trouble-shooting. Insertion of a specific DNA region into pJET1.2/blunt was done with the CloneJET PCR Cloning Kit (Fermentas, St. Leon-Rot, Germany) according to the manufacturer's recommendations. Prior to ligation into pJET1.2/blunt, the PCR products were blunted since they had been produced either with a polymerase derived from *Thermus aquaticus* or using a mixture of a DNA polymerase having proofreading activity and *Taq* polymerase (High Fidelity PCR Enzyme Mix, Fermentas, St. Leon-Rot, Germany). This enzyme transfers adenine residues to 3'- and 5'-ends. These sticky ends inhibit the ligation into pJET1.2/blunt. The DNA blunting enzyme was supplied in the kit.

For selection of positive clones, the vector encodes a restriction enzyme which is lethal to *E. coli* if the vector is re-ligated without disruption of the gene by an inserted DNA fragment. Besides this, the vector confers resistance to ampicillin. Positively transformed *E. coli* with a modified pJET1.2/blunt vector survived on LB supplemented with 100 µg/ml ampicillin and 1 % (w/v) agar-agar.

2.6.3 Gateway cloning (LR reactions)

LR reactions serve to recombine entry clones and destination vectors. To generate entry clones, a respective PCR product was integrated in the gateway compatible vector pCR8/GW/TOPO. To increase recombination efficiency, the respective entry clone was linearized with the restriction enzyme Psp1406I according to manufacturer's instructions (Fermentas GmbH, St. Leon-Rot, Germany). The digest was terminated by an incubation of

the samples at 65 °C for 20 min. Digested entry clones were directly used for LR reactions without any additional purification. To perform homologous recombination, 75 ng linearized entry clone were mixed with 75 ng of the desired destination vector and 1 µl LR Clonase II enzyme mix (Invitrogen, Carlsbad, USA). The solution was filled to a total volume of 5 µl with TE buffer pH 8.0 (10 mM Tris/HCl pH 8.0, 1 mM EDTA). Following incubation at 25 °C for 1 h, 0.5 µl Proteinase K solution was added (Invitrogen, Carlsbad, USA) and the samples were transferred to 37 °C for 10 min to terminate LR clonase activity. Afterwards, 1 µl of the LR reaction mixture was used to transform *E. coli* (see chapter 2.5.2). Selection of positive clones was performed on LB media supplemented with 1 % (w/v) agar-agar and antibiotics. The destination clones pHGWL7.0 and pHGWFS7.0 conferred resistance to spectinomycin (50 µg/ml) (Karimi *et al.* 2002, Karimi *et al.* 2005), pXCSG-YFP to ampicillin (100 µg/ml) (Witte *et al.* 2004, Feys *et al.* 2005), and pMDC83 to kanamycin (50 µg/ml) (Curtis and Grossniklaus, 2003). Putative positive clones were re-evaluated by performing colony PCRs (see chapter 2.7.4). Insertion of a specific DNA fragment in the desired orientation was verified by *E. coli* colony PCRs, restriction digests, and subsequent sequencing (see chapters 2.5.3, 2.7, 2.8).

2.7 Cleavage of double-stranded DNA with restriction enzymes

Restriction digests were used to verify the insertion of the desired PCR amplicon into the plasmid. 1 µg DNA was digested with different enzymes (Fermentas GmbH, St. Leon-Rot, Germany) depending on the plasmid and insert. Reactions were performed according to manufacturer's recommendations for approximately 1 h. Subsequently, the fragments were analyzed by agarose gel electrophoresis (see chapter 2.4.3).

2.8 Sequencing

Following cloning, plasmids were isolated and 1-2 µg were sent to GATC (GATC Biotech AG, Konstanz, Germany) for sequencing. The company uses the chain terminator principle with an ABI 3730xl system – also called Sanger sequencing (Sanger *et al.* 1977). For priming the reaction, vector specific oligonucleotides were chosen (see table M1). The resulting sequences usually had a length of approximately 500-700 bp. If the inserted region was longer, the plasmid was re-sequenced in the antisense direction. After delivery, sequences were checked for their correctness by aligning them to the original cloned DNA region with

ClustalW2.0 [http://www.ebi.ac.uk/Tools/clustalw2 (Thompson *et al.* 1994, Larkin *et al.* 2007)].

2.9 *Agrobacteria tumefaciens* modifications

2.9.1 Generation of chemically competent *Agrobacteria tumefaciens*

Chemically competent *Agrobacteria* were generated according to Weigel and Glazebrook (2002). Competent cells were generated from stocks of *Agrobacteria* strain GV3101(pMP90) (Koncz and Schell, 1986) stocks. After streaking them out on YEB (yeast extract broth) medium [0.5 % (w/v) peptone, 0.5 % (w/v) beef extract, 0.1 % (w/v) yeast extract, 0.5 % (w/v) sucrose, 0.05 % (w/v) $MgSO_4$*7 H_2O] solidified by 1 % (w/v) agar-agar and supplemented with the antibiotics rifampicin (150 µg/ml) and gentamycin (25 µg/ml). After cultivation for 1-2 days at 28 °C, 5 ml liquid YEB containing antibiotics were inoculated and incubated over night at 28 °C and continuous shaking at 200 rpm. Subsequently, the *Agrobacteria* were further propagated by enlarging the culture volume to 50-100 ml. When this culture reached an OD_{600} of approximately 0.5-1, it was cooled down on ice for 30 min and centrifuged for 5 min at 3,000 x g and 4 °C. The supernatant was discarded and the pellet redissolved in 1 ml 20 mM $CaCl_2$. This suspension was aliquoted in 100 µl portions and frozen in liquid nitrogen. For further storage they were transferred to -80 °C.

2.9.2 Transformation of *Agrobacteria tumefaciens*

Agrobacteria were also transformed according to Weigel and Glazebrook (2002). A frozen 100 µl aliquot of competent bacteria (see chapter 2.9.1) was thawed on ice and mixed with 1-3 µg of plasmid DNA. Following an incubation of 30 min, the mixture was frozen in liquid nitrogen for 5 min and transferred to 37 °C for 5 min. After addition of 1 ml YEB medium (see chapter 2.9.1) and incubation for 2-4 h at 28 °C, the samples were spread on plates containing YEB supplemented with 1 % (w/v) agar-agar and antibiotics for selection of positive clones and transferred to 28 °C for two days. Besides rifampicin (150 µg/ml) and gentamycin (25 µg/ml), spectinomycin (50 µg/ml) or kanamycin (10 µg/ml in liquid YEB, 5 µg/ml in YEB containing 1 % agar-agar) were used for selection, depending on the plasmid used for transformation. For further selection, four colonies were picked and streaked over a

quarter of a plate containing YEB supplemented with 1 % (w/v) agar-agar and antibiotics, each, and subsequently incubated for another day at 28 °C.

2.9.3 Preparation of *Agrobacteria tumefaciens* glycerol stocks

For long term storage of *A. tumefaciens* glycerol stocks were prepared. 5 ml of YEB containing antibiotics were inoculated and cultured over night at 28 °C under continuous shaking (200 rpm). Afterwards, 800 µl *A. tumefaciens* culture were mixed with 200 µl glycerol and stored at -80 °C until further use.

2.10 Isolation and transfection of *Arabidopsis thaliana* mesophyll protoplasts

Prior to protoplast isolation, necessary solutions were freshly prepared and all - except the PEG (polyethylene glycol) - were filter sterilized. The enzyme solution [20 mM MES pH 5.7 (adjusted with NaOH), 20 mM KCl, 10 mM $CaCl_2$, 0.4 M mannitol, 1.5 % (w/v) cellulase, 0.4 % (w/v) macerozyme, 0.1 % (w/v) BSA] was prepared in three steps: First, water, MES, KCl, and mannitol were mixed and heated to 70 °C for 2 min and subsequently cooled down on ice to approximately 55 °C. In a second step, all enzymes were added and the solution was incubated at 55 °C for 5 min under shaking. Afterwards, the solution was cooled down to approximately 25 °C and $CaCl_2$ and BSA were supplied, representing the third step. Mesophyll protoplasts were isolated from leaves of 4-6 week old *Arabidopsis* plants according to a slightly modified version of the Tape-*Arabidopsis* Sandwich method published by Wu *et al.* (2009). This procedure is based on the release of protoplasts from *Arabidopsis* leaves by ripping off the epidermis from the lower leaf part and incubating it in an enzyme solution for 1.5-2 h under continuous mild shaking at approximately 20 rpm. Following incubation, protoplasts which still remained in the leaves were released by rinsing them with 1 ml W5 solution (2 mM MES pH 5.7, 154 mM NaCl, 125 mM $CaCl_2$, 5 mM KCl). The solution was carefully filtered through a nylon mesh with 80 µm pore size into a plastic or glass tube with round bottom by using a glass pipette and centrifuged at 100 x g and room temperature for 1 min. The supernatant was discarded and 1 ml W5 solution added. During the following incubation on ice (0.5-2.5 h) the isolation efficiency was tested and protoplasts checked for their viability. After the recovery time, transfections were performed. 100 µl protoplast suspension were softly mixed with 20 µg desired plasmid DNA (approximately

2 µg/µl). Subsequently, 110 µl PEG (30 % (v/v) PEG, 0.2 M mannitol, 100 mM $CaCl_2$) were added. Following incubation for 7 min at room temperature, the mixture was diluted with 440 µl W5 solution to relax the protoplasts and enable DNA diffusion through their membrane. After centrifugation for 2 min at 1,000 x g and room temperature, discarding supernatants, and re-suspension of the pellets in 1 ml WI solution (2 mM MES pH 5.7, 0.5 M mannitol, 20 mM KCl), the protoplasts were incubated over night in 6-well plates covered with 1 % (w/v) BSA solution. Reporter gene activity was documented as described in chapter 2.12.

2.11 Transfection of *Arabidopsis thaliana*, *Selaginella moellendorffii*, *Physcomitrella patens*, and *Nicotiana benthamiana*

Ten day old *Arabidopsis* seedlings, young and small *Selaginella* phylloids, and *Physcomitrella* gametophytes were used to perform transfections. Prior to the procedure, *Physcomitrella* had been transferred onto fresh modified Knop medium and cultivated for ten days.

The desired *Agrobacteria* strains were cultivated in 5 ml YEB supplemented with antibiotics. To avoid possible gene silencing of the reporter gene *in planta*, an *Agrobacteria* strain expressing the very effective viral silencing suppressor P19 (Voinnet *et al.* 2003) was included in all transfection experiments and 2 x 5 ml YEB containing antibiotics were inoculated. After incubation over night at 28 °C, the *Agrobacteria* were grown to an OD_{600} of at least 0.5 in 50-200 ml cultures. Necessary volumes of *Agrobacteria* conferring the desired trait and the P19 strain were calculated according to the following equations, mixed and centrifuged at 3000 x g and room temperature for 8 min.

$$V_{construct} = n*V_{final}*0.5/OD_{600(construct)} \quad \text{and} \quad V_{P19} = n*V_{final}*0.3/OD_{600(P19)}$$

V – volume,

n – amount of infiltrated seedlings, phylloids, or gametophytes,

V_{final} - volume of infiltration suspension used

Following decantation of supernatants, pellets were resuspended in $n*V_{final}$ freshly prepared activation buffer (10 mM MES/KOH pH 5.6, 10 mM CaCl2, 150 µM acetosyringone). During

the following incubation in darkness at room temperature for 2 h, the *Agrobacteria* could recover and their virulence region was activated by actetosyringone. This activation leads to the expression of diverse genes necessary for transferring of DNA into the cell nuclei of plant hosts. Next, ten day old *Arabidopsis* seedlings, which were grown on plates containing MS medium, were flooded with the infiltration solution. The first two leaves of 6 week old tobacco plants were infiltrated with the same solution by using a syringe. The same instruments can be utilized for infiltrating leaves of adult *Arabidopsis* plants. For *Selaginella* young and small phylloids (approximately 1-2 cm) revealed to be best suited since they have a higher capability to recover. Subsequently, vacuum was applied six times for 1.5 minutes to infiltrate *Arabidopsis* seedlings. Since it is much more difficult to release the air from *Physcomitrella* and *Selaginella*, an additional vacuum application for ten minutes followed for them. If *Selaginella* still released much air during the latter vacuum, this step was repeated. Afterwards, the plants - except *Nicotiana* - were washed in autoclaved tap water and transferred to soil or fresh medium. After at least two days regeneration time reporter gene activity could be observed.

To ensure that the reporter activity was not false-positive, several negative controls were included in each experiment: Plants were infiltrated with (i) pure activation buffer, and (ii) an *Agrobacteria* strain that caused another trait as examined in the respective experiment, *e. g.* when luminescence was desired to be detected, an *Agrobacteria* strain causing fluorescence was used as negative control.

2.12 Detection of reporter gene activity

2.12.1 Detection of luciferase activity

For analyses of luciferase activity, plants were sprayed with 1 mM luciferin solution supplemented with 1 mM ATP (adenosine triphosphate) and 0.1 % (v/v) Triton-X. After incubation for 5-10 min at room temperature in darkness, luminescence was documented with the ImageQuant LAS 4000 mini device (GE Healthcare Europe GmbH, Freiburg, Germany). The exposition time was set between 10 s and 2 min depending on luminescence intensity.

2.12.2 Detection of GFP and YFP activity

Arabidopsis protoplasts were transfected with constructs causing the expression of GFP or YFP. GFP localization was documented with the fluorescence microscope Nikon Eclipse 90i (Nikon GmbH, Düsseldorf, Germany) supplemented with a camera while YFP activity was observed and documented using the fluorescence microscope system BZ-8100 (KEYENCE, Neu-Isenburg, Germany).

2.13 Measurement of photosynthetic yield

The quantum yield of photosystem II was determined using the MINI-PAM (Heiner Walz GmbH., Effeltrich, Germany). This device applies a saturating light pulse which causes a temporary total reduction of all photosynthetic reaction centers. Before and after this pulse, red fluorescence emitted by chlorophyll *a* is measured and can be used to determine the efficiency of photosynthesis. The photosynthetic yield can be calculated in dark and light acclimated plants according to the following equations.

$$\Phi_{PSII} = (F_m - F_0) / F_m = F_V / F_m$$

Maximum / Initial quantum yield of PSII (in the dark acclimated state)

$$(F_m' - F_t) / F_m' = \Delta F / F_m'$$

Effective quantum yield of photochemical energy conversion in PSII (in the light acclimated state)

The different variables of the equations are shown and defined in Fig. M1.

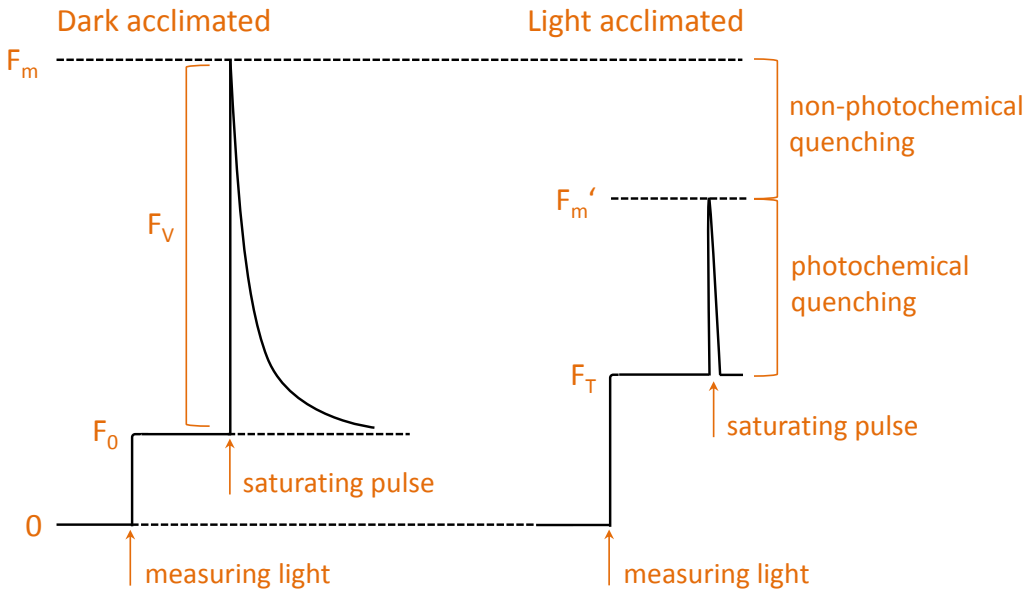

Fig. M1: Fluorescence emitted by chlorophyll a in dark or light acclimated plants due to application of measuring light, actinic light, or a photosynthetically saturating light pulse, variables in the above mentioned equations for measuring photosynthetic yield are shown (figure was adapted from Photosynthesis Yield Analyzer MiniPam, Handbook of operation, Heiner Walz GmbH, Effeltrich, Germany). measuring light - weak red pulses, F_0 – minimal fluorescence after application of the measuring light (in the dark acclimated state), F_0' – F_0 in light acclimated plants, F_m – maximum fluorescence after the saturating light pulse (in the dark acclimated state), F_v – difference between F_0 and F_m, F_m' – F_m in light acclimated plants, F_t – fluorescence intensity shortly before application of the saturating pulse (also called F).

The photosynthetic yield was measured in light acclimated *Physcomitrella* and *Arabidopsis* plants. Measuring intensity was set to 5 for *Physcomitrella* and to 10 for *Arabidopsis* whereas the intensity of the light pulse (0.8 s, >3000 µmol quanta m^{-2} s^{-1}) and distance (approximately 10 mm) between measuring device and plant remained constant.

2.14 Transcript analyses

2.14.1 Total RNA isolation from *Arabidopsis thaliana*

Arabidopsis RNA was isolated from 2-5 ten day old seedlings. The plant material was homogenized using liquid nitrogen and the Retsch Mixer Mill MM100 (Retsch, Germany). RNA which was used for RT-PCRs was isolated with the RNeasy Mini Kit (Qiagen, Hilden, Germany) while samples for qRT-PCRs were extracted with the GeneMATRIX Universal RNA Purification Kit (EURx, Poland), both according to manufacturer's instructions. Possibly remaining DNA contaminations were removed by performing on-column digestions

with RNase-free DNaseI (Fermentas GmbH, St. Leon-Rot, Germany). The kit from EURx revealed to be best suited for *Arabidopsis* seedling and yielded approximately 0.5-1 mg RNA per ml eluted solution. After RNA extraction, the RNA samples were checked for quantity, purity, and integrity (see chapters 2.14.5, 2.14.6). Afterwards, RNAs were either directly used for first strand cDNA synthesis (see chapter 2.14.7) or transferred to -80°C for further storage.

2.14.2 Total RNA isolation from *Selaginella moellendorffii*

RNA was extracted from approximately 0.1 cm^2 of young and healthy *Selaginella* phylloids. They were homogenized with liquid nitrogen using the Retsch Mixer Mill MM100 (Retsch, Germany). Following, the RNA samples for RT-PCRs were evaluated and further used as described for *Arabidopsis* seedlings (see chapter 2.14.1).

2.14.3 Total RNA isolation from *Physcomitrella patens*

Physcomitrella gametophyte bunches of approximately 1.5-2 mm diameter were collected and homogenized with liquid nitrogen and the Retsch Mixer Mill MM100 (Retsch, Germany). RNA samples for RT-PCRs and qRT-PCRs were extracted using the two different kits described for *Arabidopsis* seedlings. Being highly efficient for extracting RNA from *Arabidopsis* seedlings, the kit from EURx was less suited for *Physcomitrella*. It yielded approximately 10-50 µg RNA per ml eluted solution from gametophyte material. The RNA samples for RT-PCRs and qRT-PCRs were evaluated and further used as described for *Arabidopsis* seedlings (see chapter 2.14.1).

2.14.4 Total RNA isolation from *Chlamydomonas reinhardtii*

Chlamydomonas RNA was extracted from 100 mg dry algae pellets as described in Heiber *et al.* (2007) for ground *Arabidopsis* plant material. Afterwards, the RNA samples for RT-PCRs were evaluated and further used as described for *Arabidopsis* seedlings (see chapter 2.14.1).

2.14.5 Quantification and evaluation of nucleic acid extraction samples

All nucleic acid samples were analyzed for their quantity and purity by using the NanoPhotometer P300 (Implen, Munich, Germany). This spectro-photometrical device

measures absorbance at 230 nm, 260 nm, and 280 nm. Nucleic acid concentration was calculated according to the absorbance at 260 nm. Protein contamination is indicated by a A_{260}/A_{280} ratio lower than 1.8 for DNA samples and lower than 2.0 for RNA. A_{260}/A_{230} ratios lower than 2.0, in contrast, point to the presence of undesired sugars or phenolic substances in the sample. After this evaluation of extracted RNA, its integrity was analyzed by RNA electrophoresis. *Arabidopsis* samples showing a high quality were chosen for cDNA first strand synthesis and RT-PCRs (see chapters 2.14.7 and 2.14.8). *Physcomitrella* RNA in contrast, usually revealed low concentrations and low A_{260}/A_{230} ratios but A_{260}/A_{280} ratios ≥ 2.0. If their integrity was acceptable, they were used for cDNA first strand synthesis. To analyze the samples for DNA contaminations, RT-PCRs were performed using primers spanning the intron in the PptAPx gene (PptAPx_Q_S3, PptAPx_Q_A4 (for sequences see table M1, see chapter 2.14.8). Since the region contains an intron of 131 bp, DNA specific amplicons would appear if any contamination was present. If the cDNA samples revealed to be DNA-free, they were either diluted with RNase-free water (1:3) and used for qRT-PCRs or transferred to -80 °C for further storage.

2.14.6 Electrophoretic separation of RNA

RNA samples were separated by electrophoresis to analyze their integrity. This was performed in a 1 % (w/v) agarose gel prepared with 1 x MOPS buffer (20 mM MOPS pH 7.0, 5 mM sodium acetate, 1 mM EDTA). Before gels were poured into horizontal gel trays, agarose was melted in the buffer, the mixture was cooled down to approximately 60 °C, and formaldehyde added to a final concentration of 0.9 % (v/v). After solidification, gels were transferred to the running buffer (1 x MOPS buffer). Samples were prepared for loading as follows: 3 µl loading dye (10 mM Tris-HCl pH 7.6, 60 % (v/v) glycerol, 60 mM EDTA, 0.03 % (w/v) bromophenol blue) and 4.8 µl loading buffer [3 mM MOPS pH 7.0, 0.75 mM sodium acetate, 0.15 mM EDTA, 6.5 % (v/v) formaldehyde, 57.5 % (v/v) formamide, 0.12 mg/ml ethidium bromide] were added to 3 µl isolated RNA. Immediately after denaturation of RNA by applying 65 °C for 15 min, the samples were cooled on ice. After loading the gel, electrophoresis was performed for approximately 20 min at a constant voltage of 90 V. Ethidium bromide stained RNA bands were visualized by applying UV light (312 nm), followed by documentation of the pattern using a gel imager with a CCD camera (Intas, Göttingen, Germany).

2.14.7 First strand cDNA synthesis

Complementary DNA (cDNA) was synthesized from isolated RNA samples and used for gene expression analyses by performing qRT-PCRs. It was generated with the reverse transcriptase supplied in the High Capacity cDNA Reverse Transcription Kit (Applied Biosystems, Carlsbad, USA) without RNase inhibitor. 0.5 µg of *Arabidopsis* RNA were reverse transcribed. Since the RNA samples derived from *Physcomitrella* were low concentrated, only 40 ng were used in the total reaction volume (20 µl) containing 1 x RT Buffer, 10 mM dNTP Mix, 25 U Multiscribe Reverse Transcriptase, and 5 µM Oligo(dT) Primers (Sigma-Aldrich Chemie GmbH, Steinheim, Germany). Besides the primers, all components were supplied in the kit. To anneal the primers to RNA, the reaction mixture was incubated at 25 °C for 10 min. Afterwards, cDNA synthesis took place at 37 °C (120 min). The reverse transcription was terminated by heating the samples to 65 °C for 5 min. cDNAs were either diluted (1:2) with RNase-free water and used for qRT-PCRs or transferred to -20 °C for further storage.

2.14.8 Real-time PCR (RT-PCR) analyses

Specificity of primers used for qRT-PCRs and transcription of several genes were analyzed by RT-PCRs. For a list of primers included in RT-PCRs see table M1. The PCR mixture was prepared and the procedure followed the same protocol as described in chapter 2.4.2 for standard PCRs. Instead of genomic DNA, undiluted cDNA was used as template. The reactions were catalyzed by a heat-stable *Taq* polymerase. For each RT-PCR, a negative control was performed. This contained no template and was performed to exclude the presence of contaminations in the used reagents. Subsequent to the reaction, products were analyzed by DNA gel electrophoresis, visualized, and documented as described in chapter 2.4.3.

2.14.9 Quantitative real-time PCR (qRT-PCR) analyses

Steady state transcriptions rates were analyzed by performing qRT-PCRs with the CFX96 thermocycler (BioRAD, Munich, Germany) according to the MIQE standards published by Bustin *et al.* (2009). The principle of this method is based on the ability of SYBR Green to intercalate with double stranded DNA. Excitation with blue light (497 nm) leads to emission of green light (521 nm) which was detected by the thermocycler. The fluorescence signal

increases with the amplification of DNA catalyzed by a polymerase during PCRs. The reactions mixtures contained 3 µl diluted cDNA (1:3), Maxima SYBR Green Master Mix (Fermentas GmbH, St. Leon-Rot, Germany), and 0.6 µM transcript-specific primers (total volume: 10 µl). For a list of all primers used in qRT-PCRs see table M1. The mixtures were prepared on ice and, subsequently, transferred to the CFX96 thermocycler. PCRs were initialized with activating the hot-start polymerase by applying 95 °C for 3 min. Amplification was performed in forty cycles. Each cycle included DNA denaturation at 95 °C (15 s), primer annealing at 60 °C (30 s), and an extension step at 72 °C (30 s). To generate melting curves, each cycle was followed by another denaturation at 95 °C (15 s), a temperature decrease to 60 °C, and subsequent increase to 95 °C at a ramp speed of 0.5 °C s^{-1}. Fluorescence was detected continuously during the temperature increase.

The analyses of transcript abundance were performed in two biological replicates. These represent separated RNA isolations from two independent, but equally treated *Physcomitrella* gametophyte bunches. All qRT-PCRs carried out in three technical replicates to ensure accuracy. Additionally, controls samples containing no template were included to exclude the presence of primer dimers and contamination of primers or master mix.

2.14.10 Standardization and quantification of qRT-PCR results

All qRT-PCR results obtained for PptAPx were normalized to the transcript level of the *Physcomitrella patens* actin gene Act1 (PpAct1). Quantification of the transcript level was performed according to Livak and Schmittgen (2001). This $2^{-\Delta\Delta Ct}$ method bases on differences in the threshold cycle (Ct) values detected for a gene of interest (PptAPx) and the gene used for standardization (PpAct1) ($\Delta Ct = \Delta Ct_{PptAPx} - \Delta Ct_{PpAct1}$), on the one hand, and differences in the ΔCt detected among analyzed (treated) and reference (untreated) *Physcomitrella* gametophytes ($\Delta\Delta Ct = \Delta Ct_{treated} - \Delta Ct_{untreated}$), on the other hand.

2.15 Bioinformatics

2.15.1 BLAST searches

2.15.1.1 BLAST searches in EST databases

EST databases for *Selaginella* (JGI: http://genome.jgipsf.org/Selmo1/Selmo1.home.html), *Physcomitrella* (cosmoss: http://www.cosmoss.org/), and *Chlamydomonas* (ChlamyDB: http://www.chlamy.org/ and JGI: http://genome.jgi-psf.org) were screened for transcripts encoding APxs, Prxs, and GPxs by BLAST searches (Altschul *et al.* 1997). To identify such ESTs, TBLASTX searches were performed with the *Arabidopsis thaliana* homologs (algorithm: BLOSUM62, threshold: $1e^{-2}$-$1e^{-5}$, word size: 3). For this BLAST search, the query DNA sequence is translated into its six frames and the stop-codon is replaced by an X. The respective database is then screened for similar sequences. cDNAs of its tAPx (At4g08390) and sAPx (At1g77490), GPx1 (At2g25080), GPx7 (At4g31870) and chloroplast peroxiredoxins (2CPA: At3g11630, 2CPB: At5g06290, PrxQ: At3g26060, PrxIIE: At3g52960) were used as query sequences.

2.15.1.2 BLAST searches in genome databases

To identify genes encoding APxs, Prxs, or GPxs in the sequenced genomes of *Selaginella moellendorffii*, *Physcomitrella patens*, and *Chlamydomonas reinhardtii* were screened with BLAST searches (Altschul *et al.* 1997). TBLASTX searches were performed with the *Arabidopsis* homologs of these enzymes as described for TBLASTX searches in EST databases in chapter 2.15.1.1.

2.15.1.3 BLAST searches in protein databases

The predicted APxs, Prxs, and GPxs were investigated for their similarity to *Arabidopsis thaliana* homologs in the NCBI database (http://www.ncbi.nlm.nih.gov/, RefSeq protein). The protein queries were used to screen the protein database by BLASTP searches (algorithm: BLOSUM62, threshold: 10, word size: 3, existence: 11, extension: 1)

2.15.1.4 Genome browser applications

The *Selaginella* database at JGI (http://genome.jgipsf.org/Selmo1/Selmo1.home.html) includes sequences from two distinct haplotypes. To define the identified APx, Prx, or GPx encoding sequences to be independent genes or alleles of the same gene, their genomic environments were compared as described in chapter 2.15.6. Besides this, the genome browser of http://www.cosmoss.org was used to investigate the up- and downstream regions of the *Physcomitrella patens* thylakoid-bound APx.

Gene sequences were localized within the genomes by performing BLASTN searches (algorithm: BLOSUM62, threshold: $1e^{-5}$, word size: 11). In contrast to TBLASTX searches, these BLASTs use an untranslated query nucleotide sequence to search for similar regions with the respective genome (Altschul *et al.* 1997).

2.15.2 Determination of 5'- and 3'-ends

ESTs covering the less conserved 5'- and 3'-ends were identified by performing BLASTN searches (threshold: 10, word size: 28, match/mismatch scores: 1/-2) in the respective database using the last 200 bp at the 5'- and 3'-end of each consensus sequence as query. To identify entire coding sequences of still incomplete cDNAs, 2000 bp upstream of their 5'-ends were screened for transcription start sites using DBTSS (Wakaguri *et al.* 2008). Additional undetected 5'-exons within this region of the respective genome were predicted by FEX (Solovyev *et al.* 1994) via the Softberry-interface (http://linux1.softberry.com), BLAST searches in the EMBL Plant EST database and, manually by checking for sequence characteristics of chloroplast targeting signals (summarized in Schmidt and Mishkind 1986) and putative S, T, and R rich peptides.

Afterwards, the PeroxiBase (http://peroxibase.isb-sib.ch/search.php) database (Oliva *et al.* 2009) was screened for chloroplast peroxidases as described in the results section. Besides this, cyanobacterial PrxQs and 2CPs and extra-organellar and mitochondrial APx, GPx and PrxII were retrieved from this database for phylogenetic analyses. All collected amino acid sequences were aligned using Clustal W2.0. To calculate phylogenetic trees, incomplete sequences were removed from the analysis.

2.15.3 Discrimination of putative chloroplast and non-chloroplast isoforms

Prediction of chloroplast and non-chloroplast isoforms was performed by analyzing the amino acid sequences including putative N-terminal extensions for their chloroplast targeting probability. The online tools of choice were TargetP (Emanuelsson *et al.* 2000) and ATP (Ambiguous Targeting Predictor, http://www.cosmoss.org/bm/ATP, Mitschke *et al.* 2009). The latter program is especially suited to predict a dual localization of the query protein. It was developed using the *Physcomitrella patens* as a model plant.

2.15.4 Determination of EST counts

The number of ESTs was used as a relative measure for the expression intensity. To identify all ESTs, full length cDNAs were used as queries for BLASTN searches (threshold: 1, word size: 28, match/mismatch scores: 1/-2) within the respective EST database. Additionally, the EMBL Plant EST database was screened for corresponding ESTs. The hits were counted separately for each non-identical EST cluster.

2.15.5 Calculation of GC-contents

GC-contents were calculated based on the codon usage statistics tool CHIPS via the Mobyle-webpage (http://mobyle.pasteur.fr).

2.15.6 Prediction of the gene models

Identification of exons was achieved by alignment of the EST-assembly-based consensus sequences to genomic DNA. These sequence comparisons were generated with Clustal W2.0 (Thompson *et al.* 1994, Larkin *et al.* 2007) and via BLASTN (Altschul *et al.* 1997) searches in the respective genome.

The *Selaginella moellendorffii* database combines genomes and ESTs derived from two haplotypes (Wang *et al.* 2005, Weng *et al.* 2005, Banks *et al.* 2011). The nucleic acid sequence data derived from these haplotypes differed in only few basepairs but were localized on different scaffolds. To distinguish between specific alleles and genes, the respective genomic environments were compared for their gene structures and computationally predicted gene models provided by JGI (http://genome.jgipsf.org/Selmo1/Selmo1.home.html). If the

surrounding of an analyzed gene was similar, the two found gene models were designated as alleles, otherwise as isogenes.

2.15.7 Comparison of splice sites

Positions of splice sites were compared relative to the amino acid positions in the protein alignments depicted in the results section. The splicing site within the respective codon was designated 0, 1, and 2 according to Ahmadinejad (2008).

2.15.8 Protein alignments and protein comparison

Alignments of protein amino acid sequences were generated with the publicly available online tools MUSCLE (Edgar, 2004), ClustalW2.0 (Thompson *et al.* 1994, Larkin *et al.* 2007), and MEGA 4.1 (Tamura *et al.* 2007). The protein alignment figures presented in the results section show the comparisons by MUSCLE (MUltiple Sequence Comparison by Log-Expectation) and visualized with Jalview. MUSCLE is well suited to compare amino acid sequences. It shows higher accuracy and speed than ClustalW2.0 or T-Coffee (Notredame *et al.* 2000), two other publicly available alignment tools.

2.15.9 Calculation of phylogenetic trees

Calculation of phylogenetic trees was performed based on the ClustalW2.0 alignments using the Mega 4.1 software package (Tamura *et al.* 2007). Data retrieved for neighborhood joining were compared according to minimum evolution and maximum parsimony methods. The quality of the predicted trees was tested by calculating bootstrap values based on 500 replicates. In sequence comparisons, amino acid substitutions were weighted according to the Poisson calculation and the PAM250 matrix.

2.15.10 Secondary structure prediction and 3D-structure modeling

Secondary structure analyses were performed with PredictProtein (Rost *et al.* 2004). Transmembrane helices and their lipophilicity were predicted using TMHMM (Krogh *et al.* 2001), TMPro (Ganapathiraju *et al.* 2008), and WHEEL (http://cti.itc.virginia.edu/~cmg/Demo/wheel/wheel_instructions.html). Putative in-plane membrane anchors were detected

with AmphipaSeeK (Sapay *et al.* 2006). In addition, this tool was used to confirm Predict-Protein-based protein structure analyses. 3D structures were predicted by the publicly available alignment-based modeling tool SWISS-MODEL and the SwisspdbViewer DeepView 4.0 (Guex and Peitsch 1997, Schwede *et al.* 2003, Arnold *et al.* 2006).

2.15.11 Identification of TATA-boxes

The promoter of the *Physcomitrella* thylakoid-bond APx was screened for TATA-boxes. According to Loganantharaj (2006), the consensus sequence of these transcription initiation motifs is TATAWAW, where W can be either a T or an A.

3 Results

3.1 Data mining

3.1.1 Definition of cDNA working models

The identification of homologous genes encoding chloroplast targeted antioxidant enzymes was performed by TBLASTX searches (algorhythm: BLOSUM62, threshold: 10, word size: 3) with the coding sequences of *Arabidopsis thaliana* stromal and thylakoid ascorbate peroxidases (At4g08390 and At1g77490), GPx1 (At2g25080), GPx7 (At4g31870) and chloroplast peroxiredoxins (2CPA: At3g11630, 2CPB: At5g06290, PrxQ: At3g26060, PrxIIE: At3g52960) (Altschul *et al.* 1997) as query. EST-databases of *Chlamydomonas reinhardtii* (ChlamyDB: http://www.chlamy.org and JGI: http://genome.jgi-psf.org), *Physcomitrella patens* (cosmoss: http://www.cosmoss.org/) and *Selaginella moellendorffii* (JGI: http://genome.jgipsf.org/Selmo1/Selmo1.home.html) were chosen for screening. The collected APx, GPx, and Prx ESTs were clustered based on sequence similarity using the DNA Identity Matrix/Unity matrix of ClustalW2.0 (http://www.ebi.ac.uk/Tools/clustalw2) (Thompson *et al.* 1994, Larkin *et al.* 2007) (Fig. R1). This tool allows a fast and acceptable differentiation between expected perfect matches and isogenes-dependent variations. In this first step, no respect was given to protein targeting or localization. In the next step (Fig. R1), all non-perfectly matching ESTs were excluded to analyze for gene duplication and alternative splicing. The removed EST sequences were aligned again to find putative additional clusters (Fig. R1). In the following, consensus sequences were defined for each EST cluster. These sequences were set as working models for a gene-specific class of transcripts (Fig. R1).

Besides the EST-based search and to find putatively missed paralogs or pseudogenes, the genomes were screened by TBLASTX searches with the coding sequences of *Arabidopsis* sAPx and tAPx, its GPxs and chloroplast peroxiredoxins as query (Fig. R1). The hit sequences were compared to already identified cDNAs and checked for transcription via BLASTN searches in the corresponding EST database to define a respective sequence as functional gene or pseudogene (Fig. R1).

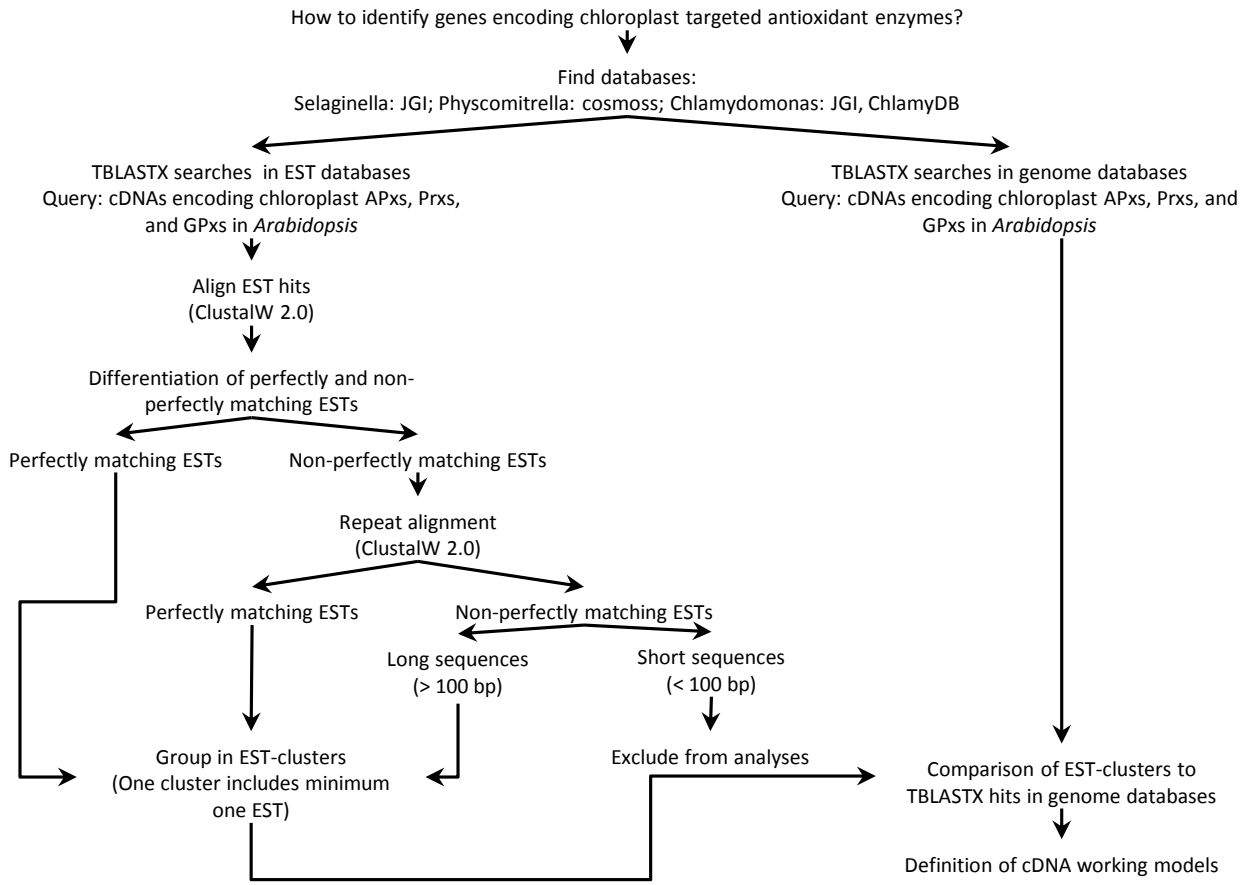

Fig. R1: Flow scheme of bioinformatic analyses for the definition of cDNA working models encoding chloroplast APxs, Prxs, or GPxs from *Selaginella moellendorffii*, *Physcomitrella patens*, and *Chlamydomonas reinhardtii*.

3.1.2 Evaluation of enzyme identity

The translated cDNA working models were analyzed for their similarity to already characterized *Arabidopsis* APxs, Prxs, and GPxs, on the one hand, and by performing BLASTP searches in the NCBI database, on the other (Fig. R2). If a predicted protein showed high similarity and presence of characteristic motifs summarized in Bréhélin *et al.* (2003), Horling *et al.* (2003), König *et al.* (2003), Kangasjärvi *et al.* (2008), Margis *et al.* (2008), and Chang *et al.* (2009), it was defined as APx, Prx, or GPx, respectively. More information about the enzyme family specific motifs will be given in the following chapters describing the identified isoforms into detail.

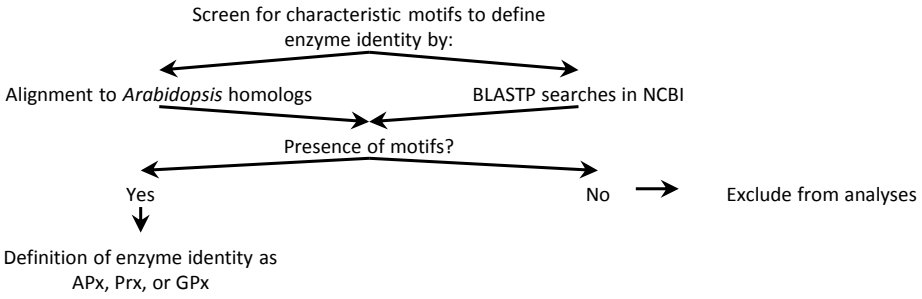

Fig. R2: Flow scheme of bioinformatic analyses. The defined *Selaginella moellendorffii*, *Physcomitrella patens*, and *Chlamydomonas reinhardtii* cDNA working models were evaluated for their enzyme identity as APx, Prx, or GPx.

3.1.3 Definition of gene models

Many of the identified working model cDNAs revealed either incomplete 3'- or 5'-termini or atypical start or stop codons. The lack of these sequence information may indicate the existence of additional exons which encode putative organellar targeting signals at the N-terminus or transmembrane anchors.

To identify the complete cDNAs, BLASTN searches in EST databases were performed with 5`- and 3`-ends of the retrieved preliminary working models as query (Fig. R3). All found ESTs were compared to the working models, checked for their similarity by using ClustalW2.0 (Thompson *et al.* 1994, Larkin *et al.* 2007), and previously defined clusters were re-defined. For each of these clusters a consensus sequence was retrieved and set as new working model (Fig. R3). For any sequence indicating a putative N-terminal or C-terminal extension the respective EST database was screened by BLASTN for so far not identified ESTs to define the entire coding sequence (Fig. R3).

For all remaining gene models without N-terminal transit peptides, the respective genomic DNA was screened 2000 bp upstream of the EST-covered region to identify start-codons and/or additional exons by DBTSS (Wakaguri *et al.* 2008) and FEX (Solovyev *et al.* 1994) (Fig. R3). Organellar targeting signals are usually localized at the N-terminus of the respective proteins. Therefore, the 2000 bp upstream of the EST-covered region were also translated into the three frames of amino acid sequences and screened not only for additional exons but also for features indicating organellar targeting sequences by hand (Fig. R3). To identify chloroplast localized APx, GPx, and Prx, the targeting probability of all predicted proteins was tested by using the publicly available online tools TargetP

(Emanuelsson *et al.* 2000) and ATP (Mitschke *et al.* 2009) (Fig. R3). Targeting probabilities were low for some of the defined cDNAs and for all predicted *Chlamydomonas reinhardtii* APxs, Prxs, and GPxs. Their N-termini were manually re-checked for the amount of hydroxylated and hydrophobic amino acids, which are highly abundant in transit peptides (Schmidt and Mishkind 1986) (Fig. R3).

Besides sequences upstream of the predicted encoding region, also 2000 bp downstream were translated into all three frames and screened for additional exons. Transmembrane helices, which anchor enzymes into membranes, are often found in the C-terminal region of proteins. The *Arabidopsis* chloroplast thylakoid-bound APx isoform represents just one example for such membrane-anchored enzymes. The probability for folding of the C-terminus of a predicted protein into a transmembrane helix was calculated by PredictProtein (Rost *et al.* 2004), TMHMM (Krogh *et al.* 2001), and TMPro (Ganapathiraju *et al.* 2008) (Fig. R3). To ingrate tightly into membranes, such helices need a highly lipophile surface. This lipophilicity of the outer helix surface was tested by WHEEL-analysis (http://cti.itc.virginia.edu/~cmg/Demo/wheel/wheel_instructions.html) (Fig. R3). If a highly lipophile helix was predicted within a yet non-EST-covered region, encoding ESTs were searched in the respective database by BLASTN (Fig. R3).

Finally, the previously predicted APx, Prx, or GPx encoding cDNAs could be designated as chloroplast or non-chloroplast targeted isoforms according to their defined C-terminus. Additionally, membrane-associated enzymes were identified due to the predicted presence of an N-terminal lipophile helix (Fig. R3). The found cDNA working models encoding chloroplast located isoforms were defined as gene models and are summarized in table R1. For more information on the amino acid sequenced of the identified organellar APxs, Prxs, and GPxs, see chapters 3.3-3.7. All obtained bioinformatic results shown in the present study were published in Pitsch *et al.* 2010.

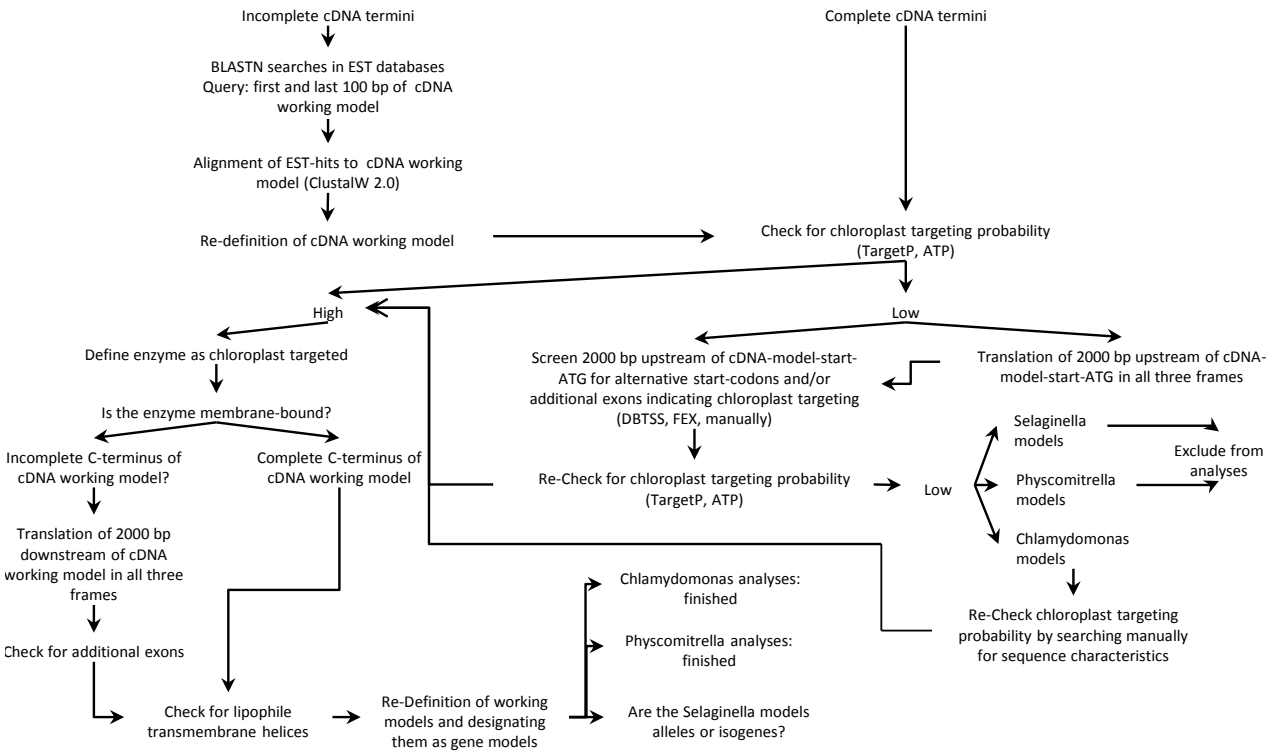

Fig. R3: Flow scheme of bioinformatic analyses for the definition of cDNA working models encoding chloroplast APxs, Prxs, or GPxs from *Selaginella moellendorffii*, *Physcomitrella patens*, and *Chlamydomonas reinhardtii*.

3.1.4 Definition of *Selaginella moellendorffi* gene models as alleles or isogenes

The JGI database combines sequences derived from two different *Selaginella* haplotypes (Wang *et al.* 2005, Weng *et al.* 2005, Banks *et al.* 2011). Hints towards the distinct haplotypes were obtained by the identification of APx, Prx, and GPx cDNAs which differed in only few base pairs. Fig. R4B shows an example for the definitions of such similar genes as alleles or isogenes.

After BLASTN searches in the genome, the only slightly dissimilar sequences revealed localization on different scaffolds pointing to the possibility that these ORFs represent either alleles or independent genes encoded in the different haplotypes. To define the identified APx, Prx, or GPx encoding cDNA working models as independent genes or alleles of the same gene, their genomic environments were compared (Fig. R4A). If the surrounding of an analyzed gene was similar, the two found gene models were designated as alleles, otherwise as isogenes. All identified *Selaginella* gene models with only few single nucleotide

polymorphisms (SNPs) encoding chloroplast which were present on two scaffold represented alleles.

A

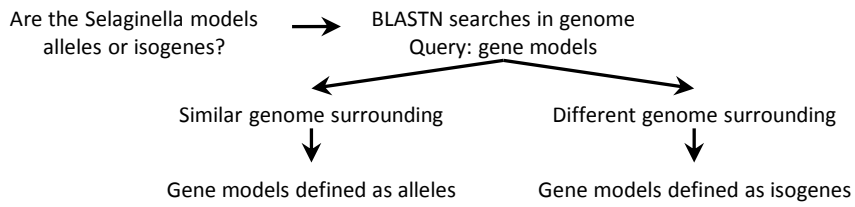

B

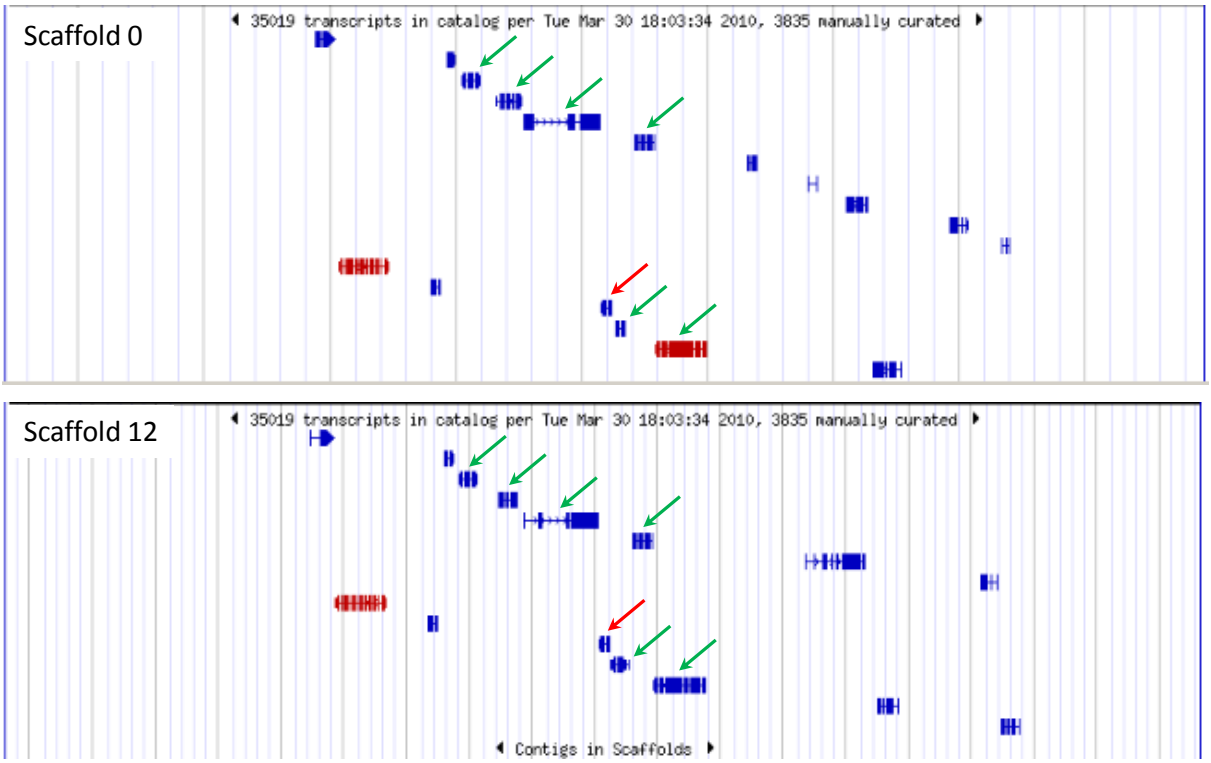

Fig. R4: A: Flow scheme of bioinformatic analyses for the re-definition of gene models from *Selaginella moellendorffii* and *Chlamydomonas reinhardtii*. B: Example for the designation of the identified *Selaginella* gene models encoding a SmGPxC as alleles or isogenes. The SmGPxC.1/2 locations on scaffold 0 (SmGPxC.1) and scaffold 12 (SmGPxC.2) are shown. SmGPxC.1/2 are indicated by red arrows. The identities of three genes to the left as well as to the right of the GPx were investigated to identify SmGPxC.1/2 as isogenes or alleles. Green arrows point to genes with equally predicted identity on both scaffolds [to the right: 1. nr_b_b_15241558 (*Arabidopsis thaliana*), 2. nr_b_b_50940087 [*Oriza sativa* (japonica cultivar-group)], 3. nr_b_b_1296955 [*Oriza sativa* (japonica cultivar-group)], to the left: 1. Phypa1_1_FilteredModels3_jgi/Phypa1_1/140302e_gw1.165.34. 1 (*Physcomitrella patens* subsp. *patens*), 2. Phypa1_1_FilteredModels3_jgi/Phypa1_1/176678 (*Physcomitrella patens* subsp. *patens*), 3. nr_b_b_63003174 (*Lemna paucicastata*)]. Since the genome surrounding on scaffolds 0 and 12 are highly similar, SmGPxC.1/2 were defined as alleles of the two different sequenced *Selaginella* haplotypes.

Table R1: Complexity and identity of APxs, Prxs, and GPxs from *Arabidopsis thaliana* (At), *Selaginella moellendorffii* (Sm), *Physcomitrella patens* (Pp), and *Chlamydomonas reinhardtii* (Cr). To determine the expression level, for *Arabidopsis*, array data were collected while for the other organisms, gene specific ESTs were counted.

Enzyme (chloroplast-targeted)	Referred to as	Length [aa]	ATP / TargetP values	Expression level	Gene code / Location in genome
Arabidopsis thaliana					
Thylakoid ascorbate peroxidase	AttAPx	426	0.62140 / 0.983	403.91	At1g77490
Stromal ascorbate peroxidase	AtsAPx	372	0.86202 / 0.864	328.86	At4g08390
2-Cys-Peroxiredoxin	At2CPA	267	0.49641 / 0.988	3184.8	At3g11630
2-Cys-Peroxiredoxin	At2CPB	274	0.71435 / 0.971	1222.76	At5g06290
Peroxiredoxin Q	PrxQ	217	0.82014 / 0.904	1835.08	At3g26060
Peroxiredoxin type II	PrxIIE	265	0.63576 / 0.936	861.2	At3g52960
Glutathione peroxidase	AtGPx1	237	0.53344 / 0.970	986.38	At2g25080
Glutathione peroxidase	AtGPx7	234	0.74449 / 0.969	66.18	At4g31870
Selaginella moellendorffii					
Thylakoid ascorbate peroxidase	SmtAPx.1	401	0.49697 / 0.916	9	7: 2423527-2425329
Thylakoid ascorbate peroxidase	SmtAPx.2	407	0.58844 / 0.704	10	36: 1259197-126991
Stromal ascorbate peroxidase	SmsAPx.1	349	0.58519 / 0.689	3	65: 2501511-248461
Stromal ascorbate peroxidase	SmsAPx.2	349	0.58519 / 0.690	6	72: 297944-296262
2-Cys-Peroxiredoxin	Sm2CPA.1	275	0.53959 / 0.943	67	96: 53633-52442
2-Cys-Peroxiredoxin	Sm2CPA.2	275	0.53959 / 0.945	60	46: 1467726-1468926
2-Cys-Peroxiredoxin	Sm2CPB.1	323	0.44061 / 0.653	0	34: 503029-503989
2-Cys-Peroxiredoxin	Sm2CPB.2	317	0.44061 / 0.725	0	18: 2038503-2040005
Peroxiredoxin Q	SmPrxQA.1	221	0.51415 / 0.930	21	21: 1420112-1421465
Peroxiredoxin Q	SmPrxQA.2	221	0.54575 / 0.928	7	31: 310820-309427
Peroxiredoxin Q	SmPrxQB.1	185	0.82512 / 0.383	0	51: 178527-179338
Peroxiredoxin Q	SmPrxQB.2	185	0.82512 / 0.410	0	55: 755418-756216
Peroxiredoxin type II	SmPrxII.1	241	0.60416 / 0.975	12	4: 3124723-3124001
Peroxiredoxin type II	SmPrxII.2	241	0.47769 / 0.954	15	91: 178039-179068
Glutathione peroxidase	SmGPxA.1	253	0.60188 / 0.523	26	107: 189067-190114
Glutathione peroxidase	SmGPxA.2	253	0.60188 / 0.523	26	40: 1392048-1393091
Glutathione peroxidase	SmGPxB.1	208	0.47597 / 0.012	8	57: 785613-784714
Glutathione peroxidase	SmGPxB.2	208	0.67471 / 0.001	0	0: 6625208-6626109
Glutathione peroxidase	SmGPxC.1	169	0.46928 / 0.111	5	0: 5532358-5531571
Glutathione peroxidase	SmGPxC.2	169	0.46928 / 0.111	1	12: 261185-260399

Enzyme (chloroplast-targeted)	Referred to as	Length [aa]	ATP / TargetP values	Expression level	Gene code / Location in genome
Physcomitrella patens					
Thylakoid ascorbate peroxidase	PptAPx	441	0.49166 / 0.842	161	424: 212264-213717
2-Cys-Peroxiredoxin	Pp2CPA	283	0.52994 / 0.968	48	30: 2368256-2370888
2-Cys-Peroxiredoxin	Pp2CPB	n. a.	0.42121 / 0.945	n. a.	1st part: scaff. 1139; 2nd part: scaff. 257
Peroxiredoxin Q	PpPrxQA	220	0.30874 / 0.809	13	233: 663095-664648
Peroxiredoxin Q	PpPrxQB	220	0.62288 / 0.977	7	30: 1873696-1872791
Peroxiredoxin Q	PpPrxQC	220	0.63957 / 0.970	13	95: 290862-289423
Peroxiredoxin type II	PpPrxIIA	266	0.54575 / 0.898	30	52: 1909032-1908279
Peroxiredoxin type II	PpPrxIIB	249	0.47646 / 0.688	24	1: 1454912-1454166
Glutathione peroxidase	PpGPxA.1	248	0.43328 / 0.869	10	115: 583295-585354
Glutathione peroxidase	PpGPxA.2	258	0.43328 / 0.869	8	115: 583295-585241
Glutathione peroxidase	PpGPxB	289	0.53257 / 0.889	0	313:1 71870-174548
Chlamydomonas reinhardtii					
Stromal ascorbate peroxidase	CrsAPxA	327	0.44733 / 0.360	JGI:5; ChlamyDB:1	7: 1855857-1852628
Stromal ascorbate peroxidase	CrsAPxB	376	0.44733 / 0.24	0	35: 346143-341772
2-Cys-Peroxiredoxin	Cr2CPA	236	0.30495 / 0.669	JGI:121; ChlamyDB:10	3: 2066498-2065265
2-Cys-Peroxiredoxin	Cr2CPB	199	0.15565 / 0.014	JGI:19; ChlamyDB:5	5: 332991-334500
2-Cys-Peroxiredoxin	Cr2CPC	184	0.13318 / 0.033	0	105: 86681-89539
Peroxiredoxin Q	CrPrxQ	197	0.44733 / 0.407	0	8: 1690093-1692044
Peroxiredoxin type II	CrPrxIIC	195	0.42189 / 0.105	JGI:3; ChlamyDB:2	1: 570401-572219
Glutathione peroxidase	CrGPxA	202	0.50985 / 0.057	0	7: 731625-733049
Glutathione peroxidase	CrGPxB	259	0.65448 / 0.649	0	95: 208056-205010
Glutathione peroxidase	CrGPxC	212	0.42097 / 0.297	JGI:2; ChlamyDB:0	4: 1977798-1976386

3.2 Comparison of predicted sequences with data resources of PeroxiBase

PeroxiBase, a novel database summarizes EST-assembly based predictions for plant peroxidases of various cellular compartments (Oliva *et al.* 2009). To find still not identified gene models for chloroplast targeted APxs, Prxs, and GPxs in *Selaginella moellendorffii*, *Physcomitrella patens*, and *Chlamydomonas reinhardtii*, the predicted sequences were compared to the available PeroxiBase data. For 22 of the 45 ORFs described here (Table R1), entries were listed in PeroxiBase. In contrast to the almost complete coverage of *Arabidopsis*, *Physcomitrella*, and *Chlamydomonas* chloroplast peroxidases, all except two of the chloroplast peroxidases of *Selaginella* were newly predicted in this study (Table R1). In addition, one (possibly silent) *Chlamydomonas* ORF and two *Physcomitrella* PrxII were newly predicted by the bioinformatic analyses presented here. Based on EST-assembly analyses described above, the N-termini of one *Physcomitrella* chloroplast APx (PeroxiBase-Entry 2497) and of one *Selaginella* 2CP (PeroxiBase-Entry 6217) could be corrected. Furthermore, the C-terminus of a *Physcomitrella* 2CP (PeroxiBase-Entry 6396), which is encoded by an incompletely assembled genome domain within the cosmoss database, could be extended by combination of sequence information split on two sequencing units. Additionally, so far not PeroxiBase-covered short sequence traces were inserted in the entries representing *Physcomitrella* PrxQC (PeroxiBase-entry 6324) and *Chlamydomonas* sAPxB (PeroxiBase-entry 2286). Besides this, the amino acid sequence of CrGPxA was corrected by addition of missing G137.

The bioinformatic studies presented above led to the prediction of 10 ORFs for chloroplast peroxidases encoded in each of the two sequenced haplotypes of *Selaginella moellendorffii*, 11 chloroplast peroxidase ORFs in *Physcomitrella patens*, and 10 in *Chlamydomonas reinhardtii* (Table R1). These gene models were compared to six well described *Arabidopsis* chloroplast peroxidases (Jespersen *et al.* 1997, Bréhélin *et al.* 2003, Horling *et al.* 2003, Navrot *et al.* 2006, Petersson *et al.* 2006, Chang *et al.* 2009) and their specific sequence characteristics will be described in the following chapters.

3.3 Ascorbate peroxidases

3.3.1 Gene copy number and protein targeting

In *Arabidopsis thaliana*, the two chloroplast APx isoforms are encoded by distinct genes, At4g08390 (AtsAPx) and At1g77490 (AttAPx) (Jespersen *et al.* 1997). Within the genomes of tobacco, spinach, and pumpkin, a single gene codes for both, sAPx and tAPx. The two enzymes result from alternative splicing (Ishikawa *et al.* 1996, Mano *et al.* 1997, Yoshimura *et al.* 1999). Rice in contrast, reveals three sAPx genes (OsAPx5-7, Teixeira *et al.* 2004) but only one gene encoding a tAPX (OsAPx8). These examples exhibit high dynamics in the gene copy number during time.

The presence of both isoforms is beneficial for plants since thylakoid-bound APxs detoxify hydrogen peroxide directly at the site of production while stromal APxs scavenge ROS which escaped tAPx (Asada 1999). Additionally, these antioxidant defense enzymes are more effective in converting hydrogen peroxide than peroxiredoxins (Prxs) (Kitajima *et al.* 2008, Kitajima 2008). Additionally, sAPxs and tAPxs may have different impacts on the chloroplast antioxidative defense during plant development (Kangasjärvi *et al.* 2008, Maruta *et al.* 2010).

After removal of the extraplastidic isoforms, EST analysis of two haplotypes of *Selaginella moellendorffii* resulted in four gene models encoding chloroplast APxs (Table R1). Two of them encode soluble isoforms (SmsAPx.1, SmsAPx.2) and two APxs anchored to membranes by C-terminal helices (SmtAPx.1, SmtAPx.2). The sequences of the SmsAPx models differed only in 7 nucleotides, while the SmtAPxs revealed nine distinct single nucleotide polymorphisms (SNPs). Comparison of the gene environment within the two *Selaginella* haplotype genomes revealed the predicted sequences being surrounded by the same genes. Thus, the predicted similar gene models represent homologous genes from these two haplotypes. It was concluded that each haplotype encodes one stromal (SmsAPx) and one thylakoid APx (SmtAPx) (Table R1).

In contrast to *Arabidopsis thaliana* and *Selaginella moellendorffii*, the bryophyte *Physcomitrella patens* encodes only one APx (Table R1). The amino acid sequence of its C-terminal extension gives strong indications for a 22 amino acid long transmembrane helix (probability = 82.8% according to TMHMM, position aa417-aa440 in the 441 amino acid long pre-protein, aa458-aa480 in Fig. R7). This led to the definition of the single chloroplast *Physcomitrella* APx as a thylakoid membrane localized isoform (PptAPx). In the NCBI database, the sequence tag is annotated as stromal APx (BQ042082) since this automated

prediction lacks the sequence information on the transmembrane anchor. The EST cluster analyses gave no indication for alternative splicing, suggesting that in *Physcomitrella patens*, all chloroplast APx activity is thylakoid-bound and that the moss does not encode any soluble APx isoform targeted to this organelle.

To the contrary of *Physcomitrella*, the green algae *Chlamydomonas reinhardtii* genome revealed two gene models, both encoding stromal ascorbate peroxidases (CrsAPxA, CrsAPxB). While the transcription of CrsAPxA was indicated by ESTs, the second gene model did not show any EST coverage. In addition to the two predicted *Chlamydomonas* APxs reported here, PeroxiBase lists a third isoform with similarities to putative chloroplast APx (ID 2805). This model was excluded from all analyses, since parts of the catalytic site, *e. g.* aa322-aa380 (numbers relative to alignment shown in Fig. R7) are strongly modified, which points to the enzyme having no ascorbate peroxidase function.

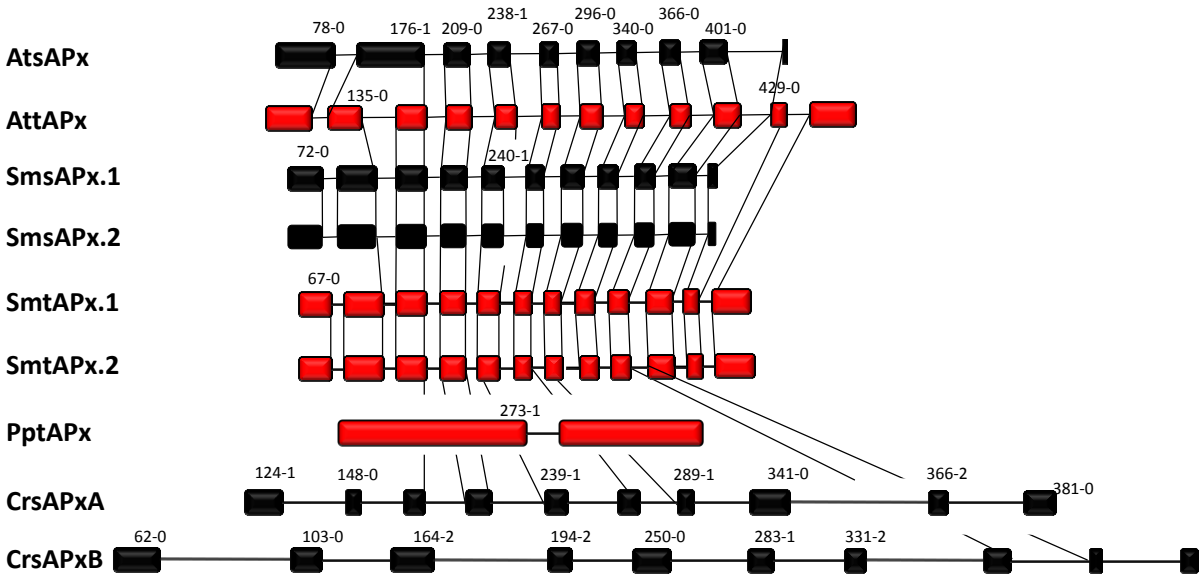

Fig. R5: Relative exon and intron lengths of chloroplast APx in *Arabidopsis thaliana* (At), *Selaginella moellendorffii* (Sm), *Physcomitrella patens* (Pp), and *Chlamydomonas reinhardtii* (Cr). tAPx are shown in red, sAPX in black. The vertical lines connect corresponding splice sites. The numbers represent positions of corresponding amino acids in the alignment shown in Fig. R7 and the relative splice sites within the corresponding codon.

3.3.2 Exon-intron structure

Evolution primarily selects for the functionality of proteins. Most non-sense mutations get discarded. Intron insertions, deletions, and splice site shifts can be tolerated more easily. Consequently, analysis of gene structures can reveal additional information on the phylogenetic relationship between genes of different organisms (Paquette *et al.* 2000). Fig. R5 shows all identified chloroplast APx gene models and a comparison of their splicing sites. The exon-ends were labeled according to Ahmadinejad (2008): their location within the amino acid sequence alignment shown in Fig. R7 and the position within the respective triplet code for the specific amino acid. Conserved splicing sites were indicated by links.

In *Arabidopsis thaliana*, the coding sequence of AtsAPx is split into 10 exons and the AttAPx is encoded by 12 exons (Fig. R5). Nine of the splice sites are conserved demonstrating that the two APx genes are of common origin. The stop codon of AtsAPx is replaced by a glutamate codon in AttAPx and the open reading frame extents into an additional exon (exon 12, Fig. R5) encoding the 22 amino acids long C-terminal transmembrane helix. In AttAPx an additional intron is inserted in the 0-position of the codon for aa135. This intron is missing in AtsAPx (Fig. R5).

The exon-intron-structure of *Selaginella* tAPx resembles that of *Arabidopsis* tAPx in both haplotypes. The splice sites are widely conserved to *Arabidopsis* tAPx from the second site onwards (Fig. R5). Like in AttAPx, the sequence encoding aa82-aa209 (Fig. R7) is split into two exons (Fig. R5). The similar gene structure indicates that SmtAPx, SmsAPx, and AttAPx evolved very likely from a common ancestor gene. As species-specific variation, the introns are all shorter in *Selaginella* than in *Arabidopsis*.

PptAPx, which is the only chloroplast targeted APx isoform encoded in the *Physcomitrella patens* genome, has the most atypical gene structure within the group of analyzed genes. The PptAPx gene model comprises only two exons. Its intron is located approximately in the mid of the transcript at a non-conserved position (273-1, relative to the amino acid position depicted in Fig. R7) (Fig. R5). Consequently, the thylakoid-bound APx isoform is not directly related to the described APx genes from the other analyzed species.

In the green alga *Chlamydomonas reinhardtii*, the two sAPx genes are each encoded by 10 exons (Fig. R5). The introns are much longer than in the *Arabidopsis thaliana* homolog increasing the size of a respective gene by a factor of 1.5 - 2. In CrsAPxA, from the third exon downstream, four splice sites are conserved with the *Arabidopsis thaliana* APxs and two

differ by only one codon (Fig. R5). For CrsAPxB, gene structure analyses revealed only one conserved splice site (aa366-0) (Fig. R5) confirming the less related nature of this gene.

3.3.3 Expression analyses

EST data indicate that the identified *Selaginella moellendorffii* ascorbate peroxidases are transcribed (Table R1). For its stromal APx less ESTs could be found than for the thylakoid-bound isoform. BLAST searches with the *Physcomitrella* gene model encoding a chloroplast APx in the respective database hit 161 ESTs with an e-value of 0 (Table R1). The *Chlamydomonas* isoforms, revealed only few ESTs for CrsAPxA, still indicating its transcription. For CrsAPxB in contrast, no transcript data were found (Table R1).

Besides collecting EST data for predicted APx genes RNA was isolated from *Chlamydomonas reinhardtii*, *Selaginella moellendorffii* and *Physcomitrella patens* and transcribed into cDNA. Subsequently, the cDNAs were tested for sAPx or tAPx expression by saturating PCR (40 cycles at optimal T_m) with primers binding specifically to the gene sequences encoding the N- and C-termini of a respective mature protein. In all analyses, single products with predicted lengths were amplified (888 bp for CrsAPxA, 900 bp for CrsAPxB, 1073 bp for PptAPx, 825 bp for SmsAPx, and 1011 bp for SmtAPx, Fig. R6). This confirmed the presence of all predicted gene models (Fig. R5) and demonstrated their expression *in planta*, even for the not-EST-covered CrsAPxB.

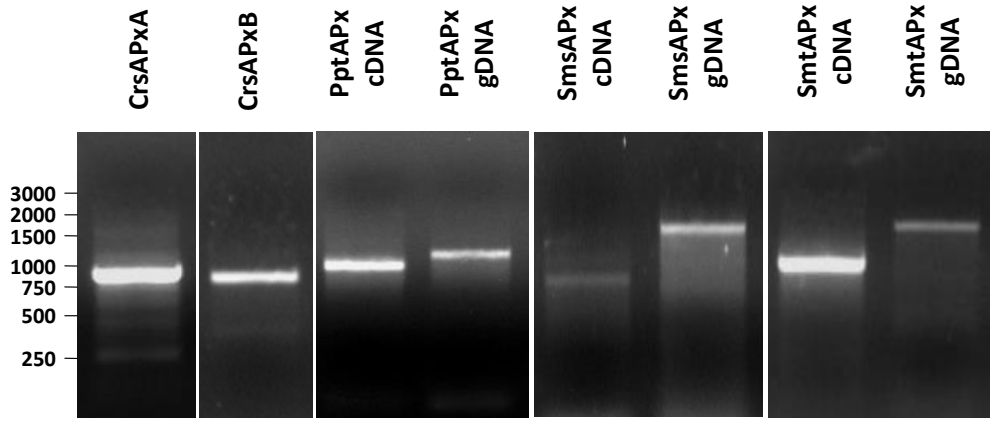

Fig. R6: PCR amplification of full-length genomic DNA (gDNA) and cDNA fragments encoding the predicted stromal and thylakoid-bound ascorbate peroxidases in *Chlamydomonas reinhardtii*, *Physcomitrella patens*, and *Selaginella moellendorffii* proving the predicted cDNA lengths. The PCRs were performed by Benjamin Witsch under the author's supervision.

3.3.4 Characteristics of the predicted proteins

The ascorbate peroxidases encoded by the identified gene models revealed to be highly similar. They showed 69-80 % identical amino acids and similarities of up to 89 % (Table R2). The only exception represented CrsAPxB with only 46 % identical and 60 % similar amino acids (Table R2). In total, 63-79% amino acid identity for sAPx and 69-79% for tAPx (Table R2) reflect a high overall similarity between *Arabidopsis*, *Selaginella*, and *Physcomitrella* chloroplast APx.

Table R2: Amino acids identity and similarity of predicted core ascorbate peroxidases from *Selaginella moellendorffii*, *Physcomitrella patens*, and *Chlamydomonas reinhardtii* to their homologs in *Arabidopsis thaliana* (Accession numbers: AtsAPx: At4g08390, AttAPx: At1g77490, aa125-aa401 in Fig. R7).

Enzyme	**Identity to *A. thaliana* homolog**	**Similarity to *A. thaliana* homolog**
SmsAPx.1/2	79/79 %	89/89 %
CrsAPxA	63 %	75 %
CrsAPxB	46 %	60 %
SmtAPx.1/2	79/80 %	87/87 %
PptAPx	69 %	82 %

However, the enzymes also show species specific differences. Besides all similarities SmsAPx shows to its homologs, this enzyme has an extended acidic and hydroxylated C-terminus (DESTS, aa406-aa410 in Fig. R5). Its sequence shows no homology to the C-terminus of any tAPx or sAPx in the other identified models (Fig. R5). Consequently, it is a specific extension of the *Selaginella* stromal APx.

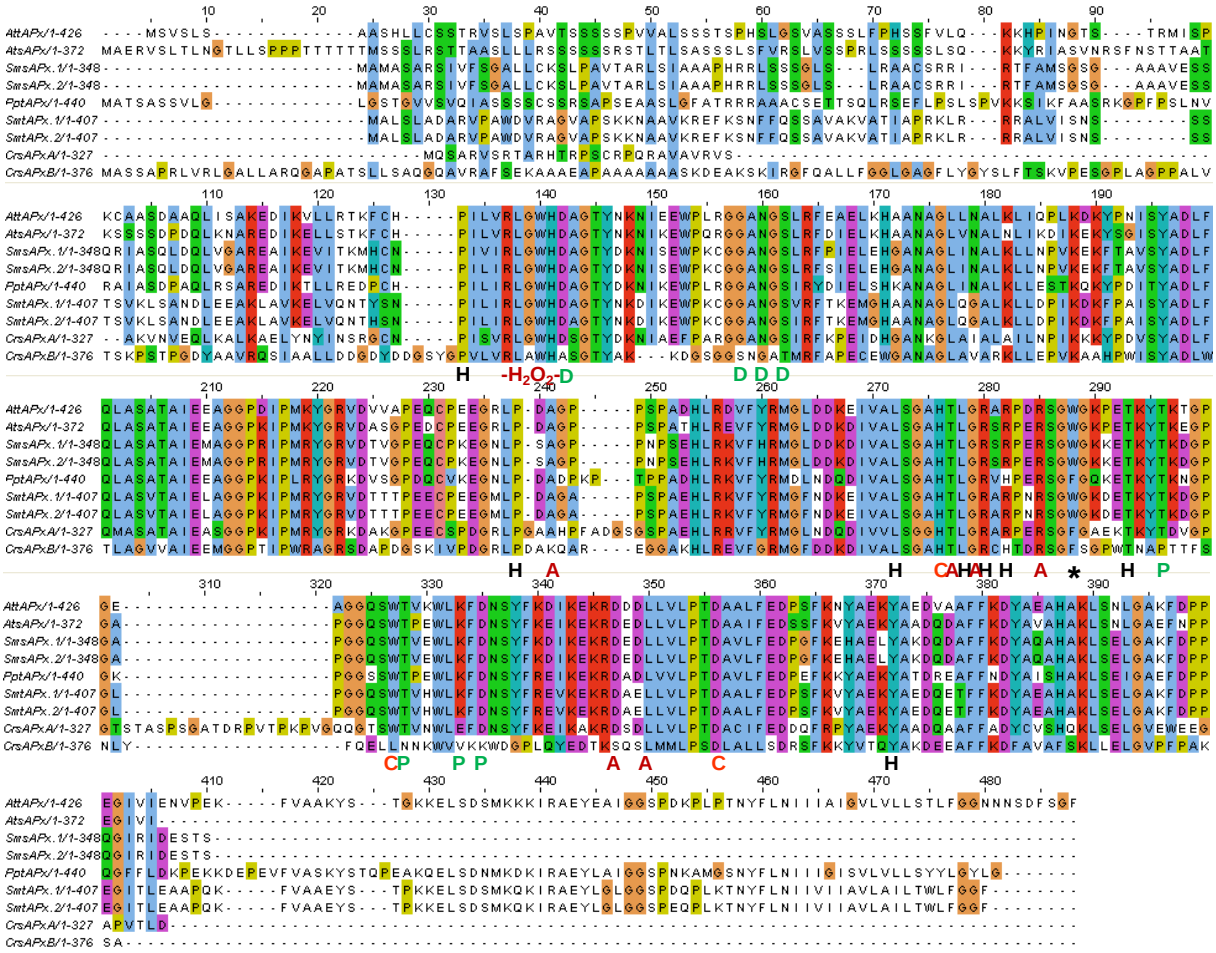

Fig. R7: Comparison of ascorbate peroxidase amino acid sequences. Amino acid sequence alignment of ascorbate peroxidases (APx) from *Arabidopsis thaliana* (At), *Selaginella moellendorffii* (Sm), *Physcomitrella patens* (Pp) and *Chlamydomonas reinhardtii* (Cr). The label "H_2O_2" marks the H_2O_2-binding site, "C" the amino acids involved in formation of the catalytic site, "P" the proximal and "D" the distal cation binding site and "H" the heme binding amino acids.

Many not N- or C-terminally localized amino acids conserve the chemical properties of a respective protein (Fig. R7). One example is E341, which is replaced by the also acidic amino acid D in both SmsAPx and AttAPx. S195 and is substituted by T and L351 by V in PptAPx.

Among the defined chloroplast targeted APxs, the amino acid residues forming the catalysis triad (H276, D356, and W327) are conserved in all identified proteins (Fig. R8), except CrsAPxB. Beside these, all proteins also have R137, W140, and H141 in common (Fig. R7), which coordinate the H_2O_2 molecule in the active site (Wada *et al.* 2003). In response to excess H_2O_2, W140 can crosslink with the heme, which irreversibly inhibits enzyme activity (Kitajima *et al.* 2007). Regarding the heme binding site, in *Physcomitrella* tAPx and *Chlamydomonas* sAPxB position R282 is replaced by an H. This exchange is usually rather found in many cytosolic than plastid APx isoforms and is suggested to prevent hydrogen

peroxide-dependent decomposition of the APx compound I in absence of ascorbate (Miyake and Asada 1996, Wada *et al.* 2003).

All other amino acids important for heme binding (P133, P238, L272, H276, L278, G279, R280, S286, and Y372, labeled "H" in Fig. R7, Raven 2003, Smith and Veitch 1998) are conserved within *Arabidopsis*, *Selaginella*, *Physcomitrella*, and *Chlamydomonas*. In general, ascorbate peroxidases bind one or two cations on the protein surface, which are involved in heme coordination (Wada *et al.* 2003). The distal cation binding site (D142, G158, N160, S162, labeled "D" in Fig. R7) is conserved in all APxs encoded by transcribed genes. In the proximal cation binding pocket (T296, T328, K333 and D335, labeled "P" in Fig. R7). K333 is exchanged by E in CrsAPxA. The higher number of negative charges provides a stronger ionic interface for the potassium ion. Superimposition of the modeled structure of CrsAPxA with AtsAPx (Fig. R8) shows that two short insertions (aa244-aa248, aa303-aa321 in Fig. R7) form loops, designated "Evolutionary VAriable LOops I and II" (EVaLo I: aa244-aa248; EVaLo II: aa303-aa321), on the protein surface.

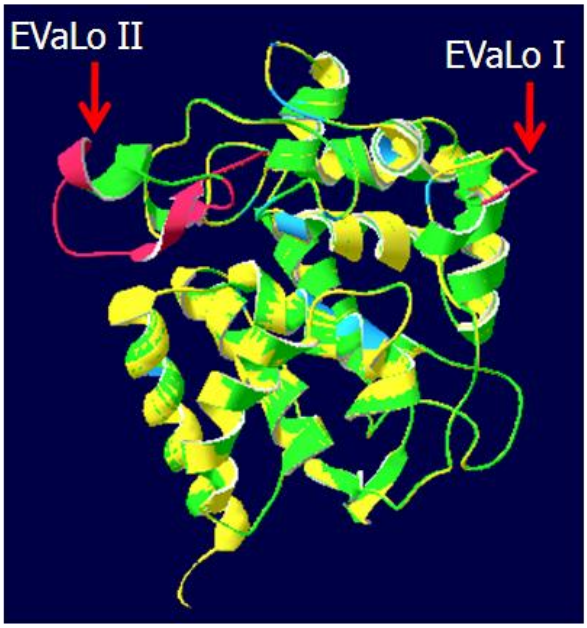

Fig. R8: Superimposition of AtsAPx (yellow) and CrsAPxA (green) structures. The two loops formed by the insertions aa244-aa248 (EVaLo I) and aa303-aa321 (EVaLO II) are shown in red.

Similar to the amino acids involved in heme coordination, the residues crucial for ascorbate binding (T277, A241, G279, R285, D347, and L350, labeled "A" in Fig. R7, Smith and Veitch 1998, Raven 2003, Wada *et al.* 2003) are widely conserved in the investigated species. In addition, several other residues (*e. g.* L138, G144, T145, Y146, K148, I150, E152, W153,

P154) also revealed to be shared by all identified enzymes (Fig. R8). The most prominent amino acid exchange is represented by the replacement of W288 by F in CrsAPxA, CrsAPxB, and PptAPx. This substitution has been published to be responsible for the elevated ascorbate specificity shown by chloroplast APxs in comparison to cytosolic isoforms (Jespersen *et al.* 1997).

3.3.5 Phylogenetic comparison

All ascorbate peroxidases encoded by the defined gene models cluster with chloroplast isoforms (Fig.s R9-R11), except CrsAPxB. Chloroplast APxs from lower and higher plants group separately. Although representing a less developed organism than *Selaginella*, the moss *Physcomitrella* encodes an APx which is closer related to *Arabidopsis*. This stands in contrast to its atypical gene structure and the total protein similarity shown in table R2. The *Selaginella* APxs showed 89 % (SmsAPx) and 87 % (SmtAPx) of similar amino acids while PptAPx revealed only 82 %. In general, the isoforms encoded by the investigated lower plants cluster together indicating that they are closer related to each other than to the higher seed plant APxs (Fig.s R9-R11). The only exception from this is represented by the *Chlamydomonas reinhardtii* sAPxB isoform. This enzyme is more homologues to the ascorbate peroxidases from fungi and non-green algae (non-chlorobionts) listed in PeroxiBase and clusters with putative extra-organellar APxs (Fig.s R9-R11). This may indicate that CrsAPxB represents an ancient antioxidative enzyme dating to times before streptophytes and chlorophytes had separated. Additionally, it might not be targeted to chloroplasts. According to sequence homology, CrsAPxB was classified as a hybrid ascorbate-cytochrome c peroxidase (Entry 2286). All this may explain, why CrsAPxB clusters far apart from the other identified and *Arabidopsis* chloroplast APxs.

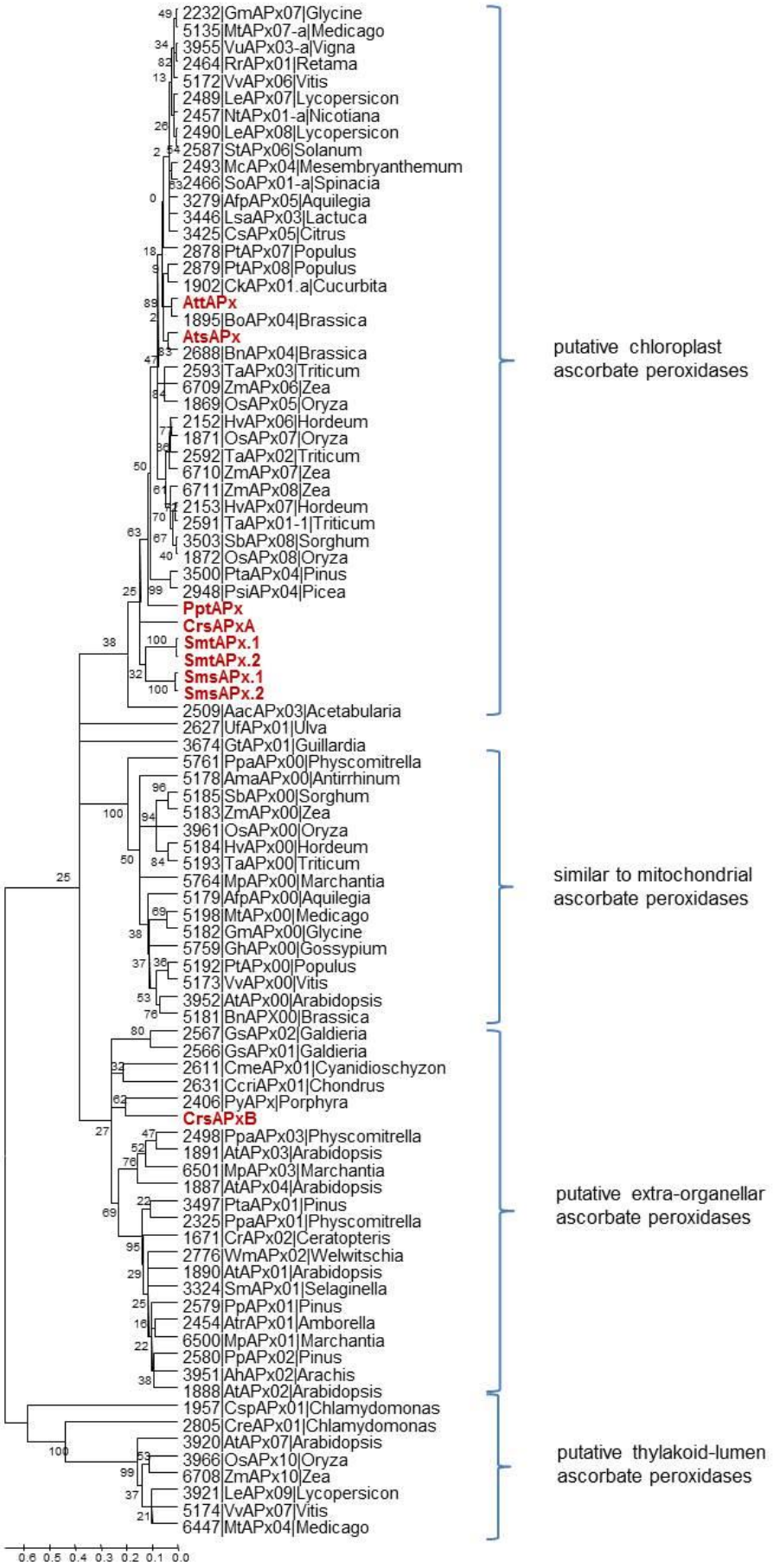

Fig. R9: Neighbor joining phylogenetic tree of APx proteins. The proteins depicted in Fig. R7 are marked in red. They are compared to all putative full-length organellar APxs listed in PeroxiBase and a selection of extra-organellar APxs. For all PeroxiBase-data, the database IDs were used. The numbers represent bootstrap values for the branches as calculated based on 500 bootstraps. Tree calculation was performed by Prof. Dr. Margarete Baier.

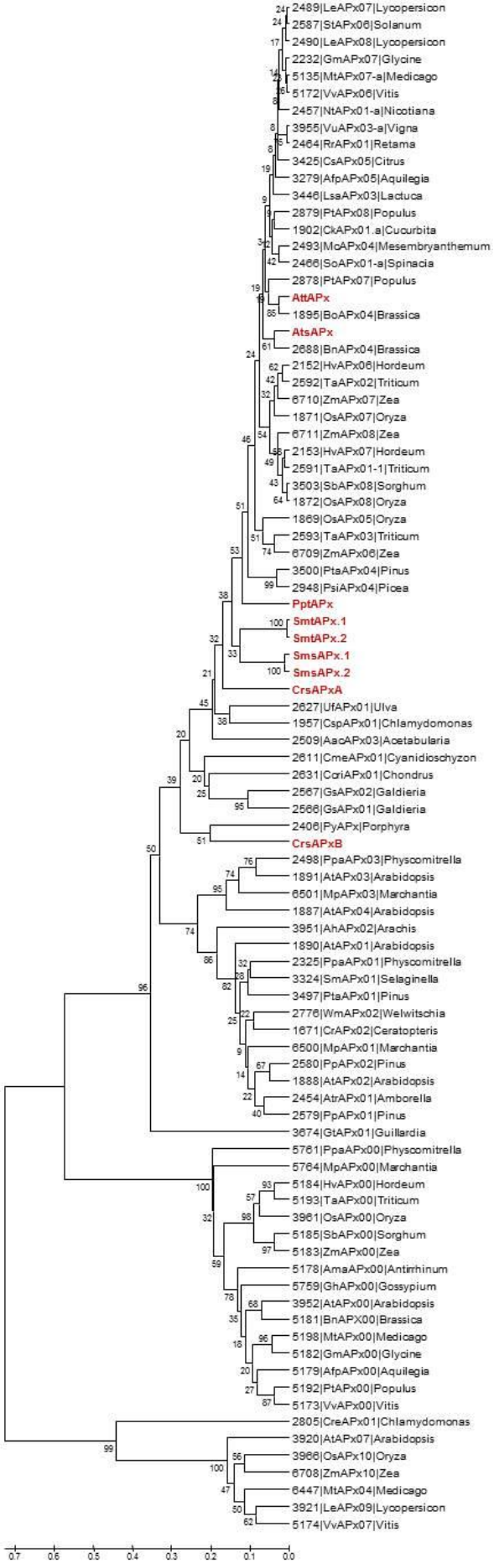

Fig. R10: Maximum parsimony phylogenetic tree of APx proteins. The proteins depicted in Fig. R7 are marked in red. They are compared to all putative full-length organellar APxs listed in PeroxiBase and a selection of extra-organellar APxs. For all PeroxiBase-data, the database IDs were used. The numbers represent bootstrap values for the branches as calculated based on 500 bootstraps. Tree calculation was performed by Prof. Dr. Margarete Baier.

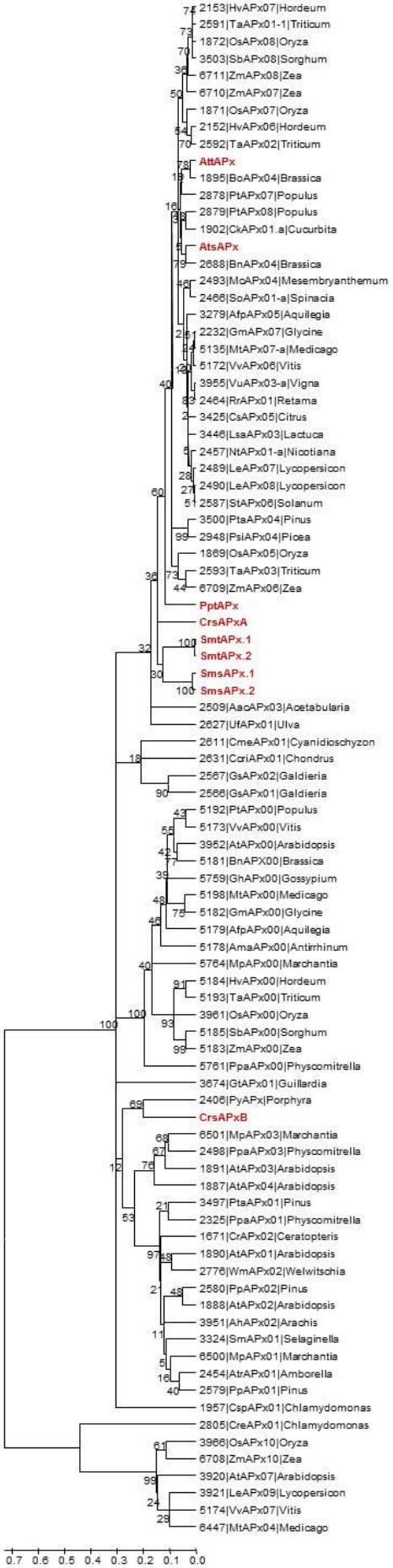

Fig. R11: Minimum evolution phylogenetic tree of APx proteins. The proteins depicted in Fig. R7 are marked in red. They are compared to all putative full-length organellar APxs listed in PeroxiBase and a selection of extra-organellar APxs. For all PeroxiBase-data, the database IDs were used. The numbers represent bootstrap values for the branches as calculated based on 500 bootstraps. Tree calculation was performed by Prof. Dr. Margarete Baier.

3.4 2-Cys peroxiredoxins

3.4.1 Gene copy number and protein targeting

The two haplotypes of *Selaginella moellendorffii* encode two pairs of almost identical 2CP, each (Sm2CPA.1/2, Sm2CPB.1/2). According to the information presently provided by the *Selaginella* database, Sm2CPB start-codons were predicted corresponding to positions 118 or 145 (relative to the positions in Fig. R13) and lacking the N-terminal extension with chloroplast targeting probability. A homologous, but incomplete putative N-terminal extension was found for Sm2CPB.2 (Fig. R13).

Alike *Arabidopsis thaliana*, the *Physcomitrella patens* genome encodes two 2CPs (Pp2CPA, Pp2CPB, Table R1, Horling *et al.* 2003). Their N-terminal targeting signals indicate that both isoforms are targeted to chloroplasts. Due to a gap between the genome scaffolds 1139 and 257 in the cosmoss database, no gene model was predictable for Pp2CPB.

In contrast to the other plant species investigated, the genome of *Chlamydomonas reinhardtii* revealed three open reading frames for 2CPs (Cr2CPA, Cr2CPB, Cr2CPC) (Table R1). Cr2CPA is identical to PRX1 and Cr2CPB to PRX2, which were previously described by Dayer *et al.* (2008). The deduced Cr2CPA protein sequence shows a typical N-terminal chloroplast targeting signal. On the contrary, the N-terminus of Cr2CPB is exceptionally short if compared to 2CP from other plants (Fig. R13). The protein was previously predicted to be cytosolic (or flagellar) (Dayer *et al.* 2008). Before Dayer *et al.*'s publication (2008), no non-chloroplast targeted 2CP isoform had been known. Thus, to identify additional exons encoding a putative targeting transit peptide the genome sequence upstream of the Cr2CPB start-ATG was screened. Since, in general and as mentioned before for APxs, the identified *Chlamydomonas* genes include longer introns than those of *Arabidopsis* and *Selaginella* (see *e. g.* Fig. R5 and R12), not only 2000 bp but 4000 bp upstream were included in the analysis. No indications were found for a putative chloroplast targeting signal. As published for the small subunit of ribulose-1,5-bisphosphate carboxylase oxygenase (RbcS) and light harvesting complex II (LHCII) subunits, protein import into chloroplasts is strongly regulated by localized translation in *Chlamydomonas* (Uniacke and Zerges 2009). These proteins show clear chloroplast targeting signals in higher plants. In the green algae *Chlamydomonas reinhardtii*, targeting to this organelle does not necessarily require strong chloroplast import signals. Nevertheless, the location of Cr2CPB remains uncertain and its predicted low chloroplast targeting probability (Table R1, Dayer *et al.* 2008) may indicate that the Cr2CPB

gene, although only weakly expressed, may encode the first identified plant non-chloroplast 2CP.

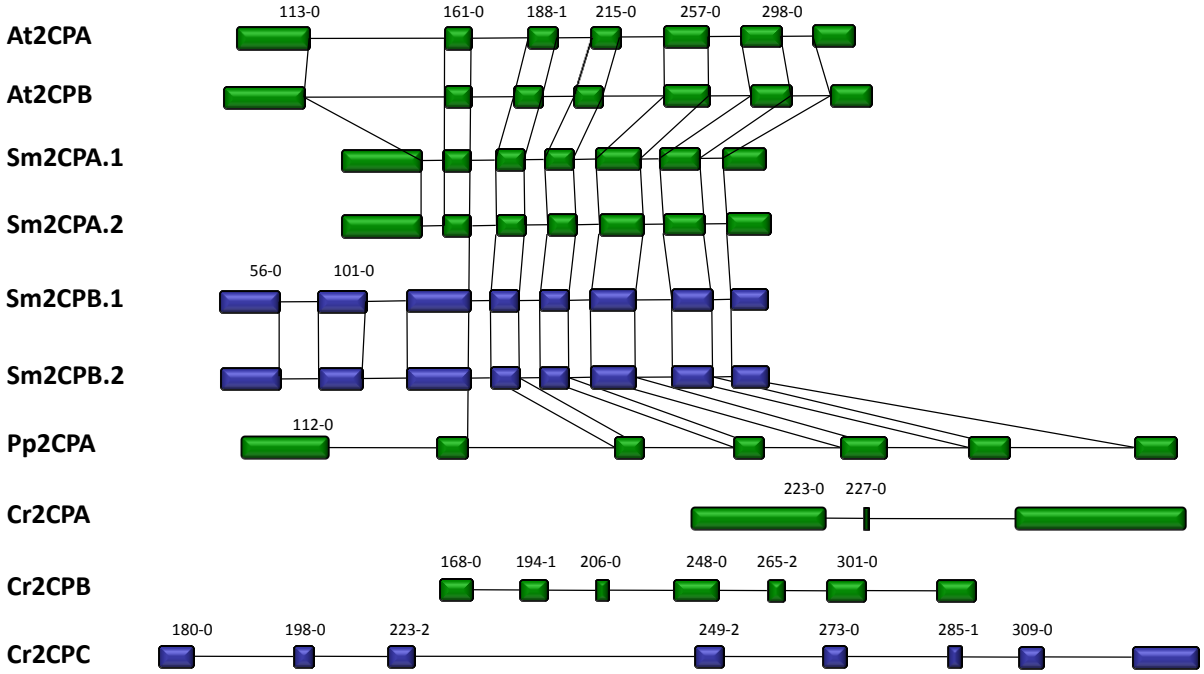

Fig. R12: Proportional comparison of the gene structures of 2CP in *Arabidopsis thaliana* (At), *Selaginella moellendorffii* (Sm), *Physcomitrella patens* (Pp), and *Chlamydomonas reinhardtii* (Cr). EST covered 2CP genes are shown in green, putatively non-expressed in blue. The vertical lines connect corresponding splice sites. The numbers represent positions of corresponding amino acids in the alignment shown in Fig. R13 and the relative splice sites within the corresponding codon.

3.4.2 Exon-intron structure

The gene structures encoding the defined chloroplast targeted 2CP isoforms were analyzed by comparison of cDNA sequences with genomic DNA (Fig. R12). The two *Arabidopsis thaliana* 2CPs show very similar structures with conserved exon-intron borders (Fig. R12). The first exon of At2CPB, which encodes the less conserved chloroplast targeting signal, is eight amino acids longer than in At2CPA. The main difference between the two genes is the length of the introns, which are slightly longer in At2CPB.

In comparison to the *Arabidopsis* 2CPs, the other streptophyte 2CPs show similar exon-intron patterns. All splice sites are conserved with Sm2CPA. In the *Physcomitrella* 2CPA and Sm2CPB genes, only the 5'-termini differ from *Arabidopsis*. For Pp2CPB, the gene structure could not be determined since its locus is interrupted. Its localization on two different scaffolds and the accompanied arrangement difficulties were unfeasible to overcome. The

introns are shorter in *Selaginella*. This decreases the total length of Sm2CPA in comparison to the *Arabidopsis* homologs. Sm2CPB shows an increased and variable length of its introns in comparison to Sm2CPA (Fig. R12). In general, the results are pointing to a high gene structure conservation within the investigated streptophytes.

The gene structures of all three 2CP isoforms identified in the *Chlamydomonas* genome are atypical if compared to their *Physcomitrella*, *Selaginella*, and *Arabidopsis* homologs (Fig. R12). Cr2CPA has only three exons while the weakly or not expressed Cr2CPB and Cr2CPC genes comprise seven and eight exons, respectively. None of the defined 2CP encoding *Chlamydomonas* genes shows any conserved splice site with the other identified chloroplast 2CPs (Fig. R12).

3.4.3 Expression analyses

BLAST searches for the *Selaginella* 2CPA gene models hit 67 (Sm2CPA.1) and 60 (Sm2CPA.2) ESTs for the two haplotypes (Table R1). For the Sm2CPB genes in contrast, no ESTs were observed (Table R1). This implies that they are putatively expressed either very weakly, not at all, or only under special circumstances. The *Physcomitrella patens* 2-Cys-peroxiredoxin A gene model revealed 48 hits in the respective database. On the contrary, for Pp2CPB no transcription could be proven by EST-coverage. Its predicted gene was split into two parts located on different scaffolds. BLAST searches using either the whole or the split cDNA sequences separately did not hit any EST with an e-value of 0 (Table R1). For the Cr2CPA gene 121 ESTs were observed in the JGI database and 10 in ChlamyDB, while Cr2CPB revealed only 19 and 5 transcripts (Table R1). Besides Cr2CPA and Cr2CPB, a third putative, but not-EST-covered 2CP gene, Cr2CPC, was identified. These data indicate Cr2CPA to be strongly expressed in relation to the other identified 2-Cys-peroxiredoxins in *Chlamydomonas*.

3.4.4 Characteristics of the predicted proteins

Despite the variability in gene structures (Fig. R12), the identified chloroplast targeted 2-Cys-peroxiredoxins share a high similarity. Especially the Sm2CPA, Pp2CPA, and Pp2CPB encoding gene models show 96-98 % similar amino acids and 85-89 % identity (Table R3) indicating a high conservation of these antioxidative enzymes. In contrast to Sm2CPA, the not EST-covered Sm2CPB isoform reveals a low similarity to the *Arabidopsis thaliana*

homologs. It shows approximately the same amount of similar amino acids as the *Chlamydomonas* 2CPA isoform, although the algae represent much more ancient photosynthetic organisms. In general, the weakly expressed or not EST-covered 2CPs (Sm2CPB, Cr2CPB, Cr2CPC) are less identical (57-73 %) and similar (71-90 %) to the *Arabidopsis thaliana* isoforms the transcribed isoforms (Table R3).

Table R3: Amino acids identity and similarity of predicted core 2-Cys peroxiredoxins from *Selaginella moellendorffii*, *Physcomitrella patens*, and *Chlamydomonas reinhardtii* to *Arabidopsis thaliana* 2-Cys peroxiredoxins (Accession numbers: At2CPA: At3g11630, At2CPB: At5g06290, aa99-aa208 in Fig. R13).

Enzyme	**Identity to A. *thaliana* homologs**		**Similarity to A. *thaliana* homologs**	
	At3g11630	**At5g06290**	**At3g11630**	**At5g06290**
Sm2CPA.1/2	86/86 %	85/85 %	97/97 %	97/97 %
Sm2CPB	70%	73%	90%	90%
Pp2CPA	85%	88%	96%	96%
Pp2CPB	86%	89%	98%	98%
Cr2CPA	76%	77%	88%	89%
Cr2CPB	57%	59%	72%	73%
Cr2CPC	58%	57%	71%	72%

The amino acid sequences of the mature 2CPs encoded by the defined gene models share many conserved positions (Fig. R13). The catalytic sites around the peroxidatic C186 (Fig. R13, aa171-aa196), around the resolving cysteine residue C311 (aa310-aa314, labeled "*" in Fig. R13) and the active pocket (P179, F182, V185, E189, W221, R265 and R295, labeled "C" in Fig. R13, Schröder *et al.* 2000) are identical in all EST-covered 2CPs. Furthermore, the GGLG-motif (aa229-aa232) is conserved in all species. Being specific for eukaryotic 2CPs, this motif stabilizes the folded structure together with the YF motif (aa332-aa333), decelerates disulfide formation and increases the sensitivity to H_2O_2 (Jönsson *et al.* 2008). Sm2CPA and Pp2CPA show charge conservative amino acid substitutions with weak sterical effects in the decamer contact phase (T243S: Sm2CPA, D256E: Pp2CPA). At position 279 in the 2CP alignment, (Fig. R13) only *Arabidopsis thaliana* shows an S while Sm2CPA, Sm2CPB, the *Physcomitrella* 2CPs, and Cr2CPA reveal an A residue. The dimer interface described by Schröder *et al.* (2000), R-Q-I-X-V-N-D, is replaced by a Q-HA/S-T-I/V-N-N consensus in most plant 2CPs (aa277-aa283, Fig. R13) (Horling *et al.* 2001). This includes also all EST

confirmed 2CPs identified in this study (Table R1, Fig. R13). Equally, the interface involved in decamer formation (L180, F182, F184, F216, A220 and W221) (labeled "T" in Fig. R13) (Schröder *et al.* 2000) revealed to be conserved (Fig. R13). Modifications were detected in the dimer and decamer interfaces in the identified proteins: As mentioned before, W221, which is also part of the active site, is replaced by F in Cr2CPB. Sm2CPB, Sm2CPA, and Pp2CPA show a G251N/R exchange while the latter two additionally reveal an I281V substitution. These two positions are known to be involved in stabilization of the enzyme dimer (Schröder *et al.* 2000).

Strongest differences were observed for the weakly or unexpressed *Selaginella* and *Chlamydomonas* 2CPs (Sm2CPB, Cr2CPB, Cr2CPC). Apart from the mentioned modifications, the isoform also shows a replacement of the YF-motif by HF (aa332-aa333, Fig. R13). Besides these, in Sm2CPB aa328-aa331 are missing. All these substitutions are pointing to the possibility that the putatively non-expressed gene does not encode a (fully) functional protein.

The *Chlamydomonas reinhardtii* 2CPs revealed low similarity to their *Arabidopsis* homologs. One prominent substitution example in these isoforms is the hydrophobic pocket around the resolving C311. In this region, G314 and K316 are replaced by N and W221 is exchanged by a less bulky F residue in Cr2CPB (Fig. R13). In *Brassica* species, W221 is replaced by G (Horling *et al.* 2001) indicating that this position is less important for an effective 2CP function than other amino acids. Another putatively critical modification is represented by the replacement of I279 to V shown within the decamer interface of Cr2CPB and Cr2CPC.

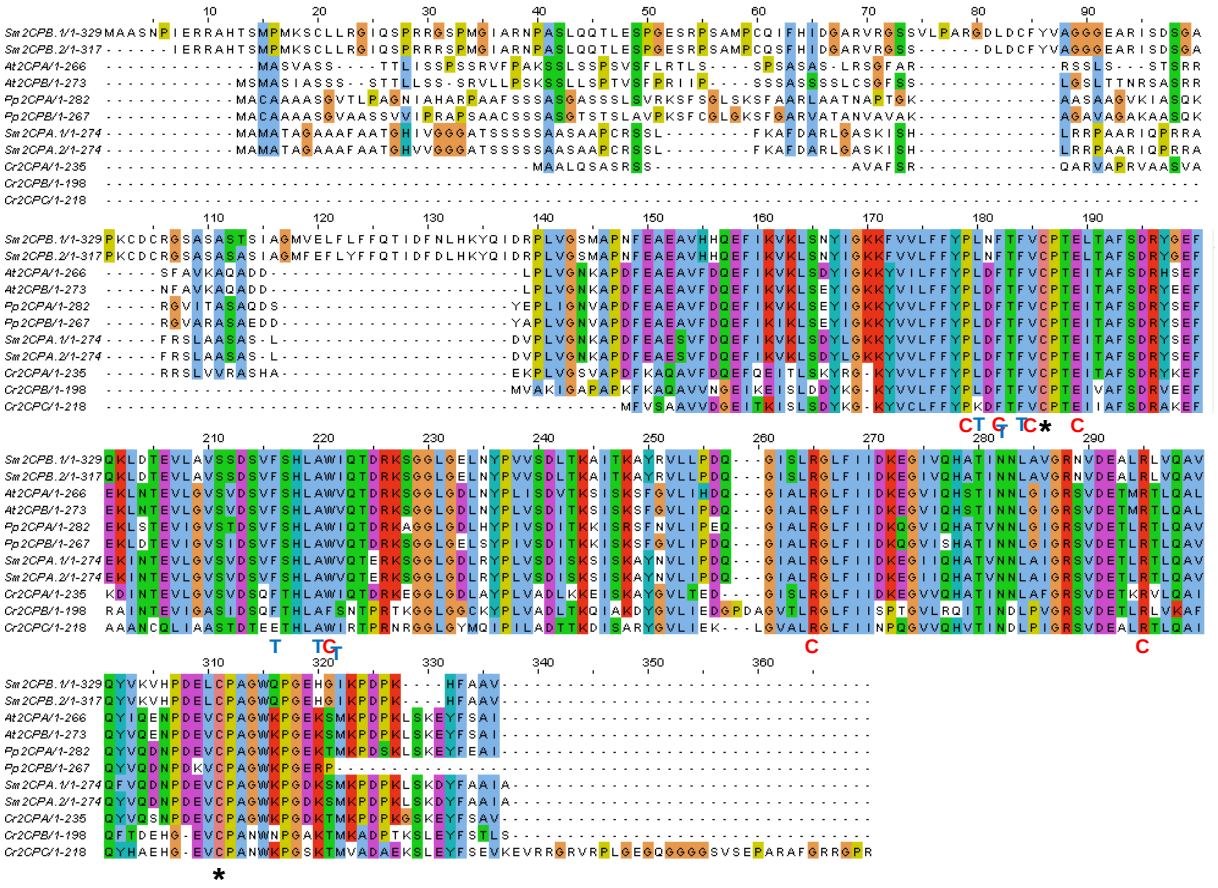

Fig. R13: Comparison of 2-Cys peroxiredoxin amino acid sequences. Amino acid sequence alignment of 2-Cys peroxiredoxins (2CP) from *Arabidopsis thaliana* (At), *Selaginella moellendorffii* (Sm), *Physcomitrella patens* (Pp), and *Chlamydomonas reinhardtii* (Cr). The peroxidatic and resolving cysteine residues are labeled with "*", "T" indicates the amino acid residues involved in decamer formation and "C" the residues forming the catalytic site.

Within the Cr2CPB protein, charged amino acids are atypically substituted. Similar exchanges are shown by Cr2CPC and partially also by Cr2CPA.The negatively charged D148, E150 and Q298 are replaced by positively and uncharged residues. E201 is exchanged by R, K or A. Uncharged S228 and L328 are substituted by K, E, R and G, and K161 (by E), K163 (by T/S), K202 (by D, A), K227 (by T/N), K272 (by P), K316 (by N), and K327 (by T/E). Besides these, K170 is deleted (Fig. R13). The mentioned uncharged amino acids are commonly widely conserved throughout the whole 2CP family (Horling *et al.* 2001, Baier and Dietz 1996). Another specific feature of the *Chlamydomonas* 2CPB isoform can be found in its C-terminus, which is involved in the attachment of 2CPs to membranes (König *et al.* 2003, Schröder *et al.* 2000). Due to S/T-substitutions at position 334, 335 and 337, the Cr2CPB C-terminus is more hydroxylated (Fig. R13). The C-terminus of the non-EST-covered Cr2CPC is extended by a G- and P-rich 33 amino acid long peptide. Nevertheless, secondary structure

analysis gave no indications that this insertion form additional α-helices or β-sheets or change the overall folding of the typical 2CPs. Similar to animal and yeast 2CPs, The 3D structure of Cr2CPC was predicted to have a long unstructured C-terminus (Schröder *et al.* 2000, Choi *et al.* 2005).

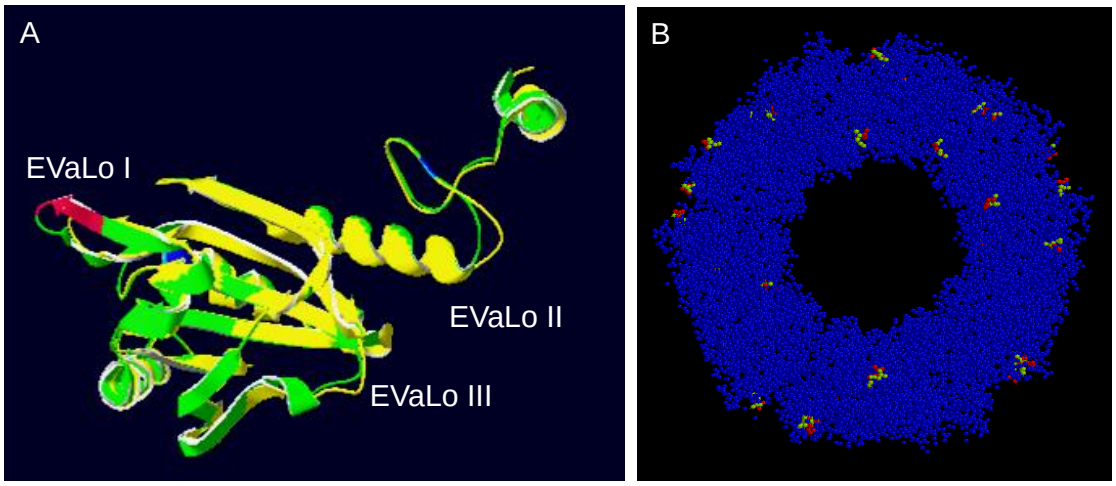

Fig. R14: Superimposition of At2CPA (yellow) and Cr2CPB (green) monomers (A) and decamers (B). The three amino acid insertion (aa258-aa260, indicated in red) extends the length of a β-sheet and modifies the protein surface. In the decameric toroid structure (B) the three EVaLos modify the inner and outer ring surface (red and green labels in B). The decameric structure was prepared by Prof. Dr. Margarete Baier.

Consistent with the degree of primary structure conservation (Table R3), modeling of the 3D-structures and subsequent iterative superimposition to the *Arabidopsis* 2CPs revealed also a high structural conservation of all identified EST-covered 2CPs. Strong differences were shown by the weakly or non-expressed isoforms. Exemplarily for the latter, Fig. R14 shows the superimposition of Cr2CPB and At2CPA. As mentioned above, within Cr2CPB, a three amino acid insertion (aa258-aa260) extends and slightly tilts the β-sheet which is involved in formation of the active site (Fig.s R13, R14, EVaLo I). Other sequence variations have an impact on the dynamic loops, designated "Evolutionary Variable Loop" II and III. EVaLo II is located on the outer surface of the 2CP toroid-decamer structure (Schröder *et al.* 2000). EVaLo III in contrast, reshapes the inner surface of the 2CP-toroid. These predicted modifications indicate a specific surface of Cr2CPB oligomers (Fig. R14B).

3.4.5 Phylogenetic comparison

Phylogenetic analyses revealed that the identified 2CPAs from non-seed plants group together and are closer related to each other than to their *Arabidopsis thaliana* homologs (Fig.s R15-R17). In the trees calculated according to neighbor joining or maximum parsimony algorithms (Fig.s R15, R16), only the *Physcomitrella* 2CPs cluster together while Sm2CPA and Sm2CPB are closer to either *Physcomitrella* or *Chlamydomonas* 2CPs. This may indicate that Sm2CPA represents a more sophisticated enzyme while the low or non-expressed Sm2CPB is a more ancient homolog. In addition, together with the *Physcomitrella* 2CPs, Sm2CPA is closer related to the *Arabidopsis* isoforms than the other defined 2-Cys-peroxiredoxins. According to the neighbor joining (Fig. R15) and minimal evolution algorithms (Fig. R18), Cr2CPA clusters into the same branch as cyanobacterial 2CPs, while Cr2CPB and Cr2CPC form an independent outgroup. Only the maximum parsimony algorithm (Fig. R16), which accounts for the most parsimonious explanation based on weighting each amino acid position discretely (Moore *et al.* 1973), clusters the three *Chlamydomonas reinhardtii* isoforms with a 2CP known from another *Chlamydomonas* (*Chlamydomonas spec.*). Nevertheless, also this group shows a closer relation to cyanobacterial 2-Cys-peroxiredoxins than to other 2CPs included in the tree calculations.

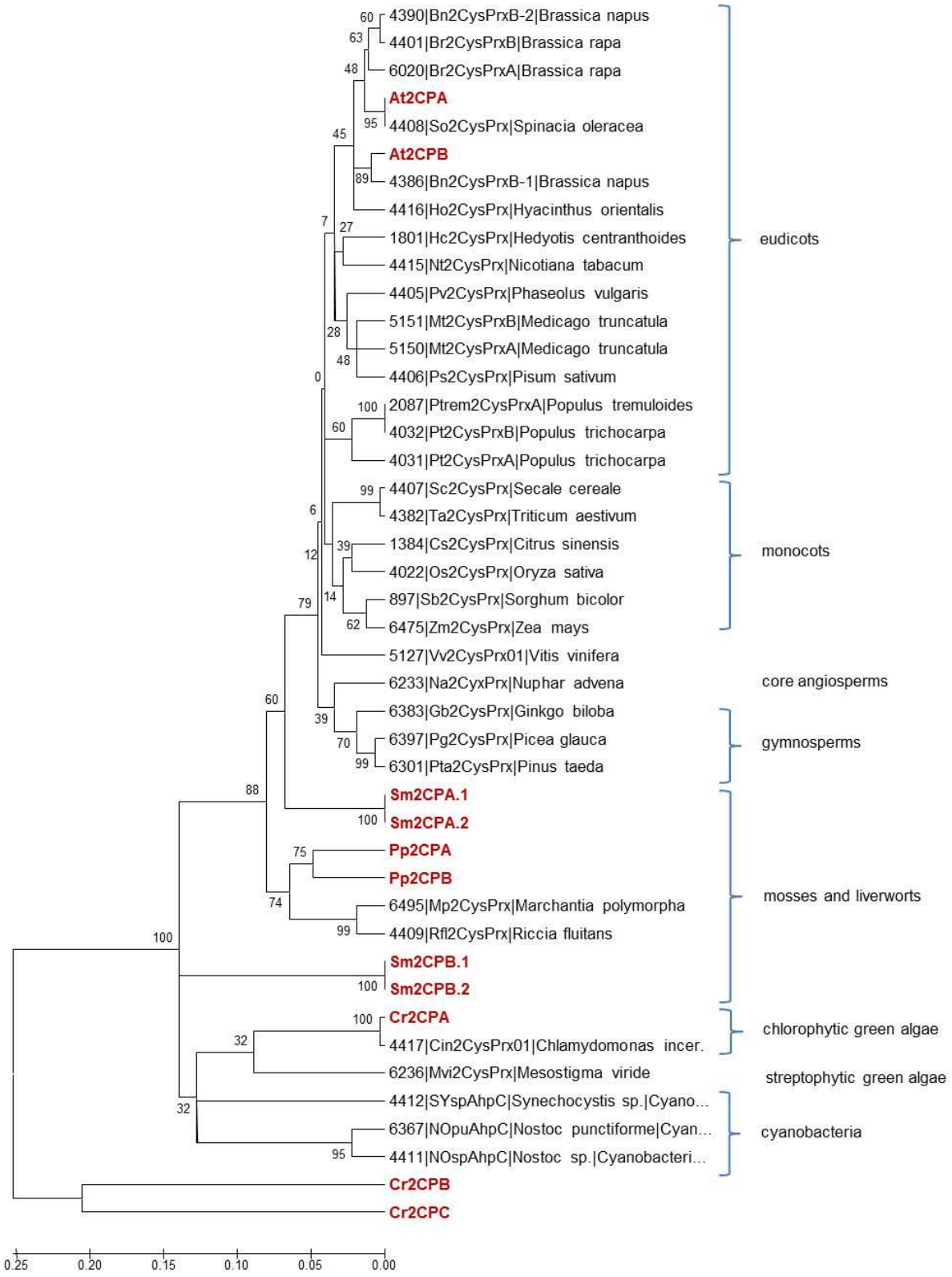

Fig. R15: Neighbor joining phylogenetic tree of the 2CP sequences shown in Fig. R13 (red) and additional 2CPs from chlorobionts and cyanobacteria as listed in PeroxiBase. For all PeroxiBase-data, the data base IDs were used. The numbers represent bootstrap values. Tree calculation was performed by Prof. Dr. Margarete Baier.

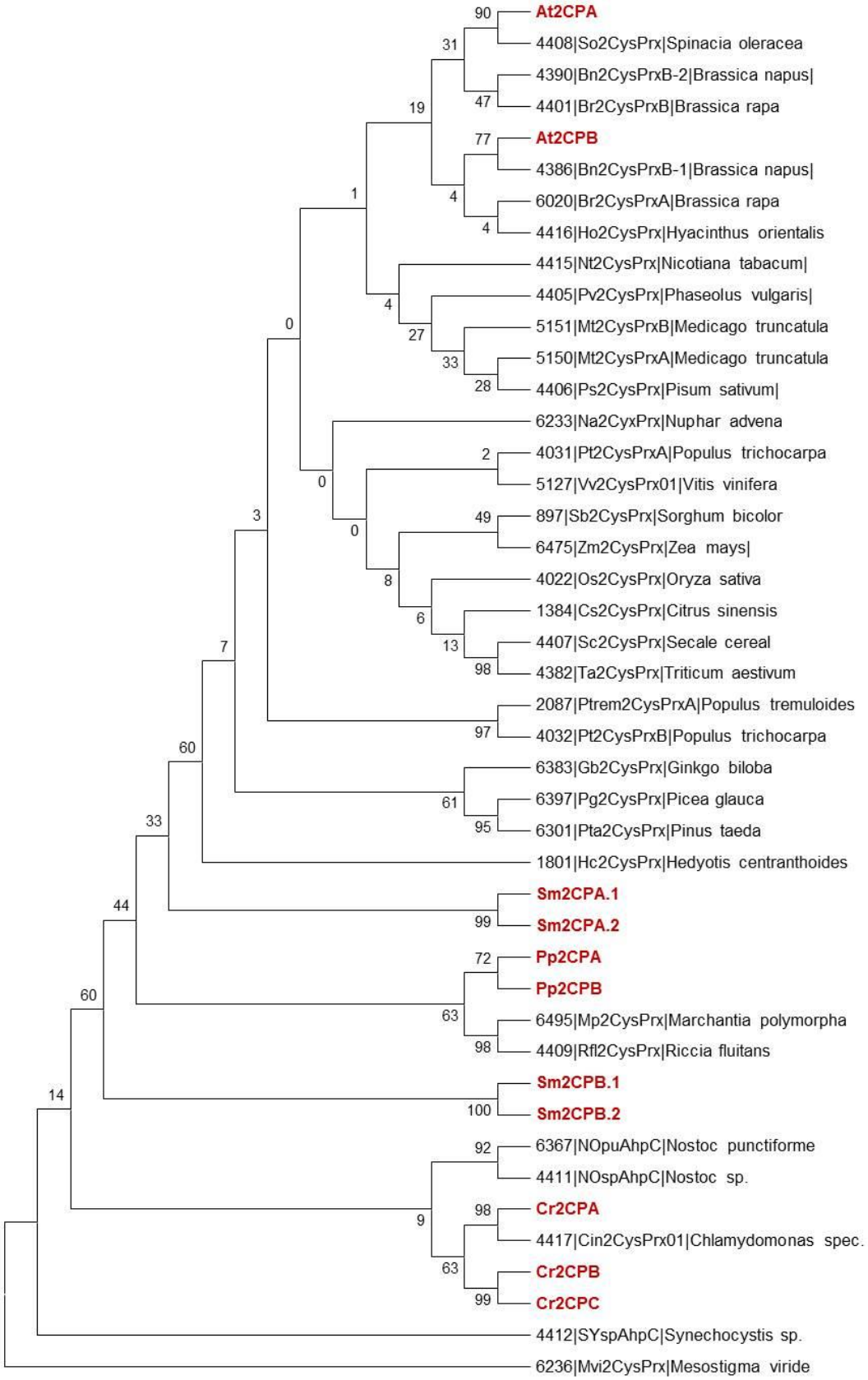

Fig. R16: Maximum parsimony phylogenetic tree of the 2CP sequences shown in Fig. R13 (red) and additional 2CPs from chlorobionts and cyanobacteria as listed in PeroxiBase. For all PeroxiBase-data, the database IDs were used. The numbers represent bootstrap values. Tree calculation was performed by Prof. Dr. Margarete Baier.

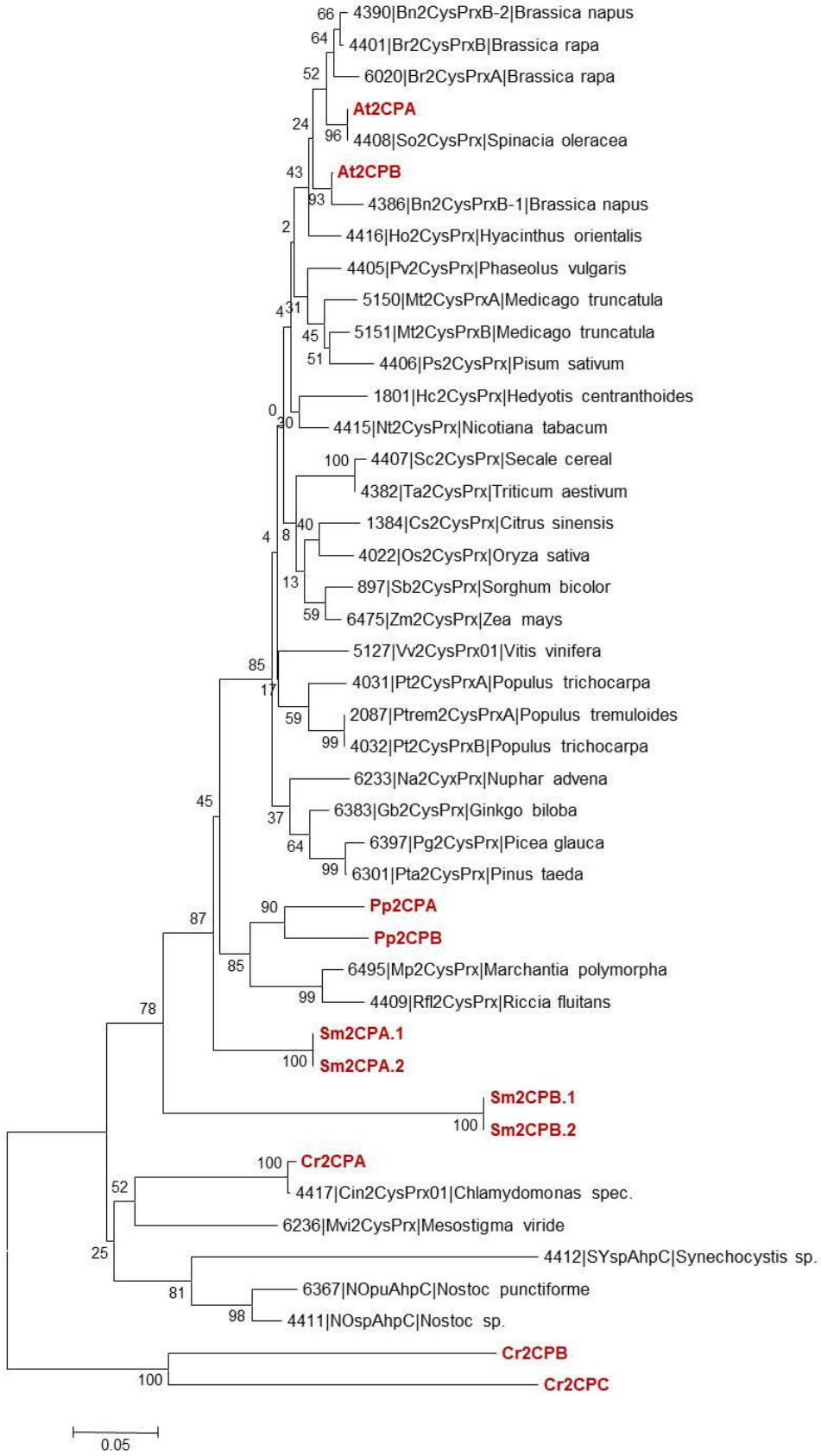

Fig. R17: Minimum evolution phylogenetic tree of the 2CP sequences shown in Fig. R13 (red) and additional 2CPs from chlorobionts and cyanobacteria as listed in PeroxiBase. For all PeroxiBase-data, the data base IDs were used. The numbers represent bootstrap values. Tree calculation was performed by Prof. Dr. Margarete Baier.

3.5 The atypical 2-Cys peroxiredoxin PrxQ

3.5.1 Gene copy number and protein targeting

The only PrxQ isoform in *Arabidopsis thaliana* is post-translationally targeted to the chloroplast thylakoid lumen (Horling *et al.* 2002, Petersson *et al.* 2006). In contrast to the seed plant, two ORFs encoding PrxQ were identified in the genome of each *Selaginella moellendorffii* haplotype (Table R1). Putatively enhancing its antioxidative defense, the bryophyte *Physcomitrella patens* expresses three chloroplast PrxQs (Table R1). As published for *Arabidopsis*, the green alga *Chlamydomonas reinhardtii* genome also revealed a single gene model coding for a chloroplast targeted PrxQ (Table R1). These results were consistent with the ones obtained by Dayer *et al.* (2008) (PRX6, here: CrPrxQ).

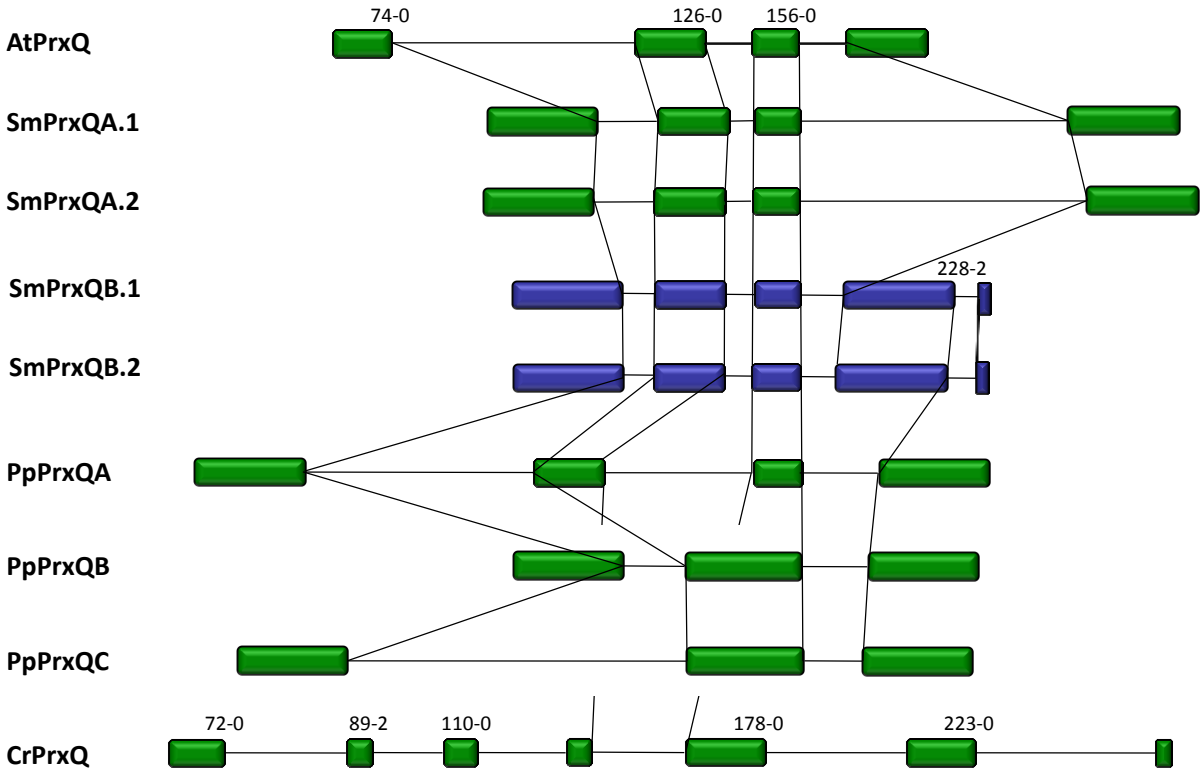

Fig. R18: Gene structures of PrxQ in *Arabidopsis thaliana* (At), *Selaginella moellendorffii* (Sm), *Physcomitrella patens* (Pp), and *Chlamydomonas reinhardtii* (Cr). Expressed PrxQ genes are shown in green, non-expressed in blue. The vertical lines connect corresponding splice sites. The numbers represent positions of corresponding amino acids in the alignment shown in Fig. R19 the relative splice site within the corresponding codon

3.5.2 Exon-intron structure

In *Arabidopsis thaliana* and *Selaginella moellendorffii*, the PrxQ gene models comprise four exons (Fig. R18). The *Physcomitrella patens* PrxQA homolog shows a similar gene structure. Its first and fourth exons have approximately the same length as in the *Selaginella* homolog (Fig. R18). The exons are separated by three introns which are longer than in AtPrxQ, SmPrxQA and SmPrxQB and elongate the entire gene (Fig. R18). The other two *Physcomitrella* PrxQ gene models (PpPrxQB, PpPrxQC) revealed to be encoded by merely three exons (Fig. R18). Their second exon combines exon2 and exon3 of AtPrxQ, SmPrxQ, and PpPrxQA. In SmPrxQB, there is an additional splice site in the last exon (corresponding to aa228-2, Fig. R18). Within *Arabidopsis*, *Selaginella*, and *Physcomitrella*, two splice sites are conserved in all identified PrxQs (aa74-0 and aa156-0, Fig. R18). PpPrxQA, the *Selaginella* and *Arabidopsis* homologs share an additional splice site at amino acid position 126-0 (Fig. R18).

The *Chlamydomonas* PrxQ gene model shows a different splice pattern. Only one splice site (corresponding to aa126-0) is conserved with the *Selaginella* and *Arabidopsis* homologs and PpPrxQA, while no splice site is shared with PpPrxQB and PpPrxQC (Fig. R18).

In general, the streptophyte gene structures show a high conservation, while they are distantly related to the *Chlamydomonas* PrxQ. This indicates that they share a common ancestor. In *Selaginella*, a gene duplication event may have led to the emergence of the two isoforms. In *Physcomitrella*, the PrxQs were triplicated. These third and second PrxQ variants were lost during evolution from mosses to higher plants.

3.5.3 Expression analyses

Evidence for the transcription of two gene models encoding SmPrxQA was found by hitting 21 (SmPrxQA.1) and 7 (SmPrxQA.2) ESTs with BLAST searches in the JGI database (Table R1). For SmPrxQB, which shows an atypical gene structure, no ESTs could be detected (Table R1). Contrasting the two *Selaginella* gene models, transcription for all three PrxQs from *Physcomitrella* was confirmed. BLAST searches revealed 13, 7, and 13 ESTs with e-values of 0 for PpPrxQA, PpPrxQB, and PpPrxQC, respectively (Table R1). In conflict with results obtained by Dayer *et al.* (2008), investigations using the *Chlamydomonas* transcript databases of JGI and ChlamyDB revealed that the single PrxQ isoform in *Chlamydomonas* is not covered by any EST (Table R1).

3.5.4 Characteristics of the predicted proteins

The *Selaginella moellendorffii* PrxQA and *Arabidopsis thaliana* PrxQ isoforms show a high degree of similarity (91 %, Table R4) while SmPrxQB is less similar (SmPrxQB.1: 80 %, SmPrxQB.2: 81%). Although the *Physcomitrella* PrxQA gene model revealed an analogous structure and PpPrxQC, the enzyme encoded by the latter shows more similar amino acids (PpPrxQA: 87 %, PpPrxQC: 91 %, Table R4). Resembling its exon-intron-pattern, the PrxQ isoform encoded in the *Chlamydomonas* genome shows the strongest differences within the investigated plant species (54 % identical and 68 % similar amino acids, Table R4). This supports the suggestion that the CrPRxQ isoform is distantly related to the streptophyte PrxQs.

PpPrxQC shows the same high similarity to its *Arabidopsis* homologs as SmPrxQA. It may be concluded that out of the three *Physcomitrella* isoforms, PpPrxQC represents the ancestor of SmPrxQA and AtPrxQ.

Table R4: Amino acids identity and similarity of predicted core peroxiredoxins Q from *Selaginella moellendorffii*, *Physcomitrella patens*, and *Chlamydomonas reinhardtii* to *Arabidopsis thaliana* peroxiredoxins Q (Accession number: At3g26060, aa98-aa222 in Fig. R19).

Enzyme	**Identity to *A. thaliana* homolog**	**Similarity to *A. thaliana* homolog**
SmPrxQA.1/2	77/77 %	91/91 %
SmPrxQB.1/2	57/58 %	80/81 %
PpPrxQA	70 %	87 %
PpPrxQB	70 %	83 %
PpPrxQC	77 %	91 %
CrPrxQ	54 %	68 %

As mentioned before, the atypical 2-Cys-peroxiredoxins have perceived less attention in plant science as typical 2CPs with respect to functional relevant motifs. The characteristic and conserved C residues are located at positions 123 (peroxidatic C) and 128 (resolving C) (Fig. R19).

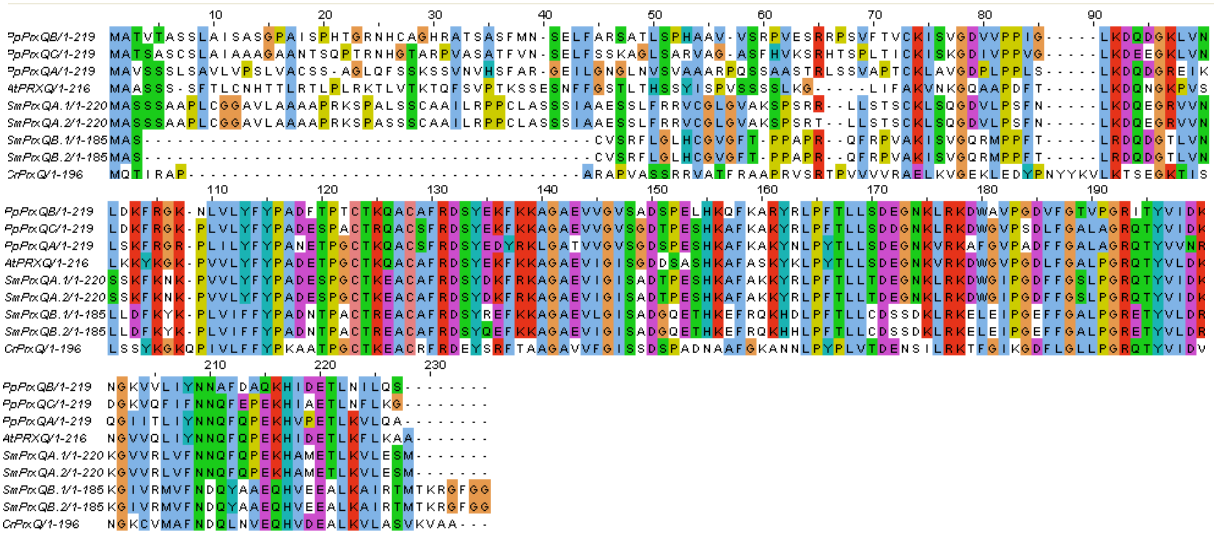

Fig. R19: Comparison of peroxiredoxin Q amino acid sequences. Amino acid sequence alignment of the here analyzed PrxQ from *Arabidopsis thaliana* (At), *Selaginella moellendorffii* (Sm), *Physcomitrella patens* (Pp), and *Chlamydomonas reinhardtii* (Cr).

Revealing 83-91 % similar amino acids, PpPrxQ, SmPrxQ, and AtPrxQ share many positively charged amino acid residues (Fig. R19). K, R, Q, and N are protonated under the acidic conditions, existing in the thylakoid lumen during light periods (Petersson *et al.* 2006). In the analyzed plant PrxQ, among the amino acids located close to the active site, aa120, aa122 and aa126 are not conserved (Fig. R20). AtPrxQ, PpPrxQA, PpPrxQB, SmPrxQB and CrPrxQ show a T residue at position 120 while it is replaced by the also hydroxylated amino acid S in SmPrxQA and PpPrxQC. In respect of enzyme activity, exchange of the positively charged Q126 to a negatively charged E in SmPrxQ and CrPrxQ and the G122T replacement in PpPrxQB may have a stronger impact. These residues affect the charge distribution close to the active site (C123-C128, Fig. R19). Besides the variation of a hydroxylated amino acid residue in the -3 position (S/T120) and P residues in the -2 and -7 position relative to the peroxidatic cysteine residue (C123) and R193, which has been suggested to be important for dimer stabilization in peroxiredoxins (Choi *et al.* 2005), there is too little information on functionally important motifs and amino acids to draw conclusions on enzyme conservation.

In contrast to the other identified PrxQs, the *Chlamydomonas* isoform, which is least similar to its *Arabidopsis* isoform, lacks negative charges at positions 118, 119, and 135 (Fig. R19). Additionally, the positive charges at positions 138, 139, 156, 175, and 200 are missing.

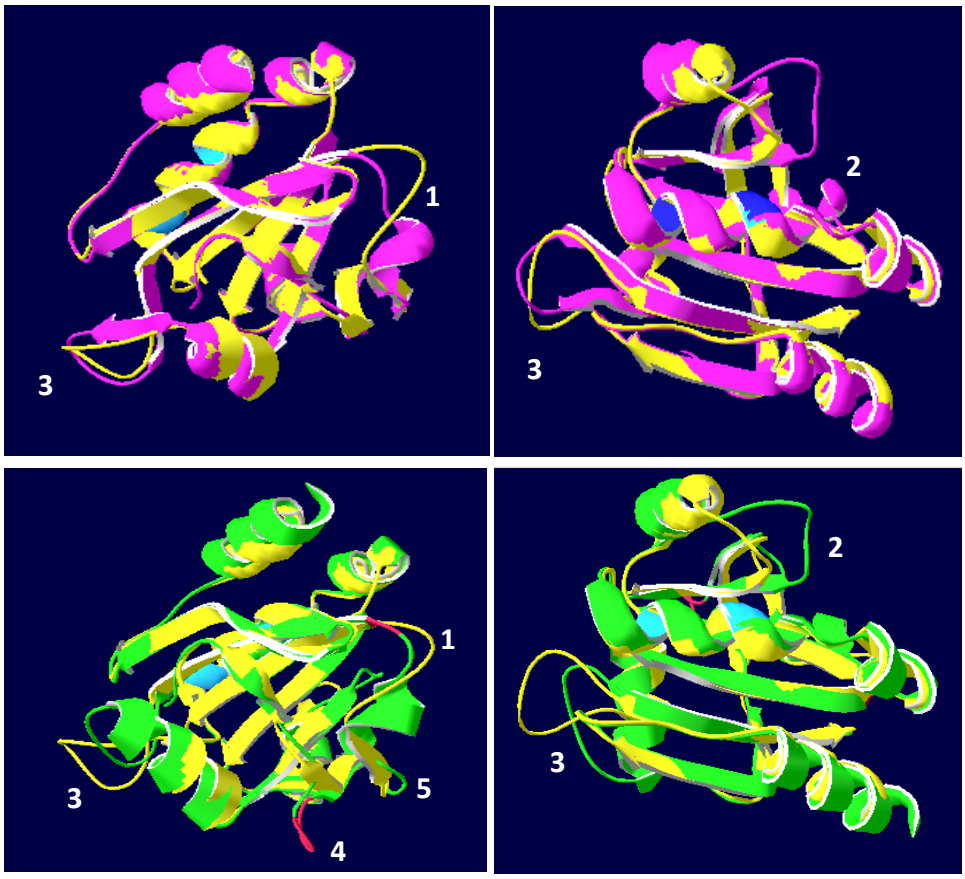

Fig. R20: Superimposition of AtPrxQ (yellow) and SmPrxQA.1 (pink) and AtPrxQ (yellow) and CrPrxQ (green) in two views. The positions of the three and five flexible elements on the protein surface are numbered in white. The peroxidatic and resolving C are labeled in blue

The peroxiredoxin type II fold was investigated by predicting their 3D-structure with SWISS-MODEL (Fig. R20). The parallel β-sheet core and the conserved α-helices confer a rigid common structure to the PrxQs encoded by *Arabidopsis*, *Selaginella*, and *Physcomitrella*. On their surfaces, three flexible loops were observed in streptophyte proteins (Fig. R20 top) and five loops in the *Chlamydomonas* PrxQ (Fig. R20 bottom). The K, R, Q, and N residues, which may be important for the pH-sensitivity of the enzyme, are evenly distributed on the protein surface.

3.5.5 Phylogenetic analyses

In comparison to non-plant PrxQs (Kong *et al.* 2000), the amino acid sequences encoded by the identified gene models revealed to be more similar within the analyzed members of the plant kingdom. Phylogenetic analyses for the identified PrxQs showed that the isoforms from lower plants are closely related and group separately from higher plants (Fig.s R21-R23). The SmPrxQ isoforms cluster together in Fig. R21 and R22, resembling their similar gene structure. It may be possible that their emergence was due to a gene duplication event.

Besides this, the peroxiredoxins Q reveal species-specific groups for the *Physcomitrella* isoforms. The same clustering is also shown within the neighbor joining and maximum parsimony analyses for *Selaginella moellendorffii* (Fig.s R21, R22). The same trees reveal the *Physcomitrella* PrxQs to be the closest relatives of the *Arabidopsis* isoform among the identified proteins.

In contrast, the *Chlamydomonas* PrxQ represents the least related enzyme to its *Arabidopsis* homolog (Fig. R21-R23). The maximum parsimony tree even shows a special group including CrPrxQ, indicating that *Chlamydomonas reinhardtii* expresses a specific type of PrxQ (Fig. R22).

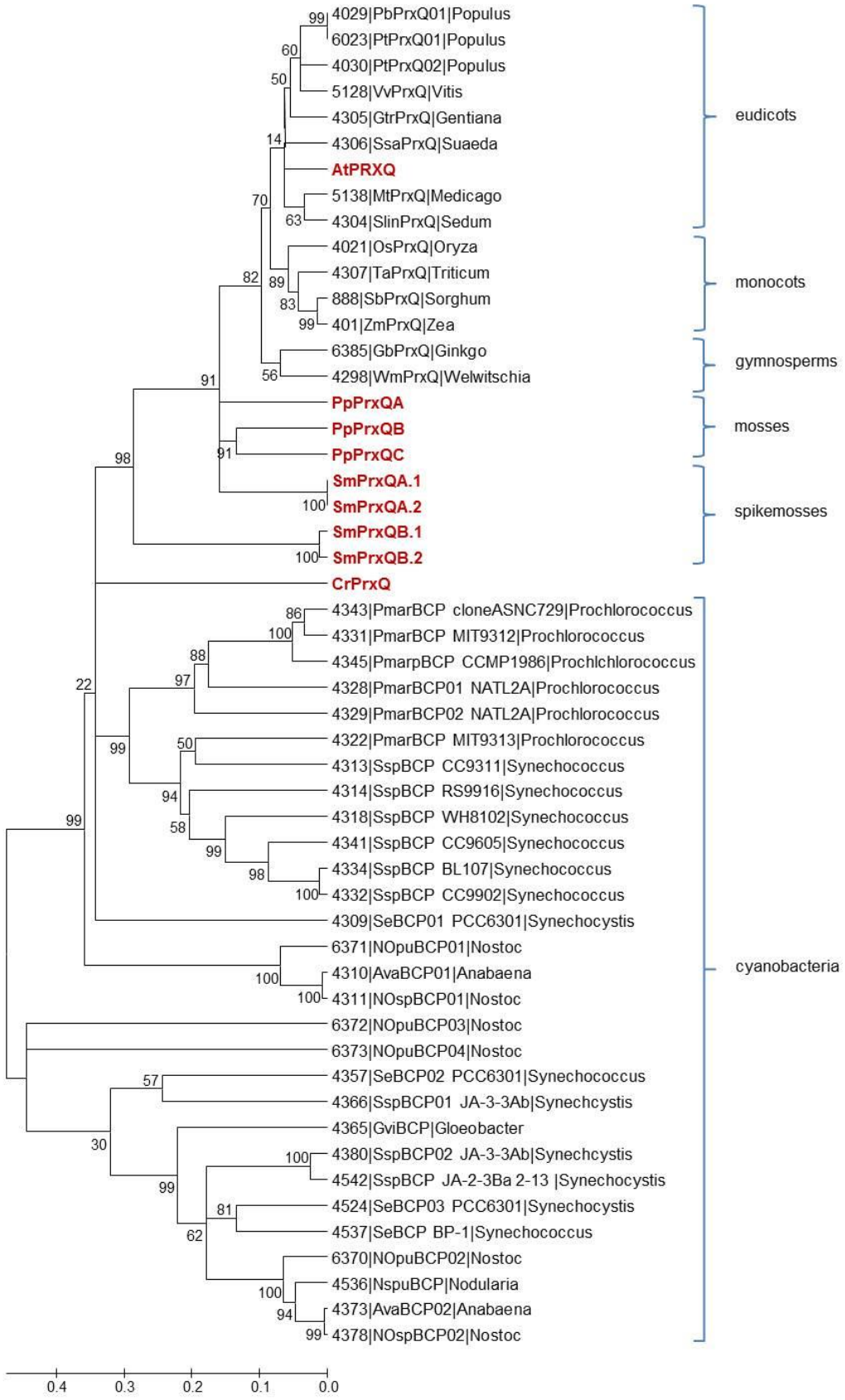

Fig. R21: Neighbor joining phylogenetic tree of the PrxQ sequences shown in Fig. R19 (red) and putative full-length PrxQ sequences of chlorobiont and cyanobacterial origin as listed in PeroxiBase. For all PeroxiBase data, the data base IDs were used. The numbers represent bootstrap values. Tree calculation was performed by Prof. Dr. Margarete Baier.

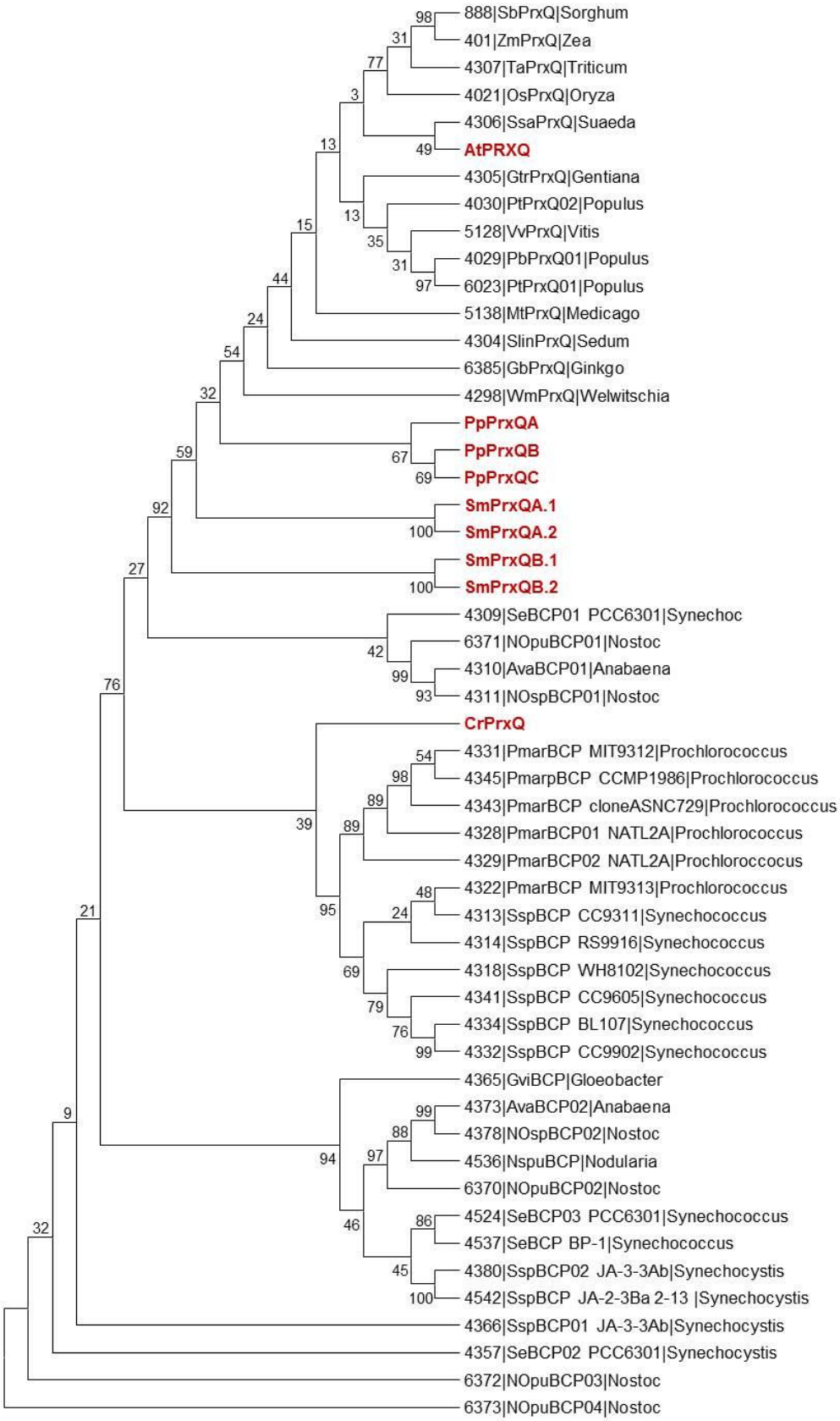

Fig. R22: Maximum parsimony phylogenetic tree of the PrxQ sequences shown in Fig. R19 (red) and putative full-length PrxQ sequences of chlorobiont and cyanobacterial origin as listed in PeroxiBase. For all PeroxiBase data, the data base IDs were used. The numbers represent bootstrap values. Tree calculation was performed by Prof. Dr. Margarete Baier.

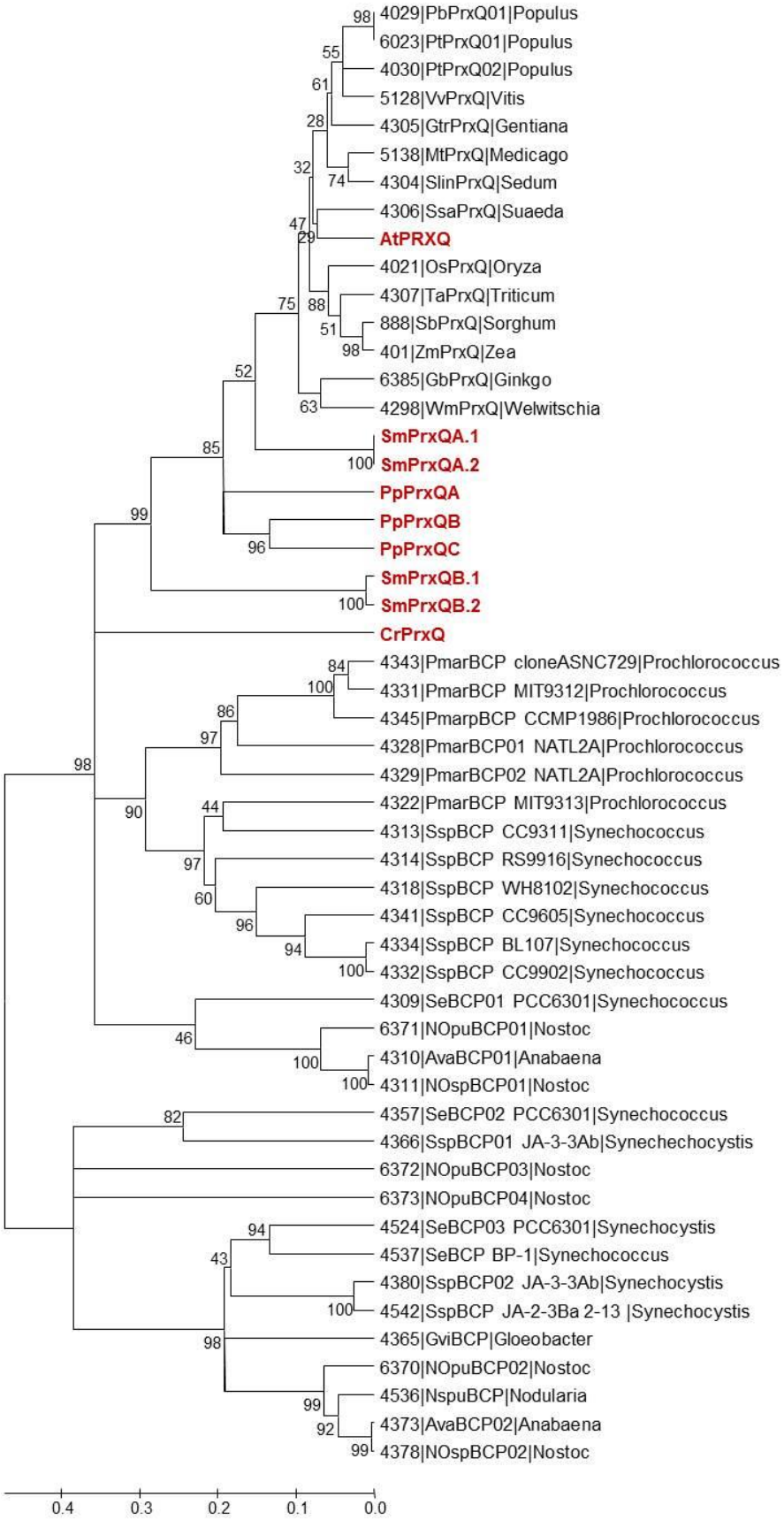

Fig. R23: Minimum evolution phylogenetic tree of the PrxQ sequences shown in Fig. R19 (red) and putative full-length PrxQ sequences of chlorobiont and cyanobacterial origin as listed in PeroxiBase. For all PeroxiBase data, the data base IDs were used. The numbers represent bootstrap values. Tree calculation was performed by Prof. Dr. Margarete Baier.

3.6 The atypical 2-Cys peroxiredoxin PrxII

3.6.1 Gene copy number and protein targeting

In *Arabidopsis thaliana*, one out of six PrxII isoforms (PrxIIE, At3g52960) is targeted to the chloroplast stroma (Horling *et al.* 2002, Bréhélin *et al.* 2003). The *Selaginella moellendorffii* haplotypes also encode two PrxII proteins with N-terminal targeting signals, each. In contrast to these more developed plants, the bryophyte *Physcomitrella patens* expresses two chloroplast targeted PrxIIs. Consistent with Dayer *et al.* (2008), one chloroplast PrxII was observed (PRX5, here: CrPrxIIC) in *Chlamydomonas reinhardtii* (Table R1).

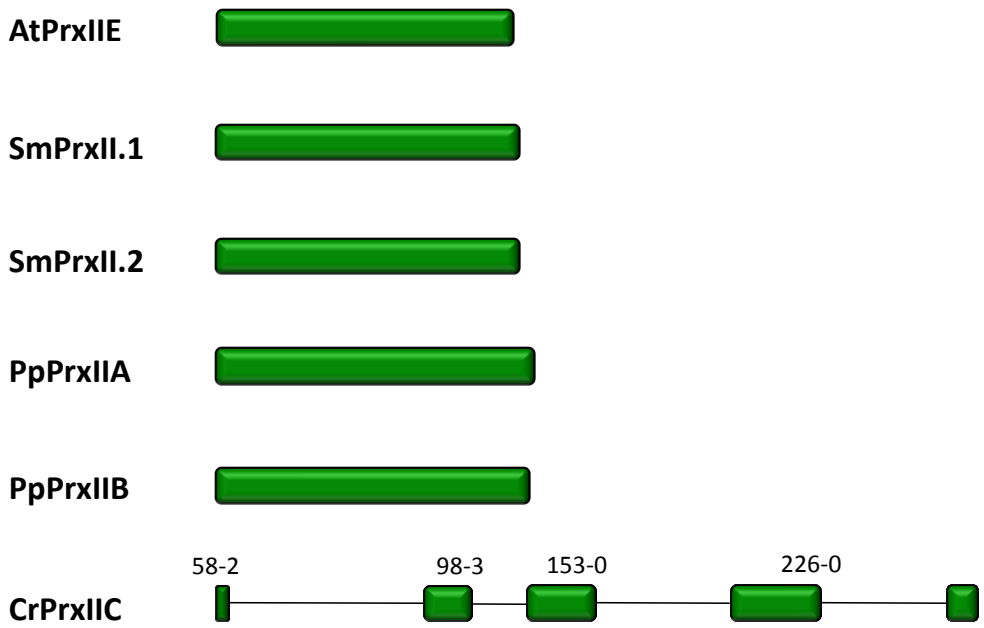

Fig. R24: PrxII gene structures of *Arabidopsis thaliana* (At), *Selaginella moellendorffii* (Sm), *Physcomitrella patens* (Pp), and *Chlamydomonas reinhardtii* (Cr). Expressed PrxII genes are shown in green. The vertical lines connect corresponding splice sites. The numbers represent position of corresponding amino acids in the alignment shown in Fig. R25 and the relative splice sites within the corresponding codon

3.6.2 Exon-intron structure

The PrxII proteins of *Arabidopsis thaliana, Selaginella moellendorffii*, and *Physcomitrella patens* are all encoded within a single exon, each (Fig. R24). In contrast, the *Chlamydomonas reinhardtii* PrxII gene show an atypical structure. It comprises five exons, which are separated by four introns of variable length (Fig R24).

3.6.3 Expression analyses

The transcription of the *Selaginella* peroxiredoxin type II isoform encoding gene models identified within the genomes of the two sequenced haplotypes was indicated by 12 (SmPrxII.1) and 15 (SmPrxII.2) ESTs (Table R1). Searches within the *Physcomitrella* transcript database revealed that the PrxII isoforms predicted for the moss are also expressed. 30 and 24 ESTs with an e-value of 0 were hit for PpPrxIIA and PpPrxIIB, respectively (Table R1). *Chlamydomonas reinhardtii* encodes a single PrxII homolog for which transcription was also indicated by EST coverage (Table R1).

3.6.4 Characteristics of the predicted proteins

The enzymes being encoded by the defined gene models share a low amount of identical amino acids (65-67 %, Table R5). Reflecting the gene structures, the *Arabidopsis*, *Selaginella*, and *Physcomitrella* isoforms showed 80-85 % similar amino acids (Table R5). Since the function and effectivity of an enzyme is often structurally conserved, this similarity may point to comparable functionality. The *Chlamydomonas reinhardtii* homolog showed the least amount of similar amino acids. The other investigated plant species PrxIIs revealed 80-85 % of similarity while the algal homolog showed 79 % similar amino acids (Table R5). Thus, the dissimilarity of CrPrxII is not as strong as indicated by its gene structure (Fig. R24).

Table R5: Amino acids identity and similarity of predicted core peroxiredoxins type II from *Selaginella moellendorffii*, *Physcomitrella patens*, and *Chlamydomonas reinhardtii* to *Arabidopsis thaliana* peroxiredoxins type II (Accession number: At3g52960, aa99-aa254 in Fig. R25).

Enzyme	**Identity to *A. thaliana* homolog**	**Similarity to *A. thaliana* homolog**
SmPrxII.1/2	66/66 %	85/85 %
PpPrxIIA	65 %	80 %
PpPrxIIB	65 %	82 %
CrPrxII	67 %	79 %

For the atypical peroxiredoxins, in contrast, only few amino acids have been reported to be essential for their activity. In general, the peroxidatic and resolving C residues are characteristic for most peroxiredoxins. In PrxIIs, these amino acids are located at positions 135 and 160, respectively (Fig. R25).

The two identified *Physcomitrella patens* gene models encode highly similar enzymes but are localized on different scaffolds. This may indicate that the presence of the two PrxIIs isoforms resulted from a gene duplication.

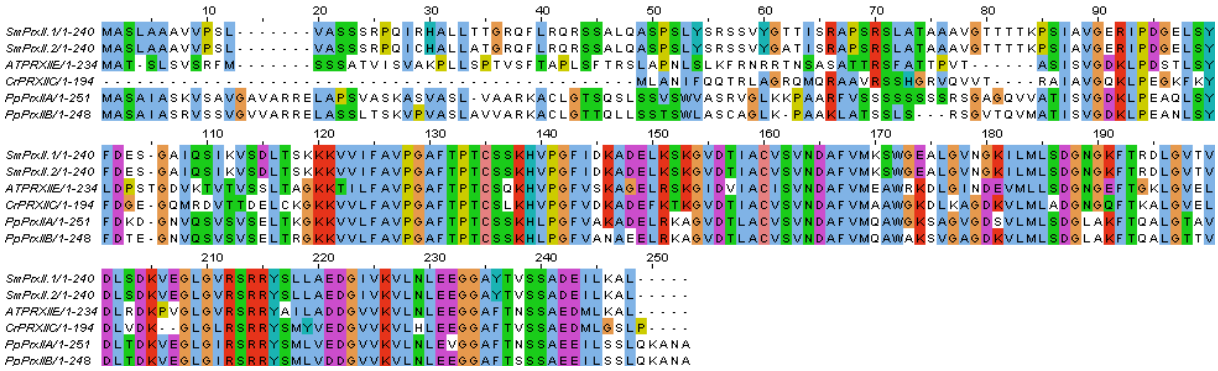

Fig. R25: Comparison of chloroplast type-II peroxiredoxin amino acid sequences. Amino acid sequence alignment of PrxII from *Arabidopsis thaliana* (At), *Selaginella moellendorffii* (Sm), *Physcomitrella patens* (Pp), and *Chlamydomonas reinhardtii* (Cr).

Recent crystal structure analyses of the poplar PrxII isoform demonstrated that F131, T132, P133, F167, V168, A171, L209, and R212 form the active site and the interface in the enzyme dimers (Echalier *et al.* 2005). Apart from position 171, which is replaced by S in SmPrxII of both haplotypes, every of the mentioned crucial amino acids is conserved in all analyzed species (Fig. R25). PrxIIs interact electrostatically with their electron donors, such as glutaredoxins (Rouhier *et al.* 2002). From the negative charges suggested to define the electrostatic surface of the poplar PrxII (Echalier *et al.* 2005), positions 242 (E/D), 243 (E/D) and 231 (E) are shared by the identified proteins. In addition, the F residue at position 131, which is part of the hydrophobic surface domain, is encoded by every of the defined gene models encoding chloroplast PrxIIs. The poplar-specific E145 is replaced by D, S, or A. The E at position 178 is substituted by small uncharged amino acids V, I, or A. Another amino acid, L137, is exchanged either by S or by Q in the here analyzed species (Fig. R25). Only the *Chlamydomonas reinhardtii* PrxII shows this residue.

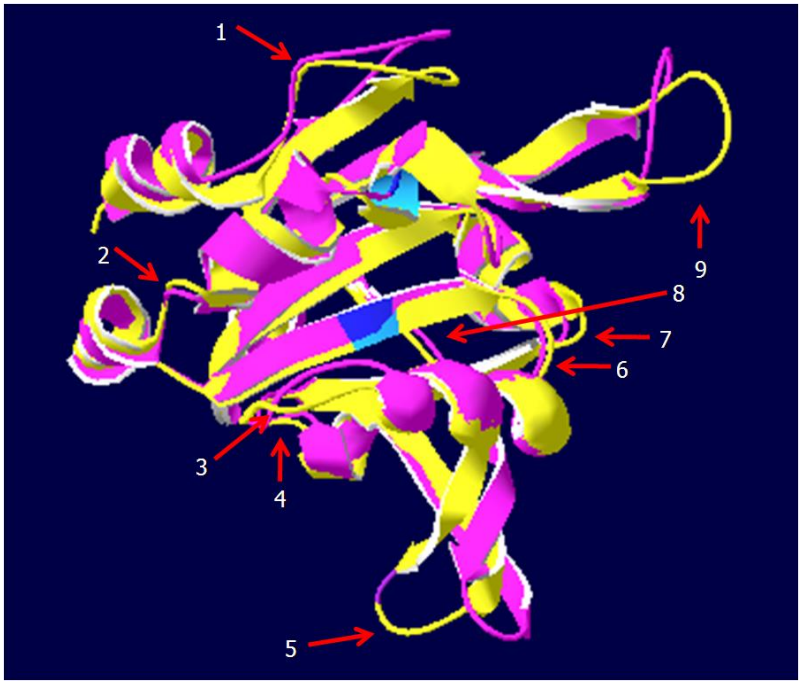

Fig. R26: Superimposition of AtPrxIIE (yellow) and SmPrxIIA.1 (pink) showing the peroxidatic and resolving C residues in blue and nine flexible loops (labeled with white numbers).

3D structural comparison showed various flexible loops on the protein surface (Fig. R26), pointing to the PrxII proteins being in general structurally less rigid than 2CPs.

Superimposition of the predicted 3D structures demonstrated that within the PrxIIs encoded by *S. moellendorffii*, *P. patens*, and *C. reinhardtii* the position of the peroxidatic C (C135) is slightly shifted if compared to their *Arabidopsis* homolog. This might be due to replacement of the positively charged Q137 by S or L (Fig. R25, R26).

In contrast to the lycophyte PrxII isoform, the two *Physcomitrella* proteins revealed atypical C-termini (Fig. R25). The eight, instead of three, amino acid long C-terminus, shown by both, has two additional hydroxylated amino acids (S246 and S247) and three (Q249, K250, N252), instead of one, positively charged residues (Fig. R25). According to Echalier *et al.* (2005), the C-terminus is exposed on the surface of PrxII proteins. Thus, the atypical tail of PpPrxIIA and PpPrxIIB may increase the hydrophilicity of the proteins.

In contrast to the *Physcomitrella* PrxIIs, the isoform encoded by *Chlamydomonas reinhardtii* revealed the shortest N-terminal extension and a deletion of V206 and E207. Although its gene structure indicates a weak relation to the streptophyte isoforms, this might indicate that CrPrxQ encodes an atypical PrxQ variant, which may have an altered function or effectivity than the other investigated isoforms.

3.6.5 Phylogenetic analyses

According to neighbor joining, minimum evolution, and maximum parsimony trees (Fig.s R27 – R29) all identified streptophyte PrxIIs group together with chloroplast homologs from other plants. They show a species-specific clustering. The *Selaginella moellendorffii* isoforms reveal to be the closest relatives to their *Arabidopsis* homologs among the identified proteins. Their most closely related homolog is encoded by *Pinus* (Fig.s R27-R29). The trees calculated according to neighbor joining and minimal evolution algorithms show that *Chlamydomonas* encodes a PrxII isoform which is more close to its *Arabidopsis* homolog than the *Physcomitrella* isoforms (Fig.s R27, R29). This may indicate that CrPrxII represents a highly sophisticate enzyme.

3.7 Glutathione peroxidases

3.7.1 Gene copy number and protein targeting

Alike peroxiredoxins, glutathione peroxidases are broad spectrum peroxidases, which detoxify H_2O_2 and a wide range of alkylhydroperoxides (Eshdat *et al.* 1997, Rouhier and Jacquot 2005, Iqbal *et al.* 2006). Plant GPx cluster into the phylogenetically ancient group of phospholipid hydroperoxides glutathione peroxidases (PHGPx, Margis *et al.* 2008). Based on sequence similarities and biochemical characterization they can alternatively be designated as a subclass of peroxiredoxins (Navrot *et al.* 2006).

The well investigated model plant *Arabidopsis thaliana* encodes seven GPx, of which three are organellar targeted by N-terminal transit peptides (Margis *et al.* 2008, Rodriguez *et al.* 2003). GPx6 (At4g11600) is suggested to be alternatively targeted to mitochondria and the cytosol, while GPx1 (At2g25080) and Gpx7 (At4g31870) are chloroplast-targeted and protect plants from photooxidative stress (Mullineaux *et al.* 1998, Rodriguez Milla *et al.* 2003, Chang *et al.* 2009).

Within the two *Selaginella moellendorffii* haplotype genomes, three different gene loci (SmGPxA, SmGPxB, SmGPxC) for GPxs similar to *Arabidopsis* GPx1 and GPx7 were identified. The protein encoded by the SmGPxA models show N-terminal extensions, characteristic for chloroplast targeting signals (Table R1). In contrast, analyses of the SmGPxB isoform revealed high ATP- but low TargetP-values (Table R1).

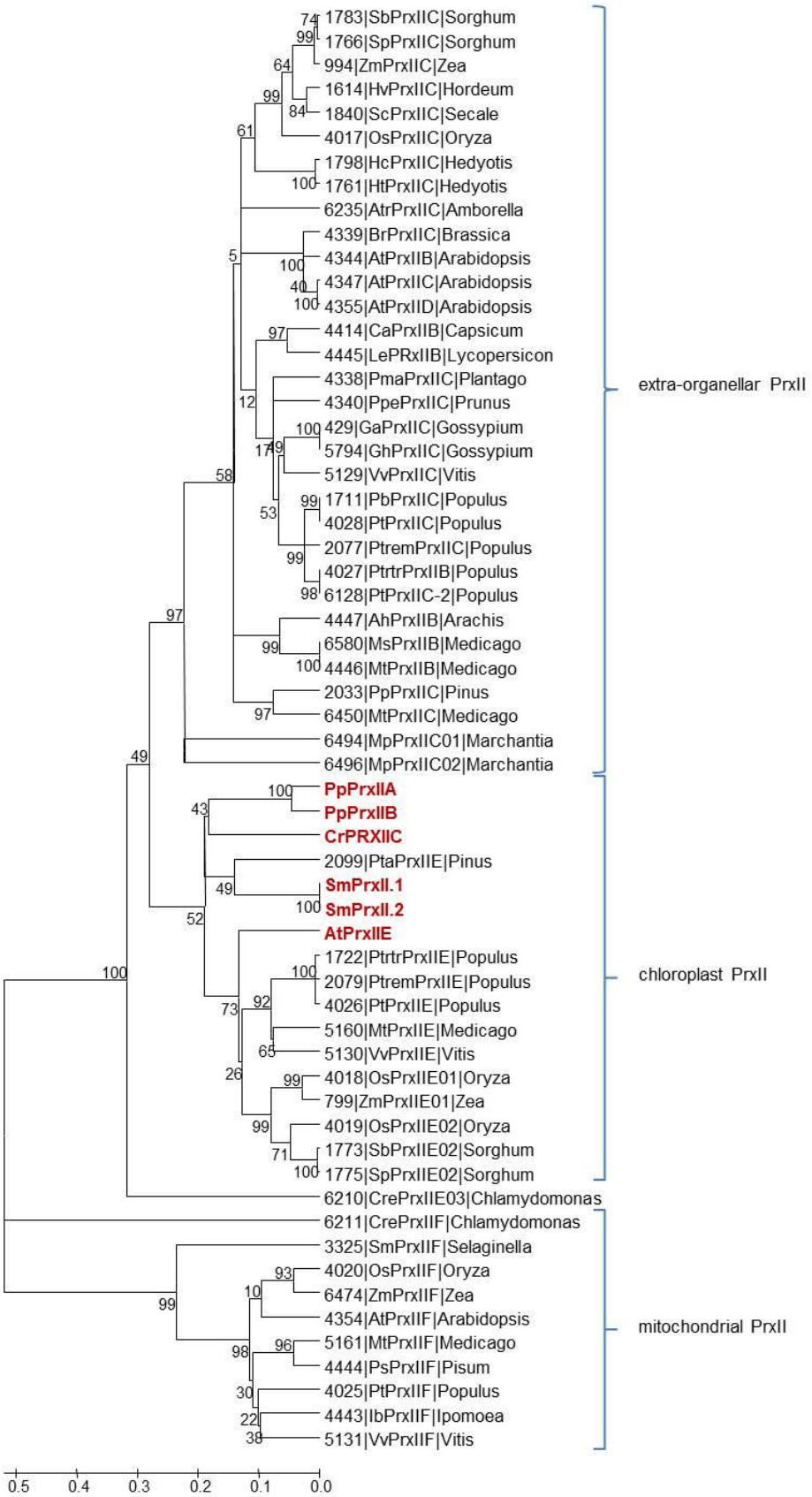

Fig. R27: Neighbor joining phylogenetic tree of the PrxII sequences shown in Fig. R25 (red) and a selection of PrxII full length sequences listed in PeroxiBase. For all PeroxiBase data, the data base IDs were used. The numbers represent bootstrap values. Tree calculation was performed by Prof. Dr. Margarete Baier.

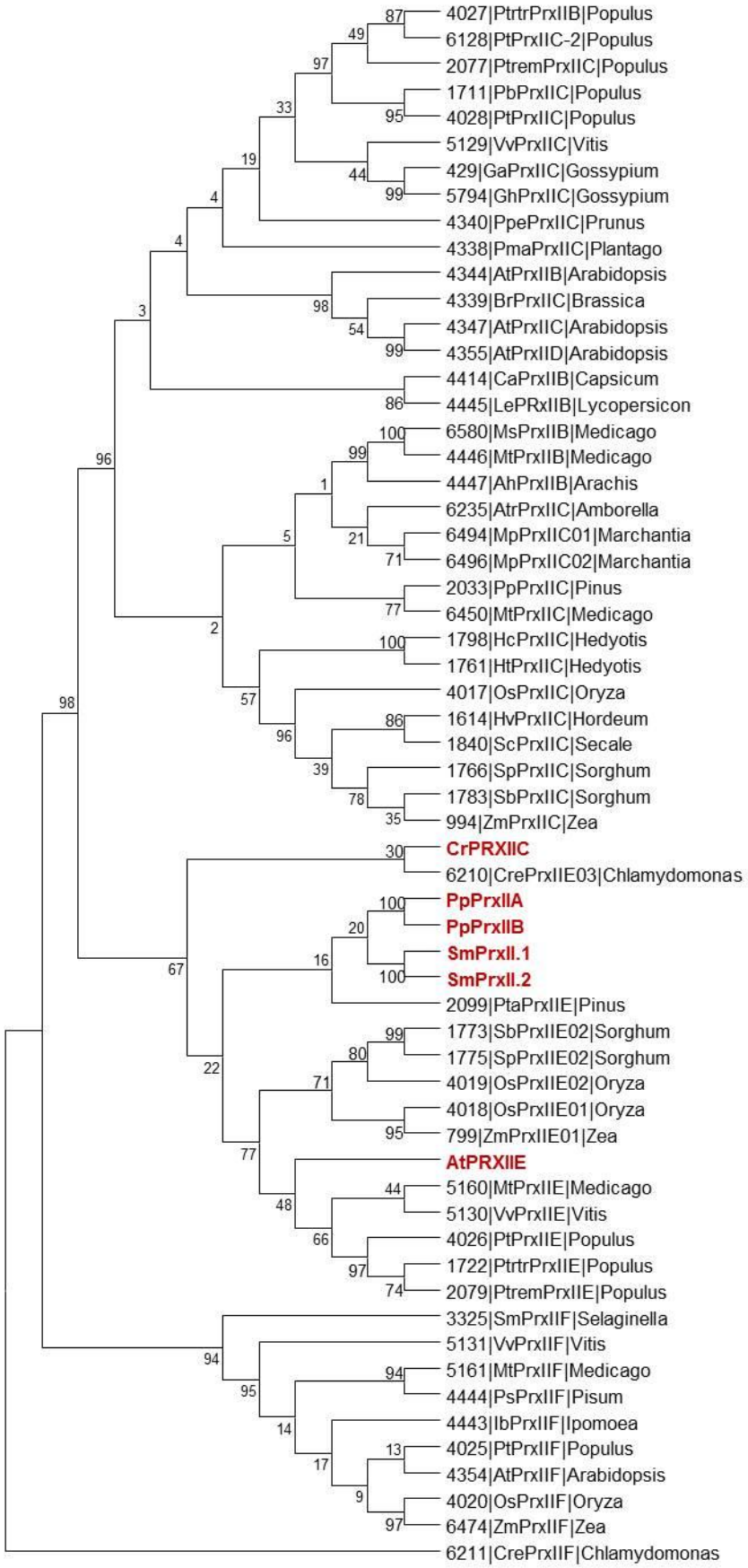

Fig. R28: Maximum parsimony phylogenetic tree of the PrxII sequences shown in Fig. R25 (red) and a selection of PrxII full length sequences listed in PeroxiBase. For all PeroxiBase data, the data base IDs were used. The numbers represent bootstrap values. Tree calculation was performed by Prof. Dr. Margarete Baier.

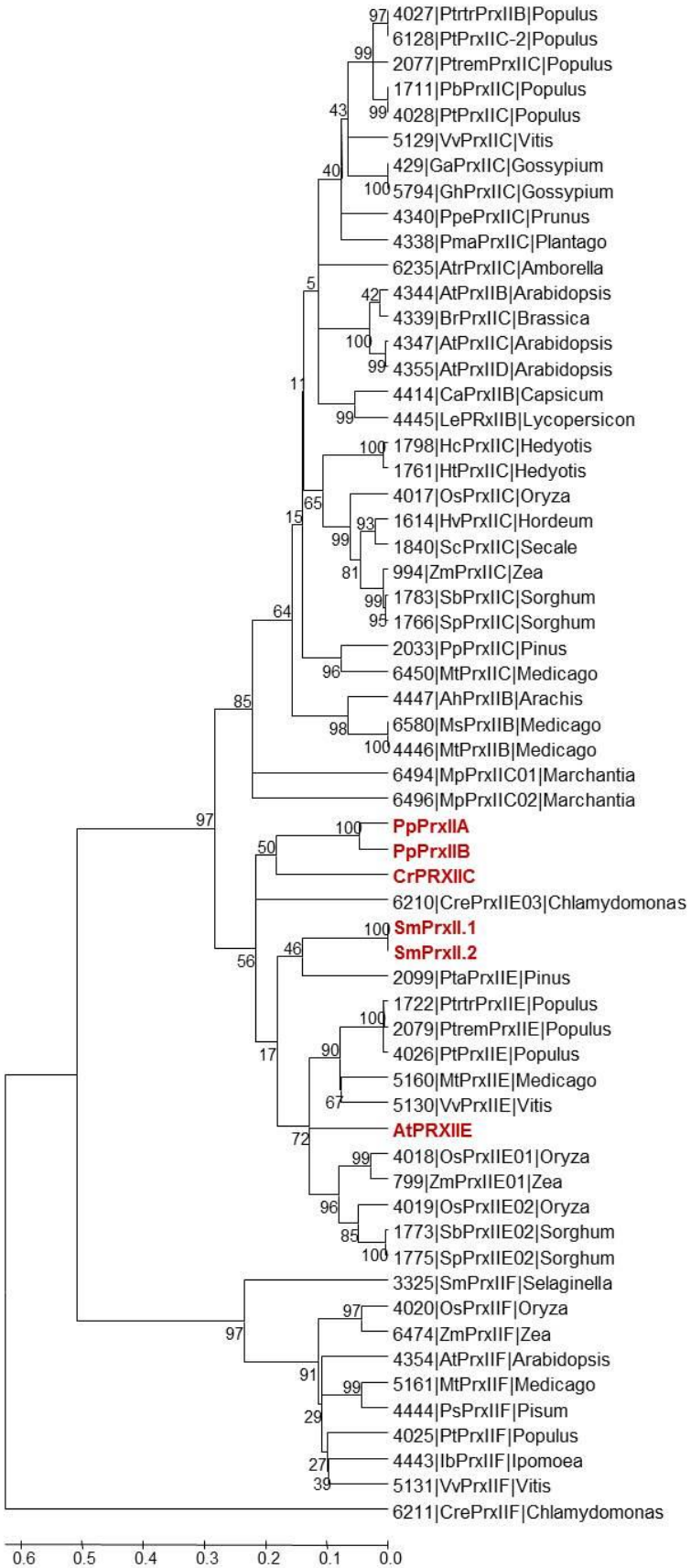

Fig. R29: Minimum evolution phylogenetic tree of the PrxII sequences shown in Fig. R25 (red) and a selection of PrxII full length sequences listed in PeroxiBase. For all PeroxiBase data, the data base IDs were used. The numbers represent bootstrap values. Tree calculation was performed by Prof. Dr. Margarete Baier.

A 18 amino acids long N-terminal α-helix (A5-W22, Fig. R32) with several hydroxylated amino acids and positive charges indicates organellar targeting and recognition of SmGPxB by the protein import complex. Besides these two GPxs, an additional gene with putative GPx function, SmGPxC, was detected in the genome of both *Selaginella* haplotypes (Table R1). Lacking an N-terminal chloroplast targeting signal (Fig. R32), this GPx may be localized in the cytosol. For this reason, less attention was spent on this isoform.

Within the *Physcomitrella patens* genome, two gene models encoding GPxs were identified. High ATP- and TargetP scores (Table R1) indicated the presence of putative organellar targeting signals.

In contrast to the two chloroplast targeted GPx isoforms identified for each of the investigated streptophytes, three organellar GPx were detected in the genome of *Chlamydomonas reinhardtii* (Table R1). These results are consistent with the previous analysis by Dayer *et al.* (2008). Two of them, CrGPxA (GPx1 in Dayer *et al.* 2008) and CrGPxB (GPx2 in Dayer *et al.* 2008), are selenoproteins (X137, Fig. 32). Fu *et al.* (2002) and Novoselov *et al.* (2002) also found a selenocysteine GPx in *Chlamydomonas*. This kind of GPxs is usually present in many animals and microbia (Lu *et al.* 2009). On the contrary, CrGPxC (GPx5 in Dayer *et al.* 2008) is a non-selenocysteine GPx (C136) like the isoforms identified for the other analyzed plant species (Fig. R32). Taken together, since it encodes seleno- as well as non-selenocysteine type GPxs *Chlamydomonas reinhardtii* shows the strongest diversification of these antioxidative defense proteins among the investigated species.

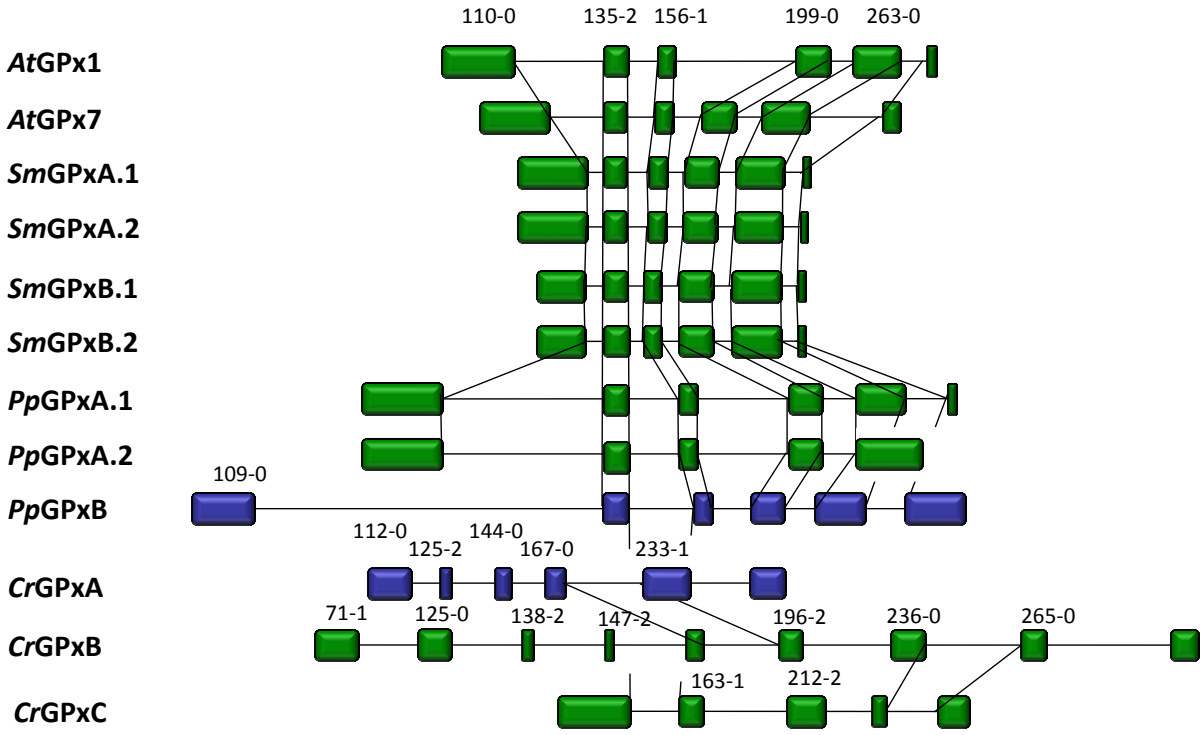

Fig. R30: GPx gene structures of *Arabidopsis thaliana* (At), *Selaginella moellendorffii* (Sm), *Physcomitrella patens* (Pp), and *Chlamydomonas reinhardtii* (Cr). Expressed GPx genes are shown in green, putatively non-expressed in blue. The vertical lines connect corresponding splice sites. The numbers represent position of corresponding amino acids in the alignment shown in Fig. R32 and the relative splice sites within the corresponding codon

3.7.2 Exon-intron structure

Most identified streptophyte gene models encoding chloroplast glutathione peroxidases comprise six exons separated by five introns. The two *Selaginella moellendorffii* GPxs reveal shorter introns, reducing the length of the total genes. Besides the similar gene structure, all splice sites are shared among EST-covered models. This conserved exon-intron structure strongly indicates a common origin of the *Arabidopsis*, *Selaginella* GPxs, and PpGPxA (Fig. R30).

The only exception from the conserved streptophyte gene structure among the expressed models is represented by PpGPxA.2. One out of the four ESTs covering the 3'-end of PpGPxA indicates alternative splicing of the last intron. A putative alternative stop-codon within the intron is indicated by this single EST. The other three ESTs perfectly cover the 3’-end of PpGPxA.1 and point to the existence of the fifth intron, which is also present in all defined *Arabidopsis* and *Selaginella* models. The single non-matching EST shows that the

Physcomitrella genome might also encode a C-terminally aberrant GPx (PpGPxA. 2) (Fig.s R30 and R32, Table R1). In general and similar to the identified APx and Prx genes, the introns in *Physcomitrella* are longer than the ones in *Arabidopsis* and much longer than in *Selaginella*. Especially the non-coding sequence in between exon1 and 2 in PpGPxB is of exceptional length (Fig. R30).

In contrast to the streptophytes, the gene structures of *Chlamydomonas reinhardtii* GPx genes are hardly conserved (Fig. R30). Except the first exon-intron border of CrGPxC (aa135-2), the *Chlamydomonas* GPx genes and the glutathione peroxidase models defined for the other analyzed plant species have no splice site in common (Fig. 30). The distant relation of the *Chlamydomonas* GPxs to streptophyte isoforms is indicated by the presence of one common splice site in CrGPxC and CrGPxB and another conserved splice site between CrGPxB and CrGPxA.

3.7.3 Expression analyses

BLASTN-searches indicated strongly different expression intensities for the homologous GPx genes in the two *Selaginella moellendorffii* haplotypes. 26 perfectly matching ESTs were detected for both gene models encoding SmGPxA, while only 8 and 0 and 5 and 1 were found for SmGPxB.1, SmGPxB.2, SmGPxC.1, and SmGPxC.2, respectively (Table R1). For the chloroplast targeted SmGPxA and SmGPxB models, cDNA fragments of the predicted size (SmGPxA.1: 417 bp, SmGPxA. 2: 415 bp, SmGPxB.1: 298 bp and SmGPxB.2: 296 bp) could be amplified by cDNA-specific saturating RT-PCR (Fig. R31). This demonstrated expressional activity of all predicted *Selaginella* genes encoding organellar GPx.

Transcription of the putatively alternatively spliced PpGPxA was indicated by 10 and 8 EST hits within the cosmoss transcript database (Table R1). To prove this gene expression activity, saturating RT-PCRs were performed with RNA isolated from sterile grown gametophytes. The reaction gave a strong signal of the expected size for PpGPxA.1 demonstrating presence of its mRNA (Fig. R31). For the splice variant PpGPxA.2, RT-PCRs with variant-specific primer combinations revealed a weak band of the expected size (361 bp) besides two larger, unspecific bands (Fig. R31). This implies the alternative splice variant PpGPxA.2 to be transcribed as well. In contrast, for the second, non-EST covered *Physcomitrella* GPx locus, PpGPxB (Table R1), expressional activity of PpGPxB could also not been shown by RT-PCR. Under the applied temperature and $MgCl_2$-conditions only unspecific, too large DNA fragments could be amplified (Fig. R31).

Within the *Chlamydomonas* transcript databases, only ESTs indicating the expression of CrGPxC could be found (Table R1). Performance of saturating RT-PCRs proved expressional activity for both, CrGPxB as well as CrGPxC (Fig. R31). In contrast, for the third *Chlamydomonas* GPx gene model, CrGPxA, no signals were observed which indicate its transcription even if a wide range of conditions (annealing temperature: 46-60°C, 1.5 - 3 mM $MgCl_2$) was applied (Fig. R31). Expression of this isoform may be either very low or restricted to very specific conditions.

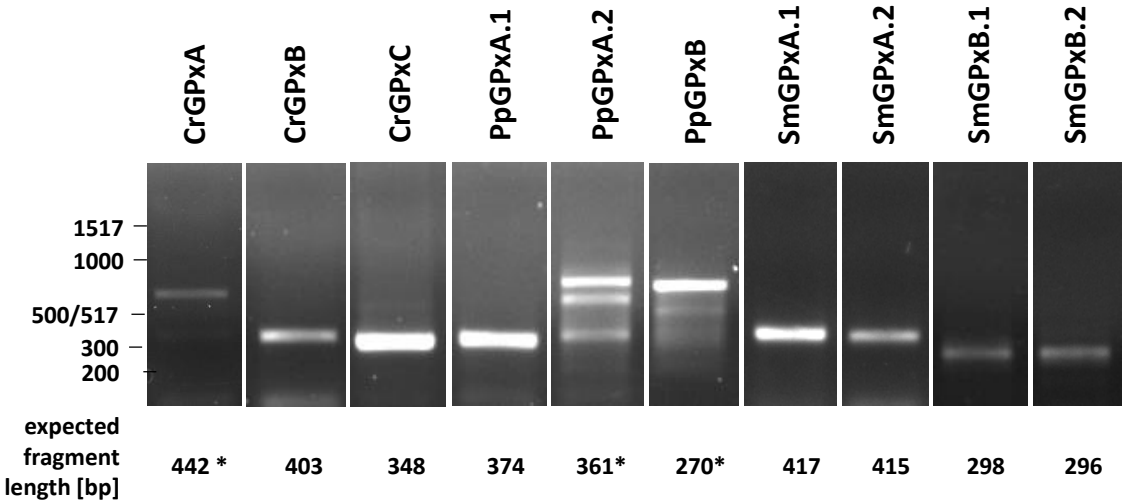

Fig. R31: PCR amplification of cDNA fragments encoding the predicted glutathione peroxidases in *Chlamydomonas reinhardtii*, *Physcomitrella patens*, and *Selaginella moellendorffii*. Samples with unspecific bands are labeled with an asterisk. The PCRs were performed by Benjamin Witsch under the author's supervision.

3.7.4 Characteristics of the predicted proteins

The glutathione peroxidases encoded by the defined gene models within the *Selaginella moellendorffii* genome revealed a high similarity to their *Arabidopsis thaliana* homologs (83-93 %, Table R6). Out of the three isoforms, SmGPxA is the most similar with up to 81 % identical amino acids (Table R6). Both PpGPxA isoforms show 90 % similar amino residues whereas the other *Physcomitrella* GPx has only 51 % of identity (Table R6). The enzymes observed for *Chlamydomonas reinhardtii* in contrast, resemble their gene structures by being most different among the identified GPx isoforms. They show only very low amounts of similar amino acids if compared to their *Arabidopsis* homologs (46-55 % identity, 62-68 % similarity, Table R6).

Table R6: Amino acids identity and similarity of predicted core glutathione peroxidases from *Selaginella moellendorffii*, *Physcomitrella patens*, and *Chlamydomonas reinhardtii* to their homologs in *Arabidopsis thaliana* (Accession numbers: AtGPx1: At2g25080, AtGPx7: At4g31870, AtGPx6: At4g11600, aa124-aa209 in Fig. R32).

Enzyme	**Identitity to *A. thaliana* homologs**			**Similarity to *A. thaliana* homologs**		
	At2g25080	**At4g31870**	**At4g11600**	**At2g25080**	**At4g31870**	**At4g11600**
SmGPxA.1/2	79/80 %	80/ 81 %	74/74 %	91/91 %	93/93%	86/87 %
SmGPxB.1/2	77/77 %	74/74 %	75/75 %	83/83 %	84/84 %	83/83 %
SmGPxC.1/2	73/73 %	74/74 %	73/73 %	84/84%	86/86 %	80/80 %
PpGPxA.1/2	80/80 %	83/83 %	78/78 %	90/90 %	90/90 %	85/85 %
PpGPxB	51%	51%	51%	74%	74%	75%
CrGPxA	48%	49%	50%	63%	62%	60%
CrGPxB	46%	46%	47%	66%	66%	67%
CrGPxC	55%	55%	52%	65%	68%	64%

As mentioned for the atypical peroxiredoxins, only few regions or amino acids crucial for a correct and effective glutathione peroxidase function have been published. Within the plant kingdom, two motifs are important for efficient glutathione peroxidases: FPCNQF and WNY/FxKFV/I (Toppo *et al.* 2008). Labeled “C” in Fig. R32, they are forming the catalytic site of the enzymes.

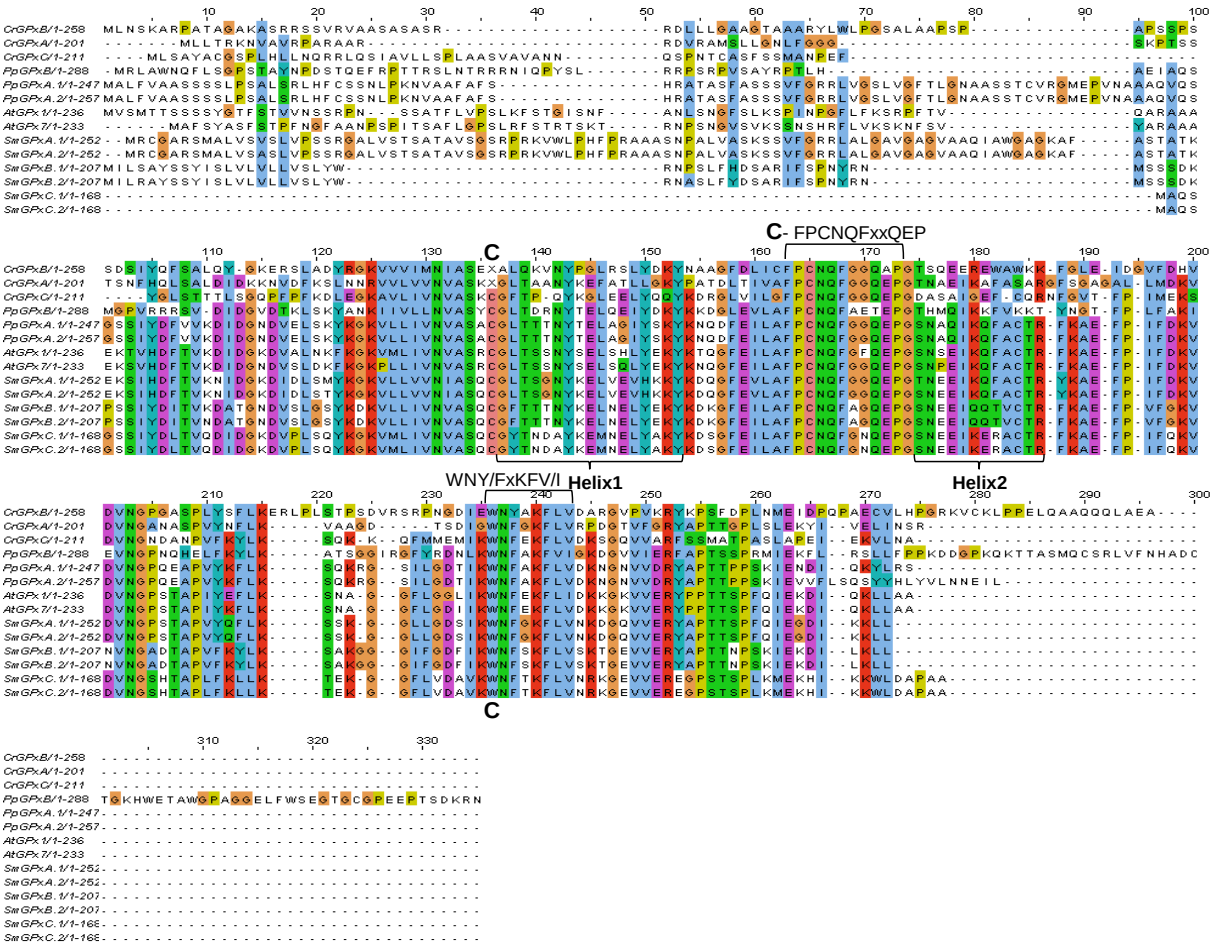

Fig. R32: Comparison of glutathione peroxidase amino acid sequences. Amino acid sequence alignment of GPx from *Arabidopsis thaliana* (At), *Selaginella moellendorffii* (Sm), *Physcomitrella patens* (Pp), and *Chlamydomonas reinhardtii* (Cr). The label "C" marks the catalytic site.

The chloroplast targeted GPxs identified in all investigated plant species show a high conservation of these regions (FPCNQF: F163 - F168), WNY/FxKFV/I: W236 - V/I243, Fig. R32).

Among all defined GPxs, PpGPxB shows the strongest sequence modifications in the domains encoding the FPCNQFxxQEP region (Fig. R32, *e. g.* Q167T). These substitutions together with several additional exchanges (*e. g.* Y/H105R and V/I117T) and the untypical C-terminal extension (Fig. R32) suggest that PpGPxB, if expressed, may not be fully functional.

Generally, the data received for the green algae *Chlamydomonas reinhardtii* are widely consistent with Dayer *et al.* (2008). CrGPxA represented an exception since its amino acid sequence could be corrected by the insertion of a G residue (G137, Fig. R32), which was missing at the position following the selenocysteine.

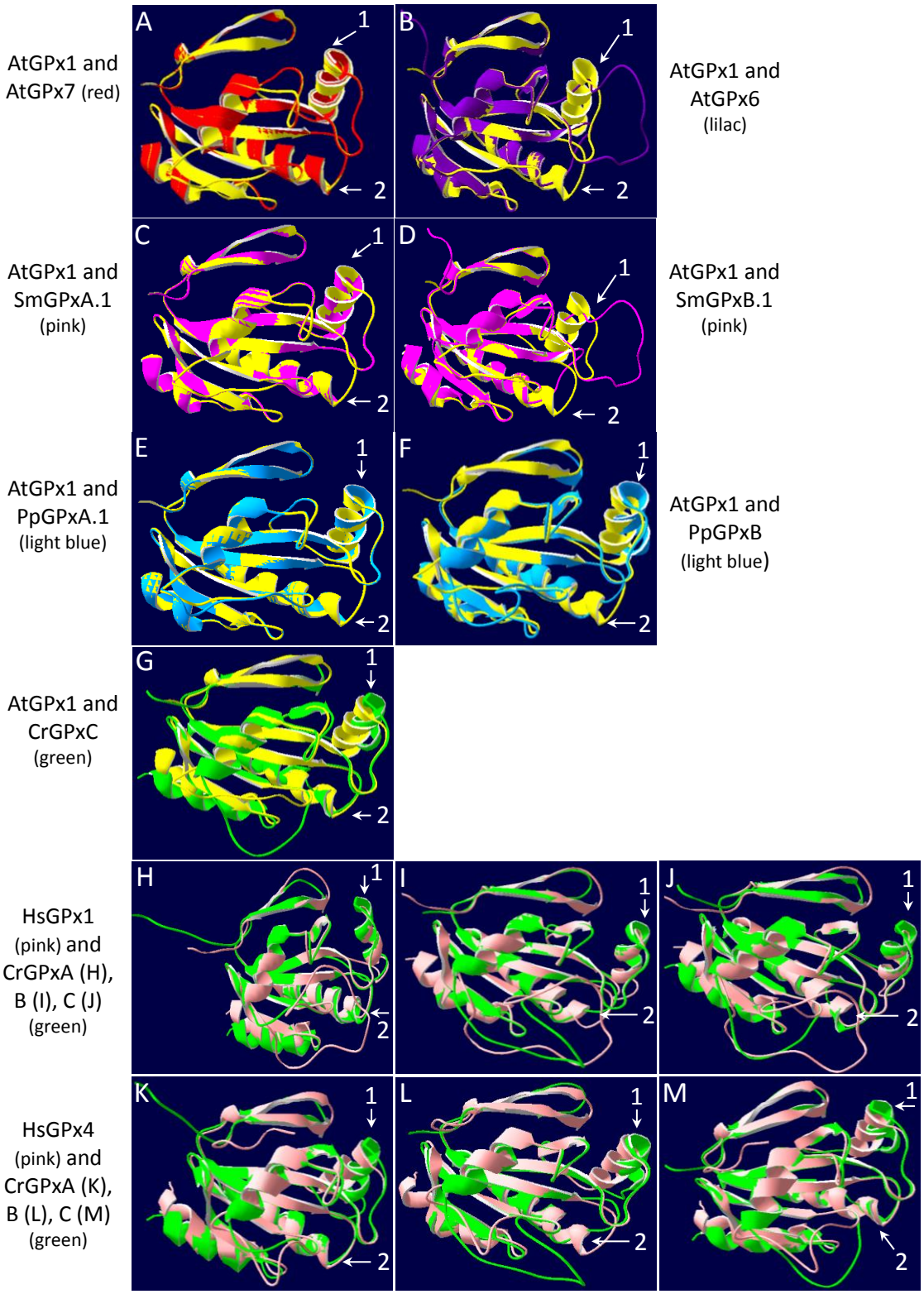

Fig. R33: Superimposition of AtGPx1 (yellow) and (A) AtGPx7 (red), (B) AtGPx6 (lilac), (C) SmGPxA.1 (pink), (D) SmGPxB.1 (pink), (E) PpGPxA.1 (light blue), (F) PpGPxB (light blue), and (G) CrGPxC (green). Superimpositions of human GPx1 (rose) and (H) CrGPxA (green), (I) CrGPxB (green), and (J) CrGPxC, Superimpositions of human GPx4 (rose) and (K) CrGPxA (green), (L) CrGPxB (green), and (M) CrGPxC (green). The arrows point at the helices 1 and 2 for which the structures of the presented proteins differ from the AtGPx1/AtGPx7 structure.

Superimposition of the AtGPx1 and AtGPx7 proteins modeled and presented by SWISSMODEL and Swiss-pdbViewer (Guex and Peitsch 1997, Schwede *et al.* 2003, Arnold *et al.* 2006) revealed no differences between their 3D structures (Fig. R34A). In contrast, AtGPx6 differed structurally by replacement of helix 2. Instead, a not structured protein domain and a shorter helix 1 were observed (Fig. R33B).

When the *Arabidopsis thaliana* GPx isoforms were compared to their *Selaginella moellendorffii* homologs, the superimpositions showed almost structural identity of SmGPxA.1 and SmGPxA.2 to AtGPx1 and AtGPx7 (Fig.s R33C). The 3D-model of SmGPxB in contrast, indicated a less structured organization of amino acid 175 to 186 (Fig. R33D). This region folds into an α-helix in SmGPxA and the *Arabidopsis* chloroplast GPx1 protein (Fig. R33C). Due to this unstructured domain, SmGPxB shows a higher similarity to mitochondrial AtGPx6 (Fig. R33D).

Superimposition of the protein models identified in *Physcomitrella patens* to the chloroplast targeted *Arabidopsis* GPxs revealed a high structural similarity of PpGPxA.1 and PpGPxA.2 to their *Arabidopsis* homologs indicating that PpGPxA is the *Physcomitrella* homolog of *Arabidopsis* GPx1 and GPx7 (Fig. R33E). In contrast and as mentioned above, the other GPx isoform found to be encoded by *Physcomitrella*, PpGPxB, shows tremendous differences (Fig. R33F). Its 3D-structure superimposed to AtGPx1 supports the suggestion that this protein may not reveal (full) glutathione peroxidase functionality.

In *Chlamydomonas*, the predicted structure of the well expressed non-selenocysteine-type CrGPxC shows several structural aberrations if compared to AtGPx1 (Fig. R33G). This may indicate CrGPxC to represent a distinct type of glutathione peroxidases. Among all differences, the aberrant twists in helix 1 and helix 2 (Fig. R33G) may have the strongest impact on enzyme function. They cause a positional change of the active site suggesting the catalytic activity of this GPx to be affected.

Despite the strong differences to AtGPx1, comparison to human GPx showed stronger structural similarity of CrGPxC to monomeric human GPx4 than to tetrameric GPx1 as do the other *Chlamydomonas* GPxs (Fig.s R34H-M). This may indicate that the CrGPxA, CrGPxB, and CrGPxC are part to the monomeric GPx cluster. Monomeric isoforms are typical for plants. Together with CrGPxC being a non-selenocysteine type GPxs, it resembles more the higher plant than animal isoforms (Novoselov *et al.* 2002, Navrot *et al.* 2006).

3.7.5 Phylogenetic analyses

Plant GPx may have evolved from a single ancestral gene by four major gene duplication events (Margis *et al.* 2008). The initial duplication was supposed to have taken place prior to separation of monocots and dicots or even before separation of gymnosperms and angiosperms. The phylogenetic analyses of the identified GPxs were performed by using the protein sequences of the defined gene models and sequences encoding plant GPxs taken from PeroxiBase. They were calculated according to the neighborhood joining, maximum parsimony and minimum evolution algorithms (Fig.s R34-R36). For *Arabidopsis thaliana* all GPxs were included, irrespective of the subcellular localization of the enzymes. The distance of the chloroplast isoforms to the other *Arabidopsis* GPx indicates that the chloroplast targeted AtGPx1 and AtGPx7 occurred as a result of a late gene duplication. This event may have taken place after separation of mitochondrial, cytoplasmic, and chloroplast paralogs. For the chloroplast GPx genes from the other investigated species, a more ancient separation can be assumed from the distant positions in the calculated phylogenetic trees (Fig.s R34-36). The variability between the three different types of phylogenetic trees makes it impossible to definitely answer the question whether chloroplast targeting was established independently for different chloroplast paralogs or prior to the final gene duplication event. The phylogenetic trees suggest early separation and independent evolution of GPx isoforms. Therefore, in contrast to the assumptions made by Margis *et al.* (2008), the phylogenetic analyses show that the gene duplication resulting in chloroplast paralogs may have occurred much earlier than the separation of angiosperms and gymnosperms.

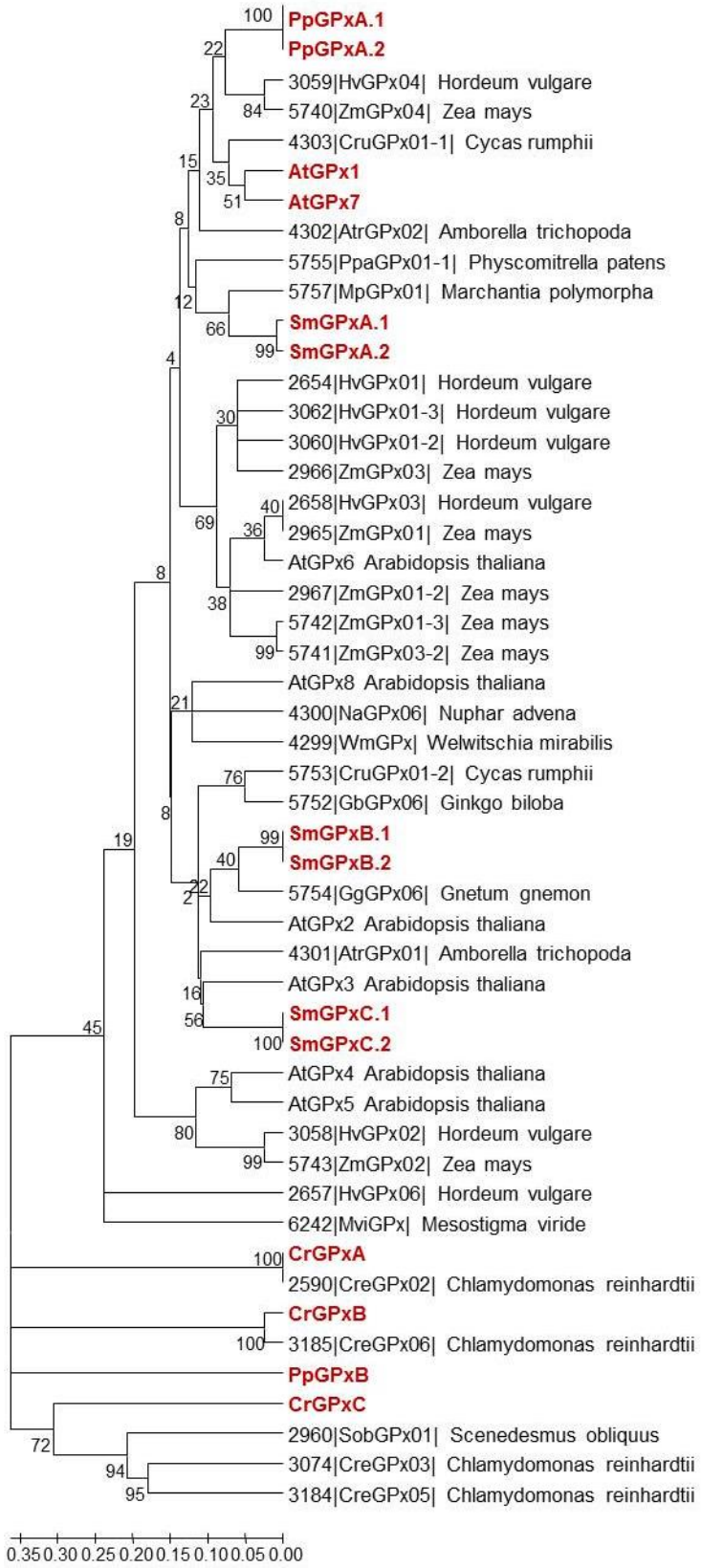

Fig. R34: Neighbor joining phylogenetic tree of the GPx sequences shown in Fig. R32 (red) and a selection of plant GPx full length sequences listed in PeroxiBase. For all PeroxiBase-data, the data base IDs were used. The numbers represent bootstrap values. Tree calculation was performed by Prof. Dr. Margarete Baier.

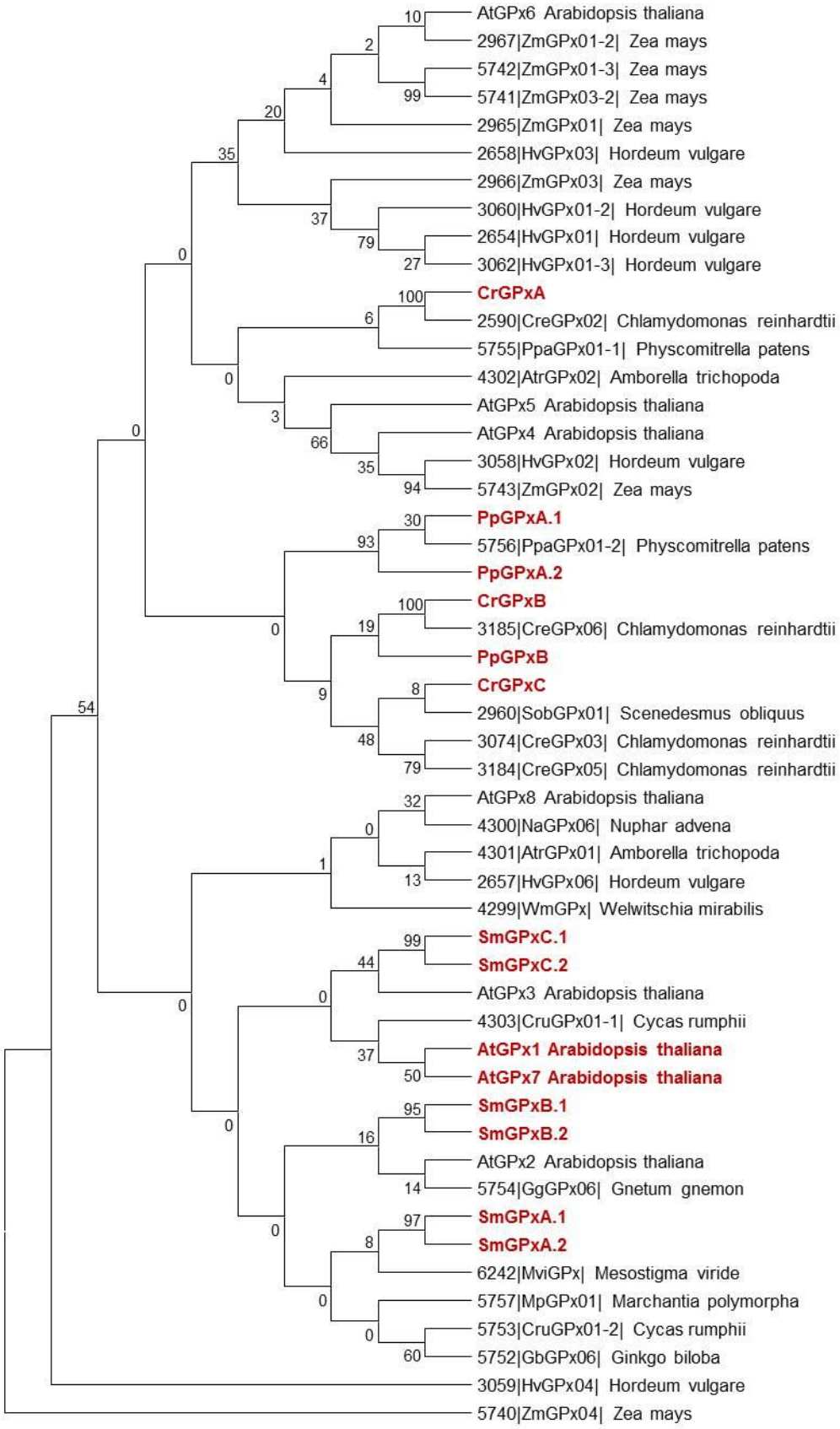

Fig. R35: Maximum parsimony phylogenetic tree of the GPx sequences shown in Fig. R32 (red) and a selection of plant GPx full length sequences listed in PeroxiBase. For all PeroxiBase-data, the data base IDs were used. The numbers represent bootstrap values. Tree calculation was performed by Prof. Dr. Margarete Baier.

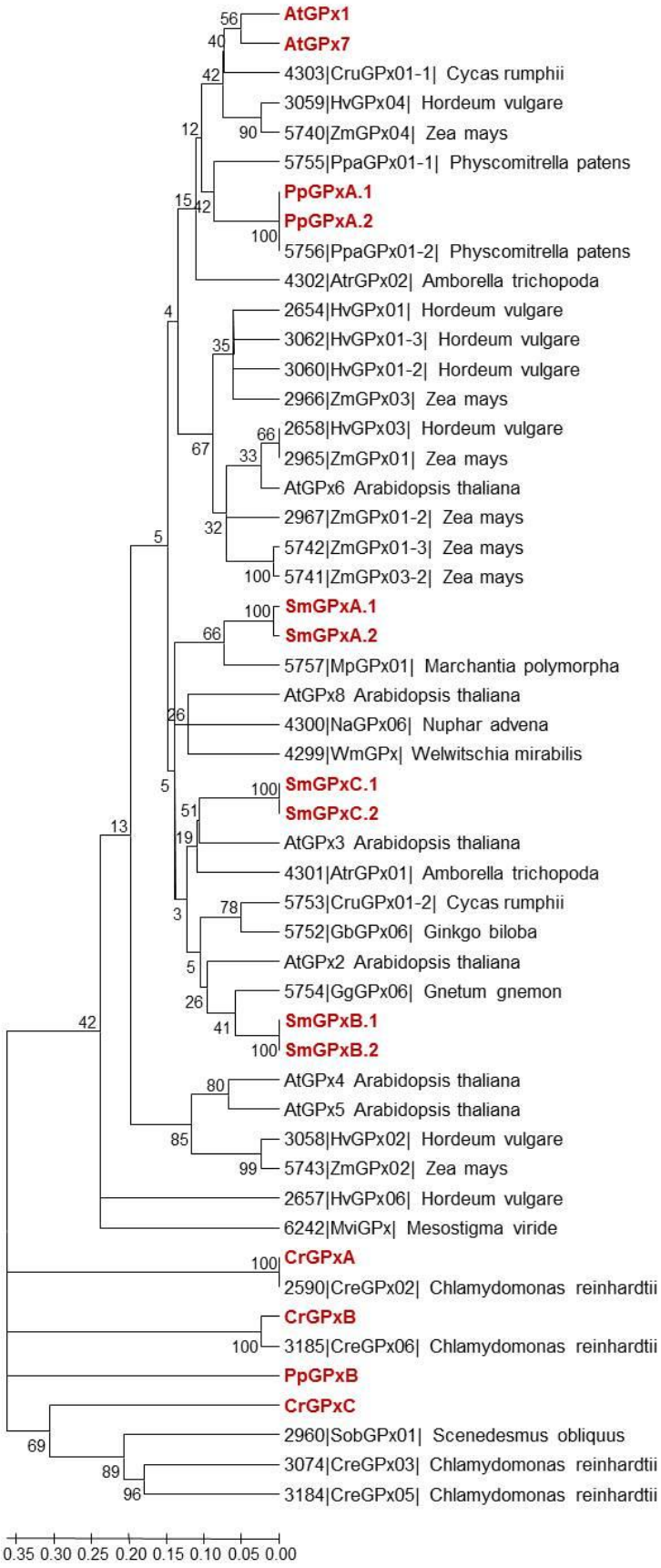

Fig. R36: Minimum evolution phylogenetic tree of the GPx sequences shown in Fig. R32 (red) and a selection of plant GPx full length sequences listed in PeroxiBase. For all PeroxiBase-data, the data base IDs were used. The numbers represent bootstrap values. Tree calculation was performed by Prof. Dr. Margarete Baier.

3.8 Relative expression of chloroplast APxs, 2CPs, PrxQs, PrxIIs, and GPxs

Microarray-based data (available from TAIR) show that sAPx and tAPx genes are weakly expressed in *Arabidopsis thaliana* if compared to its 2CPs (expression level of the entire rosette after transition to flowering: sAPx: 328.86, tAPx: 403.91, 2CPA: 3184.8, 2CPB 1222.76, Table R1). Also the other *Arabidopsis* peroxiredoxin and glutathione peroxidase encoding genes revealed a stronger expression (Table R1). In general, the 2CPs are the strongest expressed genes among the investigated antioxidant enzymes in *Arabidopsis*.

For the APxs encoded by the two *Selaginella moellendorffii* haplotypes, 3 and 6 sAPx ESTs and 9 and 10 tAPx ESTs (Table R1) were identified by EST cluster analyses. In the same data set 67 and 60 ESTs for Sm2CPA, 12 and 15 for SmPrxII, and 21 and 7 for SmPrxQ were counted (Table R1). BLAST searches using the gene models, which showed an atypical exon-intron-structure (Fig.s R5, R12, R18, R24), indicated that these isoforms are not or only weakly transcribed (Table R1). The three gene models encoding GPxs revealed different expression intensities. 26 ESTs for SmGPxA indicated its transcription, while SmGPxB was less covered (Table R1). These relative numbers indicate a rather weak expression of APx if compared to the peroxiredoxins (especially Sm2CPA) and glutathione peroxidases.

For *P. patens*, the relative EST counts indicate a strong expression of the thylakoid ascorbate peroxidase (Table R1). Among the *Physcomitrella* gene models encoding chloroplast antioxidant enzymes, PptAPx revealed the highest EST coverage. Nevertheless, for all models transcripts, which were detected within the cosmoss database, the results indicated their expression. The only exception is PpGPxB, for which not ESTs could be found (Table R1).

In *C. reinhardtii*, for CrsAPxA only 5 ESTs were counted in the JGI database, Cr2CPA expression was represented by 121 ESTs (Table R1). The other Prx genes and the GPx genes were much less active, indicating that Cr2CPA has the strongest impact on the chloroplast antioxidant system.

Taken together, 2-Cys-peroxiredoxins showed indications for the strongest transcription among the investigated gene models in *Arabidopsis*, *Selaginella*, and *Chlamydomonas*. According to the collected EST data, the order of the less expressed enzyme types varies among the plant species (Tables R1, R7). *Physcomitrella* is contrasting the seed plant, the lycophyte, and the green alga. Its single ascorbate peroxidase may have the most important role in H_2O_2 detoxification while the other antioxidant enzymes identified are less expressed

(Tables R1, R7). The EST data indicate that the moss prefers the ascorbate-dependent detoxification system while the other studied species favor the ascorbate-independent antioxidative defense in chloroplasts. However, in general, EST data need to be considered with care since also other regulatory levels are involved in the gene expression process.

In general, *Arabidopsis* encodes eight chloroplast antioxidative enzymes detoxifying hydroperoxides while the investigated lower plants have ten isoforms, each. It may be that other factors support the defense in the higher plant making it effective enough to ensure its host's fitness.

Table R7: EST-ranking of the investigated antioxidant enzyme families in *Arabidopsis thaliana*, *Selaginella moellendorffii*, *Physcomitrella patens*, and *Chlamydomonas reinhardtii*. The ranking was done according to EST counts. Rank 1 represents the highest and rank 5 the lowest amount of ESTs covering the respective enzyme family encoding genes.

EST-ranking \ Organism	*Arabidopsis thaliana*	*Selaginella moellendorffii*	*Physcomitrella patens*	*Chlamydomonas reinhardtii*
1	2-Cys-peroxiredoxins	2-Cys-peroxiredoxins	Ascorbate peroxidases	2-Cys-peroxiredoxins
2	Peroxiredoxins Q	Glutathione peroxidases	2-Cys-peroxiredoxins	Peroxiredoxins type II
3	Glutathione peroxidases	Peroxiredoxins Q	Peroxiredoxins type II	Ascorbate peroxidases
4	Peroxiredoxins type II	Peroxiredoxins type II	Peroxiredoxins Q	Glutathione peroxidases
5	Ascorbate peroxidases	Ascorbate peroxidases	Glutathione peroxidases	Peroxiredoxins Q

3.9 *Physcomitrella patens* thylakoid APx

Bioinformatic analyses revealed that the *Physcomitrella* genome encodes only a single ascorbate peroxidase which is targeted to chloroplasts (Table R1). Compared to the other investigated APx genes, its exon-intron-pattern is atypical (Fig. R5). The gene comprises only two exons while other streptophytic isoforms are encoded by ten to twelve. Despite this, EST data indicate that PptAPx is highly expressed and represents the most abundant mRNA among the ones encoding the investigated chloroplast antioxidant enzymes (Tables R1, R7). For these reasons, further investigatory focus was set on this enzyme.

3.9.1 Retrotransposonal origin

Analyses of the PptAPx gene environment revealed a strong accumulation of retrotransposonal footprints upstream and downstream of the ORF. Fig. R37 shows 51,268 bp of the *Physcomitrella* scaffold 424. The genome area spans the region in between two genes, interrupted by the PptAPx encoding ORF. The region comprises 32 transposonal footprints of different length. Long terminal repeat (LTR) retrotransposons commonly show a total length of 6.4-8.9 kbp and contain LTRs of 375-1822 bp, each.

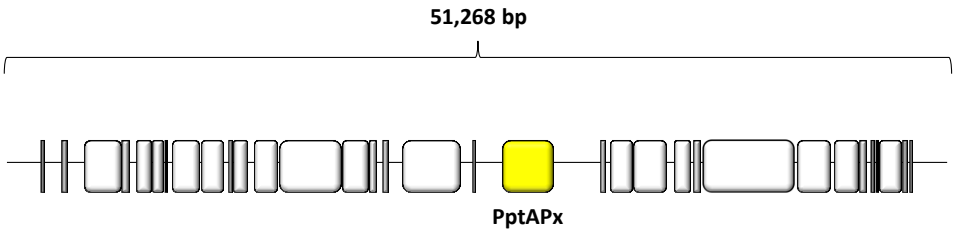

Fig. R37: Genome surrounding of the PptAPx gene on scaffold 424 (51,268 bp). The gene is labelled in yellow while retrotransposonal footprints are marked in grey.

In conclusion, the presence of retrotransposonal footprints points to the PptAPx gene being introduced at this location via retrotransposition. This supposition is supported by the gene structure of PptAPx (Fig. R5). In general, retrotransposons possess weak polyadenylation sites. The RNA transcription machinery sometimes does not recognize their termination motifs and continues transcribing until the next termination signal (Moran *et al.* 1996, Xing *et al.* 2006). This can lead to gene duplications. No traces of the original chloroplast ascorbate peroxidase encoding gene could be found within the whole *Physcomitrella* genome. Thus, this ORF got lost during evolution.

3.9.2 Transcription initiation of PptAPx

Many ESTs covered the area between the start-ATG and the TATA-box 175 bp upstream. 17 ESTs showed a longer 5'-terminus (Fig. R38, for a more detailed view see Appendix Fig. A1). It was suggested that 337 bp upstream of the PptAPx start-ATG may represent a long 5'-UTR. Due to their high number, it was assumed that the 17 ESTs were not contaminated by DNA.

Well known transcription initiation motifs are TATA-boxes. Their consensus sequence is TATAWAW, where W can be either a T or an A (Loganantharaj 2006). According to this, two TATA-boxes were predicted within the PptAPx promoter (Fig. R38). Together with the ESTs data, this indicated that there might be two transcription initiation sites controlling the expression of PptAPx (Fig. R38, for a more detailed view see Appendix Fig. A1).

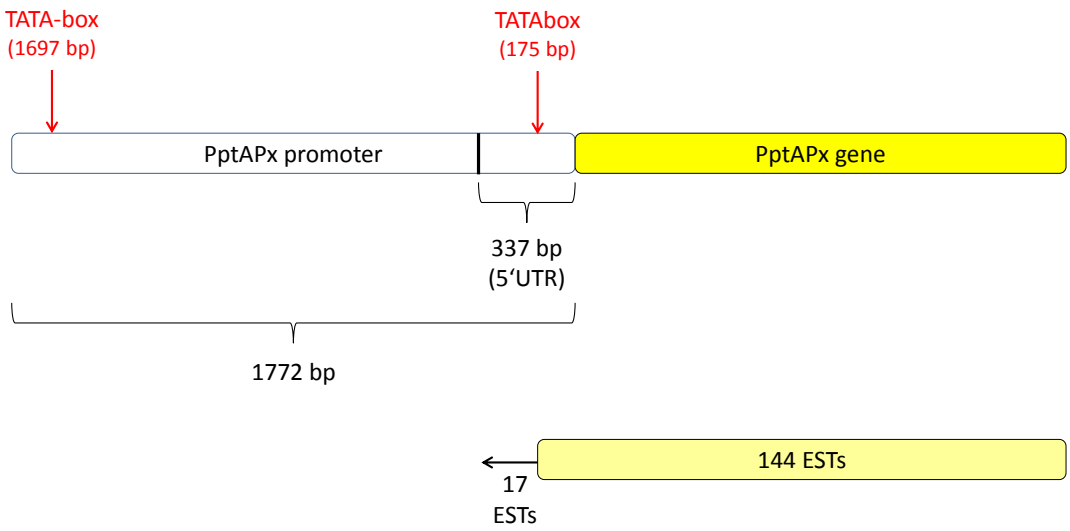

Fig. R38: PptAPx promoter, TATA-boxes, and specific ESTs. The 1772 bp promoter sequence includes the predicted 5'-UTR of 337 bp. Two TATA-boxes were detected according to the criteria listed in Loganantharaj (2006). They are located 175 bp and 1697 bp upstream of the PptAPx start-ATG. 144 ESTs cover the PptAPx gene and/or the predicted 5'-UTR downstream of the TATA-box at 175 bp, while 17 ESTs show a longer 5'-terminus. For a more detailed view on the EST-coverage see Appendix Fig. A1.

3.9.2.1 Transcription initiation sites for the *Physcomitrella* tAPx

To investigate the transcription initiation of PptAPx, different parts of its promoter were fused to a firefly luciferase gene via Gateway cloning. These areas controlled the expression of the reporter gene. As destination clone for all promoter-reporter gene analyses, the plasmid pHGWL7.0 was used (Karimi *et al.* 2005). For the *Physcomitrella* chloroplast APx isoform, three different constructs were produced. The upstream transcription regulating element (UTRE) 1/2 included 1772 bp which was set to be the whole promoter region (Fig. R39). Due to coverage, EST analyses predicted the first 337 bp upstream of the PptAPx-start-ATG to be a long 5'-UTR (Fig. R38). To verify this identity, this region was also fused to a luciferase gene. The construct was dedicated UTRE2 (Fig. R39). 1455 bp upstream of UTRE2 controlling the expression of luciferase were represented by the UTRE1 construct (Fig. R39). *Physcomitrella patens* gametophytes were transfected with *Agrobacteria* strains containing the UTRE1/2 construct.

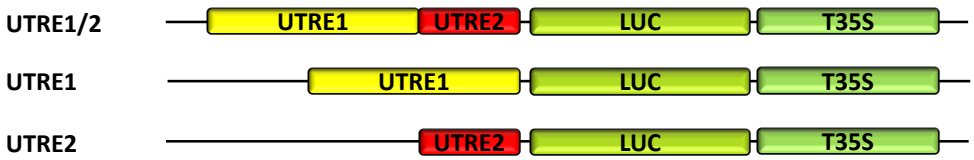

Fig. R39: PptAPx promoter::luciferase (LUC) constructs used to transfect *Physcomitrella* gametophyte colonies: UTRE1/2: 1772 bp upstream of the PptAPx start-ATG, UTRE1: 1455 bp upstream of UTRE2, UTRE2: 337 bp upstream of the PptAPx start-ATG

Following transfection, all used gametophyte colonies stayed green and healthy. Fig. R40 shows a photography and luminogram of them six days post transfection. Both, the UTRE1/2 construct, containing the whole PptAPx promoter, as well as the UTRE2 construct, representing the predicted 5'-UTR, caused development of a strong luminescence after spraying the plants with a luminol solution supplemented with ATP (Fig. R40). In contrast, when the plants were transfected with *Agrobacteria* holding the UTRE1 construct, they showed only weak luciferase activity (Fig. R40). Negative controls, no matter whether the flooding solution contained *Agrobacteria* or not, showed not luminescent activity (Fig. R40).

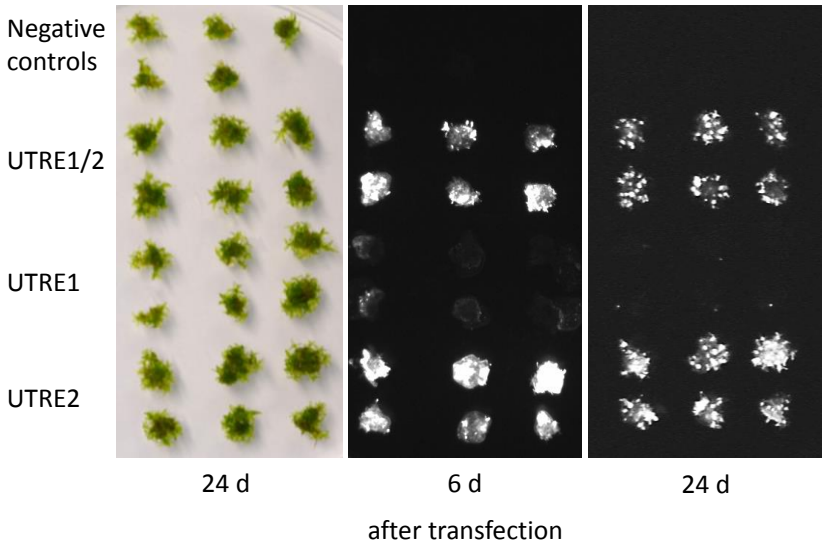

Fig. R40: Transfected *Physcomitrella* gametophytes. Two to three colonies were transfected per construct or negative control. Left: Photography, Right: Luminogram taken with a LAS4000mini. UTRE1/2 and UTRE2 constructs cause a strong LUC expression in comparison to the UTRE1 construct. Negative controls show no chemiluminescent activity. The constructs with which they were transfected are written on the left

These results indicate that the transcription of PptAPx is driven by two initiations sites (Fig. R40, R41). The first and stronger one is located within the first 337 bp upstream of the start-ATG. The fact that the UTRE1 construct also caused luminescence points to the existence of another, much weaker, initiation site, localized in a more upstream region of the genome. The strong expression driven by the whole PptAPx promoter is mainly due to the first initiation site while the other may represent an alternative and might have a minor or fine-tuning impact on the expression of the chloroplast ascorbate peroxidase. It is possible that at least one of the two transcription initiation sites represents a relic of a retrotransposon, which was installed as a functional element. Other explaining options are (i) that one of the sites arose coincidentally and (ii) that one of them is a leftover from either the APx ancestor or another gene which was replaced by retrotransposonal footprints.

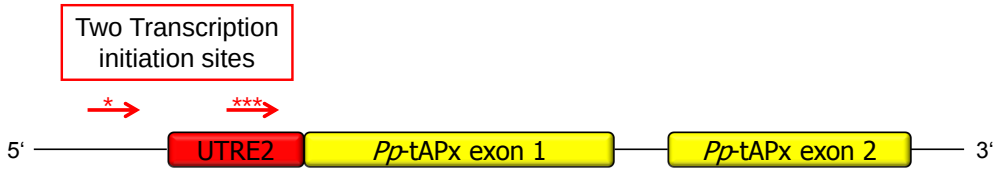

Fig. R41: Transcription initiation sites of PptAPx. The transcription of this gene is initiated at two sites: (i) within the first 337 bp upstream of the PptAPx start-ATG, which was predicted as a 5’-UTR (represented by the UTRE2 construct and, therefore, designated with the same name) and (ii) further upstream of UTRE2. They are marked by red arrows. The first initiation site drives a strong transcription if compared to the second. This variation in the transcription activity is indicated by asterisks.

3.9.3 High PptAPx expression in *Physcomitrella patens*

EST data indicated that the gene is highly expressed at least in comparison to other chloroplast antioxidant enzymes encoding genes (Table R1). Moss gametophytes showed promoter activity when transfected with *Agrobacteria* strains containing the UTRE1/2, UTRE1, or UTRE2 constructs (Fig. R39). To estimate the strength of the PptAPx promoter, its impact on the expression of luciferase was compared to chloroplast ascorbate peroxidase promoter from *Arabidopsis thaliana* which controlled the same reporter gene. One promoter-reporter gene construct was produced for each isoform. While the AttAPx promoter region was set to 1469 bp upstream of the encoding gene, the AtsAPx promoter region was represented by the first 1957 bp upstream. However, for AtsAPx 42 bp and for AttAPx 2 bp upstream of the start-ATGs were not included in the constructs. According to TAIR (www.Arabidopsis.org) they are part of their gene's 5'-UTR.

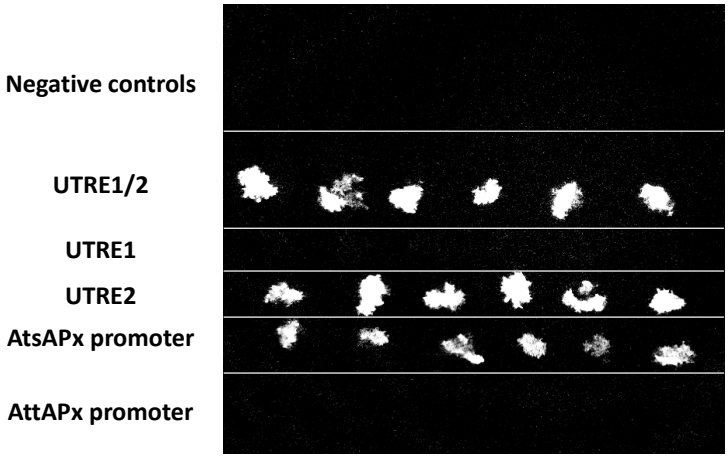

Fig. R42: *Physcomitrella* gametophyte colonies, two days after transfection. One colony was transfected per construct or negative control. The luminogram was taken with a LAS4000mini and is exemplarily for at least two experimental replicates. UTRE1/2 and UTRE2 constructs cause a strong LUC expression in comparison to the UTRE1 construct. Plants transfected with the AtsAPx promoter::LUC construct show a stronger chemiluminescence than when the AttAPx promoter::LUC construct was used, but weaker than seedlings containing UTRE1/2 and UTRE2 constructs. Negative controls show no chemiluminescent activity. The constructs with which they were transfected are written on the left.

Gametophyte colonies were transfected after ten days of cultivation in standard growth conditions. Chemiluminescence was detected, visualized, and documented after two day of recovery (Fig. R42).

As described above, usage of UTRE1/2 and UTRE2 constructs caused a strong chemiluminescence (Fig. R42). Nearly no LUC activity was visible for UTRE1. The

promoter-reporter gene constructs designed for *Arabidopsis* APxs caused different luminescence intensities. The promoter of the stromal ascorbate peroxidase revealed to drive a rather strong LUC expression in comparison to chemiluminescence conferred by the promoter of the thylakoid-bound isoform, although it was slightly weaker than the one caused by UTRE1/2 and UTRE2 (Fig. R42). Negative controls gave no luminescent signal (Fig. R42).

3.9.4 Localization and function of PptAPx

3.9.4.1 Organellar targeting of PptAPx

The identified *Physcomitrella* gene model encoding the thylakoid-bound ascorbate peroxidase was predicted to be targeted to chloroplasts by the publically available online tool TargetP (Emanuelsson *et al.* 2000) and ATP (Mitschke *et al.* 2009) (Table R1). To prove the protein localization, targeting studies had to be performed, for which different constructs were designed (Fig. R43). Localized at the N-terminus of the respective protein, transit peptides target proteins to their organellar destination. Therefore, the first 100 amino acids of PptAPx were fused to mGFP6 or YFP, respectively (Fig. R43). As positive control for targeting, fusions with the first 297 bp of the *Physcomitrella* ftsZ1-1 gene (filamentous temperature-sensitive Z1-1) were generated (Fig. R43). The PpftsZ1-1 protein was proven to be targeted to chloroplasts by Reski (2002) by transient PEG-mediated *Physcomitrella* protoplast transformation. As destination vectors, pXCSG-YFP (Witte *et al.* 2004, Feys *et al.* 2005) was chosen for YFP-fusions and pMDC83 (Curtis and Grossniklaus, 2003) for mgfp6-fusions. In both plasmids, expression of the transit peptide-fusions was driven by a CaMV35S promoter and terminated by a nos-terminator (Fig. R43).

Fig. R43: Constructs designed for organellar targeting studies in *Physcomitrella*. Left: Fusion of the PpftsZ1-1 transit peptide (region encodes the first 99 amino acids of the protein) to YFP, used for chloroplast targeting positive controls. Right: Fusion of the PptAPx transit peptide (region encodes the first 100 amino acids of the protein) to YFP. The expression of both protein fusions was controlled by a CaMV35S-promoter and terminated by a nos-terminator.

Protein targeting experiments were performed with *Physcomitrella* gametophytes. The colonies were transfected with the transit peptide-YFP fusion constructs. After two days of recovery in standard growth conditions, the targeting of PptAPx and the chloroplast targeting positive control was analyzed and documented (Fig.s R44, R45).

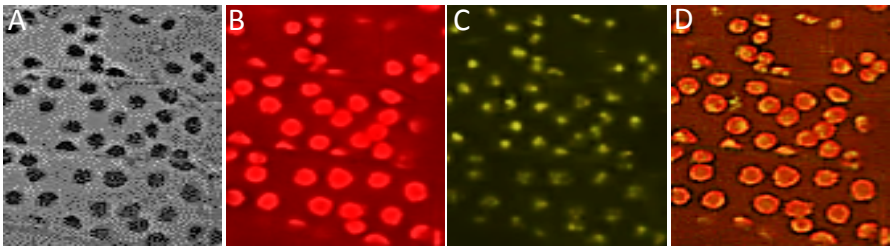

Fig. R44: Chloroplast targeting of PpftsZ1-1 in transfected *Physcomitrella* gametophytes (chloroplast targeting control). A: Light microscopic picture. Cells and chloroplasts are clearly visible. B: Picture of chlorophyll fluorescence. Chloroplasts are fluorescing (red). C: Picture of YFP fluorescence (yellow-green). Pictures were taken at a twentyfold magnification. D: Overlay of chlorophyll and YFP fluorescence. YFP is targeted to chloroplasts.

Physcomitrella leaves are single-cell layered, which facilitates the detection of fluorescence labeled targeting by fluorescence microscopy. Since YFP needs to be excited with UV light, the chlorophyll containing chloroplasts appeared red while YFP showed a yellow color. The yellowish accumulations limited to chloroplasts point to the expected targeting of PpftsZ1-1 to chloroplasts (Fig. R44).

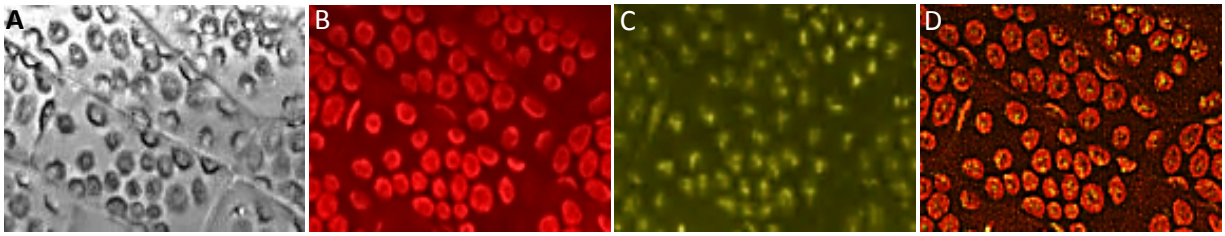

Fig. R45: Chloroplast targeting of PptAPx in transfected *Physcomitrella* gametophytes. A: Light microscopic picture. Cells and chloroplasts are clearly visible. B: Picture of chlorophyll fluorescence. Chloroplasts are fluorescing (red). C: Picture of YFP fluorescence (yellow-green). Pictures were taken at a twentyfold magnification. D: Overlay of chlorophyll and YFP fluorescence. YFP is targeted to chloroplasts.

Fig. R45 illustrates the targeting of PptAPx. As shown in Fig. R44 for the chloroplast targeted PpftsZ1-1 protein, chloroplasts showed a red fluorescence due to the excitation of chlorophyll

by UV light. The yellowish appearing YFP accumulates in these plant organelles (Fig. R45). This verified the predicted localization of PptAPx to chloroplasts in its host plant *Physcomitrella patens*.

3.9.4.2 Function of PptAPx

The PptAPx protein is targeted to chloroplasts and shows a C-terminal lipophilic transmembrane helix which implies that the protein is localized at thylakoids. Comparison to other APxs revealed two prominent variations (R282H and W288F, Fig. R7) which are usually present in cytosolic isoforms (Jespersen *et al.* 1997, Wada *et al.* 2003). R282 was published to be responsible for the inactivation of chloroplast APxs by hydrogen peroxide due to the decomposition of compound I in the absence of ascorbate (Myake and Asada 1996, Wada *et al.* 2003). The W288F substitution is suggested to cause an elevated ascorbate specificity of chloroplast APxs in comparison to cytosolic isoforms. To summarize, the variation indicates that PptAPx is less specific for ascorbate than other chloroplast APxs and more tolerant to hydrogen peroxide than other chloroplast peroxidases (Jespersen *et al.* 1997, Wada *et al.* 2003). Despite these and other amino acid exchanges, superimposition of the PptAPx protein to its *Arabidopsis* homolog showed a high probability for structural similarity pointing to the functionality of this enzyme (Fig. R46). Besides an insertion of two amino acids (aa244-245 according to Fig. R7), which change the length of one loop (indicated by a red arrow in Fig. R46), no structural dissimilarity was predicted by the overlay. Also phylogenetic analyses pointed to PptAPx being closely related to the other identified ascorbate peroxidases and, among them, even the closest relative to the *Arabidopsis* homologs (Fig.s R9-R11).

Fig. R46: Superimposition of AttAPx (yellow) and PptAPx (blue) structures. The aberrant loop formed by the insertion aa244-245 is marked with a red arrow. The SWISS MODEL building models based on the *Oriza sativa* chloroplast APx6 for PptAPx and AttAPx.

In summary, the *Physcomitrella* tAPx protein is highly similar to the *Arabidopsis* thylakoid-bound APx on amino acid as well as on structural level but shows an extremely atypical gene structure (Table R2, Fig.s R7, R46).

EST-data as well as the described comparative promoter-reporter gene studies (Table R1, see chapter 3.9.3) showed that PptAPx is highly transcribed. Different plant species overexpressing their thylakoid-bound APx show increased resistance to oxidative damage (Yabuta *et al.* 2002, Murgia *et al.* 2004). This stress can be triggered artificially by the exogenous application of methylviologen (Nakano and Asada 1980, Foyer *et al.* 1994, Palatnik *et al.* 1997, Mano *et al.* 2001, Maruta *et al.* 2010). Consequently, if the high transcript level of PptAPx corresponds to a high amount of functional protein and/or its regeneration, *Physcomitrella* should show an increased tolerance to methylviologen in comparison wildtype, *i. e.* not tAPx overexpressing, *Arabidopsis* plants.

3.9.4.3 Tolerance of *Physcomitrella patens* to methylviologen

Methylviologen, also called paraquat, transfers electrons from the iron-sulphur-cluster of photosystem I to oxygen (Nakano and Asada 1980, Babbs *et al.* 1989, Fujii *et al.* 1990), thereby leading to the formation of superoxide radicals. Other effects are the inhibition of the Calvin cycle and NADPH production (Asada 1999). The lack of NADPH causes a decrease in the chloroplast antioxidant capacity since the conversion of monodehydroascorbate to ascorbate consumes this reducing agent (Palatnik *et al.* 1997, Asada 1999). Methylviologen would finally lead to a breakdown of the water-water cycle (WWC). This scenario causes an increase in the formation of reactive oxygen species (ROS) and damage of photosystem II. The chloroplast ascorbate peroxidases were shown to be a major part of the defense against the herbicide paraquat, since they are inactivated rapidly upon treatment (Mano *et al.* 2001). This inactivation was presumed to be triggered by the lack of ascorbate and the simultaneous accumulation of hydrogen peroxide (Mano *et al.* 2001). The thylakoid-bound APx is of special importance in detoxification of hydrogen peroxide since it is located directly at the site of production and its lack or overabundance has a strong influence on the tolerance to oxidative stress (Asada 1999, Yabuta *et al.* 2002, Murgia *et al.* 2004, Tarantino *et al.* 2005).

Even if the herbicide is not completely inhibiting WWC functionality, its detrimental effect can still be measured via the decrease in photosynthesis efficiency (Bowler *et al.* 1991, McKersie *et al.* 2000). The resistance to methylviologen was increased in *Arabidopsis* mutants overexpressing tAPx (Murgia *et al.* 2004). Since the *Physcomitrella* homolog was

also shown to be strongly expressed in its native host, it was hypothesized that gametophytes could be less detrimentally affected by the herbicide.

To check the tolerance level of *Physcomitrella* gametophytes, which were cultivated for ten days in standard growth conditions, they were soaked with paraquat in concentrations of 0 µM, 25 µM, and 2 mM. As reference plants, ten day old *Arabidopsis* seedlings were used and treated equally. After application of the herbicide, *Arabidopsis* as well as *Physcomitrella* were transferred to their respective standard growth conditions. The deleterious effect of methylviologen was observed by measuring the photosynthetic yield before treatment and after two and six hours. The experiment was performed in two replicates. In total, 19-20 seedlings and nine gametophyte colonies were included. Each colony comprised at least ten *Physcomitrella* gametophytes.

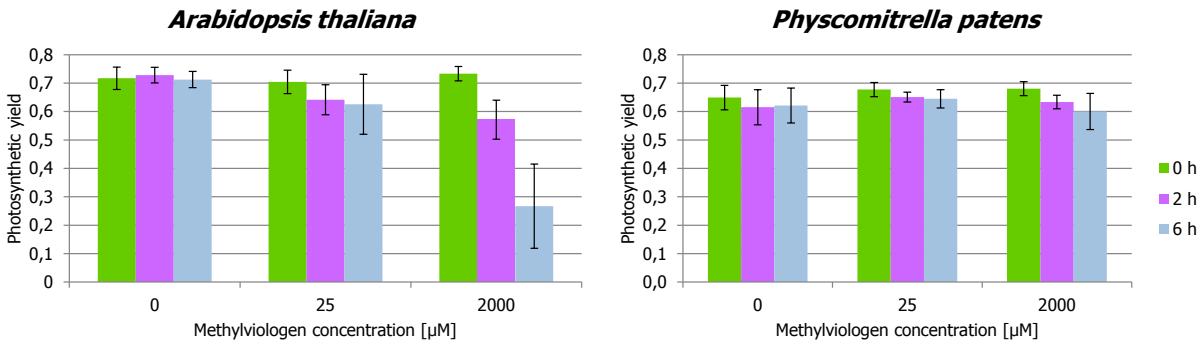

Fig. R47: Photosynthetic yield of *Arabidopsis* seedlings and *Physcomitrella* gametophytes treated with different concentrations of methylviologen (0 µM, 25 µM, 2 mM). *Arabidopsis* plants are strongly affected by methylviologen showing a strongly decreased photosynthetic yield while *Physcomitrella* reveals no evident response.

Fig. R47 shows photosynthetic yields of *Arabidopsis* and *Physcomitrella* which were treated with methylviologen. This parameter is a measure for the vitality of a respective plant or gametophyte colony. Paraquat blocks the electron acceptor site of photosystem I, thereby provoking transfer of these particles to oxygen. The created superoxide anions and its detoxification intermediate hydrogen peroxide are highly reactive and can cause severe damages. The deleterious effect decreases the fitness of a respective plant or gametophyte colony.

The *Arabidopsis thaliana* seedlings are strongly affected by methylviologen and show a tremendous decrease in vitality (Fig. R47). After six hours treatment with 2 mM

methylviologen, their photosynthetic yield was strongly decreased (Fig. R47). In contrast, the harmful effect of the herbicide was not evident in *Physcomitrella* gametophytes (Fig. R47). The moss showed a high resistance.

In conclusion, the results strongly indicate that PptAPx, which was predicted to be a thylakoid-bound APx, represents a functional tAPx enzyme. According to the results obtained for *Arabidopsis* tAPx overexpressors (Murgia et a. 2004), the increased tolerance of *Physcomitrella*, in comparison to *Arabidopsis*, may be at least partially due to the strong expression of a fully functional and highly effective thylakoid-bound APx isoform. The increased tolerance might even be supported by PptAPx being more resistant to hydrogen peroxide and less specific for ascorbate as a substrate.

3.9.5 Expressional regulation of PptAPx

It was hypothesized that the *Physcomitrella patens* tAPx encoding gene was regulated by different biotic and abiotic stimuli. To obtain evidences, moss gametophyte colonies were cultivated in standard growth conditions and subsequently treated with several chemical components and transferred to unfavorable conditions, respectively. Each colony comprised seven or more *Physcomitrella* gametophytes. The effect of these stimuli was investigated on transcript level by performance of qRT-PCRs. All results were normalized to the actin transcript level in *Physcomitrella* (PpAct1).

3.9.5.1 Posttranscriptional regulation by light intensity and chilling

Physcomitrella gametophyte colonies were subjected to varying light intensities and/or chilling temperatures for six hours. Included intensities were standard light (55 µmol quanta m^{-2} s^{-1}), excess light (1000 µmol quanta m^{-2} s^{-1}), and darkness. Since the light source used to obtain 1000 µmoles quanta m^{-2} s^{-1} emitted heat, the application of excess light was performed at 4 °C. Controls at 55 µmol quanta m^{-2} s^{-1} and 4 °C as well as at 20 °C were included.

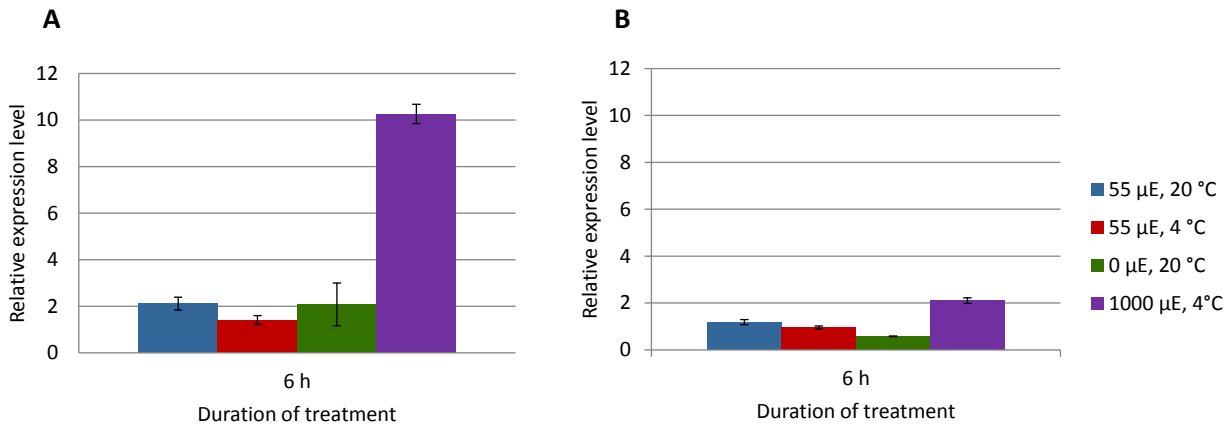

Fig. R48: Transcript level of the chloroplast thylakoid-bound ascorbate peroxidase encoding gene in *Physcomitrella patens*. Gametophyte colonies were subjected to standard light conditions (55 µmol quanta m^{-2} s^{-1}, 20 °C), excess light (1000 µmol quanta m^{-2} s^{-1}, 4°C), and darkness (0 µmol quanta m^{-2} s^{-1}, 20 °C). Temperature controls were performed at 20 °C and 4 °C. A and B represent independent qRT-PCR replicates which show varying expression levels but same trends. PptAPx transcripts levels relative to actin transcript levels are shown.

The results obtained from two independent biological replicates are shown separately since the expression level results for PptAPx varied but reveal the same trend (Fig. R48). It might be possible that the variation is due to differences in actin expression of the individual gametophyte colonies. The results show that the gene is regulated by light intensity. In comparison to standard conditions, excess light caused an accumulation of transcripts while the obtained expression level in darkness treated gametophytes either stayed unchanged or were down-regulated (Fig. R48. The transcript level decreased when a temperature of 4 °C was applied (Fig. R48). This indicates that the effect revealed by plants subjected to excess light was triggered by light intensity and not by temperature.

3.9.5.2 Expressional regulation by low molecular weight antioxidants

3.9.5.2.1 Ascorbate and dehydroascorbate

Physcomitrella gametophyte colonies were treated with the low molecular weight antioxidants ascorbate and dehydroascorbate. The former is used by ascorbate peroxidases as substrate to detoxify hydrogen peroxide (Groden and Beck 1979, Asada 1992). Two molecules are converted to monodehydroascorbate (MDHA) which in turn dissipates into dehydroascorbate and ascorbate (Bielski *et al.* 1981). Further reduction of dehydroascorbate to regenerate ascorbate is catalyzed by the dehydroascorbate reductase (DHAR) (Crook and Hopkins 1938, Crook and Morgan 1943, Foyer and Halliwell 1977). MDHA can also be

enzymatically reduced to ascorbate. The reaction is catalyzed by MDHA reductases (MDHAR) (Hossain *et al.* 1984).

Both antioxidants were applied in a concentration of 20 mM for four hours. Additionally, a treatment with 50 mM dehydroascorbate was included. Control plants were subjected to pure autoclaved tap water. The results were obtained from two independent biological replicates which were kept in standard light and temperature conditions (55 µmol quanta m^{-2} s^{-1}, 20 °C) during the treatment.

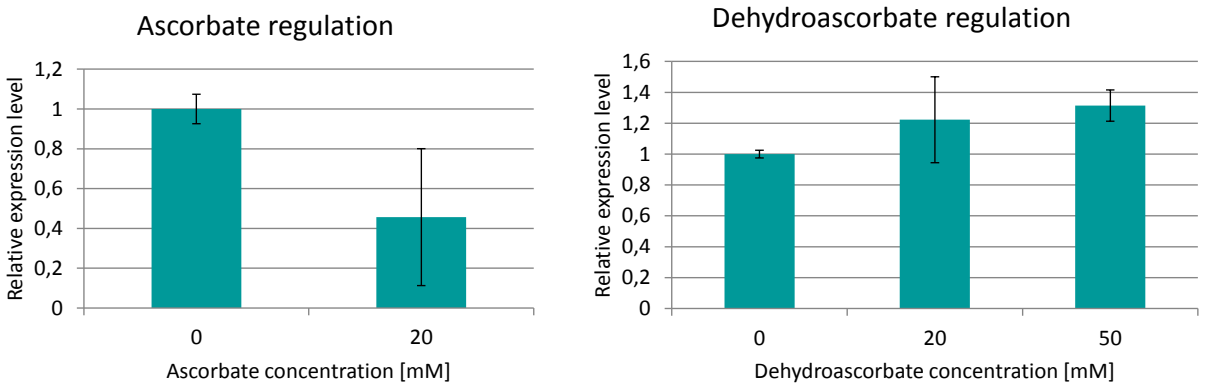

Fig. R49: Transcript level of the chloroplast thylakoid-bound ascorbate peroxidase encoding gene in *Physcomitrella patens*. Gametophyte colonies were subjected to the low molecular weight antioxidants ascorbate (concentration: 20 mM) and dehydroascorbate (concentrations: 20 mM and 50 mM). Control plants were treated with autoclaved tap water. On the left, expression levels of PptAPx in response to ascorbate are shown while the right figure displays qRT-PCR results obtained for dehydroascorbate. PptAPx transcript levels relative to actin transcript levels are shown. Controls were set to 1.

Physcomitrella gametophyte colonies treated with 20 mM ascorbate showed a decrease of the PptAPx transcript level while application of 50 mM dehydroascorbate caused an increase (Fig. R49). A lower concentration of dehydroascorbate showed an effect but it became evident when a higher concentration was used (Fig. R49). These results obtained by qRT-PCRs indicate that the PptAPx gene is transcriptionally regulated by ascorbate and dehydroascorbate.

3.9.5.2.2 Glutathione

Gametophyte colonies of *Physcomitrella patens* were also treated with another low molecular weight antioxidant: glutathione. As mentioned before, the enzyme DHAR catalyzes the regeneration of ascorbate from dehydroascorbate on the expense of glutathione. Two molecules reduced glutathione (glutathione^{red}) are oxidized during the reaction generating a

glutathione dimer (glutathione^{ox}, Wormuth *et al.* 2006). Besides this enzymatical consumption, reduced glutathione can be used by plants to directly detoxify peroxides (Larson 1988, Blokhina *et al.* 2003).

To check whether the expression of PptAPx is influenced by glutathione, both its reduced and oxidized forms where used to treat *Physcomitrella* gametophyte colonies. The investigation included 20 mM and 50 mM reduced and 10 mM oxidized glutathione. Since the oxidized form is a dimer, 10 mM may correspond to 20 mM reduced glutathione monomer. Control plants, were treated with pure autoclaved tap water. The experiment was performed in two replicates, each treatment lasted 4 h and took place at standard light and temperature conditions.

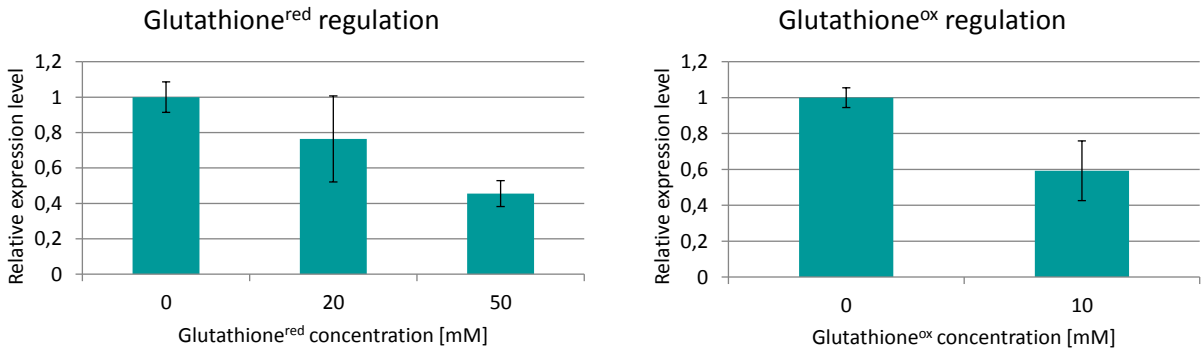

Fig. R50: Transcript level of the chloroplast thylakoid-bound ascorbate peroxidase encoding gene in *Physcomitrella patens*. Gametophyte colonies were subjected to the low molecular weight antioxidant glutathione in its reduced (concentrations: 20 mM and 50 mM) and oxidized form (concentration: 20 mM). Control plants were treated with autoclaved tap water. On the left, expression levels of PptAPx in response to reduced glutathione are shown while the right figure displays qRT-PCR results obtained for oxidized glutathione. PptAPx transcript levels relative to actin transcript levels are shown. Controls were set to 1.

Both forms of glutathione, reduced as well as oxidized, revealed to have an influence on the expression of PptAPx. 50 mM glutathione^{red} caused a decrease of the encoding mRNA molecules (Fig. R50). A lower concentration (20 mM) showed the same trend but a more evident effect was caused by a higher concentration (Fig. R50). In contrast to this, treatment of *Physcomitrella* gametophytes with 10 mM glutathione^{ox} (equating 20 mM gluathione^{red}) clearly down-regulated the transcript level of PptAPx (Fig. R50). These results demonstrate that the gene's transcription is reduced by application of glutathione, no matter if oxidized or reduced. This indicates that PptAPx is not regulated by the redox status of glutathione^{red}/ glutathione^{ox}.

3.9.5.3 Regulation by abscisic acid

Abscisic acid (ABA) is present in bryophytes as well as in higher plants (Knight *et al.* 1995, Nishiyama *et al.* 2003, Quatrano *et al.* 2007). In the latter, it mediates salt stress responses (Zhu 2002) and is involved in the closure of stomata in drought to reduce transpiration (Leung and Giraudat 1998, Zhang *et al.* 2001). Since the moss *Physcomitrella* does not have any epidermis or sturdy cuticula (Rensing *et al.* 2007) it is subjected to a high water loss. In higher plants, ABA has a regulatory impact to the chloroplast antioxidative system (Jiang and Zhang 2001, Yoshida *et al.* 2003, Baier *et al.* 2004). Richardt *et al.* (2010) supposed that ABA has similar effects in *Physcomitrella* and higher plants.

Additionally, the ABA regulatory pathway causes accumulation of hydrogen peroxide and is influenced by the redox status of ascorbate. *Arabidopsis* 2CPA is regulated by the phytohormone in a ROS-independent manner (Baier *et al.* 2004). Besides this, the regulation driven by ABA dominated the 2CPA control by the ascorbate redox status (Baier *et al.* 2004). If there are parallels in *Physcomitrella* and higher plants, the possibility that PptAPx may be regulated similarly needs to be taken into account.

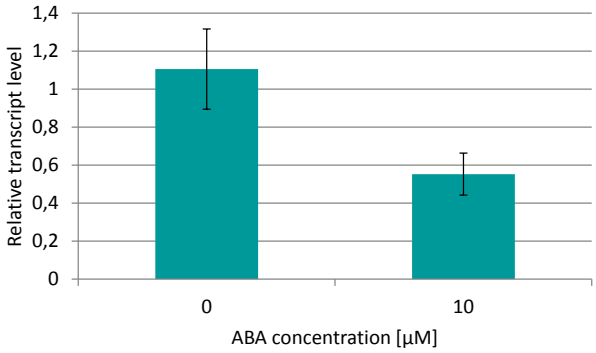

Fig. R51: Transcript level of the chloroplast thylakoid-bound ascorbate peroxidase encoding gene in *Physcomitrella patens*. Gametophyte colonies were subjected to abscisic acid (ABA, concentration: 10 mM). Control plants were treated with autoclaved tap water. The figure shows qRT-PCR results. PptAPx transcript levels relative to actin transcript levels are shown.

To investigate, whether the expression of PptAPx is influenced by the phytohormone, gametophyte colonies were treated with 10 µM ABA for one hour at standard light and temperature conditions. It is known, that the concentration and duration are sufficient to induce responsive genes in *Physcomitrella* (Richardt *et al.* 2010). Control plants, subjected to

pure autoclaved tap water, were included. qRT-PCRs were performed for two independent biological replicates.

The obtained results demonstrate that the transcription rate of PptAPx is influenced by ABA. Treatment with 10 µM of the phytohormone for one hour caused a decrease of the encoding mRNA amount (Fig. R51).

3.9.6 Parallels between *Physcomitrella patens* and the higher plants *Arabidopsis thaliana* and *Nicotiana benthamiana*

The transcription of PptAPx is initiated at two sites (Fig. R41). The strength of its promoter revealed to be high in its natural moss host. It was also stronger than the expression controlled by the *Arabidopsis* tAPx and sAPx promoters (Fig. R42). Beside this, its targeting to chloroplasts was verified (see chapter 3.9.4.1). It was investigated whether the machineries responsible for transcription initiation, increased transcription, and chloroplast targeting were preserved during evolution. The higher plant model organisms *Arabidopsis thaliana* and *Nicotiana benthamiana* were chosen to be compared to *Physcomitrella*.

3.9.6.1 Development of an effective transfection method to perform interspecies comparisons

For interspecies comparative promoter-reporter gene studies on the transcription intensity, the used transfection methods should by as similar as possible to ease the experimental work and interpretation of the obtained results. Nevertheless, the commonly used transfection procedures for *Arabidopsis*, tobacco, and *Physcomitrella* are highly different. Since, for *Arabidopsis* and the moss, they include protoplast isolation by either ripping off the epidermis or wound the plants in any other way, they are additionally accompanied by strong stress. To facilitate the comparative investigation, a transfection method suitable at least *Arabidopsis* and *Physcomitrella* was successfully developed (Fig. R52).

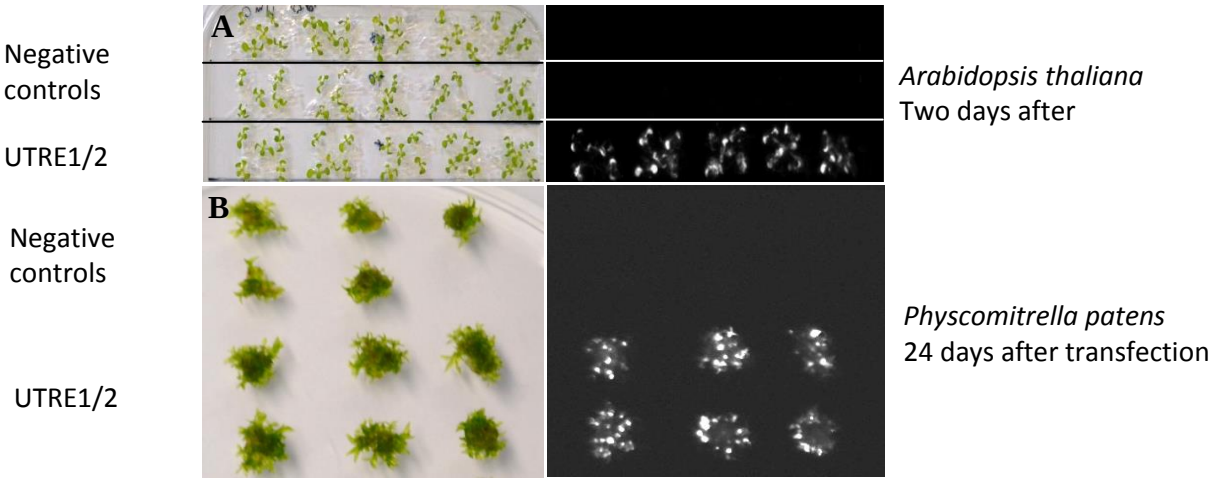

Fig. R52: Photographies (left) and luminograms (right) of 12 day old *Arabidopsis* seedlings (A) and *Physcomitrella* gametophytes (B) transfected with *Agrobacteria* containing the UTRE1/2 construct and negative controls. *Arabidopsis* and *Physcomitrella* negative controls were infiltrated with (i) the solution used for *Agrobacteria* infiltrations but without any bacteria (upper line), or (ii) a suspension of *Agrobacteria* containing a construct in which the PptAPx promoter controls the expression of a GFP/GUS protein fusion (lower line). Luciferase activity in *Arabidopsis* was detected two days of recovery after transfection while the *Physcomitrella* gametophytes were documented 24 days after transfection.

In addition, the method was applied to several spikemosses. The procedure revealed to be suited not only for the seed plant and the moss but also for various species of the spikemoss *Selaginella* for which no transfection protocol existed before (Fig. R53).

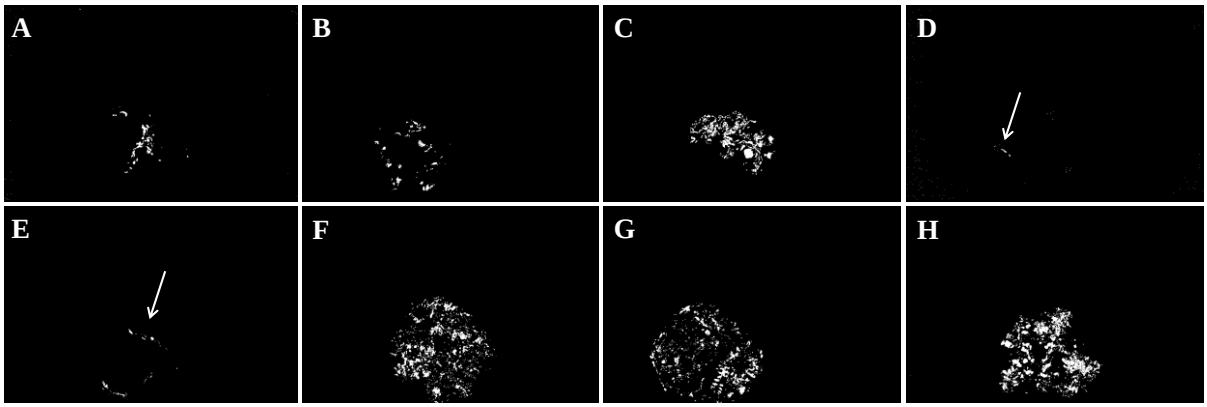

Fig. R53: Luminograms of diverse *Selaginella* species, each transfected with *Agrobacteria* containing the UTRE1/2 construct (in every luminogram placed at the bottom) and two different negative controls (in every luminogram placed at the top). A: *S. braunii*, B: *S. emmeliana*, C: *S. douglasii*, D: *S. erythropus*, E: *S. grandis*, F: *S. kraussiana*, G: *S. serpens*, H: *S. uncinata*. Negative controls were infiltrated with (i) the solution used for *Agrobacteria* infiltrations but without any bacteria (placed at the top, left), or (ii) a suspension of *Agrobacteria* containing a construct in which the PptAPx transit peptide was fused to mGFP6 under the expressional control of a CaMV35S promoter (placed at the top, right). Luciferase activity was detected two days of recovery after transfection.

3.9.6.2 PptAPx promoter activity in *Arabidopsis thaliana* and *Nicotiana benthamiana*

Comparative studies concerning the PptAPx transcription were not only performed in its natural moss host but also with *Arabidopsis thaliana* seedlings, which were transfected with the UTRE1/2, UTRE1, and UTRE2 constructs (Fig. R40). Another higher plant was used for these studies, *Nicotiana benthamiana*. *Agrobacteria* strains containing the UTRE1/2 and UTRE1 as well as the *Arabidopsis* chloroplast ascorbate peroxidase promoter-luciferase constructs were used to transfect tobacco. The infiltration of leaves from six weak old plants was performed with a syringe, not by vacuum.

Ten day old *Arabidopsis* seedlings were transfected with *Agrobacteria* strains containing UTRE1/2, UTRE1, and UTRE2 constructs, respectively. Infiltration of the two oldest leaves from six week old tobacco plants was performed with UTRE1/2 and UTRE1 *Agrobacteria* strains.

As shown before for *Physcomitrella*, also the higher plants show strong luminescence driven by the whole PptAPx promoter (UTRE1/2) and the first 337 bp upstream of the start-ATG (UTRE2) while UTRE1 causes a comparably weak luciferase activity (Fig. R54). Negative controls showed no chemiluminescence.

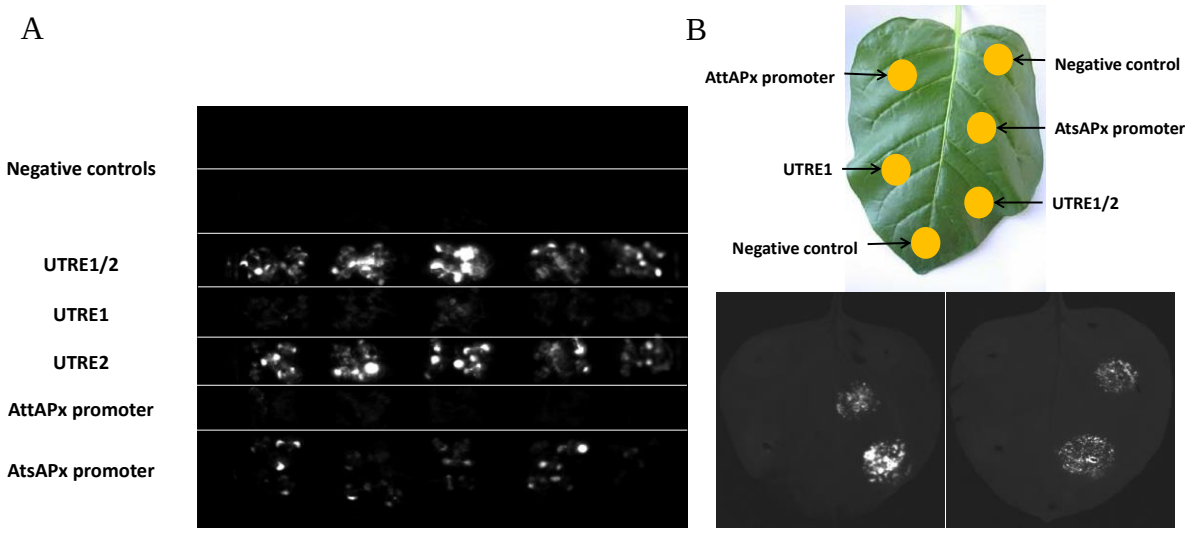

Fig. R54: A: *Arabidopsis* seedlings, two days after transfection. 25 (5x5) plantlets were transfected per construct or negative control. The luminogram was taken with a LAS4000mini and is exemplarily for at least two experimental replicates. UTRE1/2 and UTRE2 constructs cause a strong LUC expression in comparison to the UTRE1 construct. Plants transfected with the AtsAPx promoter::LUC construct show a stronger chemiluminescence than when the AttAPx promoter::LUC construct was used, but weaker than seedlings containing UTRE1/2 and UTRE2 constructs. Negative controls were infiltrated with (i) the solution used for *Agrobacteria* infiltrations but without any bacteria (A: upper line, B: leaf tip), or (ii) a suspension of *Agrobacteria* containing a construct in which the PptAPx transit peptide was fused to mGFP6 under the expressional control of a CaMV35S promoter (A: lower line, B: upper right label for negative control). These controls show no chemiluminescent activity. The constructs with which they were transfected are written on the left, B: *Nicotiana* leaves, five days after transfection. Two leaves were transfected per experiment. Top: The infiltration pattern of the constructs or negative controls is indicated in the light picture of a tobacco leaf (http://de.wikipedia.org/wiki/Datei: Tabakanbau.de-030511-DSCN0480-N_Rustica_Tabakblatt.jpg). Bottom: Luminograms were taken with a LAS4000mini and is exemplarily for at least two experimental replicates. The UTRE1/2 and AtsAPx promoter::LUC constructs cause LUC expression while all other infiltrated parts show no chemiluminescence, including negative controls.

Besides this, other ten day old *Arabidopsis* seedlings and leaves of six weeks old *Nicotiana* plants were transfected by vacuum infiltration and infiltration using a syringe, respectively. For tobacco, the two firstly developed leaves were used. In contrast to *Arabidopsis*, for which 25 seedlings were transfected per construct or negative control, each tobacco leaf was infiltrated with several constructs at once. The pattern is shown in Fig. R54B. The UTRE2 construct was omitted for *Nicotiana*. Following the transfection, *Arabidopsis* seedlings could recover for two days while *Nicotiana* plants stayed for five days in their standard growth conditions.

Both, *Arabidopsis* seedlings as well as the two oldest *Nicotiana* leaves show a strong LUC expression caused by the full length PptAPx promoter (Fig. R54). As described above, UTRE2 may be the main driving force of this strong LUC expression, at least in *Arabidopsis*, tobacco, and *Physcomitrella* (Fig. s R40, R42, R54). In both higher plant species, transfection with the UTRE1 construct yielded no or only very weak chemiluminescence (Fig. R54). Similar signals were obtained by using the *Arabidopsis* tAPx promoter controlling LUC expression (Fig. R54). In contrast and as shown in *Physcomitrella* transfection experiments, the AtsAPx also causes a rather strong luminescence, although weaker than in plants or plant parts transfected with the UTRE1/2 or UTRE2 constructs (Fig.s R42 and R54). Negative controls revealed no LUC activity (Fig. R54).

In general, the results obtained for higher plants are not different from those revealed by *Physcomitrella*. This supports the suggestion of Reski (1998a) that the principle of the promoter usage is similar among distinct plant species, no matter whether they are evolutionary distantly or closer related.

3.9.6.3 Organellar targeting of PptAPx in *Arabidopsis thaliana*

In *Physcomitrella patens* PptAPx is targeted to chloroplasts (Fig. R45). To check whether the targeting signal is functional during evolution and/or in different distantly related plants interspecific studies were performed.

For organellar targeting investigation, *Arabidopsis* protoplasts were isolated and subsequently transfected with constructs in which the transit peptide of PptAPx was fused to a plant adapted GFP (Fig. R55 right). As a positive control, the PpftsZ1-1 transit peptide was inserted in frame with the GFP (Fig. R55 left). The constructs are analogous to those used for targeting studies in *Physcomitrella* (Fig. R43). They differ in the reporter gene only.

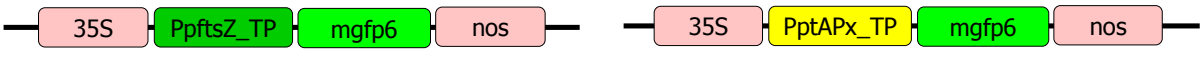

Fig. R55: Constructs designed for organellar targeting studies in *Arabidopsis*. Left: Fusion of the PpftsZ1-1 transit peptide (region encodes the first 99 amino acids of the protein) to mgfp6, used for chloroplast targeting positive controls. Right: Fusion of the PptAPx transit peptide (region encodes the first 100 amino acids of the protein) to mgfp6. The expression of both protein fusions was controlled by a CaMV35S-promoter and terminated by a *nos*-terminator.

Protein localizations of PptAPx and PpftsZ1-1, as chloroplast targeting positive control, were analyzed and documented, one night after transfection, in which the protoplasts could recover.

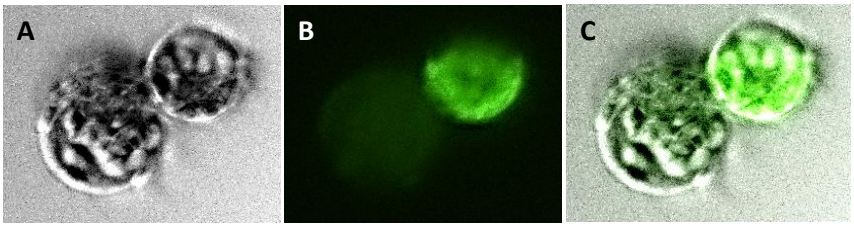

Fig. R56: Chloroplast targeting of PpftsZ1-1 in transfected *Arabidopsis* mesophyll protoplasts (chloroplast targeting control). A and B show light and fluorescence microscopic pictures of GFP expressing and not expressing protoplasts, respectively. Pictures were taken at a fortyfold magnification. C: green fluorescence merged to the light microscopic picture to visualize chloroplast targeting.

Light microscopic pictures show chloroplasts as spherical organelles inside protoplast (Fig. R56). They accumulate, so that they appear not separately. The merge of fluorescence and light microscopic pictures in Fig. R56C show the targeting of the chloroplasts localized PpftsZ1-1 protein.

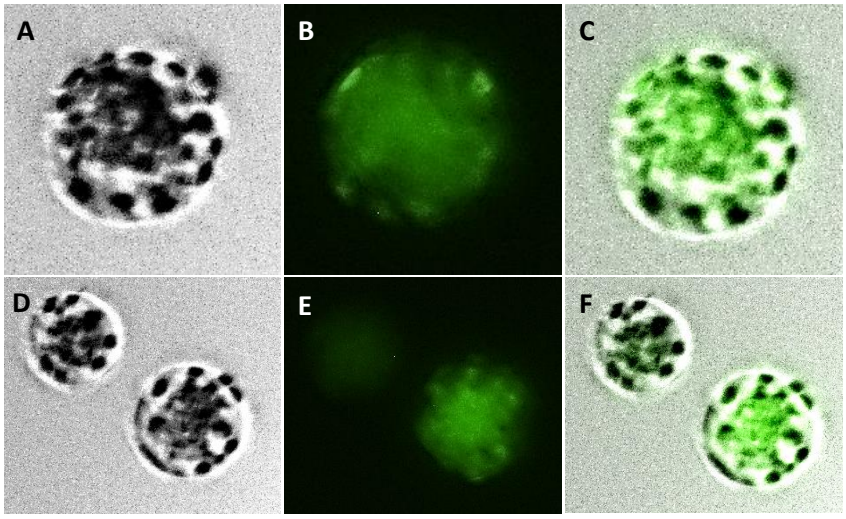

Fig. R57: Chloroplast targeting of PptAPx in transfected *Arabidopsis* mesophyll protoplasts. A, D: light microscopic pictures; B, E: fluorescence microscopic pictures. Pictures were taken at a fortyfold magnification. C and F: green fluorescence merged to the light microscopic pictures to visualize chloroplast targeting.

The documentation of the results obtained for PptAPx targeting studies in *Arabidopsis* are shown in Fig. R57. mGFP6 fluorescence is limited to chloroplasts demonstrating that PptAPx is localized to these organelles not only in its host *Physcomitrella* but also in the higher plant

Arabidopsis (Fig. R57). This indicates that the function of the transit peptide was maintained during evolution or at least in the two distantly related plant species included in the studies.

4 Discussion

Chloroplasts are one of the major sources for reactive oxygen species (ROS) within plant cells. To protect the organelles from the toxic impact, several detoxification systems are active (Jespersen *et al.* 1997, Horling *et al.* 2003, Mullineaux *et al.* 1998, Rodriguez Milla *et al.* 2003). The present study focuses on chloroplast peroxidases, which are ascorbate peroxidases (APxs), typical 2-Cys-peroxiredoxins (2CPs), peroxiredoxins Q (PrxQs), peroxiredoxins type II (PrxIIs), and glutathione peroxidases (GPxs). It was bioinformatically investigated, whether the plastid peroxide defense changed during plant evolution. The model seed plant *Arabidopsis thaliana*, the spikemoss *Selaginella moellendorffii*, the moss *Physcomitrella patens*, and the green alga *Chlamydomonas reinhardtii* were chosen for the comparing studies. It was found that, although being subjected to changes, there was an immense pressure on maintaining all three detoxification systems, since all investigated organisms showed presence of encoding genes within their genomes.

4.1 The chloroplast antioxidative defense in *Arabidopsis thaliana* and *Selaginella moellendorffii*

The higher plant *Arabidopsis thaliana* encodes eight chloroplast peroxidases: two APxs, two 2CPs, one PrxQ, one PrxII, and two GPxs (Jespersen *et al.* 1997, Horling *et al.* 2003, Mullineaux *et al.* 1998, Rodriguez Milla *et al.* 2003). The stromal APx isoform was suggested to be targeted not only to chloroplasts but also to mitochondria indicating the enzyme to be essential for hydrogen peroxide detoxification (Chew *et al.* 2003). *Selaginella moellendorffii* revealed basically the same set of genes with the addition of one more PrxQ and another GPx (Table R1).

4.2 The chloroplast antioxidative defense in *Physcomitrella patens*

In contrast to *Arabidopsis* and *Selaginella*, *Physcomitrella* encodes no stromal ascorbate peroxidase (Table R1). Kangasjärvi *et al.* (2008) published that expression of 2CPs is up-regulated in mutants which lack chloroplast APx activity. Additionally, they found that the function of sAPx is important, especially during germination. Maruta *et al.* (2010) demonstrated the importance of tAPx in later developmental stages. *Physcomitrella* highly expresses its tAPx in comparison to the other identified moss antioxidant defense genes

(Table R1, R7) and multiplied the genes encoding enzyme involved in ascorbate independent defense systems (Table R1). Like *Arabidopsis* and *Selaginella*, its genome has two ORFs for 2CPs (Table R1). The moss PrxQs and PrxIIs, in contrast, are present in two and three isoforms, demonstrating gene duplication and triplication, respectively (Table R1). In addition, three GPxs serve to protect chloroplasts (Table R1). PpGPxA appears to be a splicing variant, while PpGPxB may not be (fully) functional (Fig. R32). EST-data indicate that all of the mentioned antioxidative defense genes, except PpGPxB, are expressed (Table R1). It was published that chloroplast APxs have a three to four orders of magnitude higher peroxidase activity than peroxiredoxins (Kitajima *et al.* 2008, Kitajima 2008). Thus, a lack in ascorbate peroxidase function may demand for a strong induction and/or multiplication of alternative detoxification systems. Especially, the atypical peroxiredoxins were multiplied in the moss if compared to *Arabidopsis* and *Selaginella* (Table R1). It is possible that the higher abundance of peroxiredoxins and the high expression of PptAPx (Table R1, Fig. R45) were necessary to balance the lack of stromal APx activity and to ensure sufficient fitness of the moss to survive through times.

4.3 The chloroplast antioxidative defense in *Chlamydomonas reinhardtii*

The green alga *Chlamydomonas reinhardtii* lacks tAPx function while it has three 2CPs, one PrxQ, one PrxII, and three GPxs (Table R1). For five of these chloroplast antioxidative defense genes no ESTs could be found (CrsAPxB, Cr2CPC, CrPrxQ, CrGPxA, CrGPxB, Table R1). Thus, no obvious effort of this water organism to balance the lack of tAPx activity was found.

As plants conquered land they were challenged with new stressful conditions, such as water deficit and excess light. The tAPx isoform may have evolved as a consequence of adaptation. Kitajima (2008) suggested that the invention of a new APx, which acts directly at the site of hydrogen peroxide production, might be preferred over enhancing the effectivity of the stromal isoform(s).

Nevertheless, it may also be that one of the *Chlamydomonas* sAPxs represents an ancestor of thylakoid-bound APxs, which evolved the transmembrane anchor during time. Another possibility to explain the lack of a tAPx could be that the ancestral encoding gene existed within the *Chlamydomonas* genome but was lost during its evolution.

Since the presented data indicate that there was a strong pressure in maintaining stromal APx activity, they also suggest that sAPxs have a significant influence on the protection of chloroplasts from hydrogen peroxide. This might be a possible explanation for the strong attempts of *Physcomitrella* to compensate the lack of soluble APx activity in chloroplasts.

4.4 Composition of the chloroplast antioxidant defense during plant evolution

Although the numbers of the different members of the chloroplast antioxidant defense changed among the investigated lower plants, all encoded ten distinct hydrogen peroxide detoxifying proteins (Table R1). EST-data indicate that some of the genes are either not or only very weakly expressed (Sm2CPB, SmPrxQB, PpGPxB, CrsAPxB, Cr2CPC, CrPrxQ, CrGPxA, CrGPxB, Table R1). These genes showed the strongest differences in comparison to their *Arabidopsis* homologs (Fig.s R7, R13, R19, R25, R32). The substitutions in their amino acid sequences can have a severe influence on the functionality and effectivity of the respective enzyme. Such putative effects will be discussed later. It was suggested that higher plants, especially dicots, display the most sophisticated variant of the chloroplast antioxidative defense during plant evolution. It may be possible that their chloroplast antioxidative system in concert with various morphological adaptations to uncomfortable conditions are highly effective and make the expression of only eight different hydroperoxide detoxifying isoforms sufficient for adequate fitness to ensure survival.

EST-data indicate that 2CPs are the most expressed antioxidant enzymes in *Arabidopsis*, *Selaginella*, and *Chlamydomonas* (Tables R1, R7). The moss EST-data on 2-Cys peroxiredoxins could not be fully counted since Pp2CPB is situated on two different scaffolds making it impossible to determine the whole locus (Table R1). The available data suggest PptAPx to be the most abundant chloroplast defense enzyme in *Physcomitrella* while 2CPs take the second rank (Tables R1, R7). This moss represents the only organism among the investigated plants in which the major role of the insoluble ascorbate-dependent WWC may be prominent.

4.5 Ascorbate peroxidases

4.5.1 Evolutionary origin of chloroplast ascorbate peroxidases

The chloroplast ascorbate peroxidases identified in *Selaginella moellendorffii* and *Chlamydomonas reinhardtii* share conserved splicing sites with their *Arabidopsis thaliana* homologs (Fig. R5). The tAPx encoded by *Physcomitrella*, in contrast, showed a highly atypical gene structure with only two instead of ten to twelve exons and an unconserved splice site (Fig. R5). Nevertheless, its amino acid sequence and predicted 3D-protein folding revealed a high degree of similarity as did the *Selaginella* isoforms and CrsAPxA (Fig.s R5, R45). These results indicate that emergence of the original chloroplast targeted ascorbate peroxidase dates back to times before the division of streptophytes and chlorophytes. In phylogenetic trees, chloroplast APxs of lower plants and high plants cluster separately from each other (Fig.s R9-R11). This suggests the isoforms from evolutionary older plants to be closer related if compared to seed plant APxs.

Phylogenetic trees cluster CrsAPxB closer to non-chlorobiont APxs (Fig.s R9-R11). Beside this, it shows more similarity to cytosolic than to chloroplast isoforms (Fig. R7). It is most similar to ascorbate peroxidases from red algae (Fig.s R9-R11). Its gene structure, which shares only one conserved splice site with its *Arabidopsis* homolog points to the relation of CrsAPxB to the other investigated chloroplast isoforms (Fig. R5). It is possible that this APx represents a more ancient variant or evolved independently from other APxs. Since it shows similarity to cytosolic isoforms, its ancestor might have even been an extra-organellar isoform. In comparison to its *Arabidopsis* homolog, this enzyme shows many modifications in heme and substrate coordination sites (Fig. R7). Additionally, it was predicted to have a hybrid function as hybrid ascorbate-cytochrome c peroxidase. Its transcription was verified (Table R1, Fig. R6). In conclusion, the real function of CrsAPxB and the circumstances under which it is expressed remain to be elucidated. APxs and cytochrome c peroxidases share a common origin and both belong to the class 1 peroxidase family (Zamocky *et al.* 2000). It is suggested that this class, comprising plant, fungal, and bacterial peroxidases, evolved by gene duplication from a hydroperoxidase ancestor (Zamocky *et al.* 2000).

4.5.2 Hydrogen peroxide sensitivity of *Chlamydomonas reinhardtii* ascorbate peroxidase A

Chloroplast ascorbate peroxidases are inactivated in response to a surplus of hydrogen peroxide when the availability of ascorbate is low (Miyake and Asada 1996, Mano *et al.* 2001, Miyagawa *et al.* 2000). A chloroplast APx specific loop comprised of 16 amino acids was found to be responsible for the increased sensitivity to hydrogen peroxide in comparison to cytosolic isoforms (Yoshimura *et al.* 1998, Mano *et al.* 1997, Wada *et al.* 2003, Teixeira *et al.* 2004, Kitajima *et al.* 2006, Kitajima 2008). The development of such vulnerability was suggested to function either as a sensor for the accumulation of hydrogen peroxide or to represent a defect which was inserted during evolution (Kitajima 2008).

CrsAPxA shows two atypical loops in comparison to its *Arabidopsis* homolog (Fig. R8). They were designated "Evolutionary Variable Loop I and II" (EVaLos I and II). Located between F/W288 and W327, EVaLoII corresponds to the loop specific for chloroplast APxs (Fig. R7). In CrsAPxA, this region is elongated by 19 amino acids (Fig. R7). A *Chlamydomonas sp.* W80 strain, which also shows the chloroplast-specific loop, revealed to be more tolerant to excess hydrogen peroxide and lack of ascorbate (Takeda *et al.* 2000). The loop in this enzyme was extended by two more amino acids. It is tempting to assume that the elongated loop in CrsAPxA has an influence on the sensitivity to hydrogen peroxide. Two different suggestions can be drawn: Either the additional amino acids cause an increase or a decrease in the tolerance to the reactive oxygen species. The APx from the *Chlamydomonas sp.* W80 strain showed also an elongated version of EVaLo I (Takeda *et al.* 2000). In CrsAPxA, this loop comprised five amino acids while in the other it revealed 16 residues. Takeda *et al.* (2000) did not make any suggestions on the function of this loop. Since this region is not located in the vicinity of EVaLo II (Fig. R8), it is unlikely that it has an impact on the sensitivity of the enzyme to hydrogen peroxide.

4.6 Typical 2-Cys-peroxiredoxins

4.6.1 Evolution of typical 2-Cys-peroxiredoxins

Baier and Dietz (1997) postulated that 2-Cys-peroxiredoxins from higher plants are of endosymbiotic origin. Their conclusion was based on sequence comparison of a barley 2CP (BAS1) with isoforms encoded in the plastome of the rhodobiont *Porphyra purpurea* and cyanobacterial 2CPs. In higher plants, these nuclear encoded antioxidant enzymes are post-translationally targeted to chloroplasts (Baier and Dietz 1997) while in mammals, most of them reside in the cytosol instead of being localized in organelles (Wood *et al.* 2003). Gene structures and sequence characteristics of the identified 2CPs from *Arabidopsis*, *Selaginella*, *Physcomitrella*, and *Chlamydomonas* point to a common origin of streptophyte isoforms (Fig.s R12, R13). The *Chlamydomonas* isoforms share not a single conserved splicing site maybe indicating an independent evolution in the chlorophyte lineage (Fig. R12). These data are resembled by the calculated phylogenetic trees in which streptophyte and chlorophyte 2CPs cluster separately from each other (Fig.s R15, R17). Within the streptophytes, isoforms from gymnosperms and higher plants group apart from lower plants (Fig.s R15-R17). Additionally, the *Arabidopsis* 2CP gene structures and amino acid sequences are more similar to each other than to the *Selaginella* enzymes (Fig.s R12, R13). These results suggest the *Arabidopsis* and *Selaginella* 2-Cys-peroxiredoxins arose by distinct gene duplication events. The *Physcomitrella* isoforms also form a single cluster, which is separated from the lycophyte and the seed plant. This may point to another independent gene duplication event in the moss branch.

Phylogenetic analyses clustered Sm2CPA together with the *Physcomitrella* 2CPs closer to the *Arabidopsis* isoforms while Sm2CPB forms a separate group between streptophytes and chlorophytes (Fig.s R15-R17). The low or non-expressed Sm2CPB (Table R1) may either represent a more ancient 2-Cys-peroxiredoxin or a pseudogene in which mutations accumulated due to a lack of selective pressure on its functional activity. This hypothesis is supported by various amino acid substitutions which very likely have a strong negative impact on functionality of the protein (Fig. R13). Sm2CPA, in contrast, shows high similarity to its *Arabidopsis* homologs, suggesting that the enzyme represent a functional and more conserved variant than Sm2CPB (Table R2, Fig. R13).

4.6.2 Selective pressure on stromal 2-Cys-peroxiredoxin activity

A decrease in peroxiredoxin activity can be compensated by an increase in ascorbate peroxidase activity (Baier *et al.* 2000). APxs are more effective in detoxifying hydrogen peroxide (Kitajima *et al.* 2008, Kitajima 2008). Thus, a slight increase in ascorbate peroxidase activity may balance a strong decrease in peroxiredoxin activity. Nevertheless, sequence and structural conservation indicate a strong pressure on the functional maintenance of the Prx chloroplast detoxification system (see Results chapters 3.4-3.6). EST- and array-data suggest that in *Arabidopsis*, *Selaginella*, and *Chlamydomonas* 2CPs are the strongest expressed chloroplast antioxidant defense genes (Tables R1, R7). In *Physcomitrella*, the scaffold arrangement for the Pp2CPB locus made it difficult to count ESTs (Table R1). In contrast to ascorbate peroxidases, whose detoxification function is mainly restricted to hydrogen peroxide (Raven 2003), 2CPs are capable to reduce not only this reactive oxygen species but also a wide range of alkyl hydroperoxides (König *et al.* 2002). This may be one possible explanation for the conservation of a functional Prx system during plant evolution.

Upon severe oxidative stress APxs are inactivated by hydrogen peroxide. Their W140 (position in Fig. R7) is irreversibly cross-linked with the heme (Kitajima *et al.* 2007). The function of peroxiredoxins, in contrast, can be restored after sulfinylation of their peroxidatic C residue by *e. g.* sulfiredoxins (König *et al.* 2002, Jönsson *et al.* 2008).

Pena-Ahumada *et al.* (2006) assumed 2CPs to represent ancient stable peroxidases which are expressed prior to the activation of ascorbate peroxidases in young plant tissues. In higher plants, their stability to oxidative damage is supported by a strong accumulation of these enzymes (König *et al.* 2002). Their stability together with the regeneration option, gives 2CPs an important role in acclimation during post-stress phases. This is another possibility to explain the presence of peroxiredoxins throughout plant evolution.

4.6.3 *Chlamydomonas reinhardtii* encodes a putative cytosolic 2CP

The chloroplast targeting transit peptides of *Chlamydomonas* are shorter, less hydroxylated, and comprise fewer positively charge amino acid residues than the other investigated chloroplast antioxidant defense genes (Fig.s R7, R13, R19, R25, R32). This impeded the prediction of protein targeting for the identified *Chlamydomonas* antioxidative enzyme. Within a single celled alga, one big chloroplast covers two thirds of the cell lumen and partially surrounds the nucleus (Harris 2001). Uniacke and Zerges (2009) published that

protein import into chloroplasts is controlled by the availability of mRNA and localized translation in the green alga. The *Chlamydomonas* genome encodes three different 2CPs with unconserved gene-structures (Table R1, Fig. R12). Dayer *et al.* (2008) previously identified PRX1 (here: Cr2CPA) and PRX2 (here: Cr2CPB) but not Cr2CPC. Cr2CPA is more similar to the *Arabidopsis* homologs than Cr2CPB and Cr2CPC. The latter is either low or non-expressed while transcription of Cr2CPA and Cr2CPB was indicated by EST-data (Table R1). Besides this, the Cr2CPB and Cr2CPC isoforms show various amino acid substitutions which might have an influence on their effectivity and/or function (Fig. R13). Cr2CPB shows a more polar C-terminus than the other analyzed 2CPs and a modified KEY motif (aa330-aa332, Fig. R13) (Baier and Dietz 1996). Its C-terminus shows three proline residues. Usually, plant 2CPs have four proline residues while two residues are found in non-plant isoforms (König *et al.* 2003). Both modifications of the C-terminus suggest Cr2CPB to resemble rather non-plant 2CPs than plant isoforms (König *et al.* 2003). The streptophyte and chlorophyte lineages separated more than one billion years ago (Merchant *et al.* 2007). Chlorobionts have a common ancestor with rhodobionts. The rhodobiont *Porphyra purpurea* encodes 2CPs in its plastome (Baier and Dietz 1997). Most mammal 2CPs are localized in the cytosol (Wood *et al.* 2003) while isoforms from higher plants are found in chloroplasts (Baier and Dietz 1997). Phylogenetic analyses according to the maximum parsimony algorithm indicate the relation of all three *Chlamydomonas* 2CPs (Fig. R16). However, they show various differences in their amino acid sequences and unconserved gene structures (Fig.s R12, R13). Cr2CPB and the none EST-covered Cr2CPC reveal an extremely short N-terminus and may, therefore, lack a chloroplast targeting signal (Table R1, Fig. R13). All this suggests that *Chlamydomonas reinhardtii* still expresses either a cytosolic 2CP (Cr2CPB) of different evolutionary origin than chloroplast 2CPs of higher plants or a chloroplast 2CP with atypical amino acid sequence features.

4.7 Atypical 2-Cys-peroxiredoxins: peroxiredoxins Q and peroxiredoxins type II

4.7.1 Evolution of peroxiredoxins Q and peroxiredoxins type II

In streptophytes, PrxIIs are encoded by one single exon whereas the isoform of the investigated chlorophyte comprises five exons (Fig. R24). Despite their strong differences in gene structure, they show high amino acid sequence conservation in the species investigated (Fig. R25). The results obtained for APxs, 2CPs, and PrxQs indicate that most intron insertions took place before the divergence of mosses, ferns, and seed plants (Fig.s R5, R12, R18). For PrxIIs, gene structure and sequence analyses did not suggest any possible explanation for either the insertion of many introns in the *Chlamydomonas* isoform, or deletion of them in streptophyte PrxIIs. Similar to PrxIIs, the *Chlamydomonas* PrxQ gene structure has more exons than the streptophyte isoforms (Fig. R18). Its relation with *Selaginella* and *Arabidopsis* PrxQs is indicated by one conserved splicing site (Fig. R18). Gene structures encoding the mature parts of PrxQs revealed to be widely conserved in *Arabidopsis*, *Selaginella*, and *Physcomitrella* (Fig. R18). They are comprised of three to five exons and show common splice sites. The streptophyte genes mainly differ in the size of their introns (Fig. R18). During evolution, intron losses outnumbered intron gains (Roy and Penny 2007). The underlying mechanisms in multicellular eukaryotes are still unclear. While Roy and Penny (2007) found implications for mRNA-mediated intron loss, Niu *et al.* (2013) rather suggest other priming mechanisms. In conclusion, it is more likely that the investigated streptophytes lost their introns than that they were inserted in the chlorophyte genes.

Selaginella was found to encode two chloroplast PrxQs per haploid genome (Table R1). This indicates a gene duplication event. SmPrxQA was covered by ESTs while none was observed for the other PrxQ (Table R1). Additionally, SmPrxQB shows an atypical gene structure and reveals less amino acid similarity to its *Arabidopsis* homolog (Table R4, Fig.s R18, R19). It may be possible that the comparably low expressed SmPrxQB is less effective than SmPrxQA. If any, it might have a minor role in the protection of chloroplasts from ROS.

The bryophyte *Physcomitrella*, expresses three chloroplast PrxQs and two PrxIIs (Table R1). The gene number demonstrates an amplification of genes encoding atypical Prx if compared to *Chlamydomonas*, *Selaginella* and *Arabidopsis*. Since PpPrxQC shares the same high similarity to its *Arabidopsis* homolog as SmPrxQA (Table R4, Fig. R19), it might be possible that this *Physcomitrella* isoform represents the ancestor of AtPrxQ and SmPrxQA.

Phylogenetic analyses indicated that PrxQs are clustered in separate groups for lower and higher plants (Fig.s R21-R23). Nevertheless, gene structures indicate a common ancestor at least for streptophytes due to the presence of common splicing sites (Fig. R18). The *Chlamydomonas* PrxQ shares only one splicing site with the streptophytes suggesting that the genes are weakly related. These results may indicate, on the one hand, that PrxQ share a common origin but, on the other hand, that *Chlamydomonas* encodes an atypical PrxQ, which may be affected in effectivity and/or function.

The original PrxQ gene might have even emerged before the separation of streptophytes and chlorophytes. The gene structures for PrxIIs, in contrast, differ strongly in streptophytes and chlorophytes but phylogenetic trees cluster the identified isoforms together with their *Arabidopsis* homolog, indicating a corporate ancestor gene. Besides this, PrxIIs cluster with their chloroplast homologs (Fig.s R27-R29), which additionally supports the suggested origin from a common ancestral isoform.

4.7.2 Thylakoid localization of PrxQs may be streptophyte specific

In *Arabidopsis thaliana*, PrxQ is located in the thylakoid lumen (Petersson *et al.* 2006). In general, chloroplast proteins residing in the stroma are post-translationally targeted to the organelle by N-terminal extensions called transit peptides (Schreier *et al.* 1985, Smeekens *et al.* 1987). Smeekens *et al.* (1986, 1988) proposed that the transport to the lumenal compartment is due to transit peptides, which are composed of two domains. They comprise a "chloroplast import domain", also later called "envelope transit domain" or "envelope transfer domain" (James *et al.* 1989, Meadows *et al.* 1991, Robinson *et al.* 2001), mediating the transport into the stroma, and a second domain, the "thylakoid transfer domain", which is causes transport across thylakoid membranes (Smeekens *et al.* 1986, Smeekens *et al.* 1987, Robinson *et al.* 2001). PrxQs from *Arabidopsis*, *Selaginella*, and *Physcomitrella* show similar lengths of their transit peptides and a typical distribution of basic amino acids among many hydrophobic and hydroxylated residues (Schmidt and Mishkind 1986, Fig. R19). The *Chlamydomonas* isoform, in contrast, reveals a much shorter transit peptide, which is stronger positively charged in its second half (aa7–aa90, Fig. R19). This indicates that the "thylakoid transfer domain" (Smeekens *et al.* 1986, Smeekens *et al.* 1988) is missing in CrPrxQ. The light-harvesting chlorophyll-binding protein b1 (Lhcb1) reveals its thylakoid addressing peptide within its core sequence, not in its N-terminus, but is still targeted to these membranes (Lamppa 1988, Viitanen *et al.* 1988, Robinson *et al.* 2001). Within the whole CrPrxQ amino

acid sequence, no indications for a "thylakoid transfer domain" (Smeekens *et al.* 1986, Smeekens *et al.* 1987, Robinson *et al.* 2001) are found (Fig. R16). Therefore, the protein may be targeted to the chloroplast stroma. The *Chlamydomonas* enzyme reveals also additional modification, which separates it from streptophyte PrxQs: it lacks negative charges at positions 118, 119, 135, and positive charges at positions 138, 139, 156, 175, and 200 (positions in Fig. R19). In general, a high amount of positively charged amino acids revealed to be characteristic for the investigated streptophyte PrxQs (Fig. R19). These residues can be protonated upon the acidification of the thylakoid lumen and regulate enzyme activity. To summarize, since several of such residues are not conserved in CrPrxQ it is possible that the isoform, in contrast to streptophyte PrxQs, is not only differentially localized, but also shows another regulation of its activity.

4.8 Glutathione peroxidases

4.8.1 Evolution of glutathione peroxidases

Margis *et al.* (2008) assumed that the gene copy number of GPxs increased by gene duplication events. From the phylogenetic analyses and amino acid sequence comparison of *Arabidopsis*, *Selaginella*, *Physcomitrella*, and *Chlamydomonas* GPxs presented here (Fig.s R32, R34-R36), no clear conclusion on their general relation could be drawn. The investigated GPxs cluster with varying proteins in the different phylogenetic trees. Their gene structures indicate a common evolutionary origin of streptophyte GPxs (R34-R36). They are highly conserved in the region encoding the mature proteins (Fig. R32). All splice sites are shared among *Physcomitrella*, *Selaginella*, and *Arabidopsis* isoforms (Fig. R30). For the moss PpGPxA, EST-data indicate that the area encoding the C-terminus is alternatively spliced. The other *Physcomitrella* GPx (PpGPxB) is not covered by ESTs and its transcription could not be clearly verified (Table R1, Fig. R31). Additionally, it shows modifications in its amino acid sequence if compared to the other streptophyte GPxs (Fig. R32). If the gene is expressed, it may encode a not (fully) functional isoform. The general streptophytic conservation of GPx gene structures as well as their highly similar amino acid sequences (Fig.s R30, R32) point to a strong evolutionary pressure on the maintenance of a functional GPx detoxification system. This can be supported by the extension of exon1 in PpGPxB being accompanied by a low EST-coverage (Table R1, Fig. R30), which may point to the essentiality to conserve the GPx gene structure.

4.8.2 Latest GPx gene duplication event

The early evolution of GPxs remains unclear but some conclusions on the latest gene duplication event can be drawn. Phylogenetic analyses cluster AtGPx1 and AtGx7 together (Fig.s R34-R36), indicating that they arose from gene duplication. On the contrary, GPxs from *Selaginella* and *Physcomitrella* are not clustered in the same groups but rather far apart from each other, even if they are from the same organism (Fig.s R34-R36). It is suggested, that the gene duplication event, which led to the emergence of the two *Arabidopsis* chloroplast GPx isoforms may have taken place after the separation of non-seed and seed plants. In all phylogenetic trees, a single *Cycas* protein (5756 in PeroxiBase) represents the closest relative of the *Arabidopsis* chloroplast GPxs (Fig.s R34-R36). Since there are no paralogs of this *Cycas* enzyme, it may be possible that the latest gene duplication, leading to the creation of AtGPx1 and AtGPx7, could have happened even after the divergence of gymnosperms and angiosperms.

In minimum evolution and neighbor joining trees AtGPx1 and AtGPx7 are closely related to monocot proteins (3059 from *Hordeum vulgare* and 5740 from *Zea mays* in PeroxiBase, Fig.s R34, R36). Other included monocot GPxs share a higher similarity with the mitochondrial isoform of *Arabidopsis* (AtGPx6, At4G11600). Superimpositions of chloroplast and mitochondrial AtGPxs separated AtGPx6 from AtGPx1 (At2g25080) and AtGPx7 (At4g31870), although their gene structures are similar (Fig. R33B, TAIR database: www.Arabidopsis.org). The *Arabidopsis* chloroplast GPxs group with diverse spermatophyte enzymes, while AtGPx6 clusters exclusively with monocot proteins (Fig.s R34-R36). Consequently, the separation of the mitochondrial isoform dates back to times before the divergence of monocots and dicots. Consistent with this, one *Selaginella* chloroplast GPx (SmGPxA) showed higher similarity to AtGPx1 and AtGPx7 in superimpositions of the predicted 3D-structures, whereas the other isoform (SmGPxB) was more similar to AtGPx6 (Fig.s R33C, R33D). This indicates the identified organellar GPxs to be homologs of chloroplast AtGPx1 and AtGPx7 and mitochondrial AtGPx6, respectively, and suggests that the separation of the different organellar lineages happened prior to the separation of non-seed and seed-plants.

Phylogenetic analyses according to the neighbor joining algorithm (Fig. R34) showed that the *Arabidopsis* chloroplast GPxs cluster with enzymes of basal gymnosperms, basal angiosperms, and liverworts (*Cycas*: 4303, *Amborella*: 4302, *Marchantia*: 5757; all numbers refer to PeroxiBase). The inclusion of evolutionary old organisms, and not only monocots,

indicates that chloroplast GPxs were conserved over time and may represent more ancient isoforms than the mitochondrial AtGPx6.

4.8.3 GPx diversification in *Chlamydomonas reinhardtii*

The green alga *Chlamydomonas reinhardtii* genome encodes three GPxs (Table R1, Dayer *et al.* 2008). Only one of them represents a non-selenocysteine glutathione peroxidase (CrGPxC). This GPx type is typical for higher plants (Fig. R23, Dayer *et al.* 2008, Navrot *et al.* 2006). The other two are selenocysteine type isoforms (CrGPxA and CrGPxB) (Fig. R32, Dayer *et al.* 2008, Fu *et al.* 2002, Novoselov *et al.* 2002). Such GPxs are usually common in animals and microbia (Navrot *et al.* 2006). This is consistent with Merchant *et al* (2007), who found that some genes encoded by the *Chlamydomonas* genome resemble animal proteins while others are more similar to plant isoforms.

Although their gene structures are highly dissimilar, relation with streptophytes is indicated by one common splicing site of CrGPxC (Fig. R30). The non-selenocysteine GPx, in turn, shares one splicing site with CrGPxB and this isoforms shows a conserved splicing site with CrGPxA (Fig. R30). This indicates that the GPxs of streptophytes and chlorophytes are related. Additionally, it can be suggested that plant glutathione peroxidases evolved from a common ancestor, which is also consistent with Margis *et al* (2008). This research group suggested that plant GPx show a high sequence similarity to animal GPx4 which indicates a common eukaryotic origin (Margis *et al.* 2008). Among the *Chlamydomonas* GPxs, CrGPxC may represent the evolutionary youngest isoform since it shows one conserved streptophyte splicing site and higher similarity to the *Arabidopsis* homologs than CrGPxA and CrGPxB.

In general, the *Chlamydomonas* GPxs share only low similarity with the investigated streptophyte homologs. Together with the fact that both, seleno- as well as non-selenocysteine type GPxs are present in the green alga, this points to a parallel but independent evolution of GPxs in chlorobionts. Only the non-selenocysteine type of GPxs was maintained in plants. Throughout time, these antioxidant enzymes further diversified in the streptophyte lineage by gene duplication, such as in case of the separation of the AtGPx1/AtGPx7 ancestor from AtGPx6, and alternative splicing, which is shown by PpGPxA.

4.9 *Physcomitrella* tAPx

Physcomitrella patens revealed a single atypical chloroplast ascorbate peroxidase gene within its genome (Table R1, Fig. R5). An encoded C-terminal localized extension, which was predicted to form a helix, indicated that the APx is bound to thylakoids (Fig. R7). Although it shows a highly unconserved gene structure, its predicted protein 3D-folding and amino acid sequence are very similar to the *Arabidopsis* homolog (Fig.s R7, R46). Analyses pointed to the presence of a thylakoid-bound ascorbate peroxidase gene within the *Physcomitrella* genome, while no open reading frame (ORF) for a sAPx was found. Some plants, *e. g.* pumpkin, spinach, tobacco, and ice plant (Ishikawa *et al.* 1996, Mano *et al.* 1997, Yoshimura *et al.* 2002), encode their stromal and thylakoid-bound APx isoforms on a single gene, which is alternatively spliced. In *Physcomitrella*, all collected EST-data excluded the possibility of alternative splicing leading to the formation of a soluble ascorbate peroxidase.

Investigation on the surrounding of PptAPx within the moss genome revealed that the APx is of retrotransposonal origin (Fig. R37). This origin will be discussed later into detail. EST-data suggested that the *Physcomitrella patens* thylakoid-bound APx (PptAPx) is highly expressed in comparison to the other antioxidant defense genes bioinformatically identified in the moss (Tables R1, R7). The other investigated organisms likely expressed other detoxifying enzymes, possibly to take over the major role in their respective chloroplast defense (Table R7). For all these reasons, further focus of the present study was set on PptAPx.

4.9.1 PptAPx is of retrotransposonal origin

The surrounding within the genome revealed many LTR retrotransposonal footprints (Fig. R37) pointing to the emergence of the PptAPx gene by a retrotransposition event. In general, retrotransposons possess only weak polyadenylation sites. This can lead to addition of the DNA region in the vicinity of the retrotransposonal element since the transcription machinery stops its work not at the retrotransposonal polyadenylation site but at the next it recognizes (Moran *et al.* 1996, Xing *et al.* 2006). The additional sequence accompanies the transposon through processing and reverse transcription machineries until integration into the genome. This can lead to a duplication of the original gene (Xing *et al.* 2006, Xiao *et al.* 2008).

The *Physcomitrella* tAPx gene shows only a single and unconserved splice site (Fig. R5). This suggests that its hnRNA was spliced prior to integration into the genome. The intron

found within the PptAPx ORF was most likely inserted after the retrotransposition event and cannot result from incomplete splicing during the retrotransposition process.

Several retrotransposonal elements have been inserted into the genome in waves. Insertions took place approximately every 3.9 million years (Rensing *et al.* 2008). Mosses diverged approximately 450 million years ago (Reski 2005, Rensing *et al.* 2008). Consequently, it is not possible to date the retrotransposition leading to the emergence of PptAPx. It may even be possible that this event happened independently in mosses.

In *Physcomitrella*, no ascorbate peroxidase gene being highly similar to the retrotransposonal PptAPx or even traces of such could be detected. On the one hand, in phylogenetic trees, PptAPx clusters with other chloroplast APxs, suggesting that the ancestral gene was also a chloroplast targeted isoform (Fig.s R9-R11). On the other hand, PptAPx shows features of cytosolic APxs (Fig. R8). These facts make it difficult to draw conclusions on the identity of the original gene. Since PptAPx shares more similarity with chloroplast targeted APxs, it is likely that the ancestor was localized in these organelles. Beside this, the fate of the ancestor also remains unclear. It is possible that the original ORF, if chloroplast targeted, encoded both, sAPx and tAPx, and was alternatively spliced. The splicing site could have been lost due to the retrotransposition process or during evolution. Another option might be that the original gene was overwritten. *Physcomitrella* is known for efficient homologous recombination machinery (Hohe and Reski 2003). If the retrotransposon included the DNA region encoding the original APx gene, it showed a high degree of similarity to the part of the genome containing the ancestral APx. Consequently, the transposon may have integrated at this locus, thereby causing the extinction of the original APx. A third possibility explaining the fate of the gene might be that the newly integrated gene was more effectively expressed than its ancestor. The latter accumulated mutations and finally vanished during plant evolution. Nevertheless, it is not feasible to draw any conclusion on the real fate of the original APx.

After the retrotransposition event, expression of the just recently emerged gene had to be ensured and its fine-tuning re-established. Although, it was feasible to produce several sAPx and tAPx knock-down and knock-out mutants from different plant species (Danna *et al.* 2003, Davletova *et al.* 2005, Giacomelli *et al.* 2007, Miller *et al.* 2007, Ishikawa *et al.* 2008, Kangasjärvi *et al.* 2008, Maruta *et al.* 2010), both genes revealed to have important roles for plant fitness.

The natural habitat of *Physcomitrella* is open and disturbed (Schaefer and Zrÿd, 2001, Wolf *et al.* 2010). As a consequence, the moss can be exposed to varying light intensities. Both,

stromal and thylakoid-bound APx isoforms are important for plants. Nevertheless, it may be possible that the ancestors of the moss may have lost their original APx even before the newly emerged PptAPx had been effectively integrated into the metabolism by evolution of suitable promoter elements. If the ancestral enzyme was localized to the cytosol, the retrotransposonal PptAPx may have also existed in parallel with (a) chloroplast APx(s) and gained its transit peptide during evolution. Nevertheless, it remains unclear if the original APx was lost before, during, or after full integration of the retrotransposonal APx into the metabolism of *Physcomitrella*.

4.9.2 Chloroplast targeting of PptAPx

PptAPx is of retrotransposonal origin. It shows more features of chloroplast than of cytosolic APx isoforms. This tempts to suggest that the ancestor was rather a chloroplast localized enzyme. PptAPx itself was predicted by the online tools TargetP (Emanuelsson *et al.* 2000) and ATP (Mitschke *et al.* 2009) to be targeted to chloroplasts (Table R1). Fusions of its transit peptide to YFP verified this organellar targeting (Fig. R45). If the original APx gene was localized to chloroplasts, the retrotransposon carried the whole gene, including the encoded transit peptide, to the integration site. On the contrary, if the ancestor was not localized in chloroplasts, the targeting had to be newly established during evolution.

4.9.3 Transcriptional regulation and function of PptAPx

Prediction of TATA-boxes and EST-data for PptAPx indicated the presence of two transcription initiation sites controlling its expression (Fig. R38). Promoter deletion studies using luciferase as a reporter gene led to conformation of the EST-data (Fig.s R40, R41). Indeed, the transcription of PptAPx is initiated at two different sites. One is located within the first 337 bp upstream of the start-ATG, while the other resides further upstream. To date, such a regulation has not been published although it is known that 5'-UTRs can contain elements and motifs which influence translation (Wobbe *et al.* 2008). Nevertheless, they might have no impact on transcription initiation. It may be possible that one of the two PptAPx transcription initiation sites represents a leftover of the ancestral ascorbate peroxidase or another gene, which was replaced by the retrotransposonal footprints. Other possibilities are that one of the sites either emerged coincidentally during evolution or is a retrotransposonal relic.

Irrespective of the correct explanation, *Physcomitrella* (re-)established a high and fine-tuned transcription of its single chloroplast ascorbate peroxidase.

In detail it was found that the both sites initiate transcription at different strengths (Fig. R40). The second site revealed to be very weak while the closer site causes a strong expression of the controlled gene. *Physcomitrella* gametophytes were also transfected with other constructs, in which the expression of the reporter gene luciferase was regulated by the promoters of sAPx and tAPx from *Arabidopsis thaliana* (Fig. R42). Even in comparison to these, the whole PptAPx promoter caused a stronger luminescence. If the transcript number positively correlates with the amount of functional protein and/or its regeneration, this may indicate that *Physcomitrella* overexpresses its single thylakoid-bound APx. At least it is much higher expressed than its *Arabidopsis* homolog. From literature it is known that tAPx overexpressing mutants show an increased resistance to photo-oxidative stress than wild-type plants (Yabuta *et al.* 2002, Murgia *et al* 2004). Oxidative stress can be generated by diverse environmental factors but also artificially by application of methylviologen. This herbicide, also called paraquat, causes the accumulation of superoxide anions via transfer of electrons from photosystem I (PSI) to oxygen (Babbs *et al.* 1989, Fujii *et al.* 1990). Subsequently, hydrogen peroxide starts accumulating (Nakano and Asada 1980, Foyer *et al.* 1994, Mano *et al.* 2001, Maruta *et al.* 2010). Sufficient amounts of ascorbate cannot be regenerated from monodehydroascorbate since not enough reduction equivalents are available anymore (Palatnik *et al.* 1997). Under these conditions, chloroplast ascorbate peroxidases are rapidly inactivated (Mano *et al.* 2001, Miyagawa *et al.* 2000).

In the present study, *Physcomitrella* was shown to be highly tolerant against oxidative stress caused by the application of methylviologen if compared to *Arabidopsis* (Fig. R47). Its photosynthetic yields did not markedly decrease even if the gametophytes were treated with 2 mM paraquat. Treated with the same solution, *Arabidopsis* seedlings hardly survived (Fig. R47). *Arabidopsis* mutants overexpressing tAPx showed an increased resistance to the herbicide whereas limited tAPx expression led to an increased sensitivity (Yabuta *et al.* 2002, Murgia *et al.* 2004, Tarantino *et al.* 2005). The results indicate that *Physcomitrella* indeed expresses PptAPx at a very high level (Fig. R47). Beside this, they suggest PptAPx to be functional.

Other factors which could be supportive to the function of PptAPx, are two amino acid substitutions (R282H, W288F, positions in Fig. R7), which are typical for cytosolic isoforms. APxs localized in the cytosol are less sensitive to hydrogen peroxide and show a lower

specificity to ascorbate as a substrate (Jespersen *et al.* 1997, Wada *et al.* 2003). Since the *Physcomitrella* tAPx shows these two features, it may be less vulnerable to inactivation by hydrogen peroxide and might be capable to utilize other substrates besides ascorbate.

In general, *Physcomitrella* is known to be tolerant against many abiotic stresses causing oxidative stress, such as a surplus of salt or drought (Frank *et al.* 2005, Lunde *et al.* 2007, Wang *et al.* 2008). If the strong transcription results in high amounts of functional protein and if the amino acid substitutions have the mentioned impacts on PptAPx function and effectivity, the enzyme may represent the major defense against oxidative stress within chloroplasts.

4.9.4 Regulation of PptAPx by light and chilling temperatures on transcript level

In chilling conditions, hydrogen peroxide accumulates (Jahnke *et al.* 1991, Okuda *et al.* 1991, Asada 1999) influencing the antioxidative defense (Schöner and Krause 1990, Asada 1999, Yabuta 2002, Hu *et al.* 2008). The PptAPx transcript level is down-regulated when the gametophytes were subjected to low temperatures (Fig. R48). In contrast, excess light caused an increase in the transcript level (Fig. R48). Yoshimura *et al.* (2000) published that high light had no impact on the transcript level of spinach chloroplast APxs. Horling *et al.* (2003) showed that all chloroplast peroxiredoxins, in contrast, were stronger expressed under such stressful conditions. Thus, excess light can have an influence on the chloroplast antioxidant system.

Under these conditions, excess electrons are transferred to oxygen. The resulting superoxide is rapidly converted to hydrogen peroxide. This leads to an accumulation of this ROS and, in turn, to an increased expression of PptAPx to prevent the chloroplast from the toxic impact of hydrogen peroxide.

Excess light leads to the induction of the violaxanthin cycle. Violaxanthin is rapidly converted to zeaxanthin (Demming *et al.* 1987, Eskling *et al.* 1997). The latter is a quencher of triplet state chlorophylls (Cogdell 1985). The excess excitation energy is thereby dissipated as thermal energy. The conversion of violaxanthin to zeaxanthin consumes ascorbate leading to the formation of dehydroascorbate (Hager 1969, Demming *et al.* 1987, Eskling *et al.* 1997). In the present study, it was shown that the exogenous application of ascorbate caused to a down-regulation of the PptAPx transcript level while dehydroascorbate triggered an increase (Fig. R49). The results may indicate that ascorbate can be involved in the up-regulation of the

PptAPx transcript level by excess light. The effect would be caused by a decrease in the ascorbate content due to induction of the violaxanthin cycle (Hager 1969, Demming *et al.* 1987, Eskling *et al.* 1997).

Beside this, ABA accumulates in response to excess light and low temperatures (Ishitani *et al.* 1997, Galvez-Valdivieso *et al.* 2009). Since both, exogenous ABA application and cold treatment, caused a down-regulation of the PptAPx transcript level (Fig.s R48, R51), at least the cold response in the moss may include ABA signaling. Excess light up-regulates PptAPx transcription (Fig. R48). In conclusion, the responsible pathway might be independent from ABA. Another option may be that the light effect on PptAPx is indirectly connected with it by the ABA-dependent production of hydrogen peroxide. The ROS accumulates not only in response to an increased photosynthesis rate but also to the phytohormone. Either PptAPx transcription is directly influences or it is affected by the decreased amount of ascorbate. When ascorbate is oxidized dehydroascorbate is formed. Exogenous application of this compound caused an up-regulation of the PptAPx transcript level (Fig. R49). Consequently, the response to light could also include the abundance of ascorbate, *i. e.* its redox status.

4.9.5 Regulation of PptAPx by low molecular weight antioxidants on transcript level

The low molecular weight antioxidants glutathione and ascorbate are ubiquitous in the plant kingdom. Being present in many tissues, they accumulate to millimolar concentrations (Foyer and Halliwell 1976, Foyer and Lelandais 1996). Ascorbate as well as reduced glutathione fulfill a major part in plant defense, since they are able to detoxify hydrogen peroxide, hydroxyl radicals, superoxide, and singlet oxygen (Larson 1988). Upon stress treatment, the amounts and the redox state of glutathione and/or ascorbate can change dramatically (Maruta *et al.* 2010, Mittova *et al.* 2003). This, in turn, can influence the expression of defense genes (Wingsle and Karpinsky 1996, Horling *et al.* 2003, Mullineaux *et al.* 2005). There are several evidences that the ascorbate and glutathione pathways and signaling pathways are connected. Veljovic-Jovanovic *et al.* (2001) published that the *vtc-1* (vitamin c 1) *Arabidopsis* mutant, which is impaired in ascorbate synthesis, shows an increased glutathione levels. Ball *et al.* (2004), in contrast, found that the *Arabidopsis rax1-1* (regulator of APx2 1-1) mutant, which lacked γ-glutamylcysteine synthetase (GSH1) function, showed a constant up-regulation in the expression of a cytosolic APx. GSH1 catalyzes a step during glutathione biosynthesis (Alscher 1989, May and Leaver 1994). Thereby, Veljovic-Jovanovic *et al.* (2001) and Ball *et al.* (2004) demonstrated that the ascorbate and glutathione pathways are linked and have an

impact on each other. Maruta *et al.* (2010) showed a knock-out of chloroplast APxs affecting the redox state of glutathione. They suggested that this phenomenon might be due to different subcellular locations of their biosynthetic pathways. On the contrary, Baier *et al.* (2000) found that decreased expression of another defense gene, a 2-Cys peroxiredoxin, influences the redox state of ascorbate. All these publications prove a link between chloroplast defense genes and the low molecular weight antioxidants ascorbate and glutathione.

The *Physcomitrella* tAPx does not represent any exception from the defense genes which are regulated by ascorbate and glutathione. Its transcript level is down-regulated by application of ascorbate and up-regulated by dehydroascorbate (Fig. R49). In contrast, glutathione, no matter if reduced or oxidized, caused a decrease of PptAPx transcripts (Fig. R50). These results demonstrate that the expression of the *Physcomitrella* tAPx gene is linked to the redox state of ascorbate but not to the one of glutathione. Moreover, they prove regulation via the abundance of the substrate ascorbate. Whether this feedback control is direct or indirect remains unclear. The regulation by reduced glutathione may also represent an indirect feedback regulation. The molecule has an important role in the regeneration of ascorbate. Consequently, an elevated concentration of reduced glutathione may be a signal for sufficient ascorbate supply, which, in turn, down-regulates PptAPx transcription.

The influence of oxidized glutathione on the PptAPx transcript level may be indirect. Wingsle and Karpinsky (1996) published that in *Pinus sylvestris* needles, glutathione reductase transcription is rapidly up-regulated upon application of exogenous oxidized glutathione. If this is the same in *Physcomitrella patens*, the reduced glutathione was regenerated from the surplus of oxidized glutathione. As a result, the abundance of the previous increased, leading to a down-regulation of PptAPx. All this would be consistent with results and suggestions of Horling *et al.* (2001) for a 2CP encoded by the liverwort *Riccia fluitans*. The gene showed similar regulation as PptAPx. Another possible explanation for the decrease of PptAPx transcripts might be that higher amounts of oxidized glutathione are a signal for an increased consumption of reduced glutathione to regenerate ascorbate. This would induce the feedback regulatory pathway. There is more than one possible way to explain the regulation of PptAPx by oxidized glutathione.

Since ascorbate and reduced glutathione are important antioxidative molecules, elevated concentrations could function as a signal that there is no oxidative stress anymore. As a result, less hydrogen peroxide needs to be detoxified and the available amount of low molecular weight antioxidants is sufficient for antioxidant defense. Consequently, the abundance of

enzymes, with antioxidant function, can be decreased. Another hint to the regulation via ROS might be that the PptAPx transcript level is up-regulated by dehydroascorbate. This molecule is produced upon consumption of ascorbate by APxs to convert hydrogen peroxide to water. It is possible that the increase of dehydroascorbate is a signal for hydrogen peroxide accumulation. The amount of low molecular weight antioxidants may be not sufficient for an effective defense of the chloroplast. The regulation of PptAPx by hydrogen peroxide consents to the results obtained from gametophytes treated with excess light. In such stressful conditions, hydrogen peroxide accumulates (Mittler 2002, Maruta *et al.* 2010). According to the collected results, this may be the major signal – no matter whether direct or indirect – causing an increase in PptAPx expression to balance the status of the organelle.

Horling *et al.* (2001) proposed a model signaling pathway to regulate the expression of a 2CP in the liverwort *Riccia fluitans*. They suggested that a decrease in ROS, accompanied by an increase in ascorbate cause a down-regulation of the encoding transcripts. It may be possible that PptAPx is regulated similarly.

Finally, the regulation of PptAPx shows some similarity to the controls published for the *Arabidopsis* 2CPA. The gene encoding another antioxidative enzyme is also down-regulated upon treatment with ascorbate and its transcription revealed to be increased when hydrogen peroxide was applied (Baier *et al.* 2004). The seedlings were also exposed to different CO_2 conditions (50 ppm, 350 ppm, 2000 ppm). In high CO_2 conditions, the promotion of ribulose-1,5-bisphosphyte carboxylation causes a decrease of the NADPH/$NADP^+$ ratio in chloroplasts (Dietz and Heber 1984). In a low CO_2 environment, this ratio only slightly increases or stays at the same level (Dietz and Heber 1984, Baier *et al.* 2004). Baier *et al.* (2004) showed that the 2CPA promoter activity is positively co-regulated with the reduction state of NADPH/$NADP^+$. Besides this, most of the cellular ascorbate and glutathione are reduced even when CO_2 is low (Wormuth *et al.* 2006). The 2CPA promoter showed only a slight induction under such circumstances, following the redox state of NADPH/$NADP^+$. However, its activity was strongly decreased upon ascorbate application.

PptAPx shows a similar regulation as the *Arabidopsis* 2CPA in response to exogenous application of low molecular weight antioxidants. Additionally, a surplus of oxidized glutathione causes a decrease in the transcript level. NADPH is consumed to reduce glutathione, thereby leading to a decrease of the NADPH/$NADP^+$ ratio. In conclusion, the tAPx of *Physcomitrella* may be regulated in the same way as or similar to the 2CPA gene in *Arabidopsis*. Nevertheless, the results obtained for exogenous dehydroascorbate application

and excess light treatment contradict a positive regulation of PptAPx by the NADPH/$NADP^+$ ratio. Both cause an increase in the PptAPx transcript level (Fig.s R48, R49). Excess light conditions demand for ROS detoxification and induce the violaxanthin cycle. Both processes consume ascorbate producing dehydroascorbate (Asada 1999, Eskling *et al.* 1997). The previous is regenerated under the expense of NADPH. In conclusion, if the NADPH/$NADP^+$ ratio has an impact on PptAPx transcription it may be positive in response to exogenous $glutathione^{ox}$ and ABA application (Fig.s R50, R51) but negative upon elevated dehydroascorbate levels (Fig. R49).

4.9.6 Regulation of PptAPx by abscisic acid on transcript level

Many phytohormones, for example ABA, are present in bryophytes and angiosperms (Schumaker and Dietrich 1997, Knight *et al.* 1995, Nishiyama *et al.* 2003, Quatrano *et al.* 2007). One of them is abscisic acid (ABA). In higher plants, this hormone has an important role in tolerating and adapting to high salinity and water deficiency, upon which the ABA level increases (Zhu 2002). Richardt *et al.* (2010) suggest this phytohormone to have similar functions in *Physcomitrella*. In seed plants, ABA is known to cause accumulation of hydrogen peroxide followed by stomatal closure to prevent excess transpiration and maintain sufficient water status (Leung and Giraudat 1998, Zhang *et al.* 2001). Since *Physcomitrella* gametophytes do not have stomata, the hormone cannot have this function. However, since mosses lack an epidermis or a sturdy cuticula, their water loss is high (Rensing *et al.* 2007). This forces them to be tolerant to water deficit.

Despite Yoshimura *et al* (2000) published that ABA did not influence the transcript level of chloroplast APxs in spinach, the phytohormone is known to have an influence on the antioxidative system (Sakamoto *et al.* 1995, Yoshida *et al.* 2003, Baier *et al.* 2004). Some genes are up-regulated upon exogenous application of ABA, most likely due to the accumulation of ROS, while others are down-regulated via a ROS-independent pathway. Like published for the *Arabidopsis* 2CPA (Baier *et al.* 2004), the transcript level of PptAPx is down-regulated when gametophytes were treated with ABA (Fig.s R51). One explanation for the regulation of the APx by low molecular weight antioxidants was suggested to involve hydrogen peroxide accumulation. If this was true, the ABA regulatory pathway influencing the expression of PptAPx is independent from the increase in ROS production. Beside this, it is known that ABA biosynthesis is regulated by the redox status of ascorbate in *Arabidopsis*: It is induced when the availability of ascorbate is low (Pastori *et al.* 2003). PptAPx expression

is up-regulated in response to exogenous dehydroascorbate application but down-regulated upon ABA treatment (Fig.s R49, R51). Quatrano *et al.* (2007) published that *Physcomitrella* and angiosperms show similarities in their ABA regulatory pathway. The function of the regulatory factor Abscisic Acid Insensitive3 (ABI3) is conserved although they are present in non-homologous tissues. If the ABA regulatory pathway is also similar for *Arabidopsis* 2CPA and *Physcomitrella* tAPx, the control of PptAPx by the phytohormone would override the regulation by the redox state of ascorbate.

Besides this, a surplus of dehydroascorbate was above suggested to function as a signal of hydrogen peroxide accumulation, which may cause enhanced transcription of PptAPx. If this is the case, the down-regulating effect of ABA on PptAPx would be independent from this reactive oxygen species.

4.9.7 Major regulators of PptAPx transcript level

PptAPx transcription revealed to be regulated by the phytohormone ABA. The obtained results indicated that this pathway may depend on hydrogen peroxide during light stress but not in chilling temperatures or as response to exogenous application to otherwise unstressed gametophytes (Fig.s R48, R51, D1). It might be that these two pathways act separately from each other. Another possibility is the induction of the different signaling cascades is dependent on the dose of hydrogen peroxide or low molecular weight antioxidants. Maybe it is necessary that the ROS accumulates up to a certain threshold or that the contents of antioxidants decrease below a certain threshold to induce PptAPx transcription. In excess light conditions, this threshold might have been reached, causing the ABA down-regulating pathway to be dominated by a hydrogen peroxide dependent up-regulating cascade. This hypothesis may be supported by the finding that the *Arabidopsis vtc* mutant accumulates ABA (Pastori *et al.* 2003). These plants are impaired in ascorbate biosynthesis resulting in a low amount of the low molecular weight antioxidant (Conklin *et al.* 1996, 1997). Thus, the importance of ABA in regulatory pathways might increase with a decrease in ascorbate.

In conclusion, two major regulators of PptAPx transcription may be ABA, on the one hand, and either the amount of low molecular weight antioxidants or accumulation of hydrogen peroxide, on the other (Fig. D1). Although, dehydroascorbate also represents a low molecular weight antioxidant, its function as sensor of low ascorbate content or hydrogen peroxide accumulation overrules its antioxidative impact.

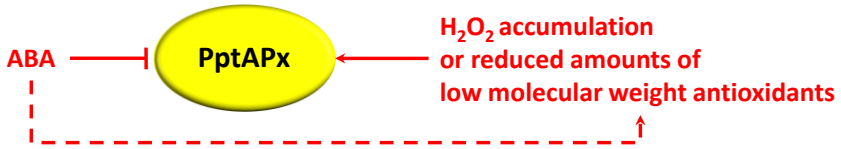

Fig. D1: Scheme of the putative PptAPx transcript level regulation by two major regulators. Exogenous application of abscisic acid (ABA) or the low molecular weight antioxidants ascorbate and reduced glutathione to otherwise unstressed gametophytes causes a decrease in the PptAPx transcript level. Hydrogen peroxide, in contrast, was suggested to trigger an increase. Higher amounts of ABA are accompanied by hydrogen peroxide accumulation. It is possible that, if the amount of this ROS accumulates to concentrations above a certain threshold, ABA pathways can be dominated by the regulatory impacts of hydrogen peroxide. Optional, not hydrogen peroxide accumulation but reduced amounts of low molecular weight antioxidants may trigger the up-regulation of the PptAPx transcript level. If their level decreases below a certain threshold, ABA dependent pathways may possibly dominate.

4.9.8 Parallels between *Physcomitrella patens* and higher plants

Additional promoter-reporter gene analyses revealed parallels in the transcriptional regulation and targeting of PptAPx between the moss *Physcomitrella patens* and higher plants. To facilitate the studies, a method to transfect several organisms at once was developed. Until then, only distinct PEG-mediated transfection/transformation procedures were known for *Arabidopsis* and *Physcomitrella* besides particle bombardment (Schaefer *et al.* 1990, Hohe *et al.* 2004, Yoo *et al*, 2007, Wu *et al.* 2009). Although the bryophyte was published to be no target of *Agrobacterium tumefaciens* (Schaefer and Zrÿd, 2001), a successful transfection assay, based on the vacuum infiltration method by Bechtold *et al* (1993), was developed. Li *et al.* (2010) published a similar, also *Agrobacteria*-mediated, method before. Nevertheless, their procedure was more time-consuming. The assay used here revealed to be highly effective since it was suitable not only for *Arabidopsis* and *Physcomitrella* but also for *Selaginella* (Fig.s R52, R53). Using this method, evolutionary comparisons are facilitated due to the possibility to transfect different plant species at once and in an equal, standardized way.

The promoter-reporter gene studies showed that the chloroplast targeting signal of PptAPx is not only functional in its host but also in *Arabidopsis* (Fig. R57). Although they have an unconserved amino acid sequence (Fig. R8, Karlin-Neumann and Tobin 1986, Bruce 2000), the results demonstrate that the way in which transit peptides target proteins chloroplasts did not change (much) during plant evolution (Soll and Alefsen 1993).

Besides *Physcomitrella* and *Arabidopsis,* a third plant species was included. The investigation concerning the PptAPx transcription also comprised *Nicotiana benthamiana*. Tobacco leaves were transfected applying the same *Agrobacteria* strains used for *Arabidopsis* and *Physcomitrella*. The infiltration was carried out not by vacuum but with a syringe. The studies showed the two sites initiating its transcription are functional not only in the moss but also in higher plants. Alike *Physcomitrella*, the first initiation site (within 337 bp upstream of the start-ATG) causes a stronger expression of the controlled luciferase gene than the second further upstream site (Fig.s R40, R54). As shown for the moss (Fig. R42), the luminescence caused by the first site was even higher than when the *Arabidopsis* sAPx and tAPx promoters were controlling luciferase expression in *Arabidopsis* and tobacco(Fig. R51). Beside this, all three organisms showed similar qualitative luminescence patterns for the AttAPx or AtsAPx promoters (Fig. R42, R54). The sAPx promoter revealed to drive a stronger luciferase expression than the tAPx promoter. Reski (1998a) suggested that the usage of promoters is similar in *Physcomitrella* and *Arabidopsis*. The results presented here clearly support this suggestion and show that the basic mechanisms leading to organellar targeting as well as transcription initiation, at least for PptAPx, are shared and effective in higher plants as well as in mosses. They were conserved during plant evolution.

4.10 Conclusions

4.10.1 Evolutionary pressure on the maintenance of APx, Prx, and GPx antioxidative detoxification systems

All investigated organisms showed presence of APxs, Prxs, and GPxs (Table R1). This demonstrates the importance of all three detoxification systems for the fitness of plants to survive through ages. Although there was enough time available to accumulate modifications in intron number or lengths and amino acid sequences, their gene and protein structures kept widely conserved in the investigated organisms (Fig.s R7, R13, R19, R25, R32). Especially, genes which were covered by ESTs showed high amino acid conservation (Table R1, Fig.s R7, R13, R19, R25, R32). The low or non-expressed isoforms, in contrast, often revealed strong differences to their respective *Arabidopsis* homolog suggesting them to represent either silent pseudogenes or, if expressed, functionally impaired or changed proteins.

It was found that the ascorbate peroxidases of *Arabidopsis*, *Selaginella*, *Physcomitrella*, and *Chlamydomonas* share a common ancestor (Fig.s R6, R9-R11). The gene structures of the

included peroxiredoxins suggest at least partially independent evolution, which resulted in putatively non-plastidic or atypical 2CP isoforms, a PrxQ which is potentially not localized in the thylakoid lumen, and a PrxII gene comprising more than one exon (Fig.s R12, R13, R18, R19, R24). Apart from this, the analyses indicated that PrxQs and PrxIIs arose from common ancestral PrxQ and PrxII isoforms, respectively (Fig.s R18, R21-R23, R27-R29). On the contrary, 2CPs evolved independently in the streptophyte and chlorophyte lineages (Fig.s R12, R15-R17). Plant GPxs evolved from a common evolutionary ancestor. Nevertheless, the GPxs included in the study differed among streptophytes and chlorophytes. The *Chlamydomonas* genome encodes three GPxs, two selenocysteine- and one non-selenocysteine type isoforms. Higher plant glutathione peroxidases are commonly non-selenocysteine isoform while selenocysteine type GPxs are usually found in animals (Navrot *et al.* 2006). While *Chlamydomonas* expresses both types, the investigated streptophytes reveal only non-selenocysteine-type GPxs.

In conclusion, the presented bioinformatic studies demonstrated that, although their individual components were target of mutations and selection, the APx, Prx, and GPx mediated chloroplast defenses were maintained during evolution and, therefore, represent crucial detoxification systems ensuring their host's survival during evolution.

4.10.2 Evolutionary pressure on *Selaginella moellendorffii* and *Arabidopsis thaliana*

The identified *Selaginella* chloroplast antioxidative defense genes most often resembled their respective *Arabidopsis* homologs. Analyses of gene structures, amino acid sequences, as well as superimpositions with proteins from the higher plant model revealed high similarities at least among the expressed isoforms. It can possibly be suggested that the evolutionary pressure on the chloroplast defense systems mediated by APxs, Prxs, and GPxs may have been stronger prior to the separation of lycophytes and higher plants than after this event. The capacity of the chloroplast antioxidative defense was sufficient for the host's fitness to endure stressful conditions, such as excess light and water deficit, and, as a consequence, to survive during evolution.

4.10.3 *Selaginella* chloroplast antioxidant defense genes have short introns

Among the investigated genes encoding chloroplast antioxidant defense enzymes, the *Selaginella* isoforms showed the shortest introns. Banks *et al.* (2011) published that the introns in *Selaginella* are in general shorter that those in found in *Physcomitrella* and *Arabidopsis*. Genome size may correlate with intron size (Deutsch and Long 1999, Vinogradov 1999, Wendel *et al.* 2002). In comparison to the other streptophytes, *Selaginella* has a small genome comprising approximately 106 Mbp (*Arabidopsis*: ~157 Mbp, *Physcomitrella*: ~480 Mbp from Bennett *et al.* 2003, Wang *et al.* 2005, and Rensing *et al.* 2008, respectively). It could be concluded that the small genome size of *Selaginella* positively correlates with its reduced intron sizes. However, from comparison to *Arabidopsis*, Banks *et al.* (2011) suggested that the shorter introns may be offset by a higher abundance of transposable elements within the *Selaginella* genome.

4.10.4 Evolutionary convergence of *Physcomitrella patens* to higher plants

The phylogenetic analyses revealed that, among the other identified APxs, *Physcomitrella* tAPx is the closest relative to *Arabidopsis* chloroplast ascorbate peroxidases (Fig.s R9-R11). In between the moss and the seed plant only higher plants were grouped. The minimum evolution tree of 2CPs as well as neighbor joining and maximum parsimony trees of PrxQ show similar clustering (Fig.s R15, R17). Additionally, amino acid sequences comparisons of the identified *Physcomitrella* antioxidant enzymes with *Arabidopsis* proteins showed high similarity indicating their functionality. Besides this, other parallels between *Arabidopsis* and *Physcomitrella* were shown. The basic mechanisms leading to chloroplast targeting, transcription initiation and intensity are similar in *Arabidopsis* and *Physcomitrella* (Fig.s R42, R45, R54, R57), at least for their chloroplast ascorbate peroxidases. Consequently, the responsible regulatory motifs are conserved and were preserved during evolution.

Mosses diverged approximately 450 million years ago (Reski 2005, Rensing *et al.* 2008). During time, this lineage, including *Physcomitrella*, further evolved. This possibly explains the phenomenon that some components of the *Physcomitrella* chloroplast antioxidative defense show a higher similarity to higher plants. The natural environment of *Arabidopsis* and the moss is open and disturbed (Schaefer and Zrÿd 2001). In addition, the ancient environmental conditions may have become even more uncomfortable for the bryophyte during time, putting a strong selective pressure on it. The convergence of the antioxidative

system towards higher plants might result from the effort of *Physcomitrella* to enhance its fitness and survive the hostile environment.

4.10.5 Evolutionary pressure on *Physcomitrella patens*: Re-integration of a retrotransposonal gene (PptAPx) into the metabolism

Only a single ORF encoding a chloroplast targeted ascorbate peroxidase was detected in the *Physcomitrella patens* genome (Table R1). A helix-forming C-terminal extension led to the designation as a thylakoid-bound isoform (Fig. R7, R46). Further studies on the surrounding within the genome showed that the gene is most likely of retrotransposonal origin indicated by many Angela-LTR retrotransposonal footprints around the ORF. No traces of the original gene could be found and its fate remains unclear. It is possible that either both genes existed in parallel or that the ancestor was lost before the retrotransposonal PptAPx could be fully integrated into the metabolism, *e. g.* by an effective (re-)established promoter regulation.

Promoter-reporter gene studies verified the predicted chloroplast targeting of PptAPx (Fig. R47). Additionally, they revealed that the transcription of PptAPx is initiated at two distinct sites (Fig.s R40, R41). Controlling the expression of a luciferase reporter gene, the first initiation site, which is closer to the start-ATG drives a much stronger luminescence than the second, further upstream, site. The strength of the first site most likely causes *Physcomitrella* to highly express PptAPx. Gametophytes transfected with constructs, in which the sAPx and tAPx promoters from *Arabidopsis* regulated the expression of luciferase, showed that the first transcription initiation site causes PptAPx to be even higher expressed than the *Arabidopsis* isoforms (Fig. R43), if the transcript number positively correlates with the amount of functional protein. Since plant overexpressors of tAPxs are more resistant to oxidative damage (Yabuta *et al.* 2002, Murgia *et al.* 2004), the high expression of PptAPx may be one explanation why *Physcomitrella* is tolerant to various uncomfortable environmental conditions causing oxidative stress, especially drought and salt surplus (Frank *et al.* 2005, Lunde *et al.* 2007, Wang *et al.* 2008). Such stress can be artificially provoked by application of the herbicide methylviologen. *Physcomitrella* showed a high resistance to this substance in comparison to the sensitivity shown by *Arabidopsis*. Consequently, PptAPx may be crucial for the survival of *Physcomitrella patens*.

Although the regulatory pathways are not fully elucidated in the moss, the transcript level was shown to be influenced various factors. Excess light caused an increased transcription while chilling triggered down-regulation (Fig. R48). Exogenous applications of ABA, ascorbate,

dehydroascorbate, reduced, and oxidized glutathione revealed to differentially influence the PptAPx transcript level (Fig.s R49-R51). Quatrano *et al.* (2007) suggested that there are parallels in regulatory pathways between *Physcomitrella* and angiosperms, at least for ABA. Additionally, the PptAPx transcription was found to be influenced analogously to *Arabidopsis* 2CPA (Fig.s R49-R51, Baier *et al.* 2004). If the regulatory pathways are similar for At2CPA and PptAPx, it can be concluded that PptAPx is two-fold redox regulated. Firstly, its expression may correlate with the NADPH/$NADP^+$ ratio. Secondly, it might be influenced by the redox regulation of the ABA pathway through ascorbate. These two might represent the primary regulation of PptAPx, since the regulation by ascorbate is dominated by the ABA influence. Secondary regulation may be triggered by the availability of low molecular weight antioxidants or the accumulation of hydrogen peroxide. This is in contrast to the response to excess light, which causes an up-regulation of the PptAPx transcript level. In this case, the suggested secondary regulatory pathways might dominate ABA signaling.

Like in *Arabidopsis* (Ishitani *et al.*1997), the results obtained for *Physcomitrella* may hint to a crosstalk of ABA-dependent and -independent regulatory pathways. Taken all together, it can be possible that the regulation by this phytohormone is similar in *Arabidopsis* and *Physcomitrella*.

After the retrotransposition event and loss of the original gene, *Physcomitrella* was forced to re-integrate its single chloroplast ascorbate peroxidase into its metabolism. A high but fine-tuned regulated expression was (re-)established. This suggests that a high evolutionary pressure was put on the moss and stresses the importance of PptAPx for the fitness of *Physcomitrella* to ensure its survival through times.

5 Summary

Plants evolved and became photosynthetically active due to the endosymbiosis of a cyanobacterium into a eukaryotic cell. By-products of the oxygenic process are cytotoxic reactive oxygen species (ROS), such as superoxide anions, hydrogen peroxide, and hydroxyl radicals. These compounds can cause severe damage by oxidation of lipids, proteins, and DNA. Within chloroplasts, ascorbate peroxidases (APxs), peroxiredoxins (Prxs), and glutathione peroxidases (GPxs) serve as peroxide scavengers. The present study focused on these enzyme families in distantly related plant species. Genomes of the lycophyte *Selaginella moellendorffii*, the moss *Physcomitrella patens*, the green alga *Chlamydomonas reinhardtii*, and the model seed plant *Arabidopsis thaliana* were analyzed for their chloroplast peroxidase genes.

The *Arabidopsis* genome encodes one stromal (sAPx) and one thylakoid-bound APx (tAPx), two 2-Cys peroxiredoxins (2CPs), one peroxiredoxin Q (PrxQ), one peroxiredoxin type II (PrxII), and two GPxs. It was found that *Selaginella* chloroplasts have the same set of peroxidases with the addition of another PrxQ and another GPx. *Physcomitrella*, in contrast, revealed to encode no stromal APx and, maybe to balance this lack, multiplied its genes for other soluble chloroplast peroxidases. It shows two 2CPs, two PrxQs, three PrxIIs, and three GPxs. Within the *Chlamydomonas* genome, two genes for sAPxs, three for 2CPs, one for a PrxQ, one for a PrxII, and three for GPxs were identified. These results show that the composition of the chloroplast antioxidant defense changed during plant evolution. The three types of peroxidases were found in all included species indicating a strong pressure on their maintenance to ensure appropriate fitness and survival of their hosts during time.

EST data suggested that 2CPs are the strongest expressed chloroplast antioxidant enzymes in *Chlamydomonas*, *Selaginella*, and *Arabidopsis*. *Physcomitrella*, in contrast, showed a strong transcription of its thylakoid-bound APx (PptAPx). Its atypical gene structure and surrounding within the genome indicated a retrotransposonal origin. After integration of PptAPx into the genome, its expressional regulation was established. The transcription is initiated at two different sites and revealed to be influenced by light intensity, temperature, low molecular weight antioxidants, and the phytohormone abscisic acid. Apart from this, the chloroplast targeting of PptAPx was verified and its functionality indicated. Since *Physcomitrella* maintained this tAPx and established its fine-tuned regulation, it is suggested that the enzyme is of essential importance for its survival during times. In addition, parallels in targeting and transcription initiation of *Physcomitrella* and higher plants were unraveled.

6 Zusammenfassung

Die Endosymbiose eines Cyanobacteriums durch eine eukaryotische Zelle führte zur Entstehung von Pflanzen und deren photosynthetischer Aktivität. Reaktive Sauerstoffspezies (engl. Reactive Oxygen Species, ROS), wie Superoxidanionen, Wasserstoffperoxid und Hydroxylradikale, sind Nebenprodukte dieses Sauerstoff produzierenden Prozesses. Diese Stoffe können durch Oxidation von Lipiden, Proteinen und DNA schwere Schäden verursachen. In Chloroplasten fungieren Ascorbatperoxidasen (APxs), Peroxiredoxine (Prxs) und Glutathionperoxidasen (GPxs) als Peroxidfänger. Die vorliegende Studie fokussiert auf diese Enzymgruppen. Sie behandelt ihr Vorkommen in verschiedenen pflanzlichen Entwicklungsstufen. Die Genome der Modellsamenpflanze *Arabidopsis thaliana*, des Lycophyten *Selaginella moellendorffii*, des Laubmooses *Physcomitrella patens* und der Grünalge *Chlamydomonas reinhardtii* wurden bezüglich der für chloroplastidäre Peroxidasen kodierenden Gene analysiert.

Das *Arabidopsis* Genom enthält ein Gen für eine stromale (sAPx) und eins für eine an Thylakoiden gebundene APx (tAPx). Zusätzlich sind zwei 2-Cys Peroxiredoxine (2CPs), ein Peroxiredoxin Q (PrxQ), ein Peroxiredoxin Typ II (PrxII) und zwei GPxs vorhanden. Diese Arbeit zeigt, dass *Selaginella* Chloroplasten das gleiche Set an Peroxidasen mit dem Zusatz einer weiteren PrxQ und einer GPx enthalten. Im *Physcomitrella* Genom jedoch, ist keine sAPx kodiert während Gene für andere chloroplastidäre Peroxidasen vervielfacht wurden. Das Vorhandensein zweier 2CPs, zweier PrxQs, dreier PrxIIs und dreier GPxs könnte einen Versuch darstellen, das Fehlen der sAPx auszugleichen. In dem Genom von *Chlamydomonas* konnten zwei Gene kodierend für sAPxs, drei für 2CPs, eines für PrxQ, eines für PrxII und drei für GPxs identifiziert werden. Diese Resultate zeigen, dass die Zusammensetzung des chloroplastidären antioxidativen Schutzes während der Pflanzenevolution starke Veränderungen erfuhr. Alle drei Peroxidasetypen waren in den untersuchten Pflanzenarten vertreten, was einen starken evolutionären Druck bezüglich ihres Erhalts erkennen lässt. Diese Enzyme sind essentiell, um eine ausreichende Fitness und damit das Überleben der Pflanzen über die Zeiten zu gewährleisten.

EST-Daten wiesen darauf hin, dass 2CPs die am stärksten exprimierten chloroplastidären antioxidativen Enzyme in *Chlamydomonas*, *Selaginella* und *Arabidopsis* sind. Im Gegensatz dazu zeigte *Physcomitrella* eine starke Transkription der tAPx (PptAPx). Die atypische Struktur des kodierenden Gens und dessen Umgebung im Genom ließen auf einen retrotransposonalen Ursprung schließen. Eine expressionale Regulation wurde im Anschluss

an die Integration von PptAPx ins Genom etabliert. Die Transkription wird an zwei unterschiedlichen Stellen initiiert und zeigte sich beeinflusst von Lichtintensität, Temperatur, niedermolekularen Antioxidantien und dem Phytohormon Abszisinsäure. Ferner wurde die Chloroplastenlokalisation von PptAPx nachgewiesen und die Funktionalität des Enzyms untersucht. Diese tAPx blieb in *Physcomitrella* erhalten und eine feinabgestimmte expressionale Regulation etabliert. Dies deutet darauf hin, dass das Enzym von wesentlicher Bedeutung für das Überleben des Laubmooses ist. Zusätzlich wurden im Zuge der Arbeiten für die vorliegende Studie Parallelen in der transkriptionellen Initiation und in der Proteinlokalisationsmaschinerie zwischen *Physcomitrella* und höheren Pflanzen aufgezeigt.

7 List of references

Ahmadinejad N (2008) Evolution of eukaryotic introns following endosymbiotic gene transfer. PhD Thesis

Alscher RG (1989) Biosynthesis and antioxidant function of glutathione in plants. Physiologia Plantarum **77:** 457-464

Altschul SF, Madden TL, Schaffer AA, Zhang JH, Zhang Z, Miller W, Lipman DJ (1997) Gapped BLAST and PSI-BLAST: a new generation of protein database search programs. Nucleic Acids Research **25:** 3389-3402

Arabidopsis Genome Inititiative (2000) Analysis of the genome sequence of the flowering plant *Arabidopsis thaliana*.
Nature **408:** 796-815

Arnold K, Bordoli L, Kopp J, Schwede T (2006) The SWISS-MODEL workspace: a web-based environment for protein structure homology modeling. Bioinformatics, Oxford University Press **22:** 195-201

Asada K (1992) Ascorbate Peroxidase - a hydrogen peroxide-scavenging enzyme in plants. Physiologia Plantarum **85:** 235-241

Asada K (1999) The water-water cycle in chloroplasts: Scavenging of active oxygens and dissipation of excess photons. Annual Review of Plant Physiology and Plant Molecular Biology **50:** 601-639

Asada K, Kiso K, Yoshikaw.K (1974) Univalent reduction of molecular oxygen by spinach chloroplasts on illumination. Journal of Biological Chemistry **249:** 2175-2181

Asada K, Urano M, Takahash.M (1973) Subcellular location of superoxide dismutase in spinach leaves and preparation and properties of crystalline spinach superoxide dismutase. European Journal of Biochemistry **36:** 257-266

Babbs CF, Pham JA, Coolbaugh RC (1989) Lethal hydroxyl radical production in paraquat-treated plants. Plant Physiology **90:** 1267-1270

Baier M, Dietz K-J (1999) The costs and benefits of oxygen for photosynthesizing plant cells. Progress in Botany **60, Springer Verlag Berlin Heidelberg:** 281-314

Baier M, Dietz KJ (1996) Primary structure and expression of plant homologues of animal and fungal thioredoxin-dependent peroxide reductases and bacterial alkyl hydroperoxide reductases. Plant Molecular Biology **31:** 553-564

Baier M, Dietz KJ (1997) The plant 2-Cys peroxiredoxin BAS1 is a nuclear-encoded chloroplast protein: its expressional regulation, phylogenetic origin, and implications for its specific physiological function in plants. Plant Journal **12:** 179-190

Baier M, Noctor G, Foyer CH, Dietz KJ (2000) Antisense suppression of 2-cysteine peroxiredoxin in *Arabidopsis* specifically enhances the activities and expression of enzymes associated with ascorbate metabolism but not glutathione metabolism. Plant Physiology **124:** 823-832

Baier M, Stroher E, Dietz KJ (2004) The acceptor availability at photosystem I and ABA control nuclear expression of 2-cys peroxiredoxin-alpha in *Arabidopsis thaliana*. Plant and Cell Physiology **45:** 997-1006

Ball L, Accotto GP, Bechtold U, Creissen G, Funck D, Jimenez A, Kular B, Leyland N, Mejia-Carranza J, Reynolds H, Karpinski S, Mullineaux PM (2004) Evidence for a direct link between glutathione biosynthesis and stress defense gene expression in *Arabidopsis*. Plant Cell **16:** 2448-2462

Banks JA (2009) *Selaginella* and 400 million years of separation. Annual Review of Plant Biology **60:** 223-238

Banks JA, Nishiyama T, Hasebe M, Bowman JL, Gribskov M, dePamphilis C, Albert VA, Aono N, Aoyama T, Ambrose BA, Ashton NW, Axtell MJ, Barker E, Barker MS, Bennetzen JL, Bonawitz ND, Chapple C, Cheng CY, Correa LGG, Dacre M, DeBarry J, Dreyer I, Elias M, Engstrom EM, Estelle M, Feng L, Finet C, Floyd SK, Frommer WB, Fujita T, Gramzow L, Gutensohn M, Harholt J, Hattori M, Heyl A, Hirai T, Hiwatashi Y, Ishikawa M, Iwata M, Karol KG, Koehler B, Kolukisaoglu U, Kubo M, Kurata T, Lalonde S, Li KJ, Li Y, Litt A, Lyons E, Manning G, Maruyama T, Michael TP, Mikami K, Miyazaki S, Morinaga S, Murata T, Mueller-Roeber B, Nelson DR, Obara M, Oguri Y, Olmstead RG, Onodera N, Petersen BL, Pils B, Prigge M, Rensing SA, Riano-Pachon DM, Roberts AW, Sato Y, Scheller HV, Schulz B, Schulz C, Shakirov EV, Shibagaki N, Shinohara N, Shippen DE, Sorensen I, Sotooka R, Sugimoto N, Sugita M, Sumikawa N, Tanurdzic M, Theissen G, Ulvskov P, Wakazuki S, Weng JK, Willats WWGT, Wipf D, Wolf PG, Yang LX, Zimmer AD, Zhu QH, Mitros T, Hellsten U, Loque D, Otillar R, Salamov A, Schmutz J, Shapiro H, Lindquist E, Lucas S, Rokhsar D, Grigoriev IV (2011) The *Selaginella* Genome Identifies Genetic Changes Associated with the Evolution of Vascular Plants. Science **332:** 960-963

Bechtold N, Ellis J, Pelletier G (1993) *In-planta Agrobacterium*-mediated gene-transfer by infiltration of adult *Arabidopsis thaliana* plants. Comptes Rendus De L Academie Des Sciences Serie Iii-Sciences De La Vie-Life Sciences **316:** 1194-1199

Bennet MD, Leitch IJ, Price HJ, Johnston JS (2003) Comparisons with *Caenorhabditis* (~100 Mb) and *Drosophila* (~175 Mb) using flow cytometry show genome size in *Arabidopsis* to be ~157 Mb and thus ~25 % larger than the *Arabidopsis* genome initiative estimate of ~125 Mb. Annals of Botany **91:** 547-557

Bielski BHJ, Allen AO, Schwarz HA (1981) Mechanism of disproportionation of ascorbate radicals. Journal of the American Chemical Society **103:** 3516-3518

Blokhina O, Virolainen E, Fagerstedt KV (2003) Antioxidants, oxidative damage and oxygen deprivation stress: a review. Annals of Botany **91:** 179-194

Blokhina OB, Chirkova TV, Fagerstedt KV (2001) Anoxic stress leads to hydrogen peroxide formation in plant cells. Journal of Experimental Botany **52:** 1179-1190

Bopp M, Brandes H (1964) Versuche zur Analyse der Protonemaentwicklung der Laubmoose. II. Über den Zusammenhang zwischen Protonemadifferenzierung und Kinetinwirkung bei der Bildung von Moosknospen. Planta **62:** 116-136

Bowler C, Slooten L, Vandenbranden S, Derycke R, Botterman J, Sybesma C, Vanmontagu M, Inze D (1991) Manganese superoxide dismutase can reduce cellular damage mediated by oxygen radicals in transgenic plants. EMBO Journal **10:** 1723-1732

Brehelin C, Meyer EH, de Souris JP, Bonnard G, Meyer Y (2003) Resemblance and dissemblance of *Arabidopsis* type II peroxiredoxins: Similar sequences for divergent gene expression, protein localization, and activity. Plant Physiology **132:** 2045-2057

Bruce BD (2000) Chloroplast transit peptides: structure, function and evolution. Trends in Cell Biology **10:** 440-447

Burns JJ (1957) Missing step in man, monkey and guinea pig required for the biosynthesis of L-ascorbic acid. Nature **180:** 552-552

Bustin SA, Benes V, Garson JA, Hellemans J, Huggett J, Kubista M, Mueller R, Nolan T, Pfaffl MW, Shipley GL, Vandesompele J, Wittwer CT (2009) The MIQE guidelines: minimum information for publication of quantitative real-time PCR experiments. Clinical Chemistry **55:** 611-622

Chae HZ, Chung SJ, Rhee SG (1994) Thioredoxin-dependent peroxide reductase from yeast. Journal of Biological Chemistry **269:** 27670-27678

Chang CCC, Slesak I, Jorda L, Sotnikov A, Melzer M, Miszalski Z, Mullineaux PM, Parker JE, Karpinska B, Karpinski S (2009) *Arabidopsis* chloroplastic glutathione peroxidases play a role in cross talk between photooxidative stress and immune responses. Plant Physiology **150:** 670-683

Chew O, Whelan J, Millar AH (2003) Molecular definition of the ascorbate-glutathione cycle in *Arabidopsis* mitochondria reveals dual targeting of antioxidant defenses in plants. Journal of Biological Chemistry **278:** 46869-46877

Cogdell RJ (1985) Carotenoids in photosynthesis. Pure and Applied Chemistry **57:** 723-728

Conklin PL, Pallanca JE, Last RL, Smirnoff N (1997) L-ascorbic acid metabolism in the ascorbate-deficient *Arabidopsis* mutant *vtc1*. Plant Physiology **115:** 1277-1285

Conklin PL, Williams EH, Last RL (1996) Environmental stress sensitivity of an ascorbic acid-deficient *Arabidopsis* mutant. Proceedings of the National Academy of Sciences of the United States of America **93:** 9970-9974

Cove DJ, Knight CD (1993) The moss *Physcomitrella patens*, a model system with potential for the study of plant reproduction. Plant Cell **5:** 1483-1488

Crook EM, Hopkins FG (1938) CLXXX. Further observations on the system ascorbic acid-glutathione-ascorbic aicd-oxidase. Biochemical Journal **32:** 1356-1363

Crook EM, Morgan EJ (1943) The reduction of dehydroascorbic acid in plant extracts. Biochemical Journal **38:** 10-15

Curtis MD, Grossniklaus U (2003) A gateway cloning vector set for high-throughput functional analysis of genes *in planta*. Plant Physiology **133:** 462-469

Danna CH, Bartoli CG, Sacco F, Ingala LR, Santa-Maria GE, Guiamet JJ, Ugalde RA (2003) Thylakoid-bound ascorbate peroxidase mutant exhibits impaired electron transport and photosynthetic activity. Plant Physiology **132:** 2116-2125

Davletova S, Schlauch K, Coutu J, Mittler R (2005) The zinc-finger protein Zat12 plays a central role in reactive oxygen and abiotic stress signaling in *Arabidopsis*. Plant Physiology **139:** 847-856

Dayer R, Fischert BB, Eggen RIL, Lemaire SD (2008) The peroxiredoxin and glutathione peroxidase families in *Chlamydomonas reinhardtii*. Genetics **179:** 41-57

Demming B, Winter K, Krüger A, F.-C. C (1987) Photoinhibition and zeaxanthin formation in intact leaves. Plant Physiology **84:** 218-224

Desikan R, Mackerness SAH, Hancock JT, Neill SJ (2001) Regulation of the *Arabidopsis* transcriptome by oxidative stress. Plant Physiology **127:** 159-172

Deutsch M, Long M (1999) Intron-exon structures of eukaryotic model organisms. Nucleic Acids Research **27:** 3219-3228

Dietz K-J (2006) The function of peroxiredoxins in plant organelle redox metabolism. Journal of Experimental Botany **57:** 1697-1709

Dietz KJ (2011) Peroxiredoxins in Plants and Cyanobacteria. Antioxidants & Redox Signaling **15:** 1129-1159

Dietz KJ, Heber U (1984) Rate-Limiting Factors in Leaf Photosynthesis. 1. Carbon Fluxes in the Calvin Cycle. Biochimica Et Biophysica Acta **767:** 432-443

Edgar RC (2004) MUSCLE: multiple sequence alignment with high accuracy and high throughput. Nucleic Acids Research **32:** 1792-1797

Elstner E (1990) Der Sauerstoff: Biochemie, Biologie, Medizin. BI-Wiss.-Verlag Mannheim, Wien, Zürich

Emanuelsson O, Nielsen H, Brunak S, von Heijne G (2000) Predicting subcellular localization of proteins based on their N-terminal amino acid sequence. Journal of Molecular Biology **300:** 1005-1016

Eshdat Y, Holland D, Faltin Z, BenHayyim G (1997) Plant glutathione peroxidases. Physiologia Plantarum **100:** 234-240

Eskling M, Arvidsson PO, Akerlund HE (1997) The xanthophyll cycle, its regulation and components. Physiologia Plantarum **100:** 806-816

Fenton HJH (1894) LXXIII. Oxidation of tartaric acid in presence of iron. Journal of the Chemical Society, Transactions **65:** 899-910

Feys BJ, Wiermer M, Bhat RA, Moisan LJ, Medina-Escobar N, Neu C, Cabral A, Parker JE (2005) *Arabidopsis* SENESCENCE-ASSOCIATED GENE101 stabilizes and signals within an ENHANCED DISEASE SUSCEPTIBILITY1 complex in plant innate immunity. Plant Cell **17:** 2601-2613

Flint DH, Tuminello JF, Emptage MH (1993) The inactivation of Fe-S cluster containing hydro-lyases by superoxide. Journal of Biological Chemistry **268:** 22369-22376

Foyer CH, Halliwell B (1976) Presence of glutathione and glutathione reductase in chloroplasts – proposed role in ascorbic-acid metabolism. Planta **133:** 21-25

Foyer CH, Halliwell B (1977) Purification and properties of dehydroascorbate reductase from spinach leaves. Phytochemistry **16:** 1347-1350

Foyer CH, Lelandais M (1996) A comparison of the relative rates of transport of ascorbate and glucose across the thylakoid, chloroplast and plasmalemma membranes of pea leaf mesophyll cells. Journal of Plant Physiology **148:** 391-398

Foyer CH, Lelandais M, Kunert KJ (1994) Photooxidative Stress in Plants. Physiologia Plantarum **92:** 696-717

Frahm J-P (2001) Biologie der Moose. Spektrum Akademischer Verlag GmbH Heidelberg-Berlin **1st volume**

Frahm J-P, Frey W (2004) Moosflora. Verlag Eugen Ulmer Stuttgart **4th volume**

Frank W, Decker EL, Reski R (2005) Molecular tools to study *Physcomitrella patens*. Plant Biology **7:** 220-227

Frey HD, Langer E, Wagner G, Weigner C (1988) Bau und Funktion der Pflanzen. Deutsches Institut für Fernstudien an der Universität Tübingen **2nd volume**

Fryer MJ (1992) The antioxidant effects of thylakoid vitamin-E(α-tocopherol). Plant Cell and Environment **15:** 381-392

Fu LH, Wang XF, Eyal Y, She YM, Donald LJ, Standing KG, Ben-Hayyim G (2002) A selenoprotein in the plant kingdom. Mass spectrometry confirms that an opal codon (UGA) encodes selenocysteine in *Chlamydomonas reinhardtii* glutathione peroxidase. Journal of Biological Chemistry **277:** 25983-25991

Fujii T, Yokoyama E, Inoue K, Sakurai H (1990) The sites of electron donation of Photosystem I to methylviologen. Biochimica Et Biophysica Acta **1015:** 41-48

Galvez-Valdivieso G, Fryer MJ, Lawson T, Slattery K, Truman W, Smirnoff N, Asami T, Davies WJ, Jones AM, Baker NR, Mullineaux PM (2009) The high light response in *Arabidopsis* involves ABA signaling between vascular and bundle sheath cells. Plant Cell **21:** 2143-2162

Ganapathiraju M, Balakrishnan N, Reddy R, Klein-Seetharaman J (2008) Transmembrane helix prediction using amino acid property features and latent semantic analysis. BMC Bioinformatics **9**

Giacomelli L, Masi A, Ripoll DR, Lee MJ, van Wijk KJ (2007) *Arabidopsis thaliana* deficient in two chloroplast ascorbate peroxidases shows accelerated light-induced necrosis when levels of cellular ascorbate are low. Plant Molecular Biology **65:** 627-644

Gorman AA, Rodgers MAJ (1992) Current perspectives of singlet oxygen detection in biological environments. Journal of Photochemistry and Photobiology B-Biology **14:** 159-176

Gorman DS, Levine RP (1965) Cytochrome F and plastocyanin - their sequence in photosynthetic electron transport chain of *Chlamydomonas reinhardtii*. Proceedings of the National Academy of Sciences of the United States of America **54:** 1665-&

Groden D, Beck E (1979) H_2O_2 Destruction by ascorbate-dependent systems from chloroplasts. Biochimica Et Biophysica Acta **546:** 426-435

Guex N, Peitsch MC (1997) SWISS-MODEL and the Swiss-PdbViewer: an environment for comparative protein modeling. Electrophoresis **18:** 2714-2723

Haber F, Weiss J (1932) Über die Katalyse des Hydroperoxides. Die Naturwissenschaften **51:** 948-950

Häflinger TJ, Wolf M (1988) Dicot weeds part 1. Documenta, CIBA-GEIGY Ltd.

Hager A (1969) Lichtbedingte pH-Erniedrigung in einem Chloroplasten-Kompartiment als Ursache der enzymatischen Violaxanthin- → Zeaxanthin-Umwandlung; Beziehungen zur Photophosphorylierung. Planta **89:** 224-243

Halliwell B (2006) Reactive species and antioxidants. Redox biology is a fundamental theme of aerobic life. Plant Physiology **141:** 312-322

Harris EH (2001) *Chlamydomonas* as a model organism. Annual Review of Plant Physiology and Plant Molecular Biology **52:** 363-406

Heiber I, Stroher E, Raatz B, Busse I, Kahmann U, Bevan MW, Dietz KJ, Baier M (2007) The redox imbalanced mutants of *Arabidopsis* differentiate signaling pathways for redox regulation of chloroplast antioxidant enzymes. Plant Physiology **143:** 1774-1788

Hill R (1939) Oxygen produced by isolated chloroplasts. Proceedings of the Royal Society of London. Series B, Biological Sciences **127:** 192-210

Hoffmann MH (2002) Biogeography of *Arabidopsis thaliana* (L.) Heynh. (Brassicaceae). Journal of Biogeography **29:** 125-134

Hohe A, Egener T, Lucht JM, Holtorf H, Reinhard C, Schween G, Reski R (2004) An improved and highly standardised transformation procedure allows efficient production of single and multiple targeted gene-knockouts in a moss, *Physcomitrella patens*. Current Genetics **44:** 339-347

Hohe A, Reski R (2003) A tool for understanding homologous recombination in plants. Plant Cell Reports **21:** 1135-1142

Horling F, Baier M, Dietz KJ (2001) Redox-regulation of the expression of the peroxide-detoxifying chloroplast 2-Cys peroxiredoxin in the liverwort *Riccia fluitans*. Planta **214:** 304-313

Horling F, Konig J, Dietz KJ (2002) Type II peroxiredoxin C, a member of the peroxiredoxin family of *Arabidopsis thaliana*: its expression and activity in comparison with other peroxiredoxins. Plant Physiology and Biochemistry **40:** 491-499

Horling F, Lamkemeyer P, Konig J, Finkemeier I, Kandlbinder A, Baier M, Dietz KJ (2003) Divergent light-, ascorbate-, and oxidative stress-dependent regulation of expression of the peroxiredoxin gene family in *Arabidopsis*. Plant Physiology **131:** 317-325

Hossain MA, Nakano Y, Asada K (1984) Monodehydroascorbate reductase in spinach chloroplasts and its participation in regeneration of ascorbate for scavenging hydrogen peroxide. Plant and Cell Physiology **25:** 385-395

Hu WH, Song XS, Shi K, Xia XJ, Zhou YH, Yu JQ (2008) Changes in electron transport, superoxide dismutase and ascorbate peroxidase isoenzymes in chloroplasts and mitochondria of cucumber leaves as influenced by chilling. Photosynthetica **46:** 581-588

Ishikawa T, Sakai K, Yoshimura K, Takeda T, Shigeoka S (1996) cDNAs encoding spinach stromal and thylakoid-bound ascorbate peroxidase, differing in the presence or absence of their 3'-coding regions. FEBS Letters **384:** 289-293

Ishikawa T, Shigeoka S (2008) Recent advances in ascorbate biosynthesis and the physiological significance of ascorbate peroxidase in photosynthesizing organisms. Bioscience Biotechnology and Biochemistry **72:** 1143-1154

Ishitani M, Xiong LM, Stevenson B, Zhu JK (1997) Genetic analysis of osmotic and cold stress signal transduction in *Arabidopsis*: Interactions and convergence of abscisic acid-dependent and abscisic acid-independent pathways. Plant Cell **9:** 1935-1949

Jahnke LS, Hull MR, Long SP (1991) Chilling stress and oxygen metabolizing enzymes in *Zea mays* and *Zea diploperennis*. Plant Cell and Environment **14:** 97-104

James HE, Bartling D, Musgrove JE, Kirwin PM, Herrmann RG, Robinson C (1989) Transport of proteins into chloroplasts - import and maturation of precursors to the 33-Kda, 23-Kda, and 16-Kda proteins of the photosynthetic oxygen-evolving complex. Journal of Biological Chemistry **264:** 19573-19576

Jespersen HM, Kjaersgard IVH, Ostergaard L, Welinder KG (1997) From sequence analysis of three novel ascorbate peroxidases from *Arabidopsis thaliana* to structure, function and evolution of seven types of ascorbate peroxidase. Biochemical Journal **326:** 305-310

Jiang MY, Zhang JH (2001) Effect of abscisic acid on active oxygen species, antioxidative defence system and oxidative damage in leaves of maize seedlings. Plant and Cell Physiology **42:** 1265-1273

Jönsson TJ, Johnson LC, Lowther WT (2008) Structure of the sulphiredoxinperoxiredoxin complex reveals an essential repair embrace. Nature **451:** 98-101

Kanematsu S, Asada K (1990) Characteristic amino-acid-sequences of chloroplast and cytosol isozymes of CuZn-superoxide dismutase in spinach, rice and horsetail. Plant and Cell Physiology **31:** 99-112

Kangasjärvi S, Lepistö A, Hännikäinen K, Piippo M, Luomala EM, Aro EM, Rintamäki E (2008) Diverse roles for chloroplast stromal and thylakoidbound ascorbate peroxidases in plant stress responses. Biochemical Journal **412:** 275-285

Karimi M, De Meyer B, Hilson P (2005) Modular cloning in plant cells. Trends in Plant Science **10:** 103-105

Karimi M, Inze D, Depicker A (2002) GATEWAY((TM)) vectors for *Agrobacterium*-mediated plant transformation. Trends in Plant Science **7:** 193-195

Karlin-Neumann GA, Tobin EM (1986) Transit peptides of nuclear-encoded chloroplast proteins share a common amino-acid framework. EMBO Journal **5:** 9-13

Karpinski S, Escobar C, Karpinska B, Creissen G, Mullineaux PM (1997) Photosynthetic electron transport regulates the expression of cytosolic ascorbate peroxidase genes in *Arabidopsis* during excess light stress. Plant Cell **9:** 627-640

Kiddle G, Pastori GM, Bernard S, Pignocchi C, Antoniw J, Verrier PJ, Foyer CH (2003) Effects of leaf ascorbate content on defense and photosynthesis gene expression in *Arabidopsis thaliana*. Antioxidants & Redox Signaling **5:** 23-32

Kitajima S (2008) Hydrogen peroxide-mediated inactivation of two chloroplastic peroxidases, ascorbate peroxidase and 2-Cys peroxiredoxin. Photochemistry and Photobiology **84:** 1404-1409

Kitajima S, Kurioka M, Yoshimoto T, Shindo M, Kanaori K, Tajima K, Oda K (2008) A cysteine residue near the propionate side chain of heme is the radical site in ascorbate peroxidase. FEBS Journal **275:** 470-480

Kitajima S, Shimaoka T, Kurioka M, Yokota A (2007) Irreversible cross-linking of heme to the distal tryptophan of stromal ascorbate peroxidase in response to rapid inactivation by H_2O_2. FEBS Journal **274:** 3013-3020

Kitajima S, Tomizawa K, Shigeoka S, Yokota A (2006) An inserted loop region of stromal ascorbate peroxidase is involved in its hydrogen peroxide-mediated inactivation. FEBS Journal **273:** 2704-2710

Knight CD, Sehgal A, Atwal K, Wallace JC, Cove DJ, Coates D, Quatrano RS, Bahadur S, Stockley PG, Cuming AC (1995) Molecular responses to abscisic-acid and stress are conserved between moss and cereals. Plant Cell **7:** 499-506

Koch E (1968) Zur photosensibilisierten Sauerstoffübertragung. Tetrahedron **24:** 6295-6318

Koncz C, Schell J (1986) The promoter of Tl-DNA gene 5 controls the tissue-specific expression of chimeric genes carried by a novel type of *Agrobacterium* binary vector. Molecular & General Genetics **204:** 383-396

Kong W, Shiota S, Shi YX, Nakayama H, Nakayama K (2000) A novel peroxiredoxin of the plant *Sedum lineare* is a homologue of *Escherichia coli* bacterioferritin co-migratory protein (Bcp). Biochemical Journal **351:** 107-114

König J, Baier M, Horling F, Kahmann U, Harris G, Schürmann P, K.-J. D (2002) The plant-specific function of 2-Cys peroxiredoxin-mediated detoxification of peroxides in the redox-hierarchy of photosynthetic electron flux. PNAS **99:** 5738-5743

König J, Lotte K, Plessow R, Brockhinke A, Baier M, Dietz K-J (2003) Reaction mechanism of plant 2-Cys peroxiredoxin. The Journal of Biological Chemistry **278:** 24409-24420

Krieger-Lizskay A (2005) Singlet oxygen production in photosynthesis. Journal of Experimental Botany **56:** 337-346

Krogh A, Larsson B, von Heijne G, Sonnhammer ELL (2001) Predicting transmembrane protein topology with a hidden Markov model: Application to complete genomes. Journal of Molecular Biology **305:** 567-580

Lamppa GK (1988) The chlorophyll a/b-binding protein inserts into the thylakoids independent of its cognate transit peptide. Journal of Biological Chemistry **263:** 14996-14999

Larkin MA, Blackshields G, Brown NP, Chenna R, McGettigan PA, McWilliam H, Valentin F, Wallace IM, Wilm A, Lopez R, Thompson JD, Gibson TJ, Higgins DG (2007) Clustal W and clustal X version 2.0. Bioinformatics **23:** 2947-2948

Larson RA (1988) The antioxidants of higher plants. Phytochemistry **27:** 969-978

Law MY, Halliwell B (1986) Purification and properties of glutathione synthetase from spinach (*Spinacia oleracea*) Leaves. Plant Science **43:** 185-191

Laxa M, Konig J, Dietz KJ, Kandlbinder A (2007) Role of the cysteine residues in *Arabidopsis thaliana* cyclophilin CYP20-3 in peptidyl-prolyl cis-trans isomerase and redox-related functions. Biochemical Journal **401:** 287-297

Leung J, Giraudat J (1998) Abscisic acid signal transduction. Annual Review of Plant Physiology and Plant Molecular Biology **49:** 199-222

Li LH, Yang J, Qiu HL, Liu YY (2010) Genetic transformation of *Physcomitrella patens* mediated by *Agrobacterium tumefaciens*. African Journal of Biotechnology **9:** 3719-3725

Liso R, Innocenti AM, Bitonti MB, Arrigoni O (1988) Ascorbic acid-induced progression of quiescent center cells from G1-phase to S-phase. New Phytologist **110:** 469-471

Livak KJ, Schmittgen TD (2001) Analysis of relative gene expression data using real-time quantitative PCR and the $2^{-\Delta\Delta CT}$method. Methods **25:** 402-408

Loganantharaj R (2006) On discriminating a TATA-box from putative TATA boxes: A case study using plant genome. Computational Systems Bioinformatics Conference, 2005. Workshops and Poster Abstracts. IEEE

Lopez-Huertas E, Corpas FJ, Sandalio LM, Del Rio LA (1999) Characterization of membrane polypeptides from pea leaf peroxisomes involved in superoxide radical generation. Biochemical Journal **337:** 531-536

Lunde C, Drew DP, Jacobs AK, Tester M (2007) Exclusion of Na^+ via sodium ATPase (PpENA1) ensures normal growth of *Physcomitrella patens* under moderate salt stress. Plant Physiology **144:** 1786-1796

Mano J, Ohno C, Domae Y, Asada K (2001) Chloroplastic ascorbate peroxidase is the primary target of methylviologen-induced photooxidative stress in spinach leaves: its relevance to monodehydroascorbate radical detected with in vivo ESR. Biochimica Et Biophysica Acta-Bioenergetics **1504:** 275-287

Mano S, Yamaguchi K, Hayashi M, Nishimura M (1997) Stromal and thylakoid-bound ascorbate peroxidases are produced by alternative splicing in pumpkin. FEBS Letters **413:** 21-26

Mapson LW (1958) Metabolism of ascorbic acid in plants. 1. Function. Annual Review of Plant Physiology and Plant Molecular Biology **9:** 119-150

Margis R, Dunand C, Teixeira FK, Margis-Pinheiro M (2008) Glutathione peroxidase family - an evolutionary overview. FEBS Journal **275:** 3959-3970

Maruta T, Tanouchi A, Tamoi M, Yabuta Y, Yoshimura K, Ishikawa T, Shigeoka S (2010) *Arabidopsis* chloroplastic ascorbate peroxidase isoenzymes play a dual role in photoprotection and gene regulation under photooxidative stress. Plant and Cell Physiology **51:** 190-200

May MJ, Leaver CJ (1994) *Arabidopsis thaliana* γ-glutamylcysteine synthetase is structurally unrelated to mammalian, yeast, and *Escherichia coli* homologs. Proceedings of the National Academy of Sciences of the United States of America **91:** 10059-10063

McCord JM, Fridovic.I (1969) Superoxide dismutase an enzymic function for erythrocuprein (hemocuprein). Journal of Biological Chemistry **244:** 6049-&

McKersie BD, Murnaghan J, Jones KS, Bowley SR (2000) Iron-superoxide dismutase expression in transgenic alfalfa increases winter survival without a detectable increase in photosynthetic oxidative stress tolerance. Plant Physiology **122:** 1427-1437

Meadows JW, Robinson C (1991) The full precursor of the 33 kDa oxygen-evolving complex protein of wheat is exported by *Escherichia coli* and processed to the mature size. Plant Molecular Biology **17:** 1241-1243

Mehler AH (1951) Studies on reactions of illuminated chloroplasts. 2. Stimulation and inhibition of the reaction with molecular oxygen. Archives of Biochemistry and Biophysics **34:** 339-351

Mehler AH, Brown AH (1952) Studies on reactions of illuminated Chloroplasts. 3. Simultaneous photoproduction and consumption of oxygen studied with oxygen isotopes. Archives of Biochemistry and Biophysics **38:** 365-370

Meinke DW, Cherry JM, Dean C, Rounsley SD, Koornneef M (1998) *Arabidopsis thaliana*: A model plant for genome analysis. Science **282:** 662

Merchant SS, Prochnik SE, Vallon O, Harris EH, Karpowicz SJ, Witman GB, Terry A, Salamov A, Fritz-Laylin LK, Marechal-Drouard L, Marshall WF, Qu LH, Nelson DR, Sanderfoot AA, Spalding MH, Kapitonov VV, Ren QH, Ferris P, Lindquist E, Shapiro H, Lucas SM, Grimwood J, Schmutz J, Cardol P, Cerutti H, Chanfreau G, Chen CL, Cognat V, Croft MT, Dent R, Dutcher S, Fernandez E, Fukuzawa H, Gonzalez-Ballester D, Gonzalez-Halphen D, Hallmann A, Hanikenne M, Hippler M, Inwood W, Jabbari K, Kalanon M, Kuras R, Lefebvre PA, Lemaire SD, Lobanov AV, Lohr M, Manuell A, Meir I, Mets L, Mittag M, Mittelmeier T, Moroney JV, Moseley J, Napoli C, Nedelcu AM, Niyogi K, Novoselov SV, Paulsen IT, Pazour G, Purton S, Ral JP, Riano-Pachon DM, Riekhof W, Rymarquis L, Schroda M, Stern D, Umen J, Willows R, Wilson N, Zimmer SL, Allmer J, Balk J, Bisova K, Chen CJ, Elias M, Gendler K, Hauser C, Lamb MR, Ledford H, Long JC, Minagawa J, Page MD, Pan JM, Pootakham W, Roje S, Rose A, Stahlberg E, Terauchi AM, Yang PF, Ball S, Bowler C, Dieckmann CL, Gladyshev VN, Green P, Jorgensen R, Mayfield S, Mueller-Roeber B, Rajamani S, Sayre RT, Brokstein P, Dubchak I, Goodstein D, Hornick L, Huang YW, Jhaveri J, Luo YG, Martinez D, Ngau WCA, Otillar B, Poliakov A, Porter A, Szajkowski L, Werner G, Zhou KM, Grigoriev IV, Rokhsar DS, Grossman AR, Annotation C, Team JA (2007) The *Chlamydomonas* genome reveals the evolution of key animal and plant functions. Science **318:** 245-251

Mereschkowsky C (1905) Über Natur und Ursprung der Chromatophoren im Pflanzenreiche. Biologisches Zentralblatt, Leipzig [etc.] VEB Georg Thieme [etc.] **25:** 595-604

Meyer Y, Verdoucq L, Vignols F (1999) Plant thioredoxins and glutaredoxins: identity and putative roles. Trends in Plant Science **4:** 388-394

Miller G, Suzuki N, Rizhsky L, Hegie A, Koussevitzky S, Mittler R (2007) Double mutants deficient in cytosolic and thylakoid ascorbate peroxidase reveal a complex mode of interaction between reactive oxygen species, plant development, and response to abiotic stresses. Plant Physiology **144:** 1777-1785

Mills GC (1957) Hemoglobin catabolism: I. Glutathione peroxidase, an erythrocyte enzyme which protects hemoglobin from oxidative breakdown. Journal of Biological Chemistry **229:** 189-197

Mitschke J, Fuss J, Blum T, Hoglund A, Reski R, Kohlbacher O, Rensing SA (2009) Prediction of dual protein targeting to plant organelles. New Phytologist **183:** 224-236

Mittler R (2002) Oxidative stress, antioxidants and stress tolerance. Trends in Plant Science **7:** 405-410

Mittova V, Theodoulou FL, Kiddle G, Gomez L, Volokita M, Tal M, Foyer CH, Guy M (2003) Coordinate induction of glutathione biosynthesis and glutathione-metabolizing enzymes is correlated with salt tolerance in tomato. FEBS Letters **554:** 417-421

Miyagawa Y, Tamoi M, Shigeoka S (2000) Evaluation of the defense system in chloroplasts to photooxidative stress caused by paraquat using transgenic tobacco plants expressing catalase from *Escherichia coli*. Plant and Cell Physiology **41:** 311-320

Miyake C, Asada K (1996) Inactivation mechanism of ascorbate peroxidase at low concentrations of ascorbate; hydrogen peroxide decomposes compound I of ascorbate peroxidase. Plant and Cell Physiology **37:** 423-430

Miyake C, Michihata F, Asada K (1991) Scavenging of hydrogen peroxide in prokaryotic and eukaryotic Algae - Acquisition of ascorbate peroxidase during the evolution of Cyanobacteria. Plant and Cell Physiology **32:** 33-43

Moran JV, Holmes SE, Naas TP, DeBerardinis RJ, Boeke JD, Kazazian HH (1996) High frequency retrotransposition in cultured mammalian cells. Cell **87:** 917-927

Mukai K, Daifuku K, Okabe K, Tanigaki T, Inoue K (1991) Structure activity relationship in the quenching reaction of singlet oxygen by tocopherol (vitamin-E) derivatives and related phenols - finding of linear correlation between the rates of quenching of singlet oxygen and scavenging of peroxyl and phenoxyl radicals in solution. Journal of Organic Chemistry **56:** 4188-4192

Mullineaux PM, Karpinski S, Jiménez A, Cleary SP, Robinson C, Creissen GP (1998) Identification of cDNAS encoding plastid-targeted glutathione peroxidase. The Plant Journal **13:** 375-379

Mullineaux PM, Rausch T (2005) Glutathione, photosynthesis and the redox regulation of stress-responsive gene expression. Photosynthesis Research **86:** 459-474

Murgia I, Tarantino D, Vannini C, Bracale M, Carravieri S, Soave C (2004) *Arabidopsis thaliana* plants overexpressing thylakoidal ascorbate peroxidase show increased resistance to paraquat-induced photooxidative stress and to nitric oxide-induced cell death. Plant Journal **38:** 940-953

Nakano Y, Asada K (1980) Spinach chloroplasts scavenge hydrogen peroxide on illumination. Plant and Cell Physiology **21:** 1295-1307

Nakano Y, Asada K (1981) Hydrogen peroxide is scavenged by ascorbate-specific peroxidase in spinach chloroplasts. Plant and Cell Physiology **22:** 867-880

Navari-Izzo F, Pinzino C, Quartacci MF, Sgherri CLM (1999) Superoxide and hydroxyl radical generation, and superoxide dismutase in PSII membrane fragments from wheat. Free Radical Research **31:** S3-S9

Navrot N, Collin V, Gualberto J, Gelhaye E, Hirasawa M, Rey P, Knaff DB, Issakidis E, Jacquot JP, Rouhier N (2006) Plant glutathione peroxidases are functional peroxiredoxins distributed in several subcellular compartments and regulated during biotic and abiotic stresses. Plant Physiology **142:** 1364-1379

Neely WC, Martin JM, Barker SA (1988) Products and relative reaction rates of the oxidation of tocopherols with singlet molecular oxygen. Photochemistry and Photobiology **48:** 423–428

Nishikimi M (1975) Oxidation of ascorbic acid with superoxide anion generated by the xanthinexanthine oxidase system. Biochemical and Biophysical Research Communications **63:** 463-468

Nishiyama T, Fujita T, Shin-I T, Seki M, H. N, Uchiyama I, A. K, Carninci P, Hayashizaki Y, Shinozaki K, Kohara Y, Hasebe M (2003) Comparative genomics of *Physcomitrella patens* gametophytic transcriptome and *Arabidopsis thaliana*: Implication for land plant evolution. PNAS **100:** 8007-8012

Niu D-K, Hou W-R, Li S-W (2013) mRNA-mediated intron losses: evidence from extraordinarily large exons. Molecular Biology and Evolution **22:** 1475-1481

Noctor G, Foyer CH (1998) Ascorbate and glutathione: Keeping active oxygen under control. Annual Review of Plant Physiology and Plant Molecular Biology **49:** 249-279

Notredame C, Higgins DG, Heringa J (2000) T-Coffee: A novel method for fast and accurate multiple sequence alignment. Journal of Molecular Biology **302:** 205-217

Novoselov SV, Rao M, Onoshko NV, Zhi HJ, Kryukov GV, Xiang YB, Weeks DP, Hatfield DL, Gladyshev VN (2002) Selenoproteins and selenocysteine insertion system in the model plant cell system, *Chlamydomonas reinhardtii*. EMBO Journal **21:** 3681-3693

Ogawa K, Kanematsu S, Takabe K, Asada K (1995) Attachment of CuZn-superoxide dismutase to thylakoid membranes at the site of superoxide generation (PSI) in spinach chloroplasts - detection by immonugold labeling after rapid freezing and substitution method. Plant and Cell Physiology **36:** 565-573

Okuda T, Matsuda Y, Yamanaka A, Sagisaka S (1991) Abrupt increase in the level of hydrogen peroxide in leaves of winter-wheat is caused by cold treatment. Plant Physiology **97:0** 1265-1267

Oliva M, Theiler G, Zamocky M, Koua D, Margis-Pinheiro M, Passardi F, Dunand C (2009) PeroxiBase: a powerful tool to collect and analyse peroxidase sequences from Viridiplantae. Journal of Experimental Botany **60:** 453-459

Palatnik JF, Valle EM, Carrillo N (1997) Oxidative stress causes ferredoxin $NADP^{(+)}$ reductase solubilization from the thylakoid membranes in methylviologen treated plants. Plant Physiology **115:** 1721-1727

Paquette SM, Bak S, Feyereisen R (2000) Intron-exon organization and phylogeny in a large superfamily, the paralogous cytochrome P450 genes of *Arabidopsis thaliana*. DNA and Cell Biology **19:** 307-317

Pastori GM, Kiddle G, Antoniw J, Bernard S, Veljovic-Jovanovic S, Verrier PJ, Noctor G, Foyer CH (2003) Leaf vitamin C contents modulate plant defense transcripts and regulate genes that control development through hormone signaling. Plant Cell **15:** 939-951

Pena-Ahumada A, Kahmann U, Dietz KJ, Baier M (2006) Regulation of peroxiredoxin expression versus expression of Halliwell-Asada-Cycle enzymes during early seedling development of *Arabidopsis thaliana*. Photosynthesis Research **89:** 99-112

Petersson UA, Kieselbach T, Garcia-Cerdan JG, Schroder WP (2006) The Prx Q protein of *Arabidopsis thaliana* is a member of the luminal chloroplast proteome. FEBS Letters **580:** 6055-6061

Pfannschmidt T, Schutze K, Fey V, Sherameti I, Oelmuller R (2003) Chloroplast redox control of nuclear gene expression - A new class of plastid signals in interorganellar communication. Antioxidants & Redox Signaling **5:** 95-101

Pitsch NT, Witsch B, Baier M (2010) Comparison of the chloroplast peroxidase system in the chlorophyte *Chlamydomonas reinhardtii*, the bryophyte *Physcomitrella patens*, the lycophyte *Selaginella moellendorffii* and the seed plant *Arabidopsis thaliana*. BMC Plant Biology **10**

Pluthero FG (1993) Rapid purification of high-activity *Taq* DNA-polymerase. Nucleic Acids Research **21:** 4850-4851

Polunin O (1971) Pflanzen Europas. BLV verlagsgesellschaft mbH, München

Priestley J (1772) XIX. Observations on different kinds of air. Philosophical Transactions of the Royal Society, London **62:** 147-264

Quatrano RS, McDaniel SF, Khandelwal A, Perroud PF, Cove DJ (2007) *Physcomitrella patens*: mosses enter the genomic age. Current Opinion in Plant Biology **10:** 182-189

Raven EL (2003) Understanding functional diversity and substrate specificity in haem peroxidases: what can we learn from ascorbate peroxidase? Natural Product Reports **20:** 367-381

Rennenberg H (1982) Glutathione metabolism and possible biological roles in higher plants. Phytochemistry **21:** 2771-2781

Rensing SA, Ick J, Fawcett JA, Lang D, Zimmer A, De Peer YV, Reski R (2007) An ancient genome duplication contributed to the abundance of metabolic genes in the moss *Physcomitrella patens*. BMC Evolutionary Biology **7**

Rensing SA, Lang D, Zimmer AD, Terry A, Salamov A, Shapiro H, Nishiyama T, Perroud PF, Lindquist EA, Kamisugi Y, Tanahashi T, Sakakibara K, Fujita T, Oishi K, Shin-I T, Kuroki Y, Toyoda A, Suzuki Y, Hashimoto S, Yamaguchi K, Sugano S, Kohara Y, Fujiyama A, Anterola A, Aoki S, Ashton N, Barbazuk WB, Barker E, Bennetzen JL, Blankenship R, Cho SH, Dutcher SK, Estelle M, Fawcett JA, Gundlach H, Hanada K, Heyl A, Hicks KA, Hughes J, Lohr M, Mayer K, Melkozernov A, Murata T, Nelson DR, Pils B, Prigge M, Reiss B, Renner T, Rombauts S, Rushton PJ, Sanderfoot A, Schween G, Shiu SH, Stueber K, Theodoulou FL, Tu H, Van de Peer Y, Verrier PJ, Waters E, Wood A, Yang LX, Cove D, Cuming AC, Hasebe M, Lucas S, Mishler BD, Reski R, Grigoriev IV, Quatrano RS, Boore JL (2008) The *Physcomitrella* genome reveals evolutionary insights into the conquest of land by plants. Science **319:** 64-69

Reski R (1998a) *Physcomitrella* and *Arabidopsis*: the David and Goliath of reverse genetics. Trends in Plant Science **3:** 209-210

Reski R (1998b) Development, genetics and molecular biology of mosses. Botanica Acta **111:** 1-15

Reski R (2002) Rings and networks: the amazing complexity of FtsZ in chloroplasts. Trends in Plant Science **7:** 103-105

Reski R (2005) Do we need another model plant? Plant Biology **7:** 219-219

Richardt S, Timmerhaus G, Lang D, Qudeimat E, Correa LGG, Reski R, Rensing SA, Frank W (2010) Microarray analysis of the moss *Physcomitrella patens* reveals evolutionarily conserved transcriptional regulation of salt stress and abscisic acid signalling. Plant Molecular Biology **72:** 27-45

Robinson C, Thompson SJ, Woolhead C (2001) Multiple pathways used for the targeting of thylakoid proteins in chloroplasts. Traffic **2:** 245-251

Rodriguez Milla MA, Maurer A, Rodriguez Huete A, Gustafson JP (2003) Glutathione peroxidase genes in *Arabidopsis* are ubiquitous and regulated by abiotic stresses through diverse signaling pathways. The Plant Journal **36:** 602-615

Rost B, Yachdav G, Liu JF (2004) The PredictProtein server. Nucleic Acids Research **32:** W321-W326

Rouhier N, Gelhaye E, Sautiere PE, Brun A, Laurent P, Tagu D, Gerard J, de Fay E, Meyer Y, Jacquot JP (2001) Isolation and characterization of a new peroxiredoxin from poplar sieve tubes that uses either glutaredoxin or thioredoxin as a proton donor. Plant Physiology **127:** 1299-1309

Rouhier N, Jacquot JP (2005) The plant multigenic family of thiol peroxidases. Free Radical Biology and Medicine **38:** 1413-1421

Roy SW, Penny D (2007) Patterns of intron loss and gain in plants: Intron loss-dominated evolution and genome-wide comparison of *O. sativa* and *A. thaliana*. Molecular Biology and Evolution **24:** 171-181

Sakamoto A, Okumura T, Kaminaka H, Sumi K, Tanaka K (1995) Structure and differential response to abscisic acid of two promoters for the cytosolic copper/zinc-superoxide dismutase genes, SodCc1 and SodCc2, in rice protoplasts. FEBS Letters **358:** 62-66

Sandalio LM, Fernández VM, Rupérez FL, del Río LA (1987) Superoxide free radicals are produced in glyoxysomes. Plant Physiology **87:** 1-4

Sanger F, Nicklein S, Coulson AR (1977) DNA sequencing with chain-terminating inhibitors. Proceedings of the National Academy of Sciences USA **74:** 5463-5467

Sapay N, Guermeur Y, Deleage G (2006) Prediction of amphipathic in-plane membrane anchors in monotopic proteins using a SVM classifier. BMC Bioinformatics **7**

Sawada Y, Ohyama T, Yamazaki I (1971) Preparation and physiological properties of green pea superoxide dismutase. Biochimica et Piophysica Acta **268:** 305-312

Schaefer D, Zrÿd J-P, Knight CD, Cove DJ (1990) Stable transformation of the moss *Physcomitrella patens*. Molecular Genetics and Genomics **226:** 418-424

Schaefer DG, Zrÿd JP (2001) The moss *Physcomitrella patens*, now and then. Plant Physiology **127:** 1430-1438

Schmidt GW, Mishkind ML (1986) The transport of proteins into chloroplasts. Annual Review of Biochemistry **55:** 879-912

Schoner S, Krause GH (1990) Protective systems against active oxygen species in spinach - response to cold-acclimation in excess light. Planta **180:** 383-389

Schreier PH, Seftor EA, Schell J, Bohnert HJ (1985) The use of nuclear-encoded sequences to direct the light-regulated synthesis and transport of a foreign protein into plant chloroplasts. EMBO Journal **4:** 25-32

Schröder E, Littlechild JA, Lebedev AA, Errington N, Vagin AA, Isupov MN (2000) Crystal structure of decameric 2-Cys peroxiredoxin from human erythrocytes at 1.7 Å resolution. Structure **8:** 605-615

Schumaker KS, Dietrich MA (1997) Programmed changes in form during moss development. Plant Cell **9:** 1099-1107

Schwede T, Kopp J, Guex N, Peitsch MC (2003) SWISS-MODEL: an automated protein homology-modeling server. Nucleic Acids Research **31:** 3381-3385

Seo MS, Kang SW, Kim K, Baines IC, Lee TH, Rhee SG (2000) Identification of a new type of mammalian peroxiredoxin that forms an intramolecular disulfide as a reaction intermediate. Journal of Biological Chemistry **275:** 20346-20354

Shen B, Jensen RG, Bohnert HJ (1997) Increased resistance to oxidative stress in transgenic plants by targeting mannitol biosynthesis to chloroplasts. Plant Physiology **113:** 1177-1183

Siefermann-Harms D (1987) The light-harvesting and protective functions of carotenoids in photosynthetic membranes. Physiologia Plantarum **69:** 561-568

Sitte P, Weiler EW, Kadereit JW, Bresinsky A, Körner C (2002) Strasburger Lehrbuch der Botanik. Spektrum akademischer Verlag Heidelberg-Berlin **35th volume**

Smeekens S, Bauerle C, Hageman J, Keegstra K, Weisbeek P (1986) The role of the transit peptide in the routing of precursors toward different chloroplast compartments. Cell **46:** 365-375

Smeekens S, Vansteeg H, Bauerle C, Bettenbroek H, Keegstra K, Weisbeek P (1987) Import into chloroplasts of a yeast mitochondrial protein directed by ferredoxin and plastocyanin transit peptides. Plant Molecular Biology **9:** 377-388

Smeekens S, Weisbeek P (1988) Protein-transport towards the thylakoid lumen - post-translational translocation in tandem. Photosynthesis Research **16:** 177-186

Smith AT, Veitch NC (1998) Substrate binding and catalysis in heme peroxidases. Current Opinion in Chemical Biology **2:** 269-278

Soll J, Alefsen H (1993) The protein import apparatus of chloroplasts. Physiologia Plantarum **87:** 433-440

Soll J, Seedorf M (1995) The protein import machinery of chloroplasts. Photosynthesis: from light to biosphere, Vol Iii**:** 725-730

Solovyev VV, Salamov AA, Lawrence CB (1994) Predicting internal exons by oligonucleotide composition and discriminant-analysis of spliceable open reading frames. Nucleic Acids Research **22:** 5156-5163

Stork T, Michel KP, Pistorius EK, Dietz KJ (2005) Bioinformatic analysis of the genomes of the cyanobacteria *Synechocystis sp.* PCC 6803 and *Synechococcus elongatus* PCC 7942 for the presence of peroxiredoxins and their transcript regulation under stress. Journal of Experimental Botany **56:** 3193-3206

Sze P (1986) A biology of the algae. Wm. C. Brown Publishers

Takeda T, Yoshimura K, Yoshii M, Kanahoshi H, Miyasaka H, Shigeoka S (2000) Molecular characterization and physiological role of ascorbate peroxidase from halotolerant *Chlamydomonas sp.* W80 strain. Archives of Biochemistry and Biophysics **376:** 82-90

Tamura K, Dudley J, Nei M, Kumar S (2007) MEGA4: Molecular evolutionary genetics analysis (MEGA) software version 4.0. Molecular Biology and Evolution **24:** 1596-1599

Tanaka T, Izawa S, Inoue Y (2005) GPX2, encoding a phospholipid hydroperoxide glutathione peroxidase homologue, codes for an atypical 2-Cys peroxiredoxin in *Saccharomyces cerevisiae*. Journal of Biological Chemistry **280:** 42078-42087

Tarantino D, Vannini C, Bracale M, Campa M, Soave C, Murgia I (2005) Antisense reduction of thylakoidal ascorbate peroxidase in *Arabidopsis* enhances paraquat-induced photooxidative stress and nitric oxide-induced cell death. Planta **221:** 757-765

Teixeira FK, Menezes-Benavente L, Galvao VC, Margis R, Margis-Pinheiro M (2006) Rice ascorbate peroxidase gene family encodes functionally diverse isoforms localized in different subcellular compartments. Planta **224:** 300-314

Teixeira FK, Menezes-Benavente L, Margis R, Margis-Pinheiro M (2004) Analysis of the molecular evolutionary history of the ascorbate peroxidase gene family: Inferences from the rice genome. Journal of Molecular Evolution **59:** 761-770

Telfer A, Dhami S, Bishop SM, Phillips D, Barber J (1994) β-Carotene quenches singlet oxygen formed by isolated photosystem II reaction centers. Biochemistry **33:** 14469-14474

Thompson JD, Higgins DG, Gibson TJ (1994) Clustal-W - Improving the sensitivity of progressive multiple sequence alignment through sequence weighting, position-specific gap penalties and weight matrix choice. Nucleic Acids Research **22:** 4673-4680

Trebst A (2003) Function of β-carotene and tocopherol in photosystem II. Zeitschrift Fur Naturforschung Section C-a Journal of Biosciences **58:** 609-620

Tryon AF, Lugardon B (1990) Spores of the Pteridophyta. Springer Verlag

Turrens JF (1997) Superoxide production by the mitochondrial respiratory chain. Bioscience Reports **17:** 3-8

Uniacke J, Zerges W (2009) Chloroplast protein targeting involves localized translation in *Chlamydomonas*. Proceedings of the National Academy of Sciences of the United States of America **106:** 1439-1444

van den Hoek C (1978) Algen. Thieme Verlag

Veljovic-Jovanovic SD, Pignocchi C, Noctor G, Foyer CH (2001) Low ascorbic acid in the *vtc-1* mutant of *Arabidopsis* is associated with decreased growth and intracellular redistribution of the antioxidant system. Plant Physiology **127:** 426-435

Verdoucq L, Vignols F, Jacquot JP, Chartier Y, Meyer Y (1999) In vivo characterization of a thioredoxin h target protein defines a new peroxiredoxin family. Journal of Biological Chemistry **274:** 19714-19722

Viitanen PV, Doran ER, Dunsmuir P (1988) What is the role of the transit peptide in thylakoid integration of the light-harvesting chlorophyll a/b protein. Journal of Biological Chemistry **263:** 15000-15007

Vinogradov AE (1999) Intron-genome size relationship on a large evolutionary scale. Journal of Molecular Evolution **49:** 376-384

Voinnet O, Rivas S, Mestre P, Baulcombe D (2003) An enhanced transient expression system in plants based on suppression of gene silencing by the p19 protein of tomato bushy stunt virus. Plant Journal **33:** 949-956

Wachter A, Wolf S, Steininger H, Bogs J, Rausch T (2005) Differential targeting of GSH1 and GSH2 is achieved by multiple transcription initiation: implications for the compartmentation of glutathione biosynthesis in the Brassicaceae. Plant Journal **41:** 15-30

Wada K, Tada T, Nakamura Y, Ishikawa T, Yabuta Y, Yoshimura K, Shigeoka S, Nishimura K (2003) Crystal structure of chloroplastic ascorbate peroxidase from tobacco plants and structural insights into its instability. Journal of Biochemistry **134:** 239-244

Wakaguri H, Yamashita R, Suzuki Y, Sugano S, Nakai K (2008) DBTSS: database of transcription start sites, progress report 2008. Nucleic Acids Research **36:** D97-D101

Wang WM, Tanurdzic M, Luo MZ, Sisneros N, Kim HR, Weng JK, Kudrna D, Mueller C, Arumuganathan K, Carlson J, Chapple C, de Pamphilis C, Mandoli D, Tomkins J, Wing RA, Banks JA (2005) Construction of a bacterial artificial chromosome library from the spikemoss *Selaginella moellendorffii*: a new resource for plant comparative genomics. BMC Plant Biology **5**

Wang XQ, Yang PF, Gao Q, Liu XL, Kuang TY, Shen SH, He YK (2008) Proteomic analysis of the response to high-salinity stress in *Physcomitrella patens*. Planta **228:** 167-177

Wang XY, Quinn PJ (2000) The location and function of vitamin E in membranes (review). Molecular Membrane Biology **17:** 143-156

Weigel D, Glazebrook J (2002) *Arabidopsis* - A laboratory manual. Cold Spring Harbor Laboratory Press, Cold Spring Harbor, New York, USA

Welinder KG (1992) Superfamily of plant, fungal and bacterial peroxidases. Current Opinion in Structural Biology **2:** 388-393

Wendel JF, Cronn RC, Alvarez I, Liu B, Small RL, Senchina DS (2002) Intron size and genome size in plants. Molecular Biology and Evolution **19:** 2346-2352

Weng JK, Tanurdzic M, Chapple C (2005) Functional analysis and comparative genomics of expressed sequence tags from the lycophyte *Selaginella moellendorffii*. BMC Genomics **6**

Wheeler GL, Jones MA, Smirnoff N (1998) The biosynthetic pathway of vitamin C in higher plants. Nature **393:** 365-369

Wingate VPM, Lawton MA, Lamb CJ (1988) Glutathione Causes a Massive and Selective Induction of Plant Defense Genes. Plant Physiology **87:** 206-210

Wingsle G, Karpinski S (1996) Differential redox regulation by glutathione of glutathione reductase and CuZn-superoxide dismutase gene expression in *Pinus sylvestris* L. needles. Planta **198:** 151-157

Witte CP, Noel LD, Gielbert J, Parker JE, Romeis T (2004) Rapid one-step protein purification from plant material using the eight-amino acid StrepII epitope. Plant Molecular Biology **55:** 135-147

Wobbe L, Schwarz C, Nickelsen J, Kruse O (2008) Translational control of photosynthetic gene expression in phototrophic eukaryotes. Physiologia Plantarum **133:** 507-515

Wolf L, Rizzini L, Stracke R, Ulm R, Rensing SA (2010) The molecular and physiological responses of *Physcomitrella patens* to ultraviolet-B radiation. Plant Physiology **153:** 1123-1134

Wood ZA, Schroder E, Harris JR, Poole LB (2003) Structure, mechanism and regulation of peroxiredoxins. Trends in Biochemical Sciences **28:** 32-40

Wormuth D, Baier M, Kandlbinder A, Scheibe R, Hartung W, Dietz KJ (2006) Regulation of gene expression by photosynthetic signals triggered through modified CO2 availability. BMC Plant Biology **6**

Wu FH, Shen SC, Lee LY, Lee SH, Chan MT, Lin CS (2009) Tape-*Arabidopsis*-Sandwich - a simpler *Arabidopsis* protoplast isolation method. Plant Methods **5**

Xiao H, Jiang N, Schaffner E, Stockinger EJ, van der Knaap E (2008) A retrotransposon-mediated gene duplication underlies morphological variation of tomato fruit. Science **319:** 1527-1530

Xing J, Wang H, Belancio VP, Cordaux R, Deininger PL, Batzer MA (2006) Emergence of primate genes by retrotransposon-mediated sequence transduction. Proceedings of the National Academy of Sciences of the United States of America **103:** 17608-17613

Yabuta Y, Motoki T, Yoshimura K, Takeda T, Ishikawa T, Shigeoka S (2002) Thylakoid membrane-bound ascorbate peroxidase is a limiting factor of antioxidative systems under photo-oxidative stress. Plant Journal **32:** 915-925

Yamasaki I, Piette LH (1961) Mechanism of free radical formation and disappearance during the ascorbic acid oxidase end peroxidase reactions. Biochimica et Biophysica Acta **50:** 62-69

Yoo SD, Cho YH, Sheen J (2007) *Arabidopsis* mesophyll protoplasts: a versatile cell system for transient gene expression analysis. Nature Protocols **2:** 1565-1572

Yoshida K, Igarashi E, Mukai M, Hirata K, Miyamoto K (2003) Induction of tolerance to oxidative stress in the green alga, *Chlamydomonas reinhardtii*, by abscisic acid. Plant Cell and Environment **26:** 451-457

Yoshimura K, Ishikawa T, Nakamura Y, Tamoi M, Takeda T, Tada T, Nishimura K, Shigeoka S (1998) Comparative study on recombinant chloroplastic and cytosolic ascorbate peroxidase isozymes of spinach. Archives of Biochemistry and Biophysics **353:** 55-63

Yoshimura K, Yabuta Y, Ishikawa T, Shigeoka S (2000) Expression of spinach ascorbate peroxidase isoenzymes in response to oxidative stresses. Plant Physiology **123:** 223-233

Yoshimura K, Yabuta Y, Ishikawa T, Shigeoka S (2002) Identification of a *cis* element for tissue-specific alternative splicing of chloroplast ascorbate peroxidase pre-mRNA in higher plants. Journal of Biological Chemistry **277:** 40623-40632

Yoshimura K, Yabuta Y, Tamoi M, Ishikawa T, Shigeoka S (1999) Alternatively spliced mRNA variants of chloroplast ascorbate peroxidase isoenzymes in spinach leaves. Biochemical Journal **338:** 41-48

Zamocky M, Janecek S, Koller F (2000) Common phylogeny of catalase-peroxidases and ascorbate peroxidases. Gene **256:** 169-182

Zhang X, Zhang L, Dong FC, Gao JF, Galbraith DW, Song CP (2001) Hydrogen peroxide is involved in abscisic acid-induced stomatal closure in *Vicia faba*. Plant Physiology **126:** 1438-1448

Zhu JK (2002) Salt and drought stress signal transduction in plants. Annual Review of Plant Biology **53:** 247-273

List of publications

Journal articles:

- **Pitsch NT, Witsch B, Baier M** (2010) Comparison of the chloroplast peroxidase system in the chlorophyte *Chlamydomonas reinhardtii*, the bryophyte *Physcomitrella patens*, the lycophyte *Selaginella moellendorffii* and the seed plant *Arabidopsis thaliana*. BMC Plant Biology 2010, **10**

- **Baier M, Pitsch NT, Mellenthin M, Guo W** (2010) Regulation of genes encoding chloroplast antioxidant enzymes in comparison to regulation of the extra-plastidic antioxidant system". In: Ascorbate-glutathione pathways and stress tolerance in plants. In Ascorbate-Glutathione Pathway and Stress Tolerance in Plants, Eds: Anjum NA, Chan M-T, Umar S. Springer

Talks:

- Comparison of the chloroplast peroxide detoxification systems in *C. reinhardtii*, *P. patens*, *S. moellendorffii*, and *A. thaliana*. Botanikertagung 2009, Leipzig, Germany

Posters:

- **Pitsch NT, Mellenthin M, Hiltscher H, Baier M** (2008) Regulation and evolution of the chloroplast antioxidant network". FESPB meeting, Tampere, Finnland

- **Pitsch NT, Baier M (**2008) Line up of the photooxidative defense during plant evolution. Photosynthesis workshop, Bochum, Germany

- **Pitsch NT, Baier M** (2009) Phylogenetic comparison of the chloroplast antioxidant network". Arabidopsis meeting, Edinburgh, UK

- **Pitsch NT, Baier M** (2011) Regulation of chloroplast APx isoforms in *Arabidopsis thaliana* and *Physcomitrella patens*. Botanikertagung, Berlin, Germany

Appendix

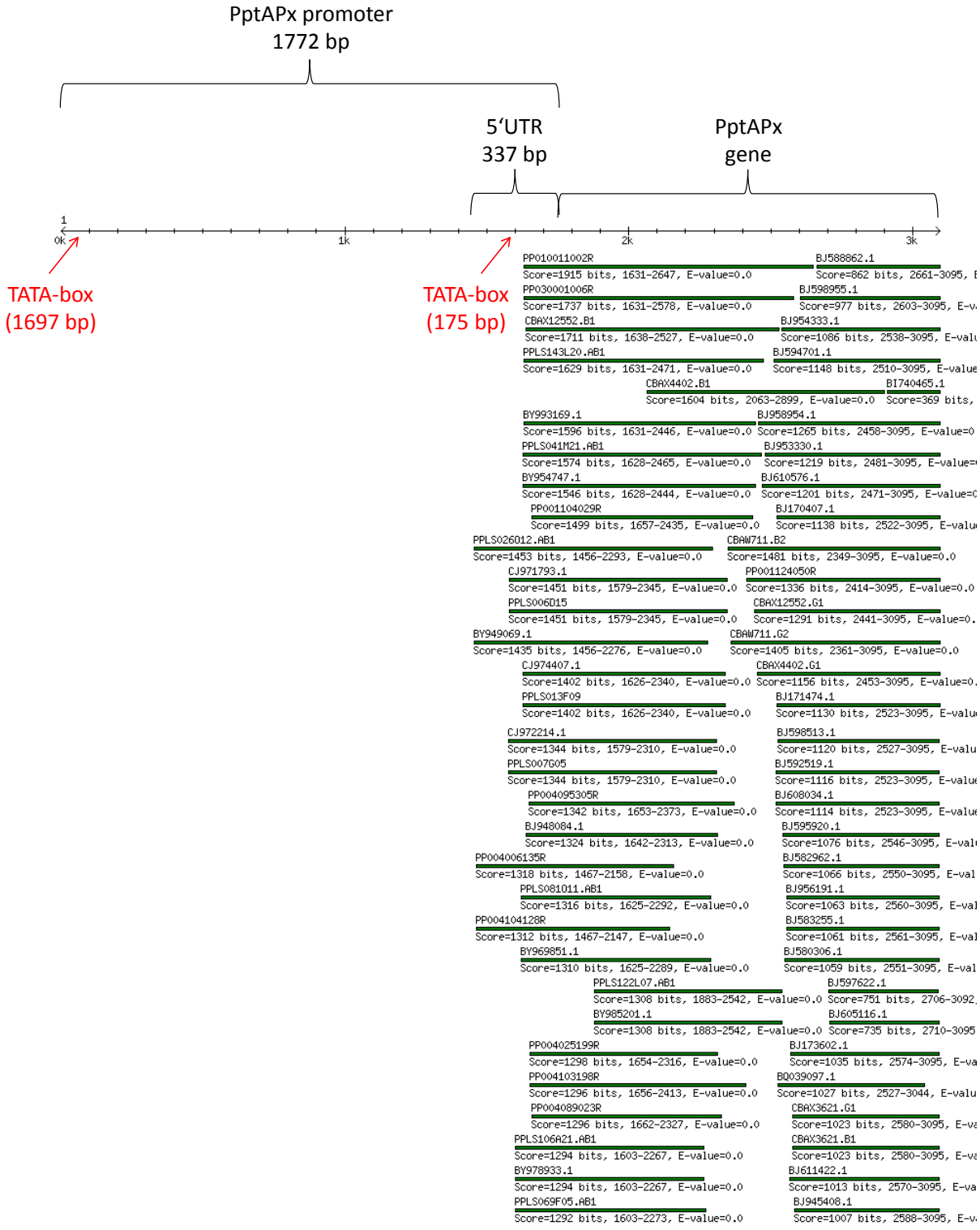

Fig. A1: PptAPx gene and its promoter, TATA-boxes, and specific ESTs. The 1772 bp promoter sequence includes the predicted 5'-UTR of 337 bp. Two TATA-boxes were detected according to the criteria listed in Loganantharaj (2006). The results were obtained with the cosmoss database genome browser. They are located 175 bp and 1697 bp upstream of the PptAPx start-ATG. 144 ESTs cover the PptAPx gene and/or the predicted 5'-UTR, downstream of the TATA-box at 175 bp, while 17 ESTs show a longer 5'-terminus. Figure is continued on next page.

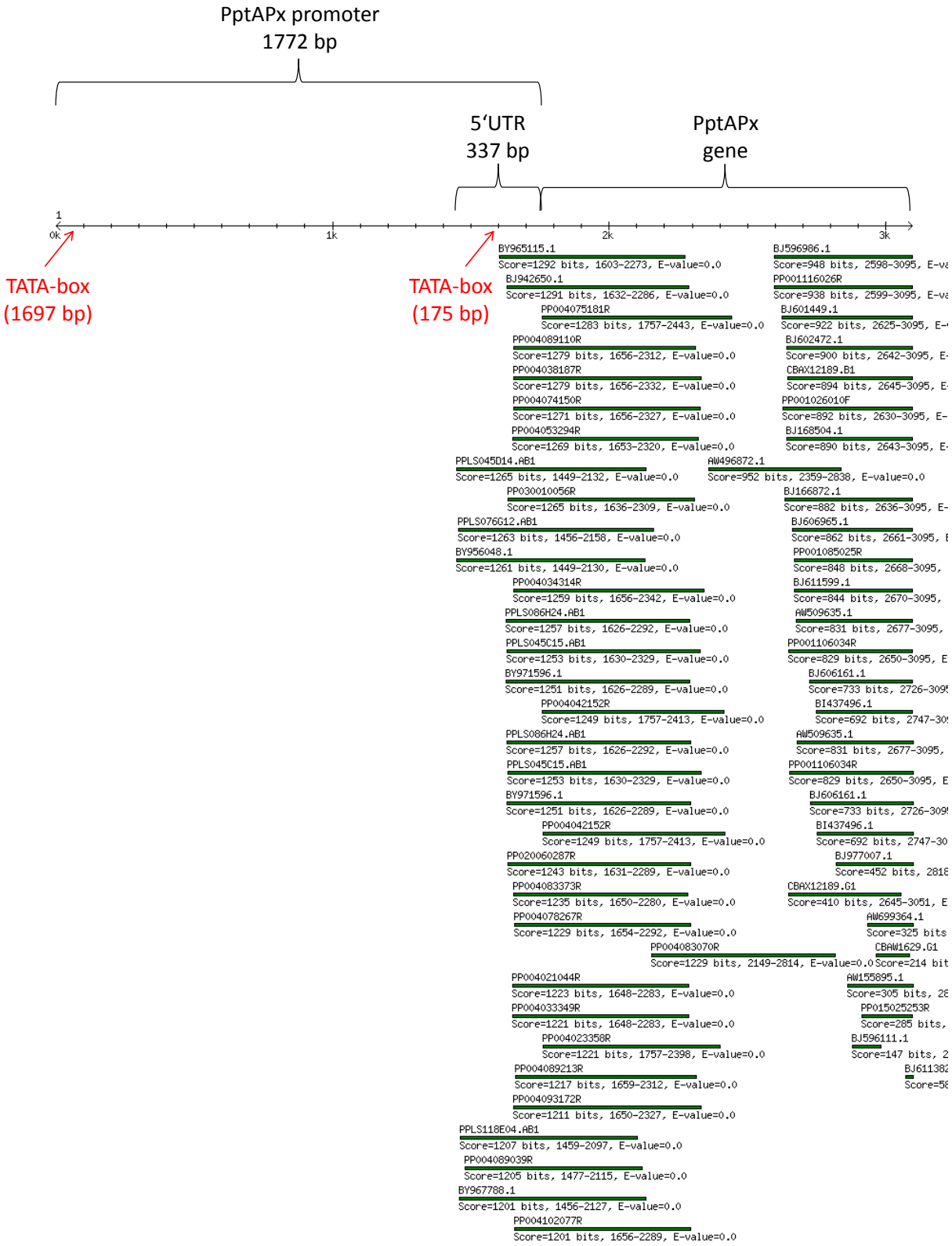

Fig. A1 (continued): PptAPx gene and its promoter, TATA-boxes, and specific ESTs. The 1772 bp promoter sequence includes the predicted 5'-UTR of 337 bp. Two TATA-boxes were detected according to the criteria listed in Loganantharaj (2006). The results were obtained with the cosmoss database genome browser. They are located 175 bp and 1697 bp upstream of the PptAPx start-ATG. 144 ESTs cover the PptAPx gene and/or the predicted 5'-UTR, downstream of the TATA-box at 175 bp, while 17 ESTs show a longer 5'-terminus. Figure is continued on next page.

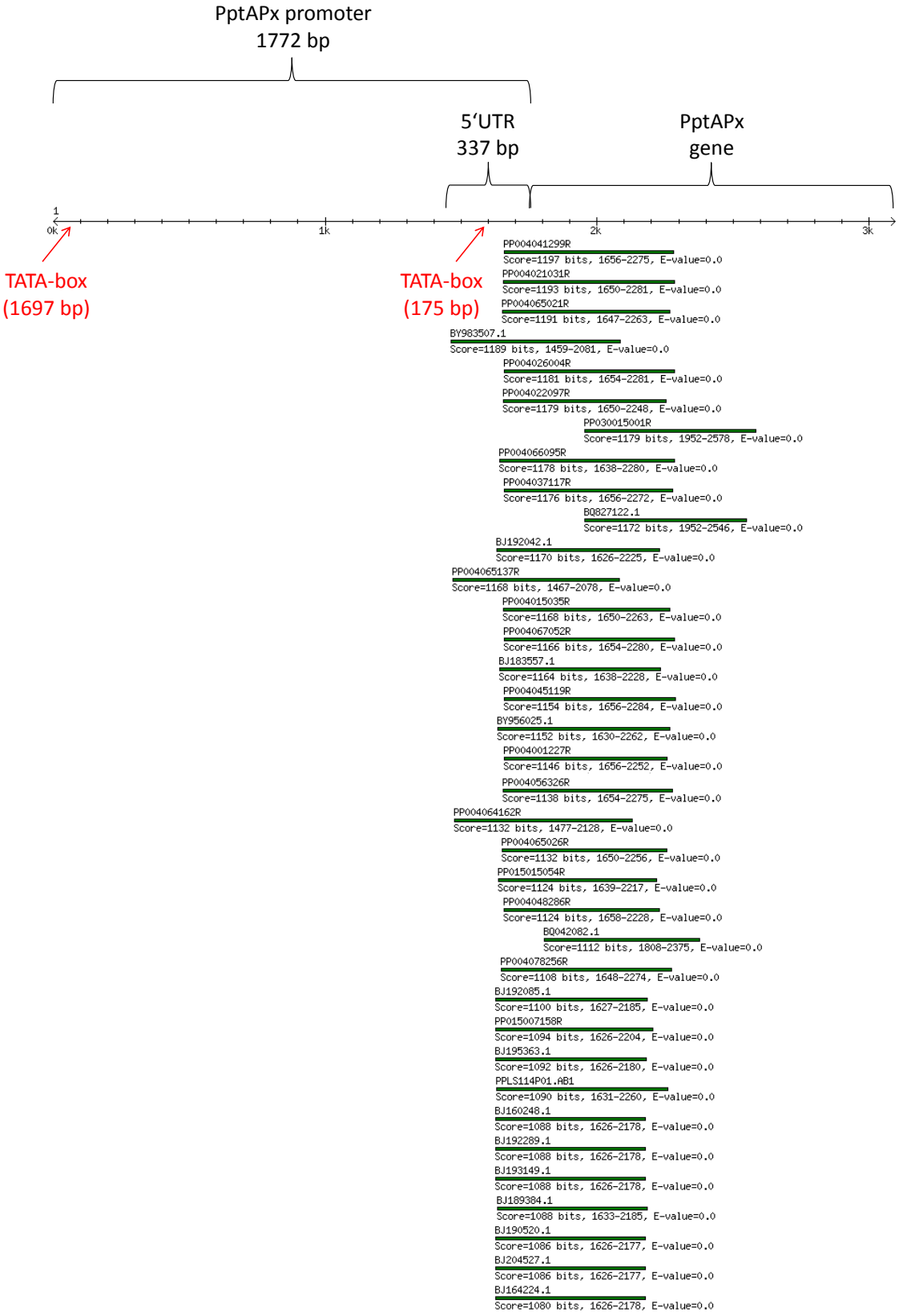

Fig. A1 (continued): PptAPx gene and its promoter, TATA-boxes, and specific ESTs. The 1772 bp promoter sequence includes the predicted 5'-UTR of 337 bp. Two TATA-boxes were detected according to the criteria listed in Loganantharaj (2006). The results were obtained with the cosmoss database genome browser. They are located 175 bp and 1697 bp upstream of the PptAPx start-ATG. 144 ESTs cover the PptAPx gene and/or the predicted 5'-UTR, downstream of the TATA-box at 175 bp, while 17 ESTs show a longer 5'-terminus. Figure is continued on next page.

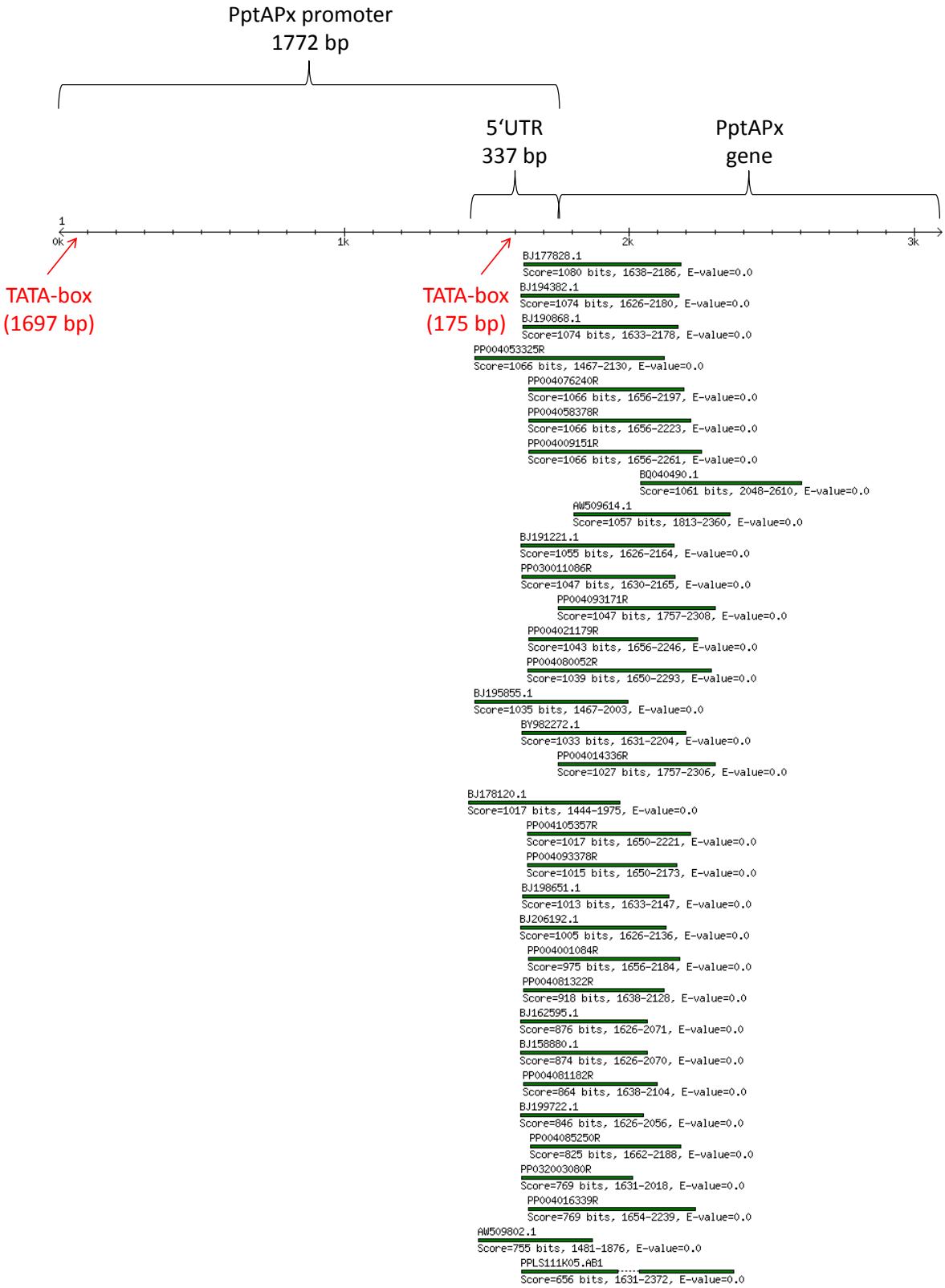

Fig. A1 (continued): PptAPx gene and its promoter, TATA-boxes, and specific ESTs. The 1772 bp promoter sequence includes the predicted 5'-UTR of 337 bp. Two TATA-boxes were detected according to the criteria listed in Loganantharaj (2006). The results were obtained with the cosmoss database genome browser. They are located 175 bp and 1697 bp upstream of the PptAPx start-ATG. 144 ESTs cover the PptAPx gene and/or the predicted 5'-UTR, downstream of the TATA-box at 175 bp, while 17 ESTs show a longer 5'-terminus.